

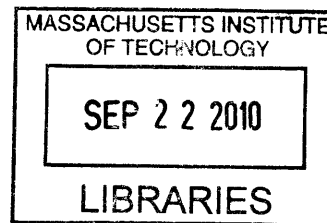
PURIFICATION AND SUBSTRATE SPECIFICITY OF NEW *C. ROSEUS* ENZYMES

by

Nancy Yerkes

B.A. Chemistry

Columbia University, 2005



ARCHIVES

SUBMITTED TO THE DEPARTMENT OF CHEMISTRY IN PARTIAL
FULFILLMENT OF THE REQUIREMENTS FOR THE
DEGREE OF DOCTOR OF PHILOSOPHY
AT THE
MASSACHUSETTS INSTITUTE OF TECHNOLOGY
SEPTEMBER 2010

© 2010 Massachusetts Institute of Technology. All rights reserved.

Signature of Author: _____

Department of Chemistry,
June 23, 2010

Certified by: _____

Sarah E. O'Connor
Latham Family Career Development Associate Professor of Chemistry
Thesis Supervisor

Accepted by: _____

Robert W. Field
Chair, Departmental Committee on Graduate Students

This doctoral thesis has been examined by a committee of the Department of Chemistry as follows:

Professor Stephen J. Lippard

Chair: _____

Professor Barbara Imperiali: _____

Professor Sarah E. O'Connor

Thesis Supervisor: _____

PURIFICATION AND SUBSTRATE SPECIFICITY OF NEW *C. ROSEUS* ENZYMES

ABSTRACT

Terpene indole alkaloids (TIAs) are a class of natural products produced in plants. Many TIAs have medicinal uses; for example, vinblastine has anti-cancer activity and ajmaline has anti-arrhythmic activity. Many TIAs did not evolve to treat human disease, however, and thus most likely do not have optimal pharmacological properties. If TIAs could be modified, the novel TIAs produced could have improved bioactivities when compared with the unmodified natural TIAs. Unfortunately, the immense structural complexity of TIAs makes cost-effective industrial-scale synthesis of the majority of TIAs and TIA analogs unfeasible. Industrial-scale production of TIAs would be improved if TIAs could be produced via reconstitution of the enzymatic pathways in a heterologous organism such as yeast. However, many of the enzymes involved in TIA biosynthesis are unknown, thereby precluding these efforts. If more TIA biosynthetic enzymes were isolated, and the substrate specificity of the enzymes were known, both natural and novel TIA analogs could be more readily produced on an industrial scale.

In this thesis I developed strategies to isolate new *C. roseus* enzymes and to make novel analogs of the anti-hypertensive agent ajmalicine and the anti-neoplastic agent isositsirikine. The NADPH-dependent reductases that produce ajmalicine and isositsirikine have not been isolated. To produce ajmalicine and isositsirikine analogs *in vitro*, two aims must be accomplished: first, the reductases forming ajmalicine and isositsirikine, ajmalicine synthase and isositsirikine synthase, must be partially purified, and second, the substrate specificity of those reductases must be determined. To satisfy the first of these aims, I developed a partial purification procedure for ajmalicine synthase and isositsirikine synthase from *Catharanthus roseus* tissue. My partial purification procedure involved acetone precipitation, ion exchange chromatography, and gel filtration chromatography. Analysis by 2D SDS-PAGE shows that the proteins have been significantly purified. I also performed crosslinking experiments with a substrate probe in attempts to isolate ajmalicine synthase and isositsirikine synthase. In the crosslinking studies four enzymes were isolated and cloned, and one has been found to have sinapyl alcohol dehydrogenase activity.

I determined the substrate specificities of ajmalicine synthase and isositsirikine synthase as well as the enzyme that precedes both enzymes in the biosynthetic pathway, strictosidine- β -glucosidase (SGD). I found that SGD, ajmalicine synthase, and isositsirikine synthase all have broad substrate specificities, which is promising for the development of novel ajmalicine and isositsirikine analogs with potentially improved therapeutic activities.

Thesis Supervisor: Sarah E. O'Connor

Title: Latham Family Career Development Associate Professor of Chemistry

ACKNOWLEDGMENTS

Most of all I thank my advisor Professor Sarah O'Connor. Sarah has been a wonderful advisor, and I am truly grateful for all the effort that she has put into my personal development. I am endlessly amazed at the amount of time Sarah spends helping all her students. Sarah's kind manner has also inspired me to be a better person.

I also thank the members of my committee at MIT, Professors Stephen Lippard and Barbara Imperiali, for all their advice, support, and time.

I thank the members of the O'Connor laboratory for their assistance, advice, and friendship: Elizabeth McCoy, with whom I had many helpful discussions, for teaching me how to express proteins, for providing invaluable assistance with the LCMS, and for providing numerous tryptamine analogs; Peter Bernhardt for his countless ideas and suggestions and for his collaboration in the des-vinyl strictosidine studies; Weerawat "Ricky" Runguphan for helpful discussion and comic relief; Aimee Usera, David Liscombe, and Nathan Ezekiel Nims for helpful advice and for their collaboration in the crosslinking experiments; Hyang-Yeol Lee for his collaboration with the aza strictosidine studies; Lesley Giddings for invaluable help with the HPLC; Weslee Glenn for assistance with the LCMS; John Cheng for assistance with computer problems in the laboratory; Justin Maresh for teaching me how to grow cell suspension cultures; and Carmen Galan for teaching me how to purify secologanin. Other laboratory members Anne Friedrich, Shi Chen, Sarah Sinnett, Jenna Caldwell, and Carla Coltharp were a pleasure to work with, too. I also thank the two undergraduate students with whom I had the privilege to work: Jia Xin "Joann" Wu and Katie Thomas.

I thank former MIT students Mary Farbman, Elvedin Lukovic, and Chiah-Hung Wu for their advice during my first two years of graduate school. I also thank my friends Mike Panas, Kristin Schleicher, Wendy Iskenderian, Brenda Goguen, Montana Childress, Lindsey McQuade, Pamela Lundin, Scott Geyer, Kevin Jones, Omar Ahmad, Wenhao Liu, Ivan Vilotijevic, and Peter Bernhardt. I thank my undergraduate advisor, Professor Ronald Breslow of Columbia University, for his continuing support.

I thank my family: my father Dave Yerkes, Heidi Yerkes, sisters Robin Horton and Lyn Yerkes, brothers-in-law John Horton and Wassim Abida, and mother Franny Yerkes. I was especially lucky to have my sister Robin live right nearby for the past four years. I also thank John Greenland for his love and support and for making me so happy. I also thank John Greenland's parents, Risa Palm and David Greenland, for all their support.

Table of Contents

CHAPTER 1: INTRODUCTION	19
I. STRUCTURE AND PHARMACOLOGICAL USES OF MONOTERPENE INDOLE ALKALOIDS (TIAs)	20
II. BIOSYNTHESIS OF TIAs	26
III. TIAs IN CATHARANTHUS TISSUE	37
IV. POTENTIAL PHARMACOLOGICAL PROPERTIES OF NOVEL TIAs.....	40
V. CLONED TIA ENZYMES.....	45
VI. SUBSTRATE SPECIFICITY OF TIA ENZYMES AND PRECURSOR DIRECTED BIOSYNTHESIS STUDIES	52
VII. THESIS OVERVIEW	56
VIII. REFERENCES	59
 CHAPTER 2: SUBSTRATE SPECIFICITY AND STEADY STATE KINETIC ANALYSIS OF STRICTOSIDINE-B- GLUCOSIDASE 65	
I. INTRODUCTION	66
II. RESULTS	75
A. <i>Novel deglycosylated strictosidine analogs</i>	80
B. <i>Steady state kinetic analysis</i>	87
III. DISCUSSION	90
IV. MATERIALS AND METHODS	98
A. <i>Synthesis of strictosidine analogs</i>	98
B. <i>LCMS analysis</i>	103
C. <i>NMR characterization</i>	104
D. <i>High-resolution mass spectrometry data</i>	104
E. <i>Assay conditions</i>	109
F. <i>Steady state kinetic analysis conditions</i>	111
V. ACKNOWLEDGMENTS.....	115

VI. REFERENCES.....	116
CHAPTER 3: PARTIAL PURIFICATION AND SUBSTRATE SPECIFICITY OF AJMALICINE SYNTHASE AND ISOSITSIRIKINE SYNTHASE.....	119
I. INTRODUCTION	121
A. <i>Previous reports of reductase activity</i>	125
B. <i>Plant enzyme purification techniques</i>	129
II. RESULTS	138
A. <i>Assay development for detection of ajmalicine synthase and isositsirikine synthase activity</i>	138
B. <i>Partial purification protocol for ajmalicine synthase and isositsirikine synthase</i>	142
C. <i>Additional purification methods</i>	151
D. <i>Novel ajmalicine and isositsirikine analogs</i>	158
III. DISCUSSION	172
IV. MATERIALS AND METHODS.....	180
A. <i>C. roseus hairy root cultures</i>	180
B. <i>C. roseus cell suspension cultures</i>	180
C. <i>Preparation of strictosidine analogs</i>	181
D. <i>High-resolution mass spectrometry data</i>	181
E. <i>NMR characterization</i>	183
F. <i>Partial purification procedure</i>	184
G. <i>LCMS data</i>	186
H. <i>Steady state kinetic analysis conditions</i>	193
I. <i>Radioactive enzyme assay</i>	197
J. <i>Chemical reduction of deglycosylated strictosidine with NaCNBH₃</i>	201
V. ACKNOWLEDGMENTS.....	202
VI. REFERENCES.....	204
CHAPTER 4: CLONING AND CHARACTERIZATION OF NOVEL C. ROSEUS ENZYMES	207

I.	INTRODUCTION	208
A.	<i>Enzyme isolation via crosslinking</i>	208
B.	<i>Cinnamyl / sinapyl alcohol dehydrogenases, malate / mannitol dehydrogenases, and 10-hydroxy geraniol oxidoreductase</i>	211
II.	RESULTS	218
A.	<i>Crosslinking experiments</i>	218
B.	<i>Characterization of enzymes isolated via crosslinking experiments</i>	225
III.	DISCUSSION.....	234
IV.	MATERIALS AND METHODS	237
A.	<i>Crosslinking experiments conditions</i>	237
B.	<i>Cloning of crosslinked enzymes</i>	238
C.	<i>Heterologous expression and purification of crosslinked enzymes</i>	239
D.	<i>DNA and amino acid sequences of crosslinked enzymes</i>	240
E.	<i>Assay conditions</i>	243
F.	<i>Steady state kinetic analysis conditions</i>	244
G.	<i>LCMS conditions</i>	245
H.	<i>High-resolution mass spectrometry data</i>	245
V.	ACKNOWLEDGMENTS:	247
VI.	REFERENCES:	248
CHAPTER 5: CONCLUSIONS AND FUTURE DIRECTIONS		251
I.	CONCLUSIONS.....	251
II.	FUTURE DIRECTIONS.....	254
III.	ACKNOWLEDGMENTS	258
IV.	REFERENCES	258

List of Figures

FIGURE 1-1: STRUCTURES OF MONOTERPENE INDOLE ALKALOIDS STRICTOSIDINE	20
FIGURE 1-2: THE STRUCTURE AND NUMBERING SYSTEM (IN BLUE) OF VINBLASTINE.....	23
FIGURE 1-3: STRUCTURES OF AJMALICINE AND ALMITRINE	24
FIGURE 1-4: STRUCTURES OF SERPENTINE, YOHIMBINE, AND ISOSITSIRIKINE	24
FIGURE 1-5: STRUCTURES OF CAMPTOTHECIN, TOPOTECAN, AND IRINOTECAN.....	25
FIGURE 1-6: STRUCTURES OF TRYPTAMINE, SECOLOGANIN, AND STRICTOSIDINE.....	26
FIGURE 1-7: THE MEVALONATE PATHWAY.....	27
FIGURE 1-8: THE NON-MEVALONATE, OR TRIOSE PYRUVATE/PHOSPHATE, PATHWAY.	28
FIGURE 1-9: FORMATION OF GERANIOL PYROPHOSPHATE.....	29
FIGURE 1-10: PROPOSED MECHANISM OF FORMATION OF IRIDOTRIAL	29
FIGURE 1-11: FORMATION OF SECOLOGANIN FROM IRIDOTRIAL.....	30
FIGURE 1-12: BIOSYNTHESIS OF L-TRYPTOPHAN	31
FIGURE 1-13: THE PROPOSED MECHANISM OF STRICTOSIDINE SYNTHASE.....	32
FIGURE 1-14: UPON DEGLYCOSYLATION BY SGD, STRICTOSIDINE CONVERTS TO A REACTIVE HEMIACETAL	33
FIGURE 1-15: IN TIA BIOSYNTHESIS, L-TRYPTOPHAN IS DECARBOXYLATED BY THE CYTOSOLIC ENZYME TRYPTOPHAN DECARBOXYLASE	34
FIGURE 1-16: THE THREE MAIN BRANCHES IN TIA BIOSYNTHESIS IN <i>C. ROSEUS</i>	36
FIGURE 1-17: PICTURES OF THE “ROSY” (LEFT) AND “LITTLE BRIGHT EYES” (RIGHT) VARIETIES OF <i>CATHARANTHUS ROSEUS</i>	37
FIGURE 1-18: <i>C. ROSEUS</i> SEEDLINGS, HAIRY ROOT CULTURE, AND CELL SUSPENSION CULTURE.....	38
FIGURE 1-19: TOPOTECAN AND IRINOTECAN	40
FIGURE 1-20: THE STRUCTURE OF THE ANTI-HISTAMINIC COMPOUND TRIPELENNAMINE	42
FIGURE 1-21: THE STRUCTURE OF A MONOAMINE OXIDASE INHIBITOR.....	42
FIGURE 1-22: THE STRUCTURES OF PARACETAMOL (ACETAMINOPHEN), <i>O</i> -METHYL PARACETAMOL, AND <i>O,O</i> -DIMETHYL PARACETAMOL ..	44
FIGURE 1-23: STRUCTURES OF INDOLE AND OTHER MOIETIES	45
FIGURE 1-24: STRUCTURES OF THE <i>S</i> -(+) AND <i>R</i> -(-) ISOMERS OF THE ANTI-HISTAMINE DEXCHLOROPHENIRAMINE.....	45
FIGURE 1-25: THE STRUCTURES OF GERANIOL AND ITS <i>CIS</i> -ISOMER NEROL	46

FIGURE 1-26: DEACETYLIPECOSIDE SYNTHASE AND DEACETYLIISOIPECOSIDE SYNTHASE.....	48
FIGURE 1-27: STRICTOSIDINE IS DEGLYCOSYLATED BY SGD.....	49
FIGURE 1-28: VINDOLINE BIOSYNTHESIS FROM TABERSONINE.....	50
FIGURE 1-29: VINBLASTINE AND VINCISTINE BIOSYNTHESIS.....	51
FIGURE 1-30: SECOLOGANIN ANALOGS ACCEPTED BY STRICTOSIDINE SYNTHASE.....	52
FIGURE 1-31: THE NUMBERING SYSTEM FOR TRYPTAMINE AND STRICTOSIDINE.....	53
FIGURE 1-32: THE SUBSTRATES NOT ACCEPTED BY STRICTOSIDINE SYNTHASE TO FORM THE CORRESPONDING STRICTOSIDINE ANALOGS.....	54
FIGURE 1-33: 2-BENZOFURAN-3-YL-ETHYLAMINE AND 2-BENZO[β]THIOPHEN-3-YL-ETHYLAMINE ARE ACCEPTED.....	54
FIGURE 1-34: PRECURSOR DIRECTED BIOSYNTHESIS STUDY.....	55
FIGURE 1-35: AJMALICINE SYNTHASE AND ISOSITSIRIKINE SYNTHASE ARE NADPH-DEPENDENT REDUCTASES.....	57
FIGURE 2-1: STRICTOSIDINE IS DEGLYCOSYLATED BY SGD TO PRODUCE A REACTIVE HEMIACETAL INTERMEDIATE.....	67
FIGURE 2-2: UPON DEGLYCOSYLATION BY SGD, STRICTOSIDINE FORMS AN AGLYCON THAT RAPIDLY INTERCONVERTS.....	68
FIGURE 2-3: PROPOSED CONCERTED HYDROLYSIS OF STRICTOSIDINE DEGLYCOSYLATION BY SGD.....	70
FIGURE 2-4: THE STRUCTURES OF 5,6-DIHYDROFLAVOPEREIRINE AND OF D-GLUCONIC ACID DELTA-LACTONE.....	71
FIGURE 2-5: DOLICHANTOSIDE IS DEGLYCOSYLATED BY SGD.....	72
FIGURE 2-6: THE STRUCTURES OF GLUCOSIDES DEACETYLIPECOSIDE, DEACETYLIISOIPECOSIDE, AND CONIFERIN.....	74
FIGURE 2-7: STRUCTURE OF STRICTOSIDINE, WITH THE NUMBERING SYSTEM SHOWN IN BLUE.....	75
FIGURE 2-8: THE STRUCTURES OF STRICTOSIDINE AND INDOLE SUBSTITUTED STRICTOSIDINE ANALOGS.....	77
FIGURE 2-9: THE STRUCTURES OF D ₄ STRICTOSIDINE AND OTHER STRICTOSIDINE ANALOGS.....	79
FIGURE 2-10: REPRESENTATIVE ASSAY USING LCMS.....	80
FIGURE 2-11: REPRESENTATIVE ASSAY USING HPLC.....	80
FIGURE 2-12: STRUCTURES OF 9-AZA STRICTOSIDINE, 12-AZA STRICTOSIDINE, BENZO STRICTOSIDINE, AND THIO STRICTOSIDINE.....	82
FIGURE 2-13: STRUCTURE OF DEACETYLIPECOSIDES.....	83
FIGURE 2-14: STRUCTURES OF VINCOSIDE AND D ₄ VINCOSIDE.....	83
FIGURE 2-15: STRUCTURE OF DES-VINYL STRICTOSIDINE ISOMERS AND ENZYMATICALLY PRODUCED DES-VINYL STRICTOSIDINE ISOMER.....	84
FIGURE 2-16: LCMS TRACE OF THE DES-VINYL STRICTOSIDINE MIXTURE.....	85
FIGURE 2-17: DES-VINYL STRICTOSIDINE MIXTURE SUBJECTED TO DEGLYCOSYLATION BY <i>B. STEAROTHERMOPHILUS</i> α -GLUCOSIDASE.....	87

FIGURE 2-18: STRICTOSIDINE, WITH PINK ARROWS INDICATING POSITIONS AT WHICH STRICTOSIDINE WAS MODIFIED	90
FIGURE 2-19: STRUCTURE OF SGD (GREEN) WITH STRICTOSIDINE (PINK) BOUND IN THE ACTIVE SITE.....	91
FIGURE 2-20: THE CRYSTAL STRUCTURE OF <i>R. SERPENTINA</i> SGD	94
FIGURE 2-21: STRUCTURE OF SWEROSIDE	98
FIGURE 2-22: STRICTOSIDINE IS PRODUCED ENZYMATICALLY WITH STRICTOSIDINE SYNTHASE	99
FIGURE 2-23: THE CHEMICAL REACTION TO FORM STRICTOSIDINE	100
FIGURE 2-24: BENZOFURAN-3-ACETONITRILE AND BENZO(B)THIOPHENE-3-ACETONITRILE ARE REDUCED WITH LiAlH_4 IN THF	102
FIGURE 2-25: DOPAMINE AND SECOLOGANIN CONDENSE IN A NONENZYMATIC REACTION	103
FIGURE 2-26: REPRESENTATIVE UV-VISIBLE TIME COURSES AT 560 NM OF THE GLUCOSE DETECTION ASSAY.....	110
FIGURE 2-27: DATA FIT FOR STEADY STATE KINETIC ANALYSIS OF SGD WITH INDOLE SUBSTITUTED STRICTOSIDINE ANALOGS.....	112
FIGURE 2-28: DATA FIT FOR STEADY STATE KINETIC ANALYSIS OF SGD WITH D_4 VINCOSIDE.	113
FIGURE 3-1: AJMALICINE SYNTHASE IS PROPOSED TO PRODUCE AJMALICINE FROM DEGLYCOSYLATED STRICTOSIDINE AND NADPH	122
FIGURE 3-2: 12-AZA ISOSITSIRIKINE , (5 <i>R</i>)-HYDROXYMETHYL ISOSITSIRIKINE ANALOG, BENZO ISOSITSIRIKINE.....	124
FIGURE 3-3: RESULTS OF A PRECURSOR DIRECTED BIOSYNTHESIS STUDY.....	125
FIGURE 3-4: TETRAHYDROALSTONINE FORMED WHEN DEGLYCOSYLATED STRICTOSIDINE WAS INCUBATED 1:2 WITH NACNBH_3	126
FIGURE 3-5: STRUCTURES OF AJMALICINE, TETRAHYDROALSTONINE, AND 19-EPI-AJMALICINE	127
FIGURE 3-6: STRUCTURES OF GEISSOSCHIZINE AND THE NATURALLY OCCURRING ISOSITSIRIKINE ISOMERS.....	129
FIGURE 3-7: STRUCTURES OF PMSF, EDTA, β -MERCAPTOETHANOL, AND PVP.	130
FIGURE 3-8: EXAMPLES OF RESINS USED IN ANION EXCHANGE CHROMATOGRAPHY AND CATION EXCHANGE CHROMATOGRAPHY.....	133
FIGURE 3-9: STRUCTURE OF REACTIVE RED AGAROSE.....	136
FIGURE 3-10: STRUCTURE OF REACTIVE GREEN AGAROSE.....	136
FIGURE 3-11: STRUCTURE OF CIBACRON BLUE AGAROSE	136
FIGURE 3-12: STRUCTURE OF REACTIVE BROWN AGAROSE	137
FIGURE 3-13: STRUCTURE OF REACTIVE YELLOW AGAROSE	137
FIGURE 3-14: THE ASSAY TO DETECT AJMALICINE SYNTHASE AND ISOSITSIRIKINE SYNTHASE ACTIVITY.....	139
FIGURE 3-15: ENZYMATIC ASSAY OF AJMALICINE SYNTHASE	140
FIGURE 3-16: ENZYMATIC ASSAY OF ISOSITSIRIKINE SYNTHASE.....	141

FIGURE 3-17: A 1D SDS-PAGE OF ACETONE PRECIPITATION FRACTIONS ONE, TWO, AND THREE.....	143
FIGURE 3-18: A 2D SDS-PAGE OF FRACTION THREE OF AN ACETONE PRECIPITATION OF <i>C. ROSEUS</i> LYSATE.	144
FIGURE 3-19: CHROMATOGRAM OF THE THIRD FRACTION OF AN ACETONE PRECIPITATION SUBJECTED TO DEAE CHROMATOGRAPHY....	145
FIGURE 3-20: A 2D SDS-PAGE OF DEAE FRACTIONS B8-9 OF A TYPICAL PURIFICATION PROCEDURE.	147
FIGURE 3-21: CHROMATOGRAM OF THE DEAE B8-9 FRACTIONS SUBJECTED TO SIZE 200 GEL FILTRATION CHROMATOGRAPHY.	149
FIGURE 3-22: A 2D SDS-PAGE OF FRACTIONS C9-12 FROM A SIZE 200 GEL FILTRATION COLUMN.	150
FIGURE 3-23: DESIGN OF PROTEIN PULLDOWN EXPERIMENT WITH SGD.....	156
FIGURE 3-24: INDOLE SUBSTITUTED STRICTOSIDINE ANALOGS	160
FIGURE 3-25: REPRESENTATIVE LCMS CHROMATOGRAMS OF ENZYMATICALLY PRODUCED AJMALICINE AND ISOSITSIRIKINE ANALOGS..	161
FIGURE 3-26: 18,19-DES-VINYL STRICTOSIDINE AGLYCONE IS REDUCED BY NADPH AND A PARTIALLY PURIFIED ENZYME FRACTION	162
FIGURE 3-27: 18,19-DES-VINYL STRICTOSIDINE AGLYCONE ISOMERS ARE COMPLETELY CONVERTED BY THE REDUCTASE ACTIVITY	163
FIGURE 3-28: REDUCTION OF 18,19-DES-VINYL STRICTOSIDINE AGLYCONE ISOMERS.....	164
FIGURE 3-29: D ₄ STRICTOSIDINE IS DEGLYCOSYLATED BY SGD TO FORM DEGLYCOSYLATED D ₄ STRICTOSIDINE.....	165
FIGURE 3-30: D ₄ VINCOSIDE IS DEGLYCOSYLATED BY SGD TO FORM DEGLYCOSYLATED D ₄ VINCOSIDE.	167
FIGURE 3-31: NACNBH ₃ REACTION.	170
FIGURE 3-32: LCMS CHROMATOGRAMS OF NACNBH ₃ REACTION	171
FIGURE 3-33: PROPOSED STRUCTURE OF THE ADDITIONAL REDUCTION PRODUCT	172
FIGURE 3-34: AN ENZYME LIKE CINNAMYL ALCOHOL DEHYDROGENASE COULD POTENTIALLY REDUCE THE IMINIUM OF CATHENAMINE. ...	175
FIGURE 3-35: PRECURSOR DIRECTED BIOSYNTHESIS STUDY.	178
FIGURE 3-36: <i>C. ROSEUS</i> HAIRY ROOT CULTURES.	180
FIGURE 3-37: AJMALICINE ANALOGS AND STANDARDS.....	187
FIGURE 3-38: AJMALICINE ANALOGS AND STANDARDS.....	188
FIGURE 3-39: LCMS CHROMATOGRAMS OF AJMALICINE ANALOGS.	191
FIGURE 3-40: LCMS CHROMATOGRAMS OF ISOSITSIRIKINE ANALOGS.....	192
FIGURE 3-41: DATA FIT FOR THE STEADY STATE KINETIC ANALYSIS OF AJMALICINE SYNTHASE.	194
FIGURE 3-42: DATA FIT FOR THE STEADY STATE KINETIC ANALYSIS OF AJMALICINE SYNTHASE.	195
FIGURE 3-43: DATA FIT FOR THE STEADY STATE KINETIC ANALYSIS OF AJMALICINE SYNTHASE	196

FIGURE 3-44: DATA FIT FOR THE STEADY STATE KINETIC ANALYSIS OF ISOSITSIRIKINE SYNTHASE	197
FIGURE 3-45: SYNTHESIS OF R^3 H-NADPH	199
FIGURE 3-46: RATES OF TRITIATED AJMALICINE FORMATION USING VARIOUS GEL FILTRATION FRACTIONS.....	200
FIGURE 4-1: COMMONLY USED PHOTO-REACTIVE GROUPS IN CROSSLINKING STUDIES	209
FIGURE 4-2: AFFINITY BASED PROTEIN PROFILING	210
FIGURE 4-3: THE STRUCTURES OF RHODAMINE AZIDE AND BIOTIN AZIDE.....	210
FIGURE 4-4: CINNAMYL ALCOHOL DEHYDROGENASES ARE NADPH-DEPENDENT ENZYMES.....	212
FIGURE 4-5: STRUCTURES OF PODOPHYLLOTOXIN, ETOPOSIDE, ETOPOSIDE PHOSPHATE, AND TENIPOSIDE	213
FIGURE 4-6: STRUCTURES OF MATAIRESINOL, SECOISOLARICRESINOL, ENTEROLACTONE, AND ENTERODIOL	213
FIGURE 4-7: CINNAMYL ALCOHOL DEHYDROGENASES ARE ZINC-DEPENDENT.....	214
FIGURE 4-8: STRUCTURES OF COMMON LIGNIN AND LIGNAN PRECURSORS.....	215
FIGURE 4-9: MALATE DEHYDROGENASE CATALYZES REVERSIBLE CONVERSION OF MALATE TO OXALOACETATE	215
FIGURE 4-10: MANNITOL DEHYDROGENASE CATALYZES CONVERSION OF D-MANNITOL TO D-MANNOSE.....	216
FIGURE 4-11: 10-HYDROXY GERANIOL OXIDOREDUCTASE CATALYZES CONVERSION OF 10-HYDROXY GERANIOL TO 10-OXO GERANIOL....	216
FIGURE 4-12: BIOSYNTHESIS OF LOGANIC ACID.....	217
FIGURE 4-13: CROSSLINKING EXPERIMENTS OF <i>C. ROSEUS</i> ENZYMES.....	220
FIGURE 4-14: A 2D SDS-PAGE OF CROSSLINKED ENZYMES USING 11-AZIDO-PENTYNYL-ESTER STRICTOSIDINE	221
FIGURE 4-15: A 2D SDS-PAGE OF CROSSLINKED ENZYMES USING 12-AZIDO-PENTYNYL-ESTER STRICTOSIDINE	221
FIGURE 4-16: SINAPALDEHYDE AND CONIFERYL ALDEHYDE WERE REDUCED BY CR-2141 AND NADPH.....	227
FIGURE 4-17: CINNAMYL ALDEHYDE DERIVATIVES NOT REDUCED BY CR-2141 AND NADPH.	228
FIGURE 4-18: NADPH-DEPENDENT PERAKINE REDUCTASE.....	235
FIGURE 4-19: THE STRUCTURES OF SINAPALDEHYDE AND DEGLYCOSYLATED 11-AZIDO-PENTYNYL-ESTER STRICTOSIDINE	237
FIGURE 4-20: A 1D SDS-PAGE OF PURIFIED CR-2141, CR-12, CR-318, AND CR-611.	240
FIGURE 4-21: A SINAPYL ALCOHOL STANDARD HAS THE SAME LCMS RETENTION TIME AS SINAPYL ALCOHOL PRODUCED IN AN ASSAY....	243
FIGURE 4-22: DATA FIT FOR STEADY STATE KINETICS OF CR-2141 WITH SINAPALDEHYDE.	245
FIGURE 5-1: ASSAY WITH MICROSOMES, SGD, NADPH, AND VARIOUS STRICTOSIDINE ANALOGS.	256
FIGURE 5-2: FOUR POTENTIAL TIAs THAT THE PRODUCT WITH m/z 325 MAY CORRESPOND TO.	257

List of Tables

TABLE 1-1: THE EIGHT SPECIES IN THE GENUS <i>CATHARANTHUS</i>	37
TABLE 1-2: THE ATOMIC RADIUS (Å) OF HYDROGEN AND HALOGEN ATOMS.....	43
TABLE 2-1: KINETIC DATA AND HILL COEFFICIENTS OF THE INDOLE SUBSTITUTED STRICTOSIDINE ANALOGS DEGLYCOSYLATED BY SGD.	89
TABLE 2-2: KINETIC DATA FOR D ₄ VINCOSIDE DEGLYCOSYLATION BY SGD.	90
TABLE 3-1: THE SPECIFIC ACTIVITIES OF AJMALICINE SYNTHASE AND ISOSITSIRIKINE SYNTHASE.....	143
TABLE 3-2: AJMALICINE SYNTHASE SPECIFIC ACTIVITY AND ISOSITSIRIKINE SYNTHASE SPECIFIC ACTIVITY OF EACH DEAE FRACTION.....	146
TABLE 3-3: AJMALICINE SYNTHASE SPECIFIC ACTIVITY AND ISOSITSIRIKINE SYNTHASE SPECIFIC ACTIVITY OF EACH SIZE 200 GEL FILTRATION FPLC FRACTION.....	149
TABLE 3-4: TABLE OF <i>C. ROSEUS</i> ESTS.....	150
TABLE 3-5: AJMALICINE SYNTHASE SPECIFIC ACTIVITY FOR THE FRACTIONS FROM A REACTIVE RED AGAROSE COLUMN.....	152
TABLE 3-6: AJMALICINE SYNTHASE SPECIFIC ACTIVITY FOR THE FRACTIONS FROM A REACTIVE RED AGAROSE COLUMN.....	152
TABLE 3-7: AJMALICINE SYNTHASE SPECIFIC ACTIVITY FOR THE FRACTIONS FROM A REACTIVE GREEN AGAROSE COLUMN.....	153
TABLE 3-8: AJMALICINE SYNTHASE SPECIFIC ACTIVITY FOR EACH FRACTION USING REACTIVE BROWN AGAROSE, CIBACRON BLUE AGAROSE, AND REACTIVE YELLOW AGAROSE.	153
TABLE 3-9: INDOLE SUBSTITUTED STRICTOSIDINES THAT FORMED THE CORRESPONDING AJMALICINE AND ISOSITSIRIKINE ANALOGS.	160
TABLE 3-10: THE STEADY STATE KINETIC DATA OF PARTIALLY PURIFIED AJMALICINE SYNTHASE.....	165
TABLE 3-11: STEADY STATE KINETIC DATA OF PARTIALLY PURIFIED AJMALICINE SYNTHASE.	166
TABLE 3-12: STEADY STATE KINETIC DATA OF PARTIALLY PURIFIED AJMALICINE SYNTHASE.	168
TABLE 3-13: STEADY STATE KINETIC DATA OF PARTIALLY PURIFIED ISOSITSIRIKINE SYNTHASE.....	169
TABLE 3-14: TRITIATED NADPH ASSAY USING VARIOUS GEL FILTRATION FRACTIONS.	201
TABLE 4-1: PROTEIN CANDIDATES 1-16 SEQUENCED FROM THE 2D SDS-PAGE	224
TABLE 4-2: BLAST RESULTS OF CR-2141.	226
TABLE 4-3: STEADY STATE KINETIC VALUES FOR SINAPALDEHYDE NADPH-DEPENDENT REDUCTION BY CR-2141.....	229
TABLE 4-4: BLAST RESULTS OF CR-12. THE 10 PROTEINS WITH THE HIGHEST SEQUENCE IDENTITY TO CR-12 ARE SHOWN	230
TABLE 4-5: BLAST RESULTS OF CR-318; THE 10 ENZYMES WITH THE HIGHEST SEQUENCE IDENTITY TO CR-318 ARE SHOWN.	232

TABLE 4-6: BLAST RESULTS OF CR-611; THE 10 ENZYMES WITH THE HIGHEST SEQUENCE IDENTITY TO CR-611 ARE SHOWN233

TABLE 4-7: SENSE AND ANTISENSE PRIMERS USED TO CLONE CR-2141, CR-12, CR-318, AND CR-611.239

List of Abbreviations

1D: one dimensional
2D: two dimensional
A. thaliana: *Arabidopsis thaliana*
ADP: adenosine diphosphate
ATP: adenosine triphosphate
BLAST: Basic Local Alignment Search Tool
Br: bromo
C. roseus: *Catharanthus roseus*
cDNA: complementary DNA
CHCl₃: chloroform
Cl: chloro
CuSO₄: copper sulfate
DCM: dichloromethane
DEAE: diethylaminoethane
DMF: dimethylformamide
DMSO: dimethylsulfoxide
EDTA: ethylenediaminetetraacetic acid
ER: endoplasmic reticulum
EST: expressed sequence tag
Et: ethyl
EtOAc: ethyl acetate
F: fluoro
FeSO₄: iron(II) sulfate
FPLC: fast performance liquid chromatography
Glc: glucose
HPLC: high performance liquid chromatography
IEF: isoelectric focusing
IPTG: isopropyl-β-D-thiogalactopyranoside
Katal: SI unit of catalytic activity
KCl: potassium chloride
K_m: Michaelis constant
LCMS: liquid chromatography mass spectrometry
MBP: maltose binding protein
Me: methyl
MeO: methoxy
MeOH: methanol
MgCl₂: magnesium chloride
MgSO₄: magnesium sulfate
MnSO₄: manganese sulfate
NaCl: sodium chloride
Na₂SO₄: sodium sulfate
PAGE: polyacrylamide gel electrophoresis
PMSF: phenylmethanesulfonyl fluoride
NaCNBH₃: sodium cyanoborohydride

NADH: nicotinamide adenine dinucleotide
NADPH: nicotinamide adenine dinucleotide phosphate
NMR: nuclear magnetic resonance
PVP: polyvinylpyrrolidone
R. serpentina: *Rauvolfia serpentina*
R_f: ratio to front
rpm: rotations per minute
r.t.: room temperature
SAM: S-adenosyl-L-methionine
SDS: sodium dodecyl sulfate
SDS-PAGE: sodium dodecyl sulfate polyacrylamide gel electrophoresis
SGD: strictosidine-β-glucosidase
STS: strictosidine synthase
*t*BuOH: *tert*-butanol
TCEP: tris(2-carboxyethyl)phosphine
TFA: trifluoroacetic acid
THF: tetrahydrofuran
TIA: terpene indole alkaloid
TLC: thin layer chromatography
Tris: tris(hydroxymethyl)aminomethane
VIGS: virus-induced gene silencing
V_{max}: maximum velocity
VT: variable temperature

Chapter 1: Introduction

- I. Structure and pharmacological uses of monoterpene indole alkaloids (TIAs)
- II. Biosynthesis of TIAs
- III. TIAs in *Catharanthus* tissue
- IV. Potential pharmacological properties of novel TIAs
- V. Cloned TIA enzymes
- VI. Substrate specificity of TIA enzymes and precursor directed biosynthesis studies
- VII. Thesis overview

I. Structure and pharmacological uses of monoterpene indole alkaloids (TIAs)

Monoterpene indole alkaloids (TIAs) are a group of secondary metabolites produced by plants that all derive from the same precursor, strictosidine **1** (Figure 1-1). There are over 2,000 TIAs, many of which have medicinal properties (Figure 1-1)¹. For example, vinblastine **2** and vincristine **3** have anti-cancer activity², ajmalicine **4** has anti-hypertensive activity³, and serpentine **5** has type II topoisomerase inhibition activity⁴. Yohimbine **6** has α_2 adrenoreceptor antagonist activity⁵, isositsirikine **7** has anti-neoplastic activity⁶, quinine **8** has anti-malarial activity⁷, ajmaline **9** has anti-arrhythmic activity⁸, and camptothecin **10** has anti-tumor activity^{1,9}.

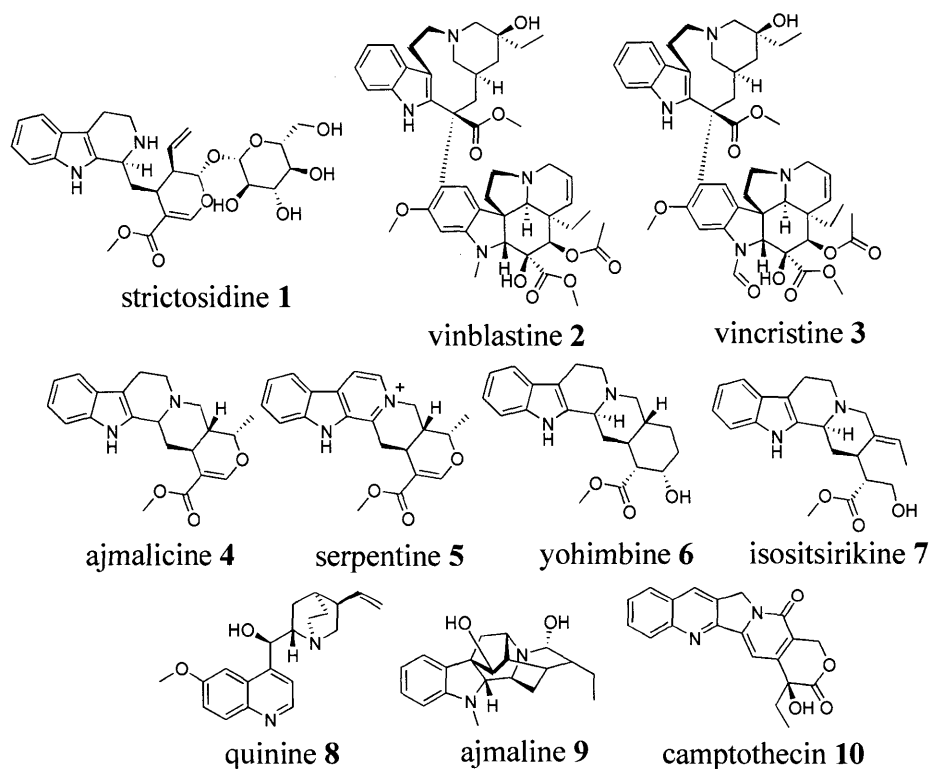


Figure 1-1: Structures of the monoterpene indole alkaloids strictosidine **1**, vinblastine **2**, vincristine **3**, ajmalicine **4**, serpentine **5**, yohimbine **6**, isositsirikine **7**, quinine **8**, ajmaline **9**, and camptothecin **10**¹.

Vinblastine **2** and vincristine **3** (Figure 1-1), which are produced by the pantropical plant *Catharanthus roseus* (Madagascar periwinkle), were discovered in the late 1950s by Dr. Robert Noble and Dr. Charles Beer. Dr. Noble had been given 25 Madagascar periwinkle leaves by his brother, who had received the leaves from a patient claiming that the leaves were popular in Jamaica for treating diabetes. Noble tested the leaves for anti-diabetic activity by crushing the dried leaves and brewing them as a tea. After having rats consume the tea, Noble tested their blood and did not find any changes in sugar levels, but he noticed that that leaves reduced the number of white blood cells. With the assistance of Beer, Noble was able to isolate the compound responsible for the reduction of white blood cells, and named the compound “vinblastine.” Noble and Beer then began clinical tests with vinblastine **2** on patients with lymphoid cancer. When vinblastine **2** was shown to have anti-cancer activity, Eli Lilly began to produce vinblastine **2** for clinical use^{2,10}. Vinblastine **2** has been produced under the names Velban®, Velsar®, and vincalukoblastine, and currently it is used in the treatment of breast cancer, testicular cancer, non-Hodgkin lymphomas, and Hodgkin’s disease^{2,10}. Vinblastine **2** is produced in the plant by the coupling of two TIAs, catharanthine and vindoline¹ (Figure 1-2).

Noble and Beer isolated an oxidized form of vinblastine **2**, named vincristine **3**, that also had anti-cancer activity. Vincristine **3** differs from vinblastine **2** in that the methyl group on N-1 of vinblastine **2** is oxidized to an aldehyde (Figure 1-2). Vincristine **3** was introduced to the clinic in 1963 and has been produced under the names leurocristine, Oncovin®, Vincasar PFS®, and Vincrex®². Vincristine **3** has proven effective against a slightly different spectrum of cancers than vinblastine **2**, and is used to treat acute leukemia, childhood leukemias, neuroblastomas, rhabdomyosarcomas, Hodgkin’s disease, and other lymphomas¹⁰.

The anti-neoplastic activity of vinblastine **2** and vincristine **3** comes from their propensity to bind to tubulin, preventing the formation of microtubules. This disruption causes dissolution of mitotic spindles, leading to metaphase arrest in dividing cells. Cells accumulate in metaphase, and this accumulation triggers cell death^{2,10}. Vinblastine **2** and vincristine **3** are often used in combination chemotherapy with DNA-alkylating drugs because action on the tubulin protein does not interfere with the action of the DNA-alkylating drugs.

A number of semi-synthetic derivatives of vinblastine **2** and vincristine **3** have been synthesized and developed as chemotherapy drugs. These include, for example, vinorelbine **11** (Navelbine®) (Figure 1-2) which was discovered in the mid-1990s by the Pierre Fabre Company and is used as an anti-mitotic chemotherapy drug against breast cancers, testicular cancers, epithelial ovarian cancers, and non-small-cell lung cancers^{2,10}. Vinorelbine **11** differs in structure from vinblastine **2** in that it contains only one methylene between the N-6' and C-9' of the catharanthine moiety, has a double bond between C-3' and C-4', and lacks a hydroxyl group at C-4' (Figure 1-2).^{2,11} Vindesine **12** (Eldesine®, Fildesin®) is another example of a semi-synthetic derivative that is currently used in chemotherapy treatments to treat lung cancer, breast cancer, melanoma, lymphoma, and leukemia¹¹. Vindesine **12** differs in structure from vinblastine **2** by having an amide instead of a methyl ester at C-3, and by having a hydroxyl instead of an acetyl group at C-4 (Figure 1-2)^{11,12}.

Vinflunine **13** (Figure 1-2) is a semi-synthetic derivative currently in late-stage clinical trials in Europe. Vinflunine **13** is obtained from vinorelbine **11** by using superacid chemistry (HF-SbF₅) to reduce the double bond between C-3' and C-4' and to introduce two fluorine atoms¹³. In clinical trials vinflunine **13** has shown less cross-resistance in multidrug-resistant

tumor cell lines than vinblastine **2**, vincristine **3**, and vinorelbine **11** have. Other halogenated derivatives have since been synthesized and are currently being tested^{2,11}.

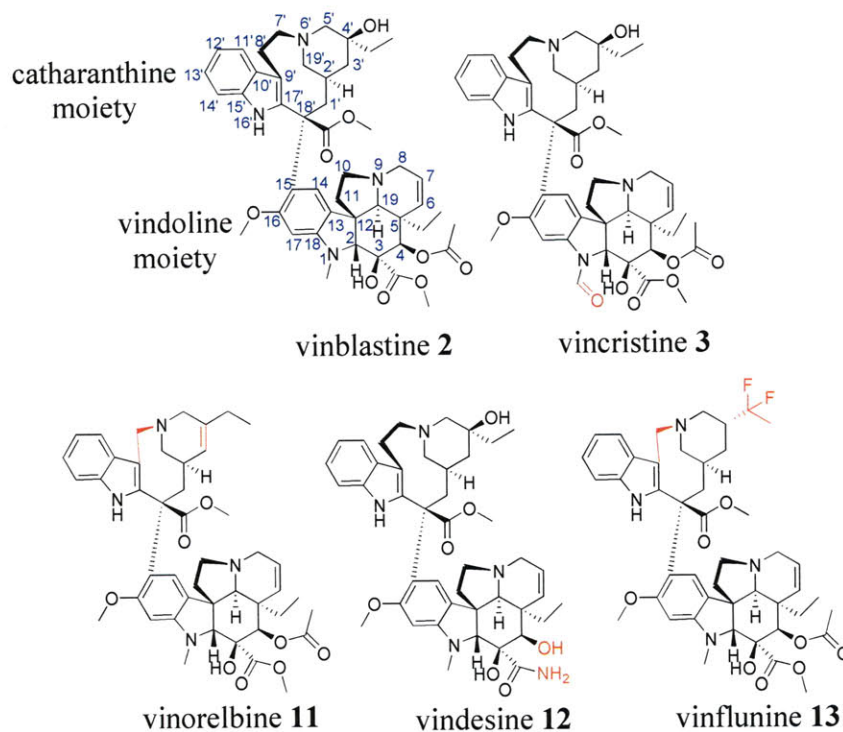


Figure 1-2: The structure and numbering system (in blue) of vinblastine **2**, which is derived from catharanthine and vindoline¹². The structures of vinorelbine **11**, vindesine **12**, and vinflunine **13** are also shown, with the moieties that differ from that of vinblastine **2** in red¹¹.

Ajmalicine **4** (Figure 1-1, Figure 1-3) is another TIA produced by *C. roseus*. Ajmalicine **4** was first used in 1957 for the treatment of hypertension. It has been marketed under the names Hydroserpan®, Lamuran®, and raubasine. When used clinically, ajmalicine **4** is often combined with a synthetic compound called almitrine **14** (Figure 1-3); this combination is called Duxil®. Duxil® is used clinically in France to treat age-related cerebral disorders and for functional rehabilitation after stroke^{3,14-16}. No ajmalicine **4** analogs have been reported or investigated as potential therapeutics.

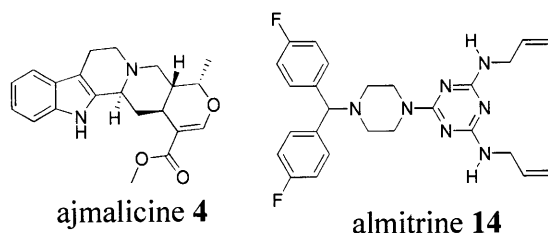


Figure 1-3: Structures of ajmalicine **4** and almitrine **14**¹⁴.

Serpentine **5**, yohimbine **6**, and isositsirikine **7** are also produced by *C. roseus* (Figure 1-4). Serpentine **5**, which is hypothesized to be produced via a peroxidase-catalyzed oxidation of ajmalicine **4**, is a type II topoisomerase inhibitor^{1,4}. Yohimbine **6** acts as an α_2 adrenoceptor antagonist and has potential clinical applications in erectile dysfunction^{1,5,17}, and isositsirikine **7** has anti-neoplastic activity⁶.

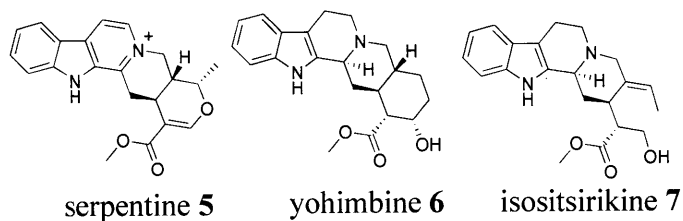


Figure 1-4: Structures of serpentine **5**, yohimbine **6**, and isositsirikine **7**.

Quinine **8** (Figure 1-1), isolated from the bark of the Cinchona tree, is most famous for its anti-malarial activity. It is believed that quinine **8** acts as an anti-malarial agent by inhibiting heme polymerase, which causes cytotoxic free heme to accumulate in the parasite. Quinine **8** also has anti-pyretic, anti-inflammatory, and analgesic activity, and is used to treat lupus and arthritis. It was the most widely used drug to treat malaria until 1944, when it was replaced by another drug, chloroquine. Quinine **8** is still used occasionally, however, because resistance has developed to chloroquine⁷.

Ajmaline **9** (Figure 1-1) is produced by the plant *Rauvolfia serpentina*¹. Ajmaline **9** is an anti-arrhythmic drug that has potent sodium channel-blocking properties. The short half life of ajmaline **9** makes ajmaline **9** a useful drug for acute intravenous treatments. Ajmaline **9** has been used to treat atrial fibrillation in patients with Wolff-Parkinson-White syndrome⁸.

Camptothecin **10** (Figure 1-1) is a topoisomerase I inhibitor that is isolated from the bark and stems of the Chinese “happy tree” *Camptotheca acuminata*, and is also produced by the plant *Ophiorrhiza pumila*¹. Although camptothecin **10** showed anti-cancer activity in clinical trials in the late 1960s, its severe toxicity prevented camptothecin **10** from being prescribed. Another drawback of camptothecin **10** is its poor water solubility, which makes drug delivery difficult. Numerous derivatives of camptothecin **10** were developed to overcome these drawbacks. Two clinically successful, water-soluble synthetic derivatives are topotecan **15** and irinotecan **16** (Figure 1-5). Topotecan **15** is used to treat lung cancer and ovarian cancer, while irinotecan **16** is primarily used to treat colon cancer⁹.

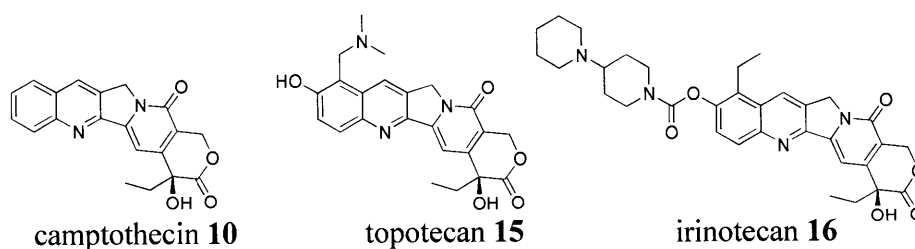


Figure 1-5: Structures of camptothecin **10**, topotecan **15**, and irinotecan **16**⁹.

II. Biosynthesis of TIAs

All TIAs are derived from a central intermediate called strictosidine **1**. Strictosidine **1** is formed by a stereoselective Pictet-Spengler condensation of the iridoid terpene secologanin **17** and tryptamine **18** catalyzed by the enzyme strictosidine synthase (Figure 1-6)¹.

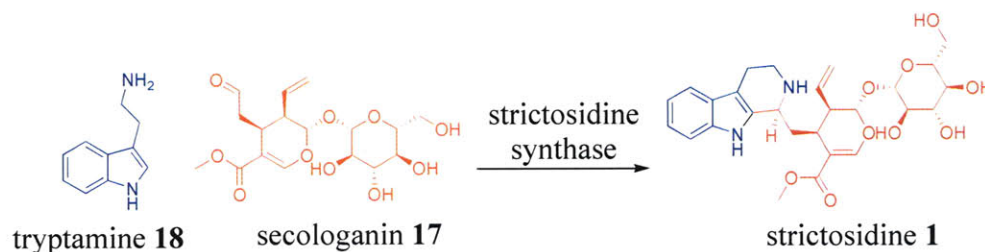


Figure 1-6: Structures of tryptamine **18**, secologanin **17**, and strictosidine **1**. Tryptamine **18** and secologanin **17** condense in a reaction catalyzed by strictosidine synthase to form strictosidine **1**¹.

The biosynthetic pathway for secologanin **17** has not been fully elucidated, and there are numerous proposed intermediates that remain uncharacterized. The mechanisms of the subcellular trafficking of biosynthetic intermediates in TIA biosynthesis also remain largely unknown¹. Secologanin **17** biosynthesis begins in the plastid¹. The precursor for all terpenoids, 3-isopentenyl pyrophosphate **19** (IPP) can be produced by either the mevalonate pathway (Figure 1-7)¹⁸ or the non-mevalonate pathway, which is also called the triose phosphate/pyruvate pathway^{18,19} (Figure 1-8). Feeding studies utilizing ¹³C glucose have shown that the triose phosphate/pyruvate pathway is most likely the pathway utilized to produce IPP for secologanin **17** biosynthesis. Once produced, IPP is converted to dimethylallyl pyrophosphate **20** (DMAPP)¹⁹.

In the mevalonate pathway (Figure 1-7), the primary hydroxyl of (*R*)-mevalonate is phosphorylated twice, and the tertiary hydroxyl is also phosphorylated. Decarboxylation then

occurs, expelling the phosphate on the tertiary hydroxyl. The simultaneous decarboxylation and phosphate expulsion produces IPP **19**, which is isomerized by isopentenyl pyrophosphate isomerase to produce DMAPP **20**¹⁸.

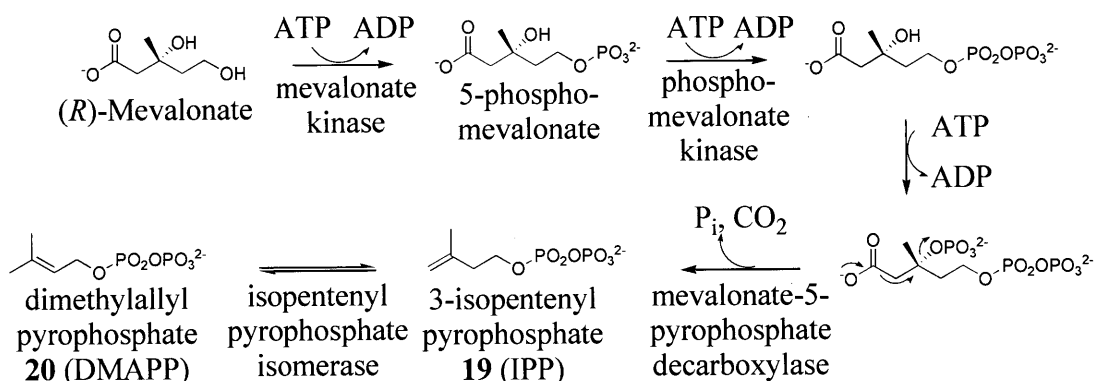


Figure 1-7: In the mevalonate pathway, dimethylallyl pyrophosphate **20** (DMAPP) is formed from (*R*)-mevalonate¹⁸.

In the non-mevalonate pathway, or triose phosphate/pyruvate pathway (Figure 1-8), 1-deoxy-D-xylulose-5-phosphate (DXP) first undergoes a rearrangement of the carbon skeleton of the molecule. Next the carbonyl group is reduced to an alcohol by NADPH and DXP reductase, forming 2-C-methylerythritol-4-phosphate (MEP). MEP then reacts with cytidine triphosphate (CTP) to form 4-diphosphocytidyl-2-C-methylerythritol (CDP-ME). CDP-ME is then phosphorylated to form 4-diphosphocytidyl-2-C-methylerythritol-2-phosphate (CDP-MEP). A cyclization reaction then occurs, forming 2-C-methylerythritol-2,4-cyclopyrophosphate (MEcPP). The intermediates and mechanisms involved in the conversion of MEcPP to 3-isopentenyl pyrophosphate **19** (IPP) are largely unknown, though it is proposed that radical reactions mediated by enzymes containing iron-sulfur clusters are involved. Once formed, IPP **19** is converted to dimethylallyl pyrophosphate **20** (DMAPP) by isopentenyl pyrophosphate isomerase¹⁸.

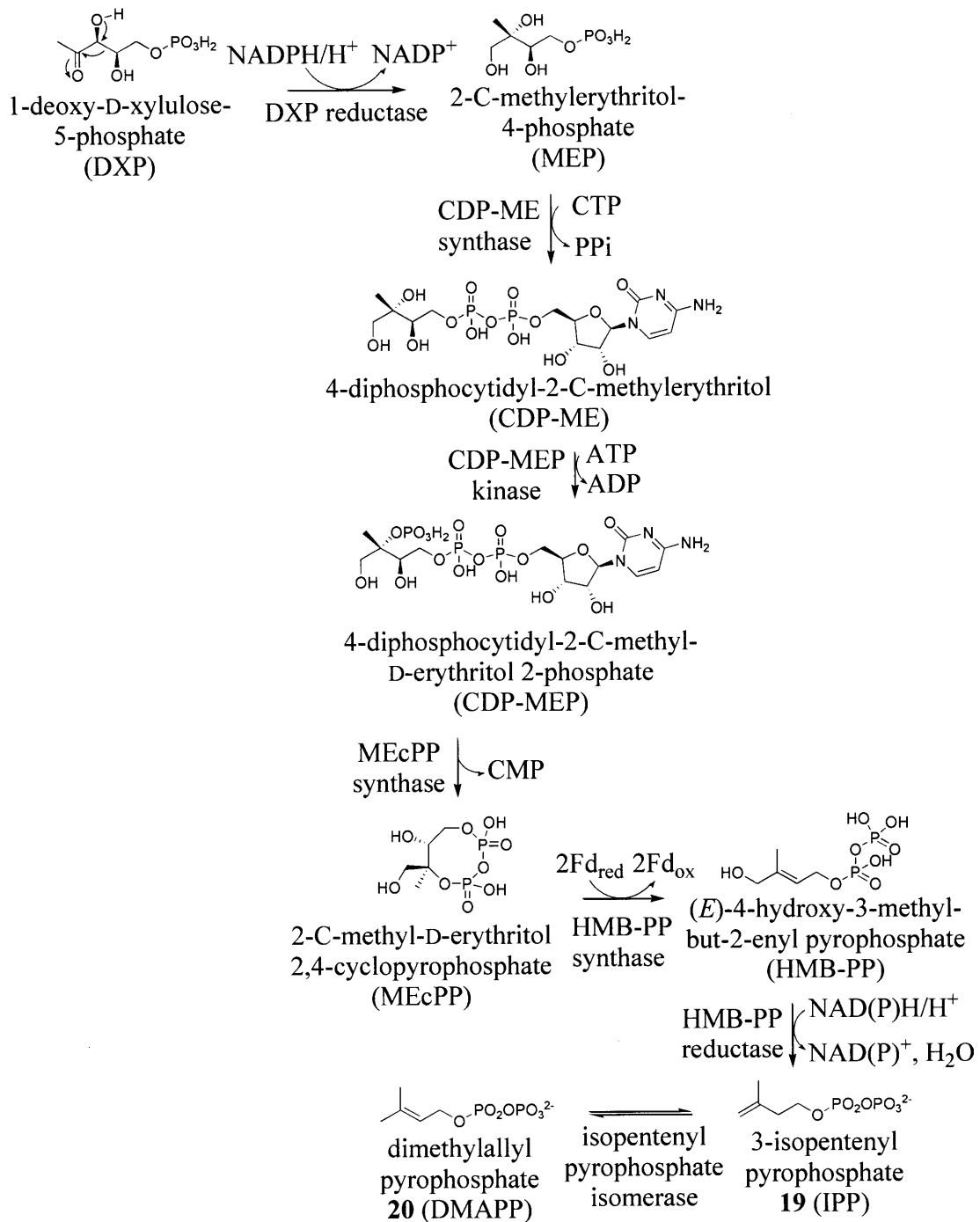


Figure 1-8: The non-mevalonate, or triose pyruvate/phosphate, pathway^{18,19}. “Fd” is an abbreviation for ferredoxin.

One unit of DMAPP **20** and one unit of IPP **19** then condense to form geraniol pyrophosphate **21** via a monoterpene synthase (Figure 1-9). Upon loss of the diphosphate, geraniol **22** is formed, which is then exported to the cytosol¹. The hydroxylation of geraniol **22** by the P450 vacuolar membrane-bound geraniol-10-hydroxylase (G10H) is the first committed step of iridoid terpene biosynthesis^{20,21}. The resulting 10-hydroxy geraniol **23** then undergoes a series of oxidations and cyclizations by yet-unidentified enzymes in the vacuole to form iridotrial **24** (Figure 1-10, Figure 1-15)^{1,22}.

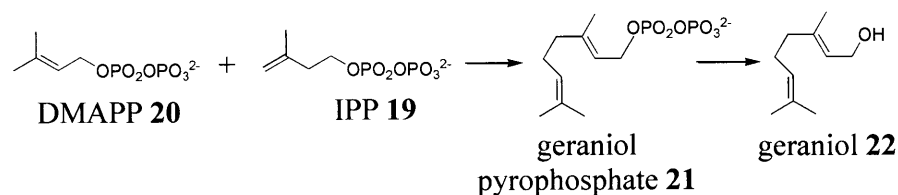


Figure 1-9: Formation of geraniol pyrophosphate **21** from one unit of dimethylallyl pyrophosphate **20** (DMAPP) and one unit of 3-isopentenyl pyrophosphate **19** (IPP)¹. Upon loss of the diphosphate, geraniol **22** is formed.

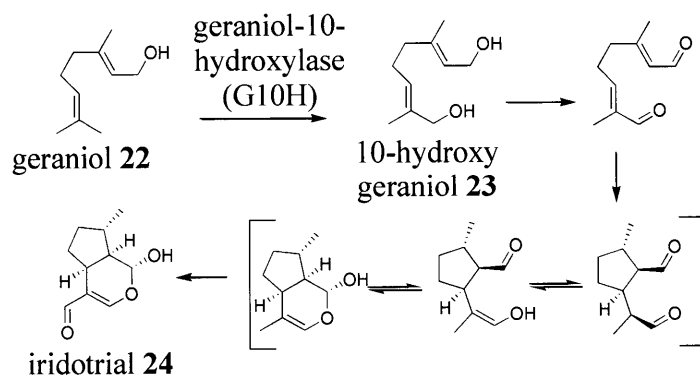


Figure 1-10: Proposed mechanism of formation of iridotrial **24** from geraniol **22**^{1,22}.

Iridotrial **24** is then oxidized, glycosylated, and esterified to form deoxyloganin¹, which is then hydroxylated to form loganin **25**. In what some have proposed to be the rate-limiting step in

indole alkaloid biosynthesis, the endomembrane-associated P450 oxidase enzyme secologanin synthase (SLS) converts loganin **25** to secologanin **17** (Figure 1-11, Figure 1-15).

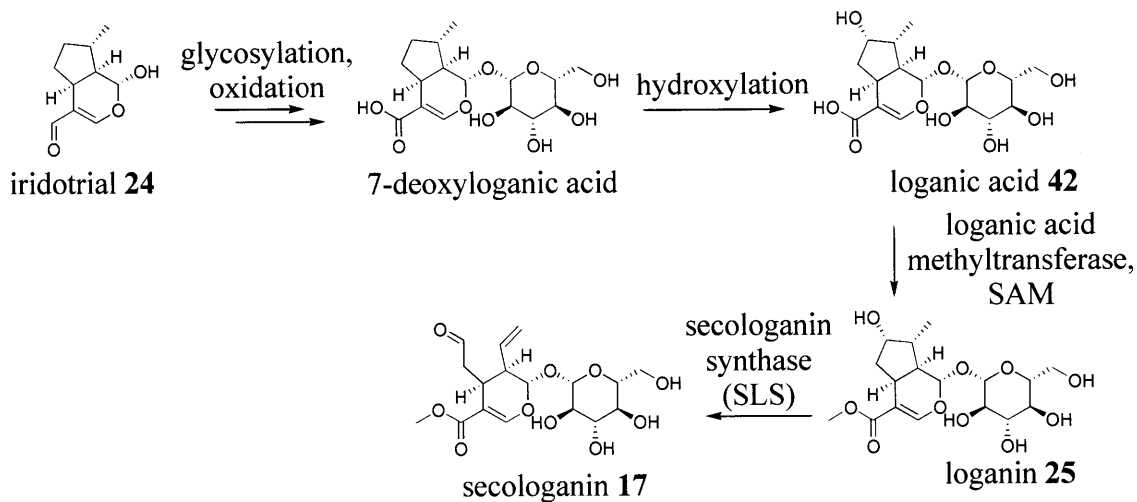


Figure 1-11: Formation of secologanin **17** from iridotrial **24**¹.

Tryptamine **18**, which reacts with secologanin **17** and strictosidine synthase to form the central intermediate strictosidine **1**, is derived from L-tryptophan **26**, which is produced by the shikimate pathway (Figure 1-12). Chorismate, the precursor of tryptophan, is converted to anthranilate by anthranilate synthase. A series of four enzymes – anthranilate phosphoribosyltransferase, *N*-(5'-phosphoribosyl) anthranilate isomerase, indole-3-glycerol phosphate synthase, and the α unit of tryptophan synthase – convert anthranilate to indole, which is converted to L-tryptophan **26** by tryptophan synthase^{23,24}.

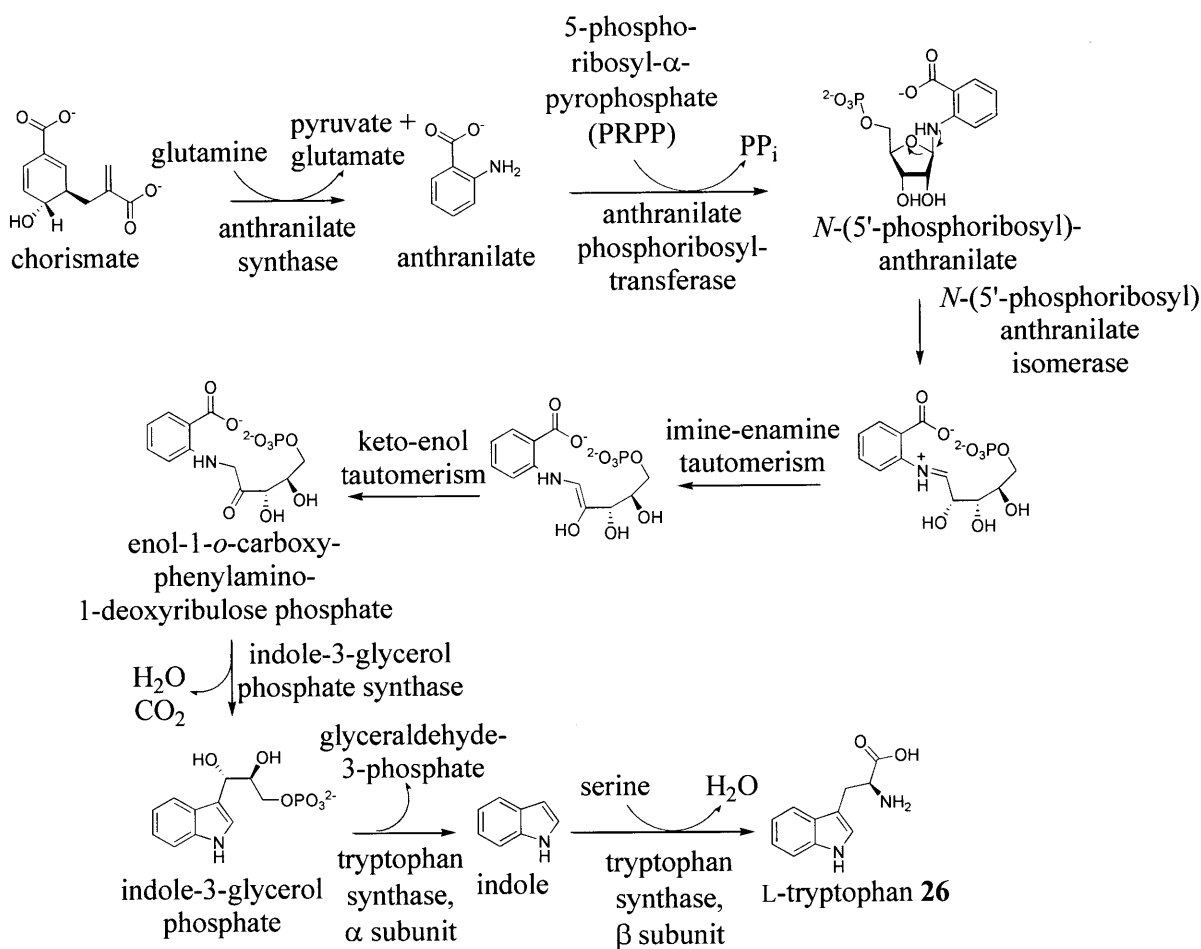


Figure 1-12: Biosynthesis of L-tryptophan **26** from chorismate^{23,24}.

L-tryptophan **26** is decarboxylated by the pyridoxal-dependent cytosolic enzyme tryptophan decarboxylase (TDC) to form tryptamine **18**, which is then transported into the vacuole (Figure 1-15)¹. Tryptamine **18** and secologanin **17** undergo a stereoselective Pictet-Spengler condensation (Figure 1-13) catalyzed by the enzyme strictosidine synthase. The resulting product, strictosidine **1**, has *S* stereochemistry at the C-3 position (Figure 1-15)¹.

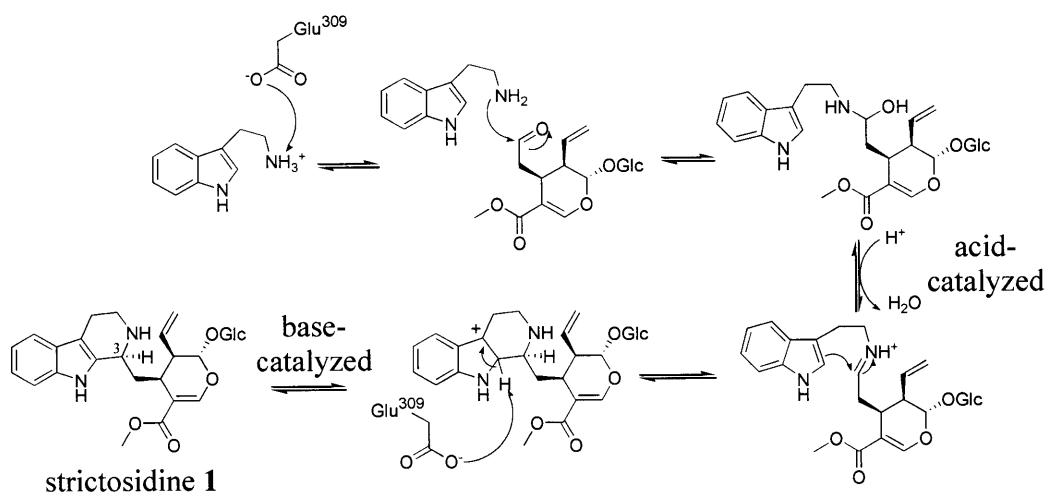


Figure 1-13: The proposed mechanism of strictosidine synthase. With strictosidine synthase, tryptamine **18** and secologanin **17** undergo a stereoselective Pictet-Spengler condensation to form strictosidine **1**¹. The C-3 position of strictosidine **1** is shown in blue. “Glc” is an abbreviation for β -glucose.

Strictosidine **1** is the central intermediate for biosynthesis of all TIAs. Strictosidine **1** is exported out of the vacuole into the cytosol, where it is then deglycosylated by the enzyme strictosidine- β -glucosidase (SGD)². SGD is a soluble enzyme associated with the endoplasmic reticulum membrane but is still accessible from the cytosol¹. Upon deglycosylation, strictosidine **1** is converted to a reactive hemiacetal intermediate (Figure 1-14, Figure 1-15). This hemiacetal is then channeled into a number of biosynthetic pathway branches that lead to hundreds of different TIAs. The reactive hemiacetal intermediate can rearrange in numerous ways, resulting in a variety of alkaloid structures. These structural frameworks are further functionalized, thereby leading to hundreds of different alkaloids (Figure 1-16). The majority of the enzymes occurring downstream of strictosidine synthase and SGD are unknown, and the mechanisms that control which alkaloids are produced at which levels are also unknown¹.

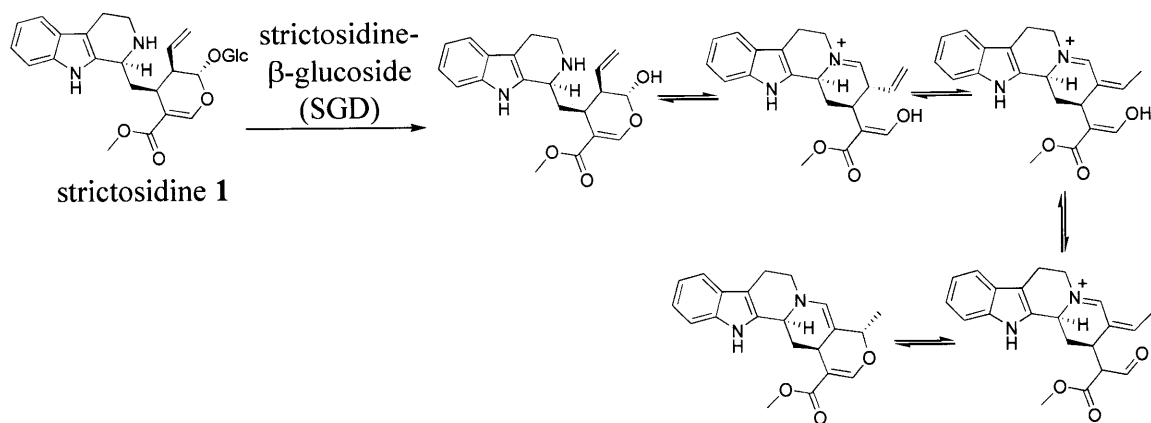


Figure 1-14: Upon deglycosylation by SGD, strictosidine **1** converts to a reactive hemiacetal that interconverts between various isomers.

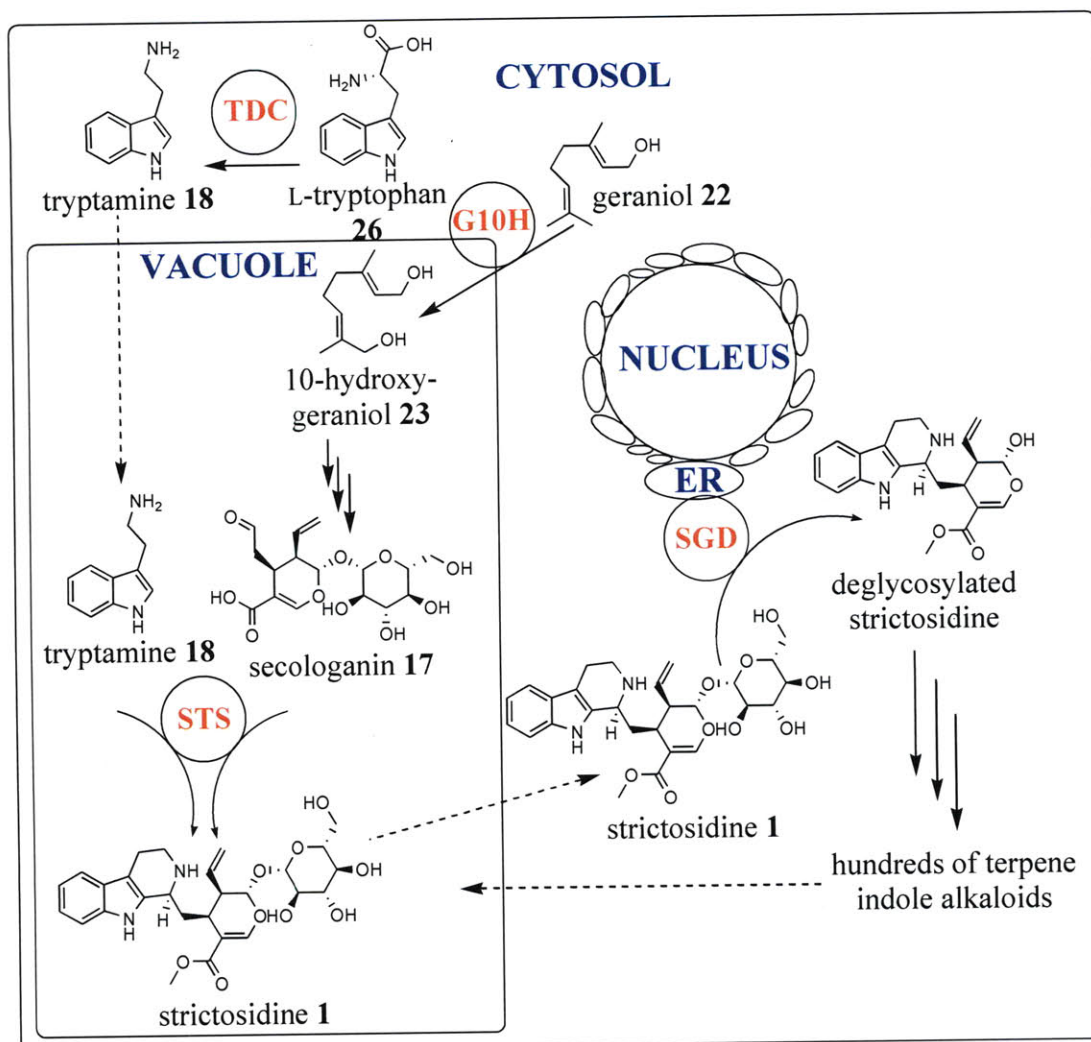


Figure 1-15: In TIA biosynthesis, L-tryptophan **26** is decarboxylated by the cytosolic enzyme tryptophan decarboxylase (TDC) to produce tryptamine **18**, which then enters the vacuole. Geraniol **22** is hydroxylated by the vacuolar membrane protein geraniol-10-hydroxylase (G10H) to form 10-hydroxy geraniol **23**, which undergoes a series of enzymatic steps to form secologanin **17**. Secologanin **17** and tryptamine **18** produce strictosidine **1** in a stereospecific Pictet-Spengler condensation catalyzed by strictosidine synthase (STS). Strictosidine **1** is then exported to the cytosol, where it is deglycosylated by SGD, which is associated with the endoplasmic reticulum (ER). Deglycosylated strictosidine is then channeled into different

biosynthetic pathways that lead to hundreds of different TIAs that are typically stored in the vacuole.

The Apocynaceae, Loganiaceae, Nyssaceae, and Rubiaceae families of plants all produce TIAs. Three different groups of TIAs produced by *C. roseus* – the corynanthe group, the aspidosperma group, and the iboga group – each have representative members that are used medicinally. Each of these structural classes is derived from strictosidine **1** (Figure 1-14, Figure 1-16). Corynanthe TIAs produced in *C. roseus* include ajmalicine **4**, serpentine **5**, yohimbine **6**, and isositsirikine **7**. Aspidosperma alkaloids include tabersonine **27** and vindoline **28**, and iboga alkaloids include catharanthine **29**. Via the action of a peroxidase, catharanthine **29** and vindoline **28** dimerize to form the anti-cancer agent vinblastine **2** (Figure 1-16)^{1,25}.

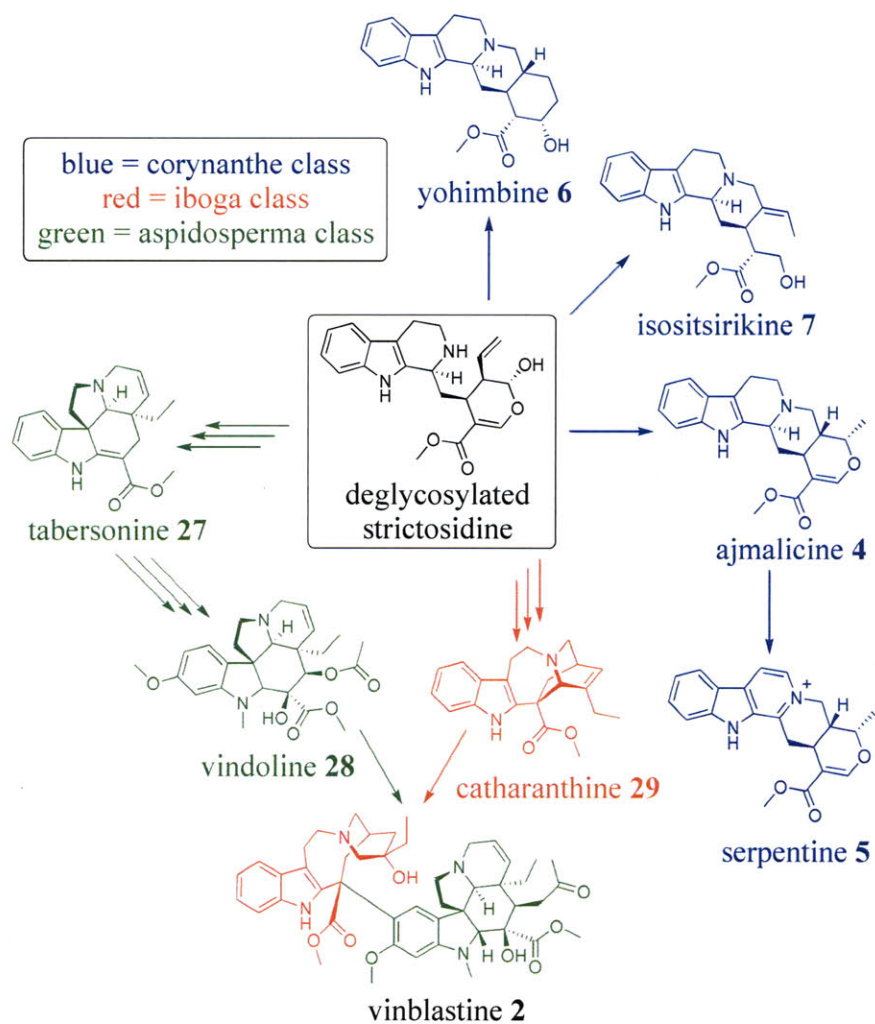


Figure 1-16: The three main branches in TIA biosynthesis in *C. roseus*. Ajmalicine 4, serpentine 5, yohimbine 6, and isositsirikine 7 from the corynanthe class are shown in blue, catharanthine 29 from the iboga class is shown in red, and tabersonine 27 and vindoline 28 from the aspidosperma class are shown in green. Vinblastine 2 is produced by the dimerization of catharanthine 29 and vindoline 28¹. All alkaloids shown derive from the strictosidine- β -glucosidase (SGD)-catalyzed deglycosylation of strictosidine 1, the central intermediate in TIA biosynthesis.

III. TIAs in *Catharanthus tissue*

Catharanthus, which belongs to the family Apocynaceae, is a genus of eight species (Table 1-1), seven of which are endemic to Madagascar. The eighth species, *Catharanthus pusillus*, is native to the Indian subcontinent. Some species of *Catharanthus* are woody, perennial shrubs that grow to heights of approximately 80 centimeters, but the more common varieties are small, cultivated ornamental plants (Figure 1-17). The flowers can be many different colors, such as red, dark red, peach, and white. *Catharanthus roseus* is also known as *Vinca rosea* and *Lochnera rosea*, as well as the common names “Old maid,” Vinca, and periwinkle¹⁴.

Members of <i>Catharanthus</i> genus	Representative alkaloids
<i>C. coriaceus</i>	none reported
<i>C. lanceus</i>	apparicine, catharine ²⁶
<i>C. longifolius</i>	cathafoline ²⁷
<i>C. ovalis</i>	vindorosine, cathovaline ²⁸
<i>C. roseus</i>	vinblastine, ajmalicine ¹
<i>C. scitulus</i>	none reported
<i>C. trichophyllus</i>	vincaleukoblastine, periformyline ²⁹
<i>C. pusillus</i>	leurosine, lochnerinine ^{30,31}

Table 1-1: The eight species in the genus *Catharanthus*, and representative alkaloids from each species, if applicable. All except for *C. pusillus* are endemic to Madagascar³².



Figure 1-17: Pictures of the “rosy” (left) and “little bright eyes” (right) varieties of *Catharanthus roseus*^{32,33}.

C. roseus has been widely studied in part because of the large number of medicinal natural products it produces. Unfortunately, many of these products are produced at low levels in the plant. To isolate one gram of vinblastine **2**, for example, approximately 500 kilograms of dried *C. roseus* leaves are needed². Also, because many different alkaloids are present in the plant, the isolation and purification of a particular alkaloid can be prohibitively difficult and expensive. The vast majority of the TIAs are structurally complex, containing numerous stereocenters, thus making industrial-scale synthesis difficult and expensive.

Three types of *C. roseus* tissue commonly used to produce TIAs are plants (both seedlings and mature plants), hairy root cultures, and cell suspension cultures (Figure 1-18). Seedlings and plants produce a greater variety of TIAs than hairy root and cell suspension cultures do, yet typically they grow more slowly and produce TIAs in lower quantities than hairy root and cell suspension cultures^{2,34}. Seedlings can also produce vindoline **28**, the precursor to the anti-cancer TIAs vinblastine **2** and vincristine **3**, whereas hairy root cultures and cell suspension cultures cannot³⁴.



seedlings



hairy root culture



cell suspension culture

Figure 1-18: *C. roseus* seedlings, hairy root culture, and cell suspension culture^{35,36}.

TIAs are also produced by hairy root cultures (Figure 1-18), a type of tissue that results upon infection of *C. roseus* seedlings with *Agrobacterium rhizogenes*^{35,37}. Hairy root tissues are

convenient to work with since the tissues can be continuously propagated, exhibit biochemical and genetic stability, and produce a diverse array of TIAs. The major alkaloids produced by hairy roots are ajmalicine **4**, serpentine **5**, catharanthine **29**, and tabersonine **27**³⁴. Hairy roots also grow relatively fast, with a doubling time of three to four days³⁸. It has been found that specific yields for many natural products are higher in hairy root cultures than in the plant. One misconception regarding hairy root cultures is that certain metabolites found in aerial parts of the plant may not be produced in hairy roots. This is not always true, however, for in many cases the site of accumulation of secondary metabolites in plants does not coincide with the site of production. For example, a naphthoquinone derivative called lawsone is found in the aerial parts of the plant henna and not in the roots. Nevertheless, lawsone is produced in hairy root cultures in significant quantities³⁹.

Plant cell suspension culture (Figure 1-18) was the subject of extensive development in the 1980s, when it was discovered that these nondifferentiated plant cells could be grown in bioreactors in liquid medium³⁹. TIAs can be produced by cell suspension cultures, which are most commonly established from callus tissue. Callus tissues are nondifferentiated cells that are grown on solid media; transfer of callus tissue to liquid media results in the formation of cell suspension cultures¹⁴. One advantage of cell suspension cultures is fast growth; cell suspension cultures typically have a doubling time of one and a half to five days³⁸. Fewer types of TIAs are typically produced in cell suspension cultures than are produced in seedlings or hairy root cultures. In the cell suspension cultures used in the research for this thesis, for example, few alkaloids apart from ajmalicine **4**, catharanthine **29**, and tabersonine **27** are observed.

IV. *Potential pharmacological properties of novel TIAs*

The vast majority of TIAs are structurally complex and cannot be made synthetically on an industrial scale. The current method for industrial-scale production of ajmalicine **4**, for example, is isolation from the plant². Plants, however, do not naturally produce TIA analogs, such as C-11 chlorinated ajmalicine. If more TIA enzymes were cloned and the substrate specificity for those enzymes are known, perhaps novel TIA analogs could be produced on the scale required for industrial production. These novel TIAs could potentially have improved activities. Though structure-activity relationship studies of ajmalicine **4** have not been performed, a variety of other analogs of TIAs have been shown to have improved or altered bioactivity. For example, the anti-cancer drugs irinotecan **16** and topotecan **15** are derived synthetically from camptothecin **10**, which is too toxic to be used clinically (Figure 1-19)⁴⁰. Vinblastine **2** analogs are also used clinically¹⁰. Novel ajmalicine **4** analogs could potentially have improved activities; for example, perhaps C-11 chlorinated ajmalicine could be shown to have better anti-hypertensive activity than naturally occurring ajmalicine **4**.

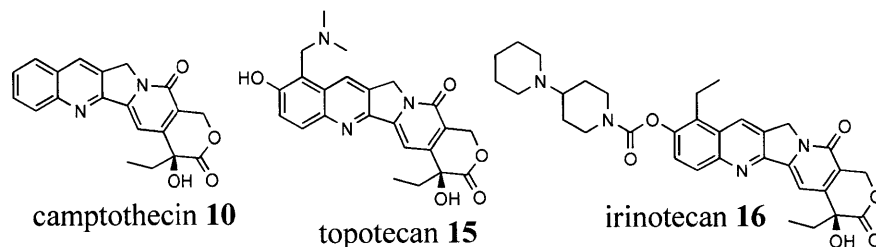


Figure 1-19: Topotecan **15** and irinotecan **16** are synthetically derived analogs of camptothecin **10**⁴⁰.

Novel TIAs can be produced by incorporating substituents at various positions of the structure. Substituents can alter the bioavailability, electron density, and conformational

properties of compounds⁴¹. Solubility and bioavailability are major factors in determining whether or not a drug candidate successfully passes clinical trials; approximately 40% of compounds fail clinical trials because of poor oral bioavailability or short half-life in plasma⁴². One limiting factor in oral bioavailability is low water solubility or high lipophilicity of a compound. A compound that is too lipophilic has difficulty diffusing through the cytosol. A sample must still be lipophilic enough, however, to traverse membranes and display appropriate pharmacokinetics⁴². According to Lipinski's Rule of Five⁴³, which are guidelines to assess whether a compound will be orally active, the octanol-water partition coefficient $\log P$ of a compound should be less than 5, where $P = [\text{drug}]_{\text{organic solvent}} / [\text{drug}]_{\text{aqueous solvent}}$.

Lipinski's Rule of Five also gives guidelines for the number of hydrogen bond donors and acceptors in a potential drug⁴³. To facilitate oral absorption and distribution, compounds should not have more than five hydrogen bond donors (NH and OH groups) or more than ten hydrogen bond acceptors (N and O atoms). Exceptions to this rule include cardiac glycosides, vitamins, anti-fungals, and antibiotics, for they typically have active transporters that take them across membranes⁴².

Halogens are frequently incorporated as substituents in drug candidates⁴⁴: indeed, one out of every three drugs contains a halogen⁴¹. Halogenation of a compound makes a compound more lipophilic, improving the ability of the compound to traverse the membrane. One drawback of halogenated compounds, however, is that they tend to accumulate in lipid tissue⁴⁴.

Halogenation often improves the bioactivity of a compound. In the series of anti-histaminic compounds shown in Figure 1-20, for example, the fluorinated ($X = \text{F}$) and chlorinated ($X = \text{Cl}$) derivatives show three to four fold higher activity than the parent

nonhalogenated compound, tripeleennamine **30** (X = H) (Figure 1-20)⁴¹. Similarly, with a monoamine oxidase inhibitor **31** (Figure 1-21), the brominated (X = Br) and trifluoromethyl (X = CF₃) derivatives show sixfold and twelvefold lower IC₅₀ values than the parent compound **31**^{41,45}. In a third example, the antibiotic clorobiocin is reported to have eight fold higher activity against *Bacillus subtilis* bacteria than its des chloro analog^{46,47}.

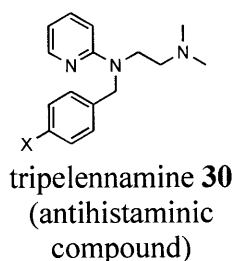
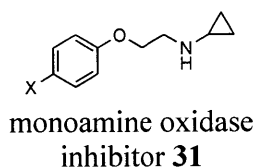


Figure 1-20: The structure of the anti-histaminic compound tripeleennamine **30** (X = H)⁴¹.



monoamine oxidase inhibition	IC ₅₀ (nM)
X = H	1200
X = Br	200
X = CF ₃	100

Figure 1-21: The structure of the monoamine oxidase inhibitor **31**⁴¹.

Fluorine is the most widely used halogen in drug discovery efforts. It is the smallest halogen and is isosteric to hydrogen (Table 1-2). Fluorine increases the lipophilicity of a molecule; although fluorine is only slightly more lipophilic than hydrogen, trifluoromethyl is significantly more lipophilic than methyl, and trifluoromethyl groups are often used as replacement for methyl groups to improve the pharmacological activity of a compound. Additionally, carbon-fluorine bonds are stronger than carbon-hydrogen bonds; fluorine thus imparts oxidative stability to a compound. Fluoro derivatives are often more stable to metabolic

degradation. For example, CF₃ groups are generally biostable, whereas CH₃ groups are easily oxidized by cytochrome P450s present in the human liver⁴⁸.

Atomic radius (Å)	Bond	Interatomic distance (Å)	Bond strength (kcal mol ⁻¹)
hydrogen: 0.29	C-H	1.14	93
fluorine: 0.64	C-F	1.45	114
chlorine: 0.99	C-Cl	1.74	72
bromine: 1.14	C-Br	1.90	59
iodine: 1.33	C-I	2.12	45

Table 1-2: The atomic radius (Å) of hydrogen and halogen atoms, and the bond, interatomic distance, and bond strength of carbon-hydrogen and carbon-halogen bonds⁴¹.

After fluorine, chlorine is the second most frequently used halogen in drug discovery efforts. Like fluorine, chlorine also increases the lipophilicity of a compound and can serve as a metabolic obstruction⁴¹. Bromine is used less frequently than fluorine or chlorine, and is most often incorporated as a bromo aryl moiety. Iodine is the least-used halogen because of the weakness of the carbon-iodine bond. The weak carbon-iodine bond allows iodide ions to be formed easily, which can trigger unwanted reactions in the human body⁴¹.

Methylation also alters the properties of a potential drug by increasing the lipophilicity of the compound. As with halogenated compounds, the increase in lipophilicity facilitates the compound's traversing membranes but also impedes diffusion in the aqueous cytosol⁴⁴. Aryl methyl groups can be oxidized in the body to carboxylic acids, which aids in the elimination of the compound by improving its water solubility. Methylation can also prevent certain side effects by obstructing reactions from occurring at a given position. For example, *ortho*-methyl paracetamol **33** and *ortho, ortho*-dimethyl paracetamol **34** have lower hepatotoxicity than the

analgesic and anti-pyretic paracetamol **32** (acetaminophen) (Figure 1-22). It is believed that methylation at the *ortho* positions to the phenolic hydroxy group of paracetamol **32** prevents metabolic hydroxylation at those *ortho* positions⁴⁴.

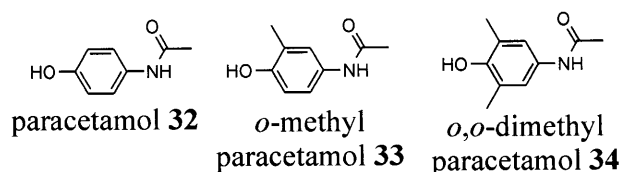


Figure 1-22: The structures of paracetamol **32** (acetaminophen), *o*-methyl paracetamol **33**, and *o,o*-dimethyl paracetamol **34**⁴⁴.

Hydroxylation and methoxylation also alter the properties of a potential drug by, conversely, increasing its water solubility. Hydroxylation also introduces potential new hydrogen-bonding centers, which can influence the binding of the compound to its target⁴⁴.

If a compound of interest contains a heterocycle, substitution of alternate, isosteric heterocycles has been shown to alter the bioactivity of the compound. For example, an indole **35** moiety can be substituted with an aza-indole **36**, a benzofuran **37**, or a benzothiophene **38** moiety (Figure 1-23)⁴⁹. Intriguing biological properties have been reported for numerous compounds containing aza-indole **36**, benzofuran **37**, and benzothiophene **38** moieties⁵⁰⁻⁵⁷, and numerous drugs⁵⁸⁻⁶⁰ contain such moieties. Aza compounds, for example, typically have high water solubility and unique hydrogen-bonding properties⁶¹.

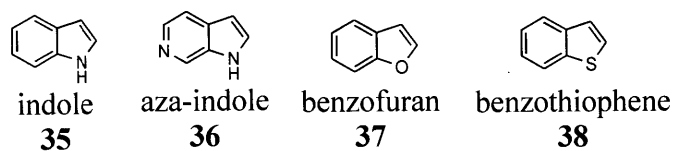


Figure 1-23: Structures of indole **35**, aza-indole **36**, benzofuran **37**, and benzothiophene **38** moieties. In the aza-indole **36** moiety the nitrogen on the benzene ring can also be in other positions on the benzene ring.

Different stereoisomers of a compound can have vastly different bioactivities⁶². For example, the *S*-(+)-isomer of the anti-histamine dexchloropheniramine **39** is approximately two hundred times more powerful than the *R*-(-) isomer **40** (Figure 1-24)⁴². Altering the stereochemistry at a chiral center is yet another way to potentially alter the bioactivity of a compound.

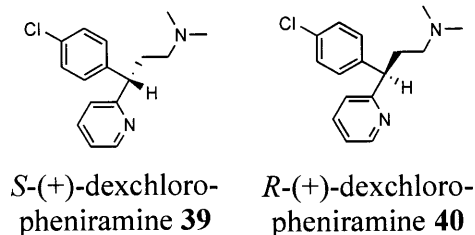


Figure 1-24: Structures of the *S*-(+) **39** and *R*-(-) **40** isomers of the anti-histamine dexchloropheniramine⁴².

V. Cloned TIA enzymes

A potentially useful way of making large amounts of TIAs and plant-derived natural products in general is by heterologous reconstitution in yeast. Unfortunately, only a few of the cDNA sequences encoding the enzymes of TIA biosynthesis in *C. roseus* have been cloned. These enzymes include geraniol-10-hydroxylase (G10H), loganic acid methyltransferase

(LAMT), secologanin synthase (SLS), strictosidine synthase (STS), strictosidine- β -glucosidase (SGD), and several enzymes that occur late in the biosynthesis of vindoline¹.

Geraniol-10-hydroxylase (G10H) is a 56 kDa cytochrome P450 monooxygenase that catalyzes the first committed step of iridoid terpene biosynthesis, the conversion of geraniol **22** to 10-hydroxy geraniol **23** (Figure 1-10). Geraniol-10-hydroxylase has been heterologously expressed in yeast and functionally characterized^{20,21}. Hydroxylation of geraniol **22** and its *cis*-isomer nerol **41** were observed in a reconstituted system with geraniol-10-hydroxylase and NADPH-cytochrome P450 reductase²¹. Geraniol-10-hydroxylase has a K_m of 5.5 μ M for geraniol **22** and 11 μ M for nerol **41** (Figure 1-25)²².

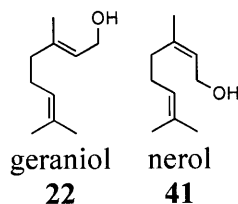


Figure 1-25: The structures of geraniol **22** and its *cis*-isomer nerol **41**.

The enzyme loganic acid methyltransferase (LAMT) methylates loganic acid **42**, converting it to loganin **25** (Figure 1-11). Loganic acid methyltransferase has been cloned and expressed in *E. coli*⁶³. Previous enzymatic studies with partially purified enzyme have shown that loganic acid **42** is the substrate for the methylation reaction catalyzed by loganic acid **42** methyltransferase^{22,64}. Loganic acid methyltransferase was reported to have an unusually high K_m of 14.76 ± 1.7 mM for loganic acid **42** and 742.1 ± 37 μ M for S-adenosyl-L-methionine, a turnover of 19.6 min^{-1} , a pH optimum of 7.5, and a temperature optimum of 32°C ^{63,64}.

Secologanin synthase (SLS), the P450 oxidase that converts loganin **25** to secologanin **17** (Figure 1-11), has been cloned and expressed in *E. coli* as a translational fusion with the *C. roseus* P450 reductase⁶⁵. Secologanin synthase was isolated from a cDNA library of a *C. roseus* cell suspension culture⁶⁶⁻⁶⁸. Secologanin synthase was shown to accept only loganin **25** as a substrate, and has a pH optimum of 7.5 and a temperature optimum of 30°C⁶⁸.

Strictosidine synthase (STS) catalyzes the formation of strictosidine **1** from secologanin **17** and tryptamine **18** (Figure 1-6, Figure 1-13). Strictosidine synthase is absolutely stereoselective, forming only strictosidine **1** and not the C-3 *R* diastereomer vincoside **43**. Recombinant strictosidine synthase expressed in *E. coli* has been kinetically characterized: the K_m for tryptamine **18** and secologanin **17** are reported to be 6.2 μM and 39 μM , respectively, and the k_{cat} is 78.2 min^{-1} . The optimal pH and temperature are reported to be 6.8 and 30°C, respectively⁶⁹. Strictosidine synthase from *Rauwolfia serpentina* has been crystallized, and the structure is a six-bladed β -propeller fold⁷⁰. The only currently known enzymes that are functionally related to strictosidine synthase are deacetylipecoside synthase, deacetyloipecoside synthase⁷¹, and norcoclaurine synthase⁷². Deacetylipecoside synthase catalyzes the condensation of secologanin **17** and dopamine **44** to produce deacetylipecoside **45**, while deacetyloipecoside synthase catalyzes the condensation of secologanin **17** and dopamine **44** to produce deacetyloipecoside **46**, leading to the family of monoterpenoid tetrahydroisoquinoline alkaloids (Figure 1-26)⁷¹. Norcoclaurine synthase catalyzes the condensation of 4-hydroxyphenylacetaldehyde **47** and dopamine **44** to produce (*S*)-norcoclaurine **48**, leading to the family of benzyloquinoline alkaloids (Figure 1-26)^{70,72}. The amino acid sequence of norcoclaurine synthase, which has been cloned, is not at all similar to that of strictosidine synthase.

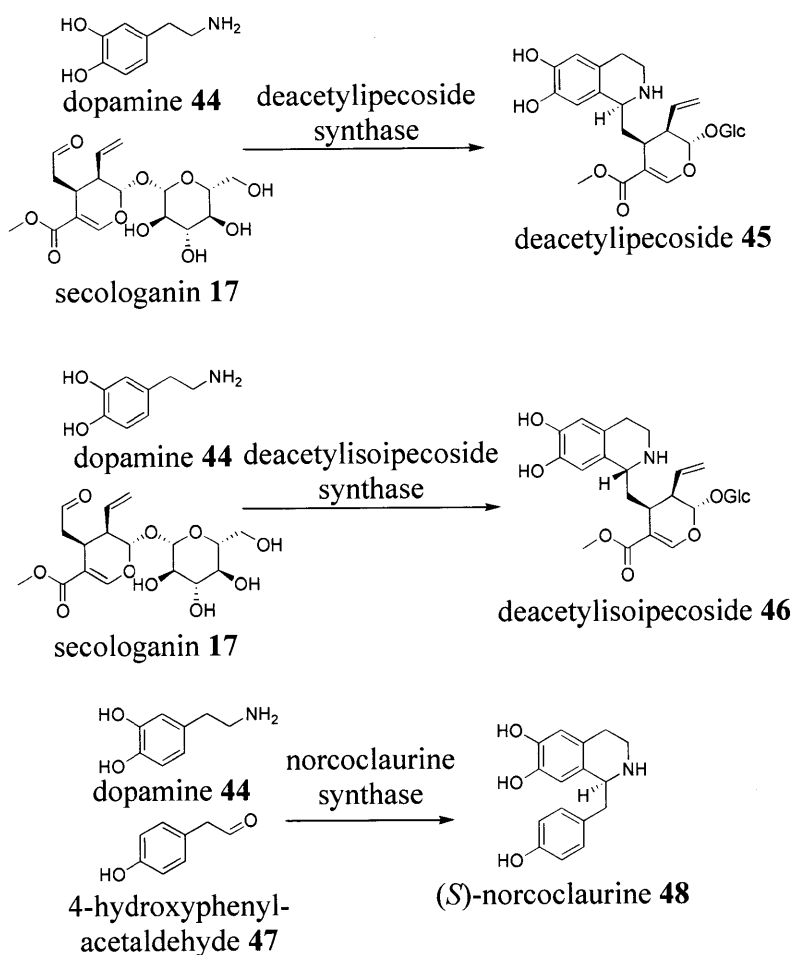


Figure 1-26: Deacetylpecoside synthase and deacetylisoipecoside synthase catalyze the condensation of dopamine **44** and secologanin **17** to produce deacetylpecoside **45** and deacetylisoipecoside **46**, respectively⁷¹. Norcoclaurine synthase catalyzes the condensation of dopamine **44** and 4-hydroxyphenylacetaldehyde **47** to produce (*S*)-norcoclaurine **48**⁷².

Strictosidine- β -glucosidase (SGD) catalyzes the deglycosylation of strictosidine **1**, the central TIA intermediate (Figure 1-14, Figure 1-27). SGD exists as a high molecular weight complex formed from aggregates of 4, 8, or 12 monomers, with the monomer having a molecular weight of 63 kDa. The main products of SGD deglycosylation of strictosidine **1** are cathenamine **49** and glucose **50**, though other isomers of cathenamine **49** are also formed (Figure 1-27).⁷³⁻⁷⁶

SGD from *C. roseus* has an optimum pH between 6 and 6.4⁷⁴, an optimum temperature of 30°C⁷⁷, and reported K_m values ranging from 18 to 200 μM ^{77,78}. SGD is discussed in further detail in Chapter 2.

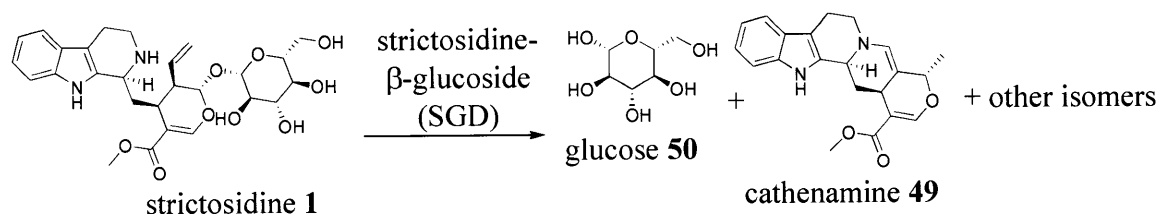


Figure 1-27: Strictosidine **1** is deglycosylated by SGD to produce glucose **50**, cathenamine **49**, and other isomers of cathenamine **49**.

Tabersonine **27** is transformed to vindoline **28** in six reactions that have been studied extensively by De Luca and coworkers (Figure 1-28)¹. Many of the enzymes in the biosynthetic pathway leading to vindoline **28** have been cloned. The first step is an aromatic hydroxylation of tabersonine **27** at C-11 by the microsomal cytochrome P450 monooxygenase tabersonine 16-hydroxylase⁶⁶. The hydroxyl group is then methylated by the cytosolic S-adenosyl-L-methionine (SAM)-dependent 16-hydroxytabersonine *O*-methyltransferase (OMT)⁷⁹. The 2,16 double bond is then hydrated by an unknown enzyme². A thylakoid-associated SAM-dependent 2,16-dihydro-11-hydroxytabersonine-*N*-methyltransferase (NMT) then methylates N-1, producing desacetoxyvindoline⁸⁰. The C-17 of desacetoxyvindoline is then hydroxylated by the cytosolic 20-oxoglutarate-dependent dioxygenase (D17H)⁸¹. Vindoline is finally produced by 4-*O*-acetylation by the cytosolic 17-*O*-deacetylvindoline-17-*O*-acetyltransferase⁸² (Figure 1-28). The vindoline **28** produced is then coupled with catharanthine **29** by the known peroxidase 3',4'-anhydrovinblastine synthase to produce a 5',6' iminium dimer⁸³. The 5',6' iminium is then reduced, producing α -3',4'-anhydrovinblastine **51**. Hydroxylation of the 3',4' double bond yields

vinblastine **2**, and further oxidation of the N-1-methyl group yields vincristine **3** (Figure 1-29).

The enzymes that act after the dimerization step, however, are uncharacterized¹.

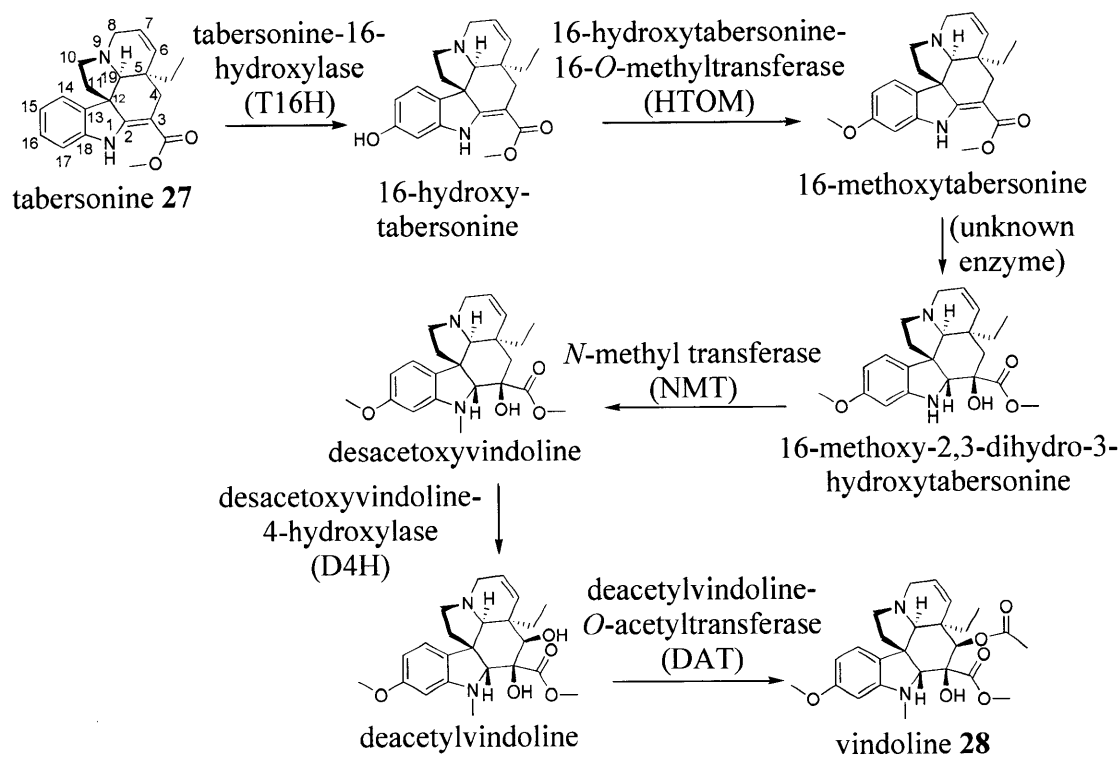


Figure 1-28: Vindoline **28** biosynthesis from tabersonine **27**^{1,66,79-82}, with the numbering system for tabersonine **27** shown in blue¹².

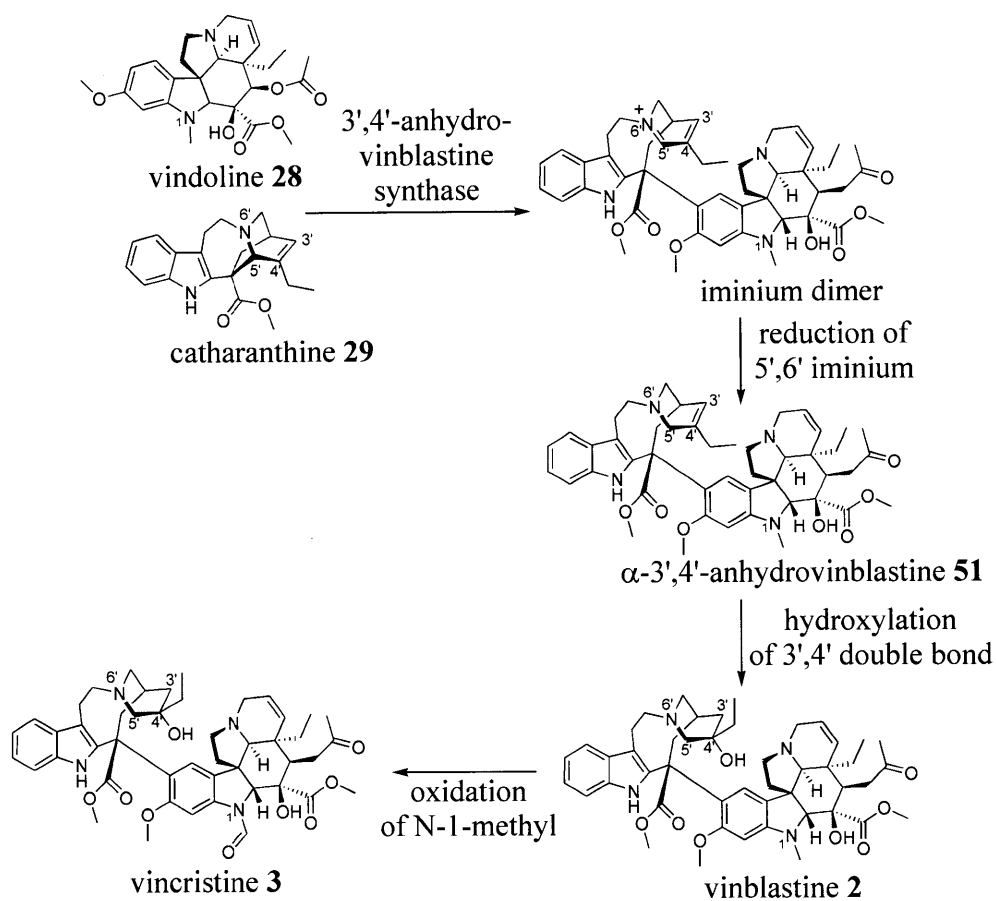


Figure 1-29: Vinblastine 2 and vincristine 3 biosynthesis from catharanthine 29 and vindoline 28^{1,83}, with the numbering system shown in blue¹².

VI. Substrate specificity of TIA enzymes and precursor directed biosynthesis studies

Strictosidine **1**, the central intermediate in TIA biosynthesis, is produced by a stereoselective Pictet-Spengler condensation of secologanin **17** and tryptamine **18**⁸⁴. The substrate specificity of strictosidine synthase was studied to determine which novel strictosidine **1** analogs can be produced enzymatically^{85,86}. Once formed, these strictosidine **1** analogs could potentially be incorporated into various biosynthetic pathways to form novel TIAs with improved or altered biological activities. Numerous secologanin **17** and tryptamine **18** analogs were shown to be accepted by strictosidine synthase. *In vitro* studies have shown that strictosidine synthase is able to accept ethyl-ester secologanin **52**, allyl-ester secologanin **53**, and pentynyl-ester secologanin **54** (Figure 1-30)⁸⁶.

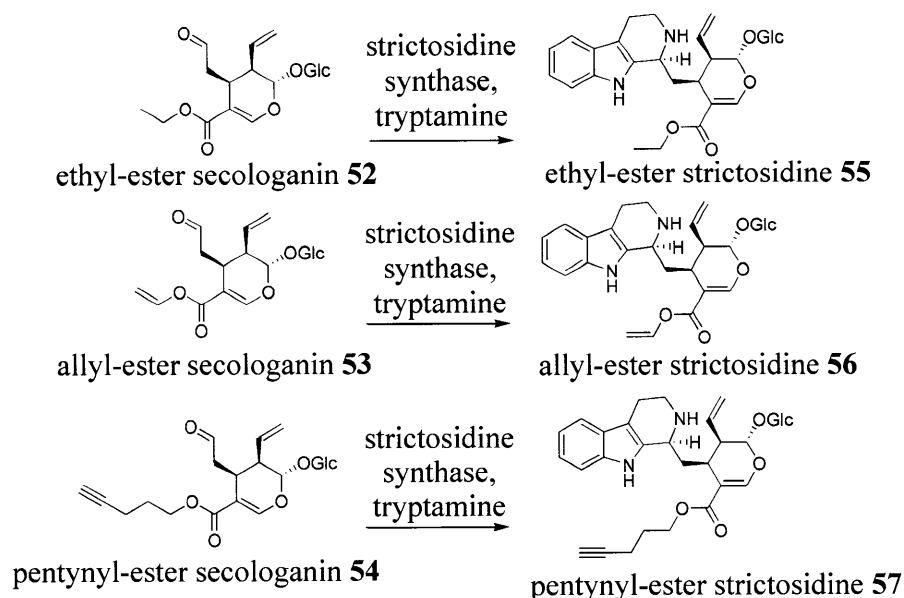


Figure 1-30: Secologanin **17** analogs accepted by strictosidine synthase include ethyl-ester secologanin **52**, allyl-ester secologanin **53**, and pentynyl-ester secologanin **54**^{69,86,87}.

A variety of indole-substituted tryptamine **18** analogs are also accepted by strictosidine synthase. The tryptamine **18** and strictosidine **1** numbering systems are shown below in Figure

1-31. The 4-, 5-, 6-, and 7- positions of tryptamine correspond to the 9-, 10-, 11-, and 12-positions of strictosidine **1**, respectively. Tryptamine **18** analogs that are accepted by strictosidine synthase to form the corresponding strictosidine **1** analogs include 4-fluoro, 5-fluoro, 6-fluoro, 7-fluoro, 4-methyl, 6-methyl, 7-methyl, 5-hydroxy, 6-methoxy, 5,6-dihydroxy tryptamine, and α -methyl tryptamine^{70,86,88}. Tryptamine analogs tested that are not accepted by strictosidine synthase include 5-methyl, 5-chloro, 5-bromo, 5,7-dihydroxy, 5-methoxy tryptamine, N-methyl tryptamine, and N- ω -methyl tryptamine⁸⁶.

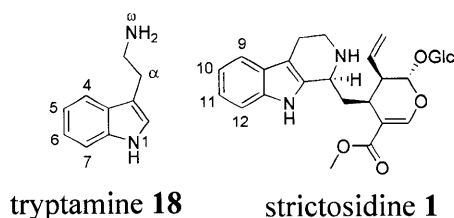


Figure 1-31: The numbering system for tryptamine **18** and strictosidine **1** indole substituents is shown in blue. The 4-, 5-, 6- and 7- positions of tryptamine **18** correspond to the 9-, 10-, 11-, and 12-positions of strictosidine **1**, respectively⁸⁶. The α -position and the N-1 nitrogen and N- ω nitrogen of tryptamine **18** are indicated in blue.

Different heterocyclic amines were also assayed with strictosidine synthase. *N*-methyl tryptamine **58**, 2-(1*H*-Pyrrol-3-yl)-ethylamine **59**, and 2-(1*H*-Imidazol-4-yl)-ethylamine **60** are not accepted by strictosidine synthase to form the corresponding strictosidine **1** analogs (Figure 1-32). However, 2-benzofuran-3-yl-ethylamine **61** and 2-benzo[*b*]thiophen-3-yl-ethylamine **62** form benzo strictosidine **1-a** and thio strictosidine **1-b**, respectively (Figure 1-33). The 2-benzo[*b*]thiophen-3-yl-ethylamine **62** substrate was accepted so slowly by strictosidine synthase that a quantitative enzymatic kinetic analysis was not possible. The 2-benzofuran-3-yl-ethylamine **61** substrate had a K_m value similar to that of tryptamine, but it had a much lower

k_{cat} ; we speculate that catalysis is slowed by the electron-deficient nature of the benzofuran ring⁸⁶.

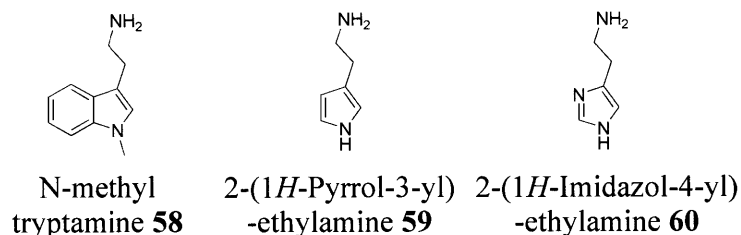


Figure 1-32: The substrates N-methyl tryptamine **58**, 2-(1*H*-Pyrrol-3-yl)-ethylamine **59**, and 2-(1*H*-Imidazol-4-yl)-ethylamine **60** are not accepted by strictosidine synthase to form the corresponding strictosidine analogs⁸⁶.

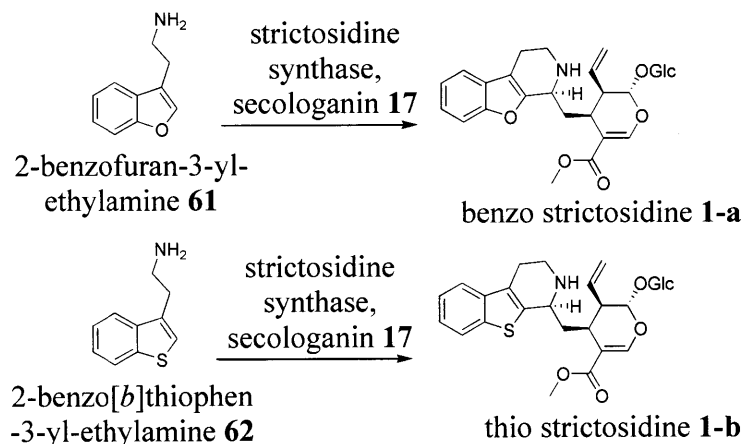


Figure 1-33: The substrates 2-benzofuran-3-yl-ethylamine **61** and 2-benzo[*b*]thiophen-3-yl-ethylamine **62** are accepted by strictosidine synthase to form benzo strictosidine **1-a** and thio strictosidine **1-b**, respectively⁸⁶.

Precursor directed biosynthesis studies

To probe the capacity of the biosynthetic machinery to produce novel alkaloids, tryptamine **18** analogs were also co-cultured with hairy root cultures in precursor directed

biosynthesis studies (Figure 1-34), and it was found that many of the enzymes in TIA biosynthesis can accept alternative substrates^{34,36}. The substrates 4-7-fluoro, 4-7-chloro, 4-7-bromo, 4-7-methyl, and 4-7-methoxy tryptamine, as well as benzo strictosidine **1-a**, were co-cultured with hairy root cultures for two weeks. The cultures were then extracted with methanol and the alkaloid content was analyzed. The corresponding ajmalicine **4**, serpentine **5**, isositsirikine **7**, akuammicine **63**, catharanthine **29**, tabersonine **27**, and vindoline **28** analogs were observed, indicating that numerous enzymes downstream of SGD are able to accept alternative substrates³⁶.

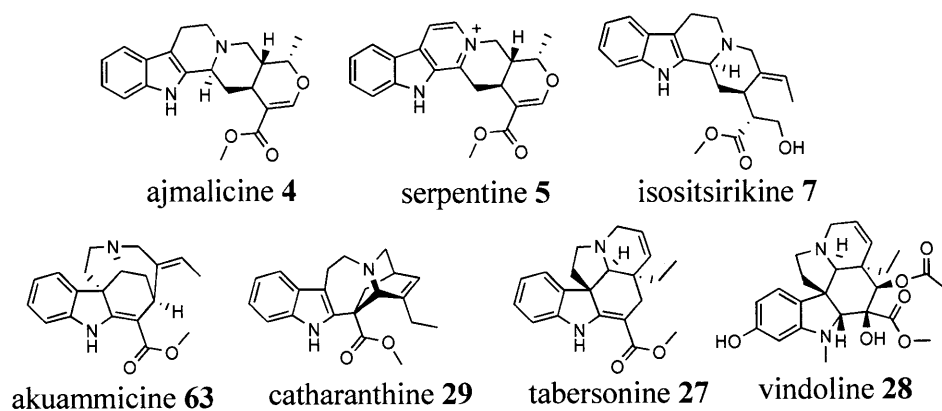


Figure 1-34: The substrates 4-7-fluoro, 4-7-chloro, 4-7-bromo, 4-7-methyl, and 4-7-methoxy tryptamine, as well as benzo strictosidine **1-a**, were incorporated into hairy root cultures and produced the corresponding ajmalicine **4**, serpentine **5**, isositsirikine **7**, akuammicine **63**, catharanthine **29**, tabersonine **27**, and vindoline **28** analogs³⁴.

VII. *Thesis overview*

Because of synthetic complexity of TIAs, cost-effective industrial-scale synthesis of many TIAs is currently not feasible. A potential strategy to produce large amounts of TIAs is heterologous reconstitution of the pathway in yeast⁸⁹. Unfortunately, only a few of the enzymes found in TIA biosynthesis in *C. roseus*, strictosidine synthase, strictosidine- β -glucosidase (SGD), and several enzymes that occur late in the biosynthesis of vindoline¹ have been cloned.

There are reports of natural product analogs that have proven to be more pharmaceutically useful than the parent natural product; for example, the camptothecin **10** analogs topotecan **15** and irinotecan **16** (Figure 1-5) are used clinically, yet the natural product camptothecin **10** is too toxic and water insoluble to be used as a drug⁹. If the substrate specificity of TIA enzymes were known, novel TIAs could be produced on an industrial scale once the enzymes were isolated and cloned. A library of novel TIAs could be created, and assayed in a variety of pharmaceutical screens.

In this thesis I discuss my work studying the enzymes strictosidine- β -glucosidase (SGD), ajmalicine synthase, and isositsirikine synthase. As described, SGD deglycosylates strictosidine **1**, the central intermediate of TIA biosynthesis. Ajmalicine synthase and isositsirikine synthase are NADPH-dependent reductase enzymes that reduce the reactive hemiacetal moiety generated by the action of SGD (Figure 1-35). Ajmalicine synthase produces ajmalicine **4**, which is used to treat hypertension³, and isositsirikine synthase produces isositsirikine **7**, which has anti-neoplastic activity⁶. In this thesis I developed strategies to make novel ajmalicine **4** and isositsirikine **7** analogs *in vitro*. The NADPH-dependent reductase enzymes that produce the anti-hypertensive agent ajmalicine **4** and the anti-neoplastic agent isositsirikine **7** have not been isolated. I developed a partial purification procedure for ajmalicine synthase and isositsirikine

synthase from *C. roseus* hairy root and cell suspension cultures. I also performed crosslinking experiments with a substrate probe in attempts to isolate ajmalicine synthase and isositsirikine synthase. In my substrate specificity studies I found that ajmalicine synthase and isositsirikine synthase have broad substrate specificity substrate specificity, which is promising for the development of novel ajmalicine **4** and isositsirikine **7** analogs with potentially improved therapeutic activities.

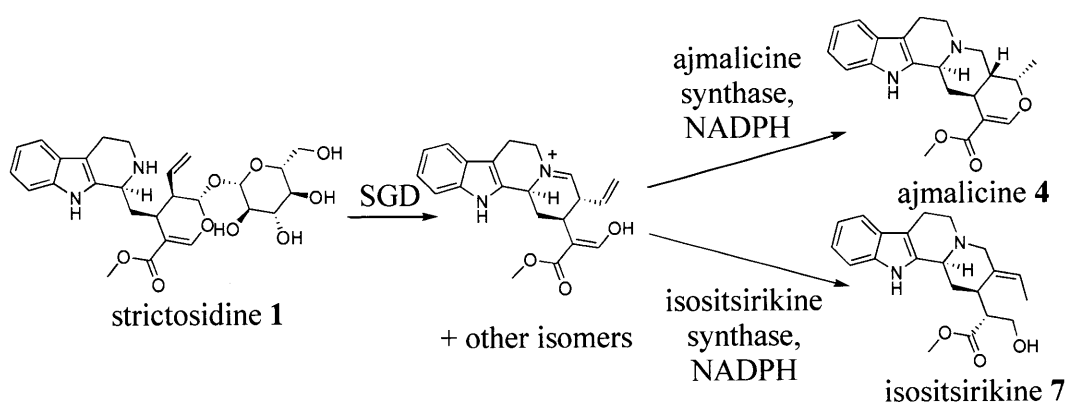


Figure 1-35: Strictosidine **1** is deglycosylated by SGD. Ajmalicine synthase and isositsirikine synthase are NADPH-dependent reductases that reduce deglycosylated strictosidine to ajmalicine **4** and isositsirikine **7**, respectively.

Chapter 2 describes my work determining which strictosidine **1** analogs are accepted by SGD. I assayed strictosidine **1** analogs containing modified indole, methyl ester, vinyl, and glucose moieties, as well as the diastereomer of strictosidine **1**, vincoside **43**. I also discuss the steady state kinetic analysis studies that I performed to obtain a quantitative assessment of the substrate specificity of this enzyme. Chapter 3 discusses the partial purification procedure that I developed for ajmalicine synthase and isositsirikine synthase. Efforts to clone these enzymes are described. I also describe deglycosylated strictosidine **49** analogs that I found were accepted by

ajmalicine synthase and isositsirikine synthase to produce new corynanthe type alkaloids. Chapter 4 describes the enzymes that have been isolated and cloned by a crosslinking strategy. One of these enzymes has been found to have sinapyl alcohol dehydrogenase activity. Finally, chapter 5 discusses future directions of the project.

VIII. *References*

- (1) O'Connor, S. E.; Maresh, J. J. Chemistry and biology of monoterpene indole alkaloid biosynthesis. *Natural Products Reports* **2006**, *23*, 532-47.
- (2) van der Heijden, R.; Jacobs, D. I.; Snoeijer, W.; Hallard, D.; Verpoorte, R. The Catharanthus alkaloids: pharmacognosy and biotechnology. *Current Medicinal Chemistry* **2004**, *11*, 607-28.
- (3) Allain, H.; Bentue-Ferrer, D. Clinical efficacy of almitrine-raubasine: an overview. *European Neurology* **1998**, *39*, 39-44.
- (4) Dassonneville, L.; Bonjean, K.; De Pauw-Gillet, M. C.; Colson, P.; Houssier, C.; Quetin-Leclercq, J.; Angenot, L.; Bailly, C. Stimulation of topoisomerase II-mediated DNA cleavage by three DNA-intercalating plant alkaloids: cryptolepine, matadine, and serpentine. *Biochemistry* **1999**, *38*, 7719-26.
- (5) Yonezawa, A.; Yoshizumii, M.; Ebiko, M.; Amano, T.; Kimura, Y.; Sakurada, S. Long-lasting effects of yohimbine on the ejaculatory function in male dogs. *Biomedical Research* **2005**, *26*, 201-206.
- (6) Mukhopadhyay, S.; El-Sayed, A.; Handy, G.A.; Cordell, G.A. Catharanthus alkaloids XXXVII. 16-Epi-Z-isositsirikine, a monomeric indole alkaloid with antineoplastic activity from *Catharanthus roseus* and *Rhazya stricta*. *Journal of Natural Products* **1983**, *46*, 409-13.
- (7) Prudhomme, J.; McDaniel, E.; Ponts, N.; Bertani, S.; Fenical, W.; Jensen, W.; Le Roch, K. Marine actinomycetes: a new source of compounds against the human malaria parasite. *PLoS One* **2008**, *3*, e2335.
- (8) Brugada, J.; Brugada, P.; Brugada, R. The ajmaline challenge in Brugada syndrome: a useful tool or misleading information? *European Heart Journal* **2003**, *24*, 1085-86.
- (9) Bomgaars, L.; Berg, S.L.; Blaney, S.M. The development of camptothecin analogs in childhood cancers. *The Oncologist* **2001**, *6*, 506-16.
- (10) Emory Winship Cancer Institute, <http://www.cancerquest.org/index.cfm?page=525>, accessed April 21, 2010.
- (11) Ishikawa, H.; Colby, D. A.; Seto, S.; Va, P.; Tam, A.; Kakei, H.; Rayl, T. J.; Hwang, I.; Boger, D. L. Total synthesis of vinblastine, vincristine, related natural products, and key structural analogues. *Journal of the American Chemical Society* **2009**, *131*, 4904-16.
- (12) Bau, R.; Jin, K.K. Crystal structure of vinblastine. *Journal of the Chemical Society Perkins Transactions I* **2000**, 2079-82.
- (13) Hong, J.; Chen, S.-H. *Case studies in natural-product optimization*; Humana Press: Totowa, New Jersey, 2005.
- (14) Zhou, M.-L.; Shao, J.-R.; Tang, Y.-X. Production and metabolic engineering of terpenoid indole alkaloids in cell cultures of the medicinal plant *Catharanthus roseus* (L.) G. Don (Madagascar periwinkle). *Biotechnology and Applied Biochemistry* **2009**, *52*, 313-23.
- (15) Chan, P.; Li, Z.Z.; Hu, P.; Sarbach, S.D.; Guez, D. Neurologic and histologic evaluation of almitrine and raubasine (Duxil) in middle cerebral art. *European Journal of Pharmacology* **1993**, *231*, 175-82.
- (16) Li, S.; Long, J.; Ma, Z.; Xu, Z.; Li, J.; Zhang, Z. Assessment of the therapeutic activity of a combination of almitrine and raubasine on functional rehabilitation following ischaemic stroke. *Current Medical Research and Opinion* **2004**, *20*, 409-15.

- (17) Kernohan, A.F.; McIntyre, M.; Hughes, D.M.; Tam, S.W.; Worcel, M.; Reid, J.L. An oral yohimbine/L-arginine combination (NMI 861) for the treatment of male erectile dysfunction: a pharmacokinetic, pharmacodynamic and interaction study with intravenous nitroglycerine in healthy male subjects. *British Journal of Clinical Pharmacology* **2005**, *59*, 85-93.
- (18) McMurry, J.; Begley, T. *The Organic Chemistry of Biological Pathways*; Roberts and Company Publishers: Greenwood Village, Colorado, 2005.
- (19) Contin, A.; van der Heijden, R.; Lefeber, A. W.; Verpoorte, R. The iridoid glucoside secologanin is derived from the novel triose phosphate/pyruvate pathway in a *Catharanthus roseus* cell culture. *FEBS Letters* **1998**, *434*, 413-16.
- (20) Collu, G.; Garcia, A.A.; Heijden, R.; Verpoorte, R. Activity of the cytochrome P450 enzyme geraniol 10-hydroxylase and alkaloid production in plant cell cultures. *Plant Science* **2002**, *162*, 165-72.
- (21) Collu, G.; Unver, N.; Peltenburg-Looman, A.M.G.; Heijden, R.; Verpoorte, R.; Memelink, J. Geraniol 10-hydroxylase, a P450 enzyme involved in terpenoid indole alkaloid biosynthesis. *FEBS Letters* **2001**, *508*, 215-20.
- (22) El-Sayed, M.; Verpoorte, R. *Catharanthus* terpenoid indole alkaloids: biosynthesis and regulation. *Phytochemistry Reviews* **2007**, *6*, 277-305.
- (23) Voet, D.; Voet, J.G. *Biochemistry*; John Wiley & Sons: Danvers, Massachusetts, 2004.
- (24) Dewick, P.N. *Medicinal Natural Products: A Biosynthetic Approach*; 2 ed.; John Wiley & Sons, Ltd: West Sussex, England, 2001.
- (25) Sottomayor, M.; Duarte, P.; Figueiredo, R.; Barceló, A.R. A vacuolar class III peroxidase and the metabolism of anticancer indole alkaloids in *Catharanthus roseus*. *Plant Signaling and Behavior* **2008**, *3*, 899-901.
- (26) Abraham, D.J.; Farnsworth, N.R.; Blomster, R.N.; Rhodes, R.E. Structure elucidation and chemistry of *Catharanthus* alkaloids II. Isolation and partial structure of catharine, a dimeric indole alkaloid from *C. zanceus* and *C. roseus*. *Journal of Pharmaceutical Sciences* **2006**, *56*, 401-403.
- (27) Jacquier, M.J.; Vercauteren, J.; Massiot, G.; Men-Olivier, L.L.; Pussetta, J.; Sevenet, T. Alkaloids of *Alstonia plumosa*. *Phytochemistry* **1980**, *21*, 2973-77.
- (28) Cordell, G.A. *The alkaloids: chemistry and biology*; Academic Press: San Diego, California, 1998; Vol. 51.
- (29) Mukhopadhyay, S.; Cordell, G.A. *Catharanthus* alkaloids. XXXVI. Isolation of vincalkebostine (VLB) and periformyline from *Catharanthus trichophyllus* and pericyclivine from *Catharanthus roseus*. *Journal of Natural Products* **1981**, *44*, 335-39.
- (30) Tin-Wa, M.; Fong, H.H.; Blomster, R.N.; Farnsworth, N.R. *Catharanthus* alkaloids. XXI. Isolation of lochnerinine, one of the cytotoxic principles of *C. pusillus*. *Journal of Pharmaceutical Sciences* **1968**, *57*, 2167-69.
- (31) Tin-Wa, M.; Farnsworth, N.R.; Fong, H.H.; Trojanek, J. *Catharanthus* alkaloids. XXV. Isolation of leurosine and ursolic acid from *C. pusillus*. *Lloydia* **1970**, *33*, 261-63.
- (32) Mishra, M.P., <http://www.ecosensorium.org/2009/09/vinca-rosea-sadabahaar-or-madagascar.html>, accessed April 19, 2010. 2010.
- (33) National Tropical Botanical Garden, <http://www.ntbg.org/pwr/resources/photos/1404.jpg>, accessed May 20, 2010.

- (34) McCoy, E., O'Connor, S.E. Directed biosynthesis of alkaloid analogs in the medicinal plant *Catharanthus roseus*. *Journal of the American Chemical Society* **2006**, *128*, 14276-77.
- (35) Runguphan, W.; Maresh, J. J.; O'Connor, S. E. Silencing of tryptamine biosynthesis for production of nonnatural alkaloids in plant culture. *Proceedings of the National Academy of Sciences USA* **2009**, *106*, 13673-78.
- (36) McCoy, E. Substrate analogs to investigate alkaloid biosynthesis in *C. roseus*. Ph.D. dissertation, Massachusetts Institute of Technology, 2009.
- (37) Runguphan, W.; O'Connor, S. E. Metabolic reprogramming of periwinkle plant culture. *Nature Chemical Biology* **2009**, *5*, 151-53.
- (38) Bhadra, R.; Vani, S.; Shanks, J. Production of indole alkaloids by selected hairy root lines of *Catharanthus roseus*. *Biotechnology and Bioengineering* **1993**, *41*, 581-92.
- (39) Shanks, J.V.; Morgan, J. Plant 'hairy root' culture. *Current Opinion in Biotechnology* **1999**, *10*, 151-55.
- (40) Cragg, G.M.; Kingston, D.G.I.; Newman, D.J. *Anticancer agents from natural products*; Taylor & Francis: New York, New York, 2005.
- (41) Wermuth, C.G. *The practice of medicinal chemistry*; Harcourt Brace and Company: New York, New York, 1996.
- (42) Silverman, R.B. *The organic chemistry of drug design and drug action*; Elsevier Academic Press: Oxford, United Kingdom, 2004.
- (43) Lipinski, C.A.; Lombardo, F.; Dominy, B.W.; Feeney, P.J. Experimental and computational approaches to estimate solubility and permeability in drug discovery and development settings. *Advanced Drug Delivery Reviews* **2001**, *46*, 3-26.
- (44) Thomas, G. *Medicinal chemistry: an introduction*; John Wiley & Sons: New York, New York, 2000.
- (45) Newman, A.H.; Allen, A.C.; Izenwasser, S.; Katz, J.L. Novel 3- α -(diphenylmethoxy)tropane analogs: potent dopamine uptake inhibitors without cocaine-like behavioral profiles. *Journal of Medicinal Chemistry* **1994**, *1994*, 2258-61.
- (46) Eustaquio, A.S.; Gust, B.; Luft, T.; Li, S.-M.; Chater, K.F.; Heide, L. Clorobiocin biosynthesis in *Streptomyces*: identification of the halogenase and generation of structural analogs. *Chemistry and Biology* **2003**, *10*, 279-88.
- (47) Eustaquio, A.S.; Gust, B.; Li, S.-M.; Pelzer, S.; Wohlleben, W.; Chater, K.F.; Heide, L. Production of 8'-halogenated and 8'-unsubstituted novobiocin derivatives in genetically engineered *Streptomyces coelicolor* strains. *Chemistry and Biology* **2004**, *11*, 1561-72.
- (48) Muller, K.; Faeh, C.; Diederich, F. Fluorine in pharmaceuticals: looking beyond intuition. *Science* **2007**, *317*, 1881-86.
- (49) Muranaka, A.; Yasuike, S.; Liu, C.Y.; Kurita, J.; Kakusawa, N.; Tsuchiya, T.; Okuda, M.; Kobayashi, N.; Matsumoto, Y.; Yoshida, K.; Hashizume, D.; Uchiyama, M. Effect of periodic replacement of the heteroatom on the spectroscopic properties of indole and benzofuran derivatives. *Journal of Physical Chemistry A* **2009**, *113*, 464-73.
- (50) Guo, H.F.; Shao, H.Y.; Yang, Z.Y.; Xue, S.T.; Li, X.; Liu, Z.Y.; He, X.B.; Jiang, J.D.; Zhang, Y.Q.; Si, S.Y.; Li, Z.R. Substituted benzothiophene or benzofuran derivatives as a novel class of bone morphogenetic protein-2 up-regulators: synthesis, structure-activity relationships, and preventive bone loss efficacies in senescence accelerated mice (SAMP6) and ovariectomized rats. *Journal of Medicinal Chemistry* **2010**, *53*, 1819-20.

- (51) Davis, R. L.; Kahramana, C.; Prinsa, T.J.; Beavera, Y.; Cooka, T.G.; Crampa, J.; Cayanana, C.S.; Gardinera, E.M.M.; McLaughlinb, M.A.; Clark, A.F.; Hellberg, M.R.; Shiaua, A.K.; Noble, S.A.; Borchardta, A.J. Benzothiophene containing Rho kinase inhibitors: efficacy in an animal model of glaucoma. *Bioorganic and Medicinal Chemistry Letters* **2010**, *In press*.
- (52) Wang, S.; Beck, R.; Blench, T.; Burd, A.; Buxton, S.; Malic, M.; Ayele, T.; Shaikh, S.; Chahwala, S.; Chander, C.; Holland, R.; Merette, S.; Zhao, L.; Blackney, M.; Watts, A. Studies of benzothiophene template as potent factor IXa (FIXa) inhibitors in thrombosis. *Journal of Medicinal Chemistry* **2010**, *53*, 1465-72.
- (53) Albaneze-Walker, J.; Rossen, K.; Reamer, R.A.; Volante, R.P.; Reider, P.J. Synthesis of benzofuroquinolizine for alpha-2 adrenoceptor antagonist MK-912: an O-analogue of the Pictet-Spengler reaction. *Tetrahedron Letters* **1999** *40*, 4917-20.
- (54) Kawakubo, H.; Okazaki, K.; Nagatani, T.; Takao, K.; Hasimoto, S.; Sugihara, T. Potent anticonflict activity and lessening of memory impairment with a series of novel [1]benzothieno[2,3-C]pyridines and 1,2,3,4-tetrahydro[1]benzothieno[2,3-C]pyridines. *Journal of Medicinal Chemistry* **1990** *33*, 3110-16.
- (55) Perry, N.B.; Ettouati, L.; Litaudon, M.; Blunt, J.W.; Munro, M.H.H. Alkaloids from the antarctic sponge kirkpatrickia-varialosa. 1. Variolin-b, a new antitumor and antiviral compound. *Tetrahedron* **1994**, *50*, 3987-92.
- (56) Schumacher, R.W.; Davidson, B.S. Didemnolines a-d, new N9-substituted beta-carbolines from the marine ascidian *Didemnum* sp. *Tetrahedron* **1995**, *51*, 10125-30.
- (57) Trimurtulu, G.; Faulker, D.J.; Perry, N.B.; Ettouati, L.; Litaudon, M.; Blunt, J.W.; Munro, M.H.G.; Jameson, G.B. Alkaloids from the antarctic sponge *Kirkpatrickia-varialosa*. 2. variolin-a and N(3')-methyl tetrahydrovariolin-b. *Tetrahedron* **1994**, *50*, 3993-4000.
- (58) Schafer, J.I.M.; Liu, H.; Tonetti, D.A.; Jordan, V.C. The interaction of raloxifene and the active metabolite of the antiestrogen EM-800 (SC 5705) with the human estrogen reporter. *Cancer Research* **1999**, *59*, 4308-13.
- (59) Lu, P.; Schrag, M.L.; Slaughter, D.E.; Raab, C.E.; Shou, M.; Rodrigues, A.D. Mechanism-based inhibition of human liver microsomal cytochrome P450 1A2 by zileuton, a 5-lipoxygenase inhibitor. *Drug Metabolism and Disposition* **2003**, *31*, 1352-60.
- (60) Croxtall, J.D.; Plosker, G.L. Sertaconazole: a review of its use in the management of superficial mycoses in dermatology and gynaecology. *Drugs* **2009**, *69*, 339-59.
- (61) Merour, J.Y.; Joseph, B. Synthesis and reactivity of 7-azaindoles (1H-pyrrolo[2,3-b]pyridine). *Current Organic Chemistry* **2001**, *5*, 471-506.
- (62) De Camp, W.H. The FDA perspective on the development of stereoisomers. *Chirality* **1989**, *1*, 2-6.
- (63) Murata, J.; Roepke, J.; Gordon, H.; De Luca, V. The leaf epidermone of *Catharanthus roseus* reveals its biochemical specialization. *The Plant Cell* **2008**, *20*, 524-42.
- (64) Madyastha, K.M.; Guarnaccia, R.; Baxter, C.; Coscia, C.J. S-adenosyl-L-methionine: loganic acid methyltransferase. *The Journal of Biological Chemistry* **1973**, *248*, 2497-2501.
- (65) Irmeler, S.; Schroder, G.; St-Pierre, B.; Crouch, N.P.; Hotze, M.; Schmidt, J.; Strack, D.; Matern, U.; Schroder, J. Indole alkaloid biosynthesis in *Catharanthus roseus*: new enzyme activities and identification of cytochrome P450 CYP72A1 as secologanin synthase. *The Plant Journal* **2000**, *24*, 797-804.

- (66) Schroder, G.; Unterbusch, E.; Kaltenbach, M.; Schmidt, J.; Strack, D.; De Luca, V.; Schroder, J. Light-induced cytochrome P450-dependent enzyme in indole alkaloid biosynthesis: tabersonine 16-hydroxylase. *FEBS Letters* **1999**, *458*, 97-102.
- (67) Yamamoto, H.; Katano, N.; Ooi, A.; Inoue, K. Transformation of loganin and 7-deoxyloganin into secologanin by *Lonicera japonica* cell suspension cultures. *Phytochemistry* **1998**, *50*, 417-22.
- (68) Yamamoto, H.; Katano, N.; Ooi, A.; Inoue, K. Secologanin synthase which catalyzes the oxidative cleavage of loganin into secologanin is a cytochrome P450. *Phytochemistry* **2000**, *53*, 7-12.
- (69) Chen, S.; Galan, M.C.; Coltharp, C.; O'Connor, S.E. Redesign of a central enzyme in alkaloid biosynthesis. *Chemistry and Biology* **2006**, *13*, 1137-41.
- (70) Ma, X.; Panjekar, S.; Koepke, J.; Loris, E.; Stockigt, J. The structure of *Rauvolfia serpentina* strictosidine synthase is a novel six-bladed beta-propeller fold in plant proteins. *The Plant Cell* **2006**, *18*, 907-20.
- (71) De-Eknamkul, W.; Suttipanta, N.; Kutchan, T.M. Purification and characterization of deacetylpecoside synthase from *Alangium lamarckii* Thw. *Phytochemistry* **2000**, *55*, 177-81.
- (72) Samanani, N.; Facchini, P.J. Purification and characterization of norcoclaurine synthase, the first committed enzyme in benzyloisoquinoline alkaloid biosynthesis in plants. *The Journal of Biological Chemistry* **2002**, *277*, 33878-83.
- (73) Geerlings, A.; Ibanez, M. M.; Memelink, J.; van Der Heijden, R.; Verpoorte, R. Molecular cloning and analysis of strictosidine beta-D-glucosidase, an enzyme in terpenoid indole alkaloid biosynthesis in *Catharanthus roseus*. *The Journal of Biological Chemistry* **2000**, *275*, 3051-56.
- (74) Gerasimenko, I.; Sheludko, Y.; Ma, X.; Stockigt, J. Heterologous expression of a *Rauvolfia* cDNA encoding strictosidine glucosidase, a biosynthetic key to over 2000 monoterpenoid indole alkaloids. *European Journal of Biochemistry* **2002**, *269*, 2204-13.
- (75) Warzecha, H.; Gerasimenko, I.; Kutchan, T.M.; Stoeckigt, J. Molecular cloning and functional bacterial expression of a plant glucosidase specifically involved in alkaloid biosynthesis. *Phytochemistry* **2000**, 657-66.
- (76) Barleben, L.; Panjekar, S.; Ruppert, M.; Koepke, J.; Stockigt, J. Molecular architecture of strictosidine glucosidase: the gateway to the biosynthesis of the monoterpenoid indole alkaloid family. *The Plant Cell* **2007**, *19*, 2886-97.
- (77) Heimscheidt, T.; Zenk, M.H. Glucosidases involved in indole alkaloid biosynthesis of *Catharanthus* cell culture. *Federation of the Societies of Biochemistry and Molecular Biology Letters* **1992**, *110*, 187-191.
- (78) Luijendijk, T.J.C.; Stevens, L.H.; Verpoorte, R. Purification and characterization of strictosidine beta-D-glucosidase from *Catharanthus roseus* cell suspension cultures. *Plant Physiology and Biochemistry* **1998**, *36*, 419-25.
- (79) Levac, D.; Murata, J.; Kim, W.S.; De Luca, V. Application of carborundum abrasion for investigating the leaf epidermis: molecular cloning of *Catharanthus roseus* 16-hydroxytabersonine-16-O-methyltransferase. *The Plant Journal* **2007**, *53*, 225-36.
- (80) Liscombe, D.K.; Usera, A.R.; O'Connor, S.E. A homolog of tocopherol C-methyltransferases catalyzes N-methylation in anticancer alkaloid biosynthesis. *Submitted* **2010**.
- (81) Vazquez-Flota, F.; De Carolis, E.; Alarco, A.-M.; De Luca, V. Molecular cloning and characterization of desacetoxylvindoline-4-hydroxylase, a 2-oxoglutarate dependent-

dioxygenase involved in the biosynthesis of vindoline in *Catharanthus roseus* (L.) G. Don. *Plant Molecular Biology* **1997**, *34*, 935-48.

(82) Fahn, W.; Stöckigt, J. Purification of acetyl-CoA: 17-O-deacetylvindoline 17-O-acetyltransferase from *Catharanthus roseus* leaves. *Plant Cell Reports* **1990**, *8*, 613-16.

(83) Sottomayor, M.; López-Serrano, M.; DiCosmo, F.; Barceló, R. Purification and characterization of alpha-3',4'-anhydrovinblastine synthase (peroxidase-like) from *Catharanthus roseus* (L.) G. Don. *FEBS Letters* **1998**, *428*, 299-303.

(84) Maresh, J. J.; Giddings, L. A.; Friedrich, A.; Loris, E. A.; Panjikar, S.; Trout, B. L.; Stockigt, J.; Peters, B.; O'Connor, S. E. Strictosidine synthase: mechanism of a Pictet-Spengler catalyzing enzyme. *Journal of the American Chemical Society* **2008**, *130*, 710-23.

(85) Bernhardt, P.; McCoy, E.; O'Connor, S. E. Rapid identification of enzyme variants for reengineered alkaloid biosynthesis in periwinkle. *Chemistry and Biology* **2007**, *14*, 888-97.

(86) McCoy, E.; Galan, M.C.; O'Connor, S.E. Substrate specificity of strictosidine synthase. *Bioorganic and Medicinal Chemistry Letters* **2006**, *16*, 2475-78.

(87) Galan, M.C., McCoy, E.; O'Connor, S.E. Chemoselective derivatization of alkaloids in periwinkle. *Chemical Communications* **2007**, 3249-51.

(88) Loris, E. A.; Panjikar, S.; Ruppert, M.; Barleben, L.; Unger, M.; Schubel, H.; Stockigt, J. Structure-based engineering of strictosidine synthase: auxiliary for alkaloid libraries. *Chemistry and Biology* **2007**, *14*, 979-85.

(89) Keasling, J. From yeast to alkaloids. *Nature Chemical Biology* **2008**, *4*, 524-25.

Chapter 2: Substrate Specificity and Steady State Kinetic Analysis of Strictosidine- β -Glucosidase

- I. Introduction
- II. Results
 - A. Novel deglycosylated strictosidine analogs
 - B. Steady state kinetic analysis
- III. Discussion
- IV. Materials and Methods
 - A. Synthesis of strictosidine analogs
 - B. LCMS analysis
 - C. NMR characterization
 - D. High-resolution mass spectrometry data
 - E. Assay conditions
 - F. Steady state kinetic analysis conditions
- V. Acknowledgments
- VI. References

The results described in this chapter have been reported in the following publications:

- Nancy Yerkes, Jia Xin Wu, Elizabeth McCoy, M. Carmen Galan, Shi Chen, Sarah E. O'Connor. Substrate specificity and diastereoselectivity of strictosidine glucosidase, a key enzyme in monoterpene indole alkaloid biosynthesis. *Bioorganic and Medicinal Chemistry Letters* 18 (2008) 3095-98.
- Peter Bernhardt*, Nancy Yerkes*, Sarah E. O'Connor. Bypassing stereoselectivity in the early steps of alkaloid biosynthesis. *Organic and Biomolecular Chemistry* 7 (2009) 4166-68. (*co-first authors)
- Hyang-Yeol Lee, Nancy Yerkes, Sarah E. O'Connor. Aza-tryptamine substrates in natural product biosynthesis. *Chemistry and Biology* 16 (2009) 1225-29.

I. *Introduction*

Strictosidine- β -glucosidase (SGD) is the enzyme that acts after strictosidine synthase in monoterpene indole alkaloid (TIA) biosynthesis. SGD deglycosylates the central TIA intermediate strictosidine **1**, producing a reactive aglycone **49** that can rearrange in numerous ways¹. This reactive aglycone **49** and its isomers then enter multiple biosynthetic pathways, ultimately producing hundreds of different TIAs (Figure 2-1)⁷³.

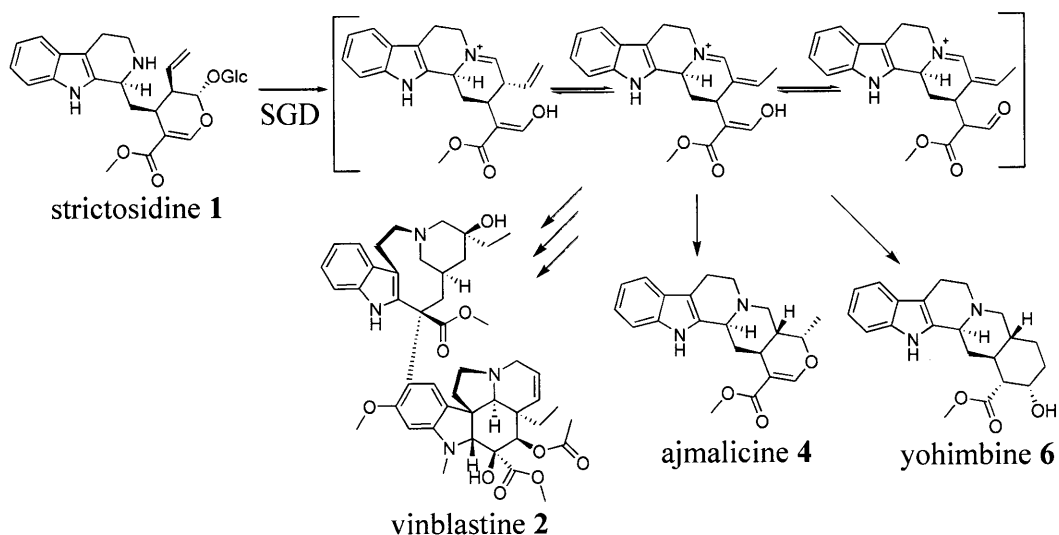


Figure 2-1: Strictosidine **1** is deglycosylated by SGD to produce a reactive hemiacetal intermediate that can rearrange in many ways. Different enzymes then act to produce hundreds of different TIAs, such as vinblastine **2**, ajmalicine **4**, and yohimbine **6**¹.

This reactive aglycone **49** forms a mixture of isomers in equilibrium, including 4,21-dehydrogeissoschizine **64** and cathenamine **49** (Figure 2). The compound 4,21-dehydrogeissoschizine **64** is a proposed intermediate for other TIAs, including the anti-cancer agents vinblastine **2** and vincristine **3**. Cathenamine **49** is reported to be the major product *in vitro* of strictosidine **1** deglycosylation by SGD (Figure 2-2)¹.

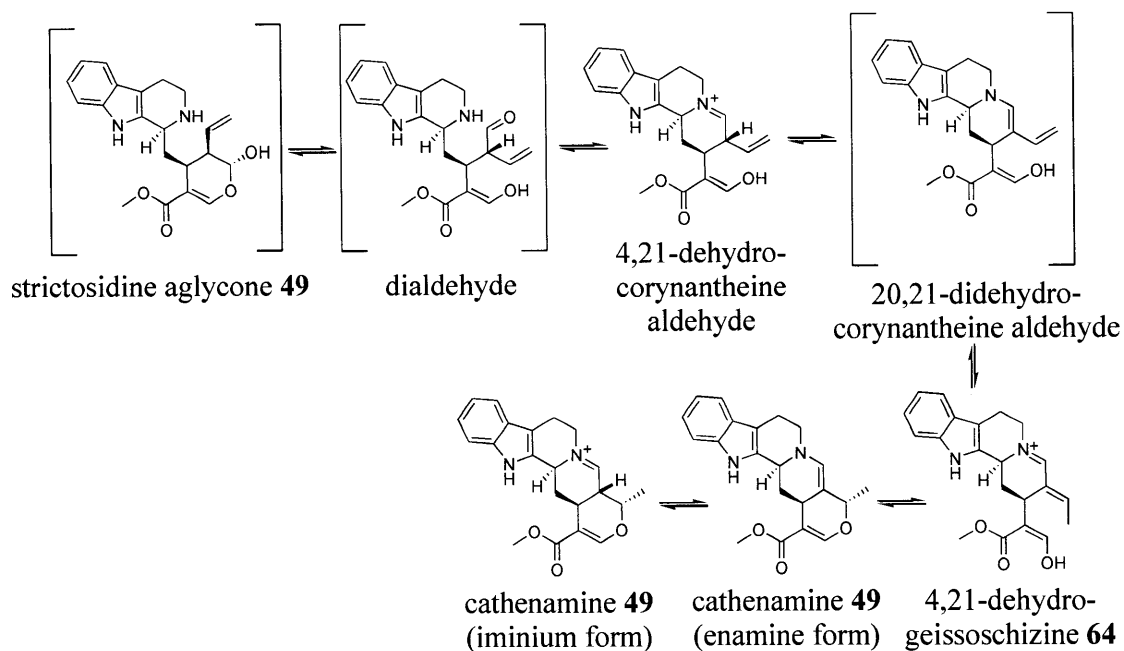


Figure 2-2: Upon deglycosylation by SGD, strictosidine **1** forms an aglycone **49** that rapidly interconverts between various isomers¹.

In 2000, a SGD cDNA clone was isolated from a *C. roseus* cDNA library, and then expressed in *Saccharomyces cerevisiae*. The recombinant SGD protein was shown specifically to deglycosylate strictosidine **1**; several other glucosides tested were not deglycosylated⁷³⁻⁷⁵. SGD can also be heterologously expressed in *E. coli*. The optimum pH of SGD from *C. roseus* was found to be between 6 and 6.4⁷⁴. It was also discovered that SGD expression could be induced by the plant hormone methyl jasmonate, which is known to increase alkaloid production when provided to *C. roseus* seedlings and cell suspension cultures⁷³.

SGD has also been cloned from *Rauvolfia serpentina*. Unlike SGD from *C. roseus*, SGD from *R. serpentina* lacks a C-terminal signal sequence predicted to direct it to the endoplasmic reticulum (ER). The *in vitro* deglycosylation of SGD from *R.*

serpentina is believed to proceed through the same mechanism as in *C. roseus*. The amino acid sequence of SGD from *R. serpentina* is 70% identical to that of the enzyme from *C. roseus*⁷⁴, though the optimum pH of SGD from *R. serpentina* was found to be between 5 and 5.2, somewhat lower than the pH optimum observed for *C. roseus*. Sequence alignment studies indicate that SGD is part of the glycosyl hydrolase family 1⁷⁶.

SGD from *R. serpentina* has been recently crystallized (PDB: 2FJ6)⁷⁶. The crystal structure of SGD from *R. serpentina* shows that this enzyme has a $(\beta/\alpha)_8$ barrel fold, 13 α -helices, and 13 β -strands. Eight parallel β -strands form a β -barrel that is the core of the structure. The β -barrel is surrounded by eight helices, and the binding site for strictosidine **1** is located in the barrel⁷⁶. At the base of the β -barrel there are several charged, hydrophilic residues that appear to interact with the glucose moiety. At the entrance of the pocket there are several hydrophobic residues – Phe-221, Trp-388, Gly-386, Met-275, Thr-210, and Met-297 – that surround the indole moiety of strictosidine **1** (Figure 2-3)⁷⁶.

The amino acid residues Glu-207 and Glu-416 are conserved in SGD and in all other glucosidases of the glycosyl hydrolase family 1. In the proposed concerted hydrolysis of strictosidine **1** deglycosylation by SGD, Glu-416 acts as a nucleophile, attacking the C-1' position of the glucose moiety of strictosidine **1**, and Glu-207 acts as a proton donor (Figure 2-3A)⁷⁶. Barleben *et al.* report that a Glu207Gln mutant had no detectable hydrolysis activity (Figure 2-3B), which suggests the importance of the Glu-207 residue in catalysis⁷⁶.

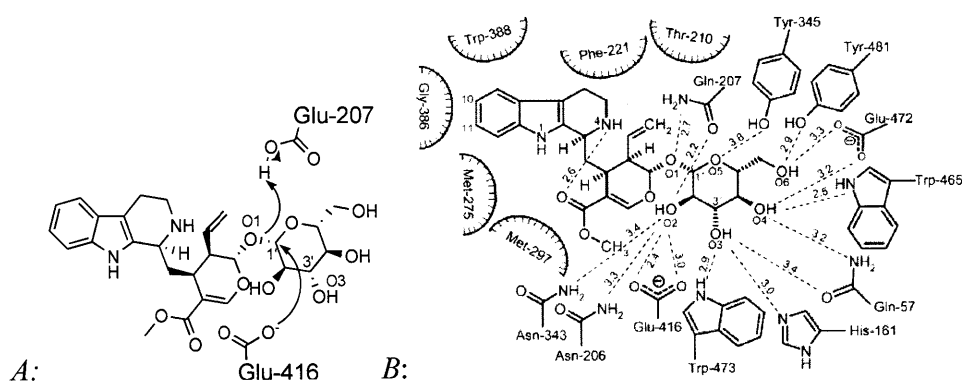


Figure 2-3: *A*: In the proposed concerted hydrolysis of strictosidine **1** deglycosylation by SGD, Glu-416 acts as a nucleophile, attacking the C-1' position of the glucose moiety of strictosidine **1**, and Glu-207 acts as a proton donor⁷⁶. *B*: Figure of the active site of the inactive SGD mutant Glu207Gln. This figure is taken from Barleben *et al.*⁷⁶

Native PAGE of *C. roseus* SGD has shown three different protein bands at approximately 250, 500, and 630 kDa. In contrast, under denaturing conditions, one protein band of 63 kDa is observed, suggesting that SGD can form aggregates of 4, 8, or 12 monomers⁷³. SGD has also been found to be glycosylated, though because recombinant protein from *E. coli* is active, glycosylation does not appear to be essential for activity⁷³.

SGD from *C. roseus* has a C-terminal KKXKX sequence that likely directs it to the ER⁷³⁻⁷⁵. An *in situ* localization method and a sucrose gradient analysis have also indicated that SGD is likely associated with the ER⁷³. In the *in situ* localization method, cells and protoplasts of *C. roseus* containing SGD activity were incubated with 2 mM strictosidine **1** and analyzed by fluorescence microscopy. Strictosidine **1** deglycosylation by SGD produces a yellow degradation product, 5,6-dihydroflavopereirine **66** (Figure 2-4), that has low solubility in water. The degradation product is derived from 4,21-

dehydrogeissoschizine **64**, which is in equilibrium with cathenamine **49**². After strictosidine **1** and SGD were incubated for ten minutes with the protoplasts, a yellow-colored degradation product, 5,6-dihydroflavopereirine **66**, appeared. Longer incubation times resulted in more intense coloration in the area where the ER is located and less dense coloration throughout the cytosol. Samples taken from the incubation mixture throughout the incubation period showed a disappearance of strictosidine **1** by HPLC, indicating SGD activity². An additional study was performed in which the SGD inhibitor D-gluconic acid δ -lactone **67** (Figure 2-4) was added. In protoplasts in which D-gluconic acid δ -lactone **67** was present, no yellow coloration was observed⁷³. In a sucrose gradient analysis of SGD in *C. roseus* lysate, SGD activity was found in the 47% sucrose fraction along with an ER marker enzyme, also suggesting that SGD is possibly associated with the ER⁷³.

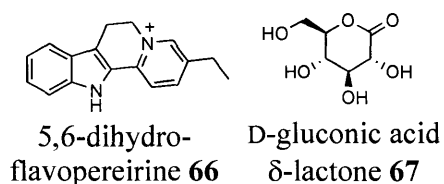


Figure 2-4: The structures of 5,6-dihydroflavopereirine **66**, a degradation product of 4,21-dehydrogeissoschizine **64**, and of D-gluconic acid δ -lactone **67**, an inhibitor of SGD².

We have hypothesized that the enzymes acting downstream of SGD are also located near the ER, because the deglycosylated strictosidine isomers are reactive and have poor solubility, thus making transportation by diffusion to other sites difficult. It is unknown whether there are specific carrier proteins for various TIA intermediates⁷³.

It was found by Gerasimenko *et al.*⁷⁴ that when SGD was incubated with *N*- β -methyl strictosidine (dolichantoside **68**), several products formed, including a product called isocorreantine A **69** (Figure 2-5). The formation of isocorreantine A **69** and not a cathenamine **49** analog led the researchers to believe that the dialdehyde intermediate produced upon deglycosylation is released from SGD and further rearrangements occur spontaneously. The researchers suggest that the divergence leading to the numerous TIA biosynthetic pathways occurs at a later stage than strictosidine deglycosylation, after the formation of 4,21-dehydrogeissoschizine **64**⁷⁴.

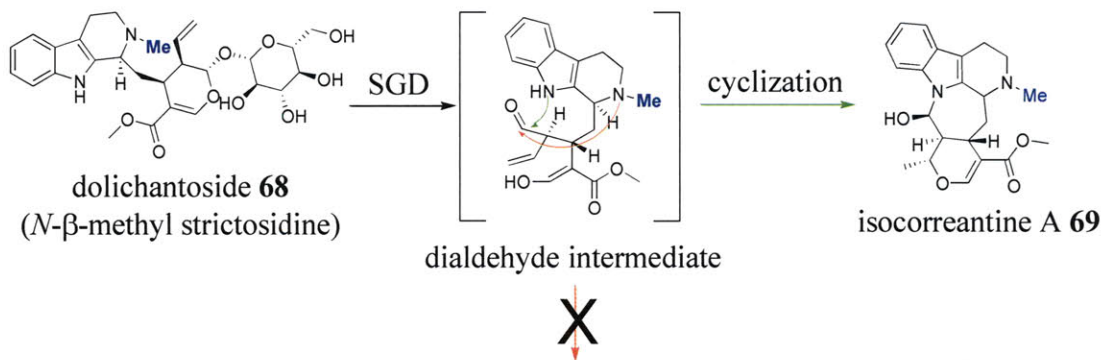


Figure 2-5: Dolichantoside **68** is *N*- β -methyl strictosidine; the methyl group that differentiates dolichantoside **68** from strictosidine **1** is labeled in blue. Dolichantoside **68** is deglycosylated by SGD to form a dialdehyde intermediate. Upon deglycosylation, the indole nitrogen attacks the aldehyde (green arrow) and then cyclizes to form isocorreantine A **69**. Attack by the methylated nitrogen (red arrow) does not occur⁷⁴.

Deglycosylation of strictosidine **1** by SGD may also play a role in *C. roseus* plant cell defense. The aglycone **65** produced by strictosidine **1** deglycosylation by SGD has been shown to have anti-microbial activity against a number of microorganisms⁷⁶. Though its detailed ecological relevance is not clear, this is not an unprecedented finding:

many glucosidases found in other plants also have defense-related functions. Deglycosylation in a variety of other plants leads to the formation of toxic or bitter small molecules that are known to be defensive, such as isothiocyanates⁹⁰, DIMBOA⁹¹, or cyanide⁹².

Strictosidine **1** is a unique central intermediate. It is rare for a glucoside to act as a precursor at the beginning of a biosynthetic pathway, and for the precursor to become activated by deglycosylation. Glucosides more typically appear in natural product biosyntheses at the end of biosynthetic pathways, acting as a means of converting end products into water-soluble compounds. Once water-soluble, the end products can easily be stored in plant vacuoles. SGD is thus a unique glucoside in that it has both defensive and synthetic importance⁷⁶.

Besides SGD, there are only two other examples of biosynthetic pathways in which a glucosidase has synthetic relevance. In isoquinoline alkaloid biosynthesis, the central intermediate glucosides deacetylisopecoside **45** and deacetylpecoside **46** are deglycosylated (Figure 2-6)⁹³ and then go on to form numerous isoquinoline alkaloids. In lignin biosynthesis, the glucoside coniferin **70** (Figure 2-6) is deglycosylated to form coniferyl alcohol⁹⁴, which is a precursor to lignin⁷⁶.

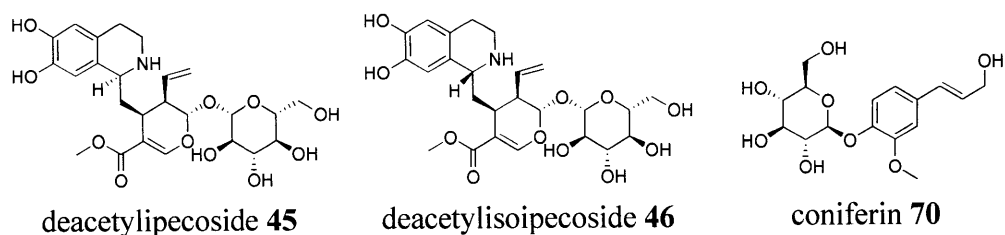


Figure 2-6: The structures of glucosides deacetylpecoside **45**, deacetylisoipecoside **46**, and coniferin **70**.

Numerous tryptamine **18** and secologanin **17** analogs have been reported to be accepted by strictosidine synthase to form strictosidine **1** analogs^{36,86,87}, and directed biosynthesis studies have shown that the TIA pathway can produce a variety of novel alkaloids by utilizing nonnatural substrate analogs³⁴. For novel alkaloids derived from strictosidine **1** analogs to be produced, these analogs must be accepted by SGD. This chapter discusses my work in determining which strictosidine **1** analogs are accepted by SGD. I assayed a broad scope of strictosidine **1** analogs containing modified indole, methyl ester, vinyl, and glucose moieties, as well as the diastereomer of strictosidine **1**, vincoside **43**. I also performed steady state kinetic analysis on numerous substrates to determine whether SGD acts as a bottleneck in the production of novel alkaloids.

II. Results

Strictosidine analogs

To determine whether SGD acts as a gatekeeper in the production of novel TIAs, I synthesized a broad array of strictosidine **1** analogs in one step from tryptamine and secologanin analogs (Figure 2-7 – Figure 2-9). To determine the substrate specificity of SGD, I altered numerous moieties of strictosidine **1**, including the indole ring, methyl ester, and glucose moieties. I modified numerous positions, including the C-20 vinyl position, the C-5 α position, and the C-3 position. Further details on the synthesis and characterization of all strictosidine **1** analogs described herein are in the Materials and Methods section.

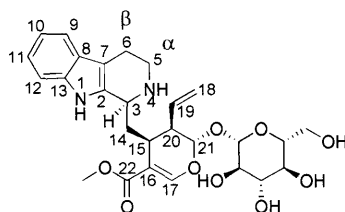


Figure 2-7: Structure of strictosidine **1**, with the numbering system shown in blue. The 5 position is commonly referred to as the α position, and the 6 position is commonly referred to as the β position⁹⁵.

The indole substituted strictosidine analogs synthesized included 9-fluoro **1-c**, 10-fluoro **1-d**, 11-fluoro **1-e**, 12-fluoro **1-f**, 9-methyl **1-g**, 10-methyl **1-h**, 11-methyl **1-i**, 12-methyl **1-j**, 9-chloro **1-k**, 10-chloro **1-l**, 12-chloro **1-m**, 9-bromo **1-n**, 10-bromo **1-o**, 10-hydroxy **1-p**, 10-isopropyl **1-q**, 10-methoxy **1-r**, and 11-methoxy **1-s** (Figure 2-7, Figure 2-8).

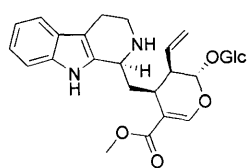
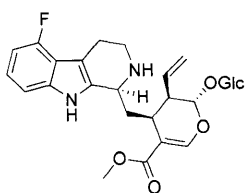
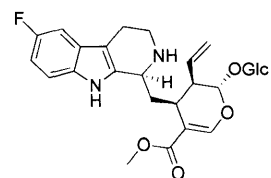
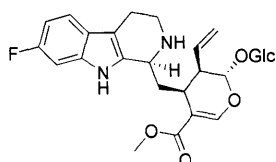
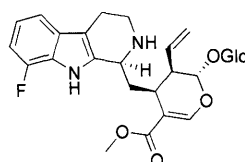
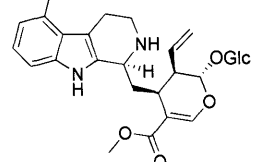
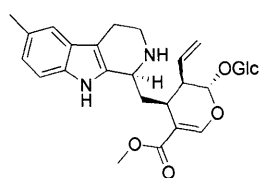
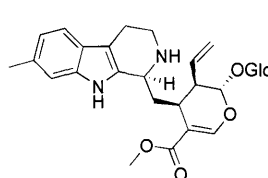
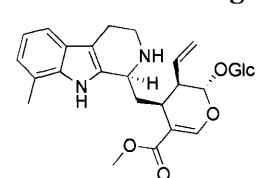
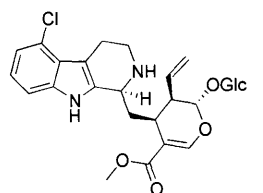
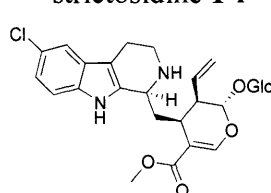
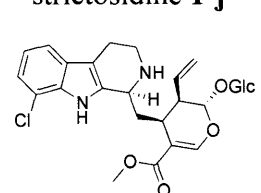
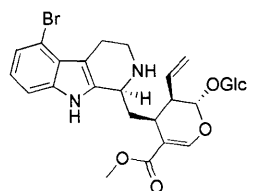
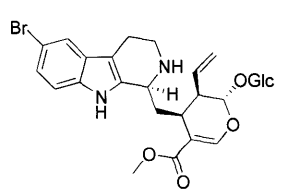
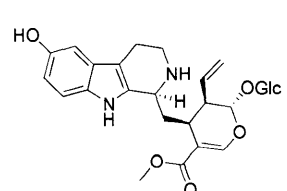
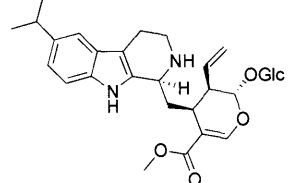
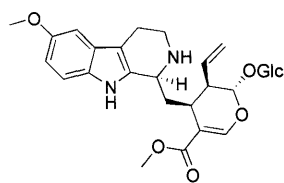
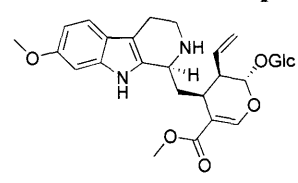
strictosidine **1**9-fluoro
strictosidine **1-c**10-fluoro
strictosidine **1-d**11-fluoro
strictosidine **1-e**12-fluoro
strictosidine **1-f**9-methyl
strictosidine **1-g**10-methyl
strictosidine **1-h**11-methyl
strictosidine **1-i**12-methyl
strictosidine **1-j**9-chloro
strictosidine **1-k**10-chloro
strictosidine **1-l**12-chloro
strictosidine **1-m**9-bromo
strictosidine **1-n**10-bromo
strictosidine **1-o**10-hydroxy
strictosidine **1-p**10-isopropyl
strictosidine **1-q**10-methoxy
strictosidine **1-r**11-methoxy
strictosidine **1-s**

Figure 2-8: The structures of strictosidine **1** and indole substituted strictosidine analogs **1-c** through **1-s**.

In addition to indole substituted strictosidine **1** analogs, I also synthesized isotopically labeled d_4 strictosidine **1-1**, vincoside **43**, d_4 vincoside **43-1**, pentynyl-ester strictosidine **1-t**, 10-fluoro- α -methyl strictosidine **1-u**, α -dimethyl strictosidine **1-v**, 9-aza strictosidine **1-w**, 12-aza strictosidine **1-x**, benzo strictosidine **1-a**, and thio strictosidine **1-b** (Figure 2-9). I also chemically synthesized a diastereomeric mixture **45-1** of deacetylipecoside and deacetyloisopecoside isomers from dopamine and secologanin. Because the products could not be separated and thus completely characterized, despite extensive efforts, it is possible that an alternate regioisomer is also present in this mixture (Figure 2-9, **45-1**). Hereafter, the mixture of all these various isomers will be called “deacetylipecosides **45-1**” (Figure 2-9). Dr. Peter Bernhardt generously provided des-vinyl strictosidine isomers **1-y**, as well as a diastereomerically pure des-vinyl strictosidine isomer produced enzymatically with strictosidine synthase **1-z** (Figure 2-9).

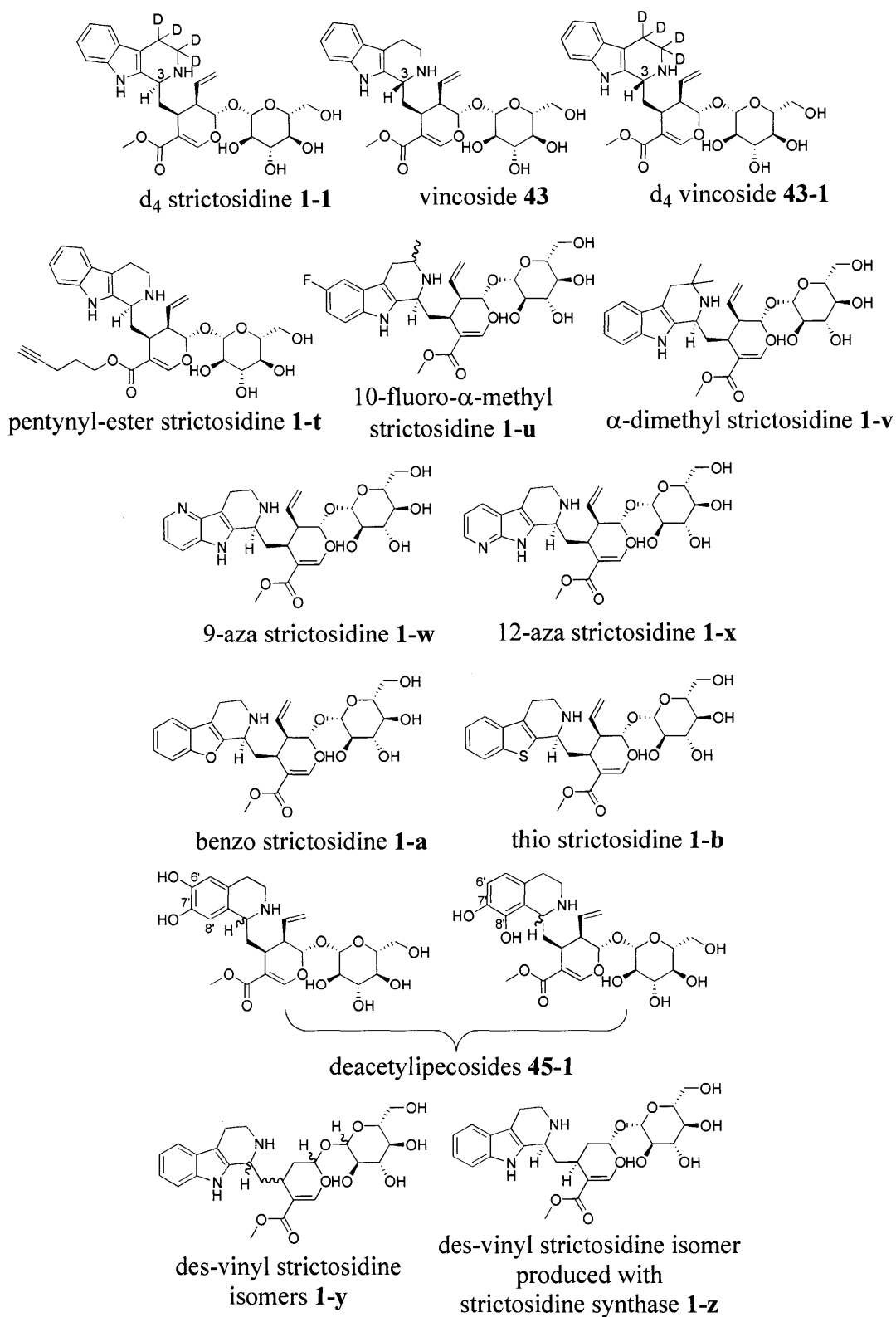


Figure 2-9: The structures of d₄ strictosidine **1-1**, vincoside **43**, d₄ vincoside **43-1**, pentynyl-ester strictosidine **1-t**, 10-fluoro- α -methyl strictosidine **1-u**, α -dimethyl strictosidine **1-v**, 9-aza strictosidine **1-w**, 12-aza strictosidine **1-x**, benzo strictosidine **1-a**, thio strictosidine **1-b**, deacetylipecosides **45-1**, des-vinyl strictosidine isomers **1-y**, and des-vinyl strictosidine isomer produced with strictosidine synthase **1-z**. The C-3 position of vincoside **43**⁹⁵ and the 6', 7' and 8' positions of deacetylipecosides **45-1**⁹⁶, are labeled in blue.

SGD Assay

SGD from *C. roseus* was expressed in *E. coli* as an N-terminal maltose-binding protein (MBP) or as a C-terminal hexa-His-tag fusion using a codon-optimized synthetic gene. To assay SGD activity, strictosidine analogs **1-a** through **1-z** were incubated with SGD in 0.15 M citrate phosphate buffer, pH 6. Three analytical methods were used to detect SGD activity: LCMS, HPLC, and a colorimetric glucose-detection assay. With both LCMS and HPLC, disappearance of strictosidine **1** analog and formation of deglycosylated strictosidine **49** analog could be observed (Figure 2-10, Figure 2-11). A glucose-detection assay with the Amplex® Red Glucose/Glucose Oxidase Assay Kit from Invitrogen was used as further verification of SGD activity; upon deglycosylation the free glucose is oxidized by glucose oxidase. The H₂O₂ that results reacts with Amplex® Red and horseradish peroxidase to generate a fluorescent compound, resorufin.

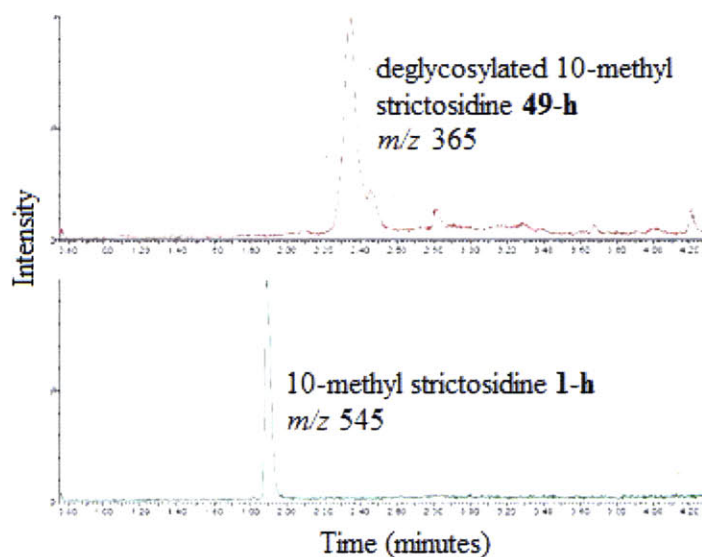


Figure 2-10: Representative assay using LCMS. Selected ion chromatograms of an assay of 10-methyl strictosidine **1-h** with SGD showing starting material and product.

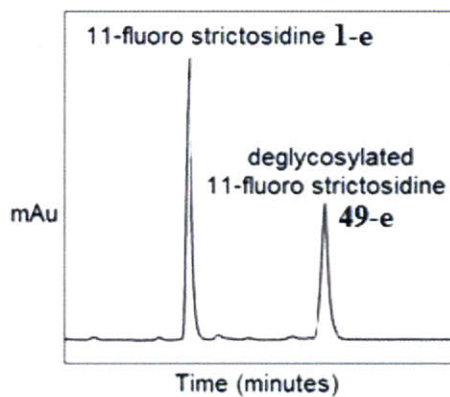


Figure 2-11: Representative assay using HPLC. HPLC chromatogram of an assay of 11-fluoro strictosidine **1-e** with SGD, with the absorbance at 238 nm measured.

A. *Novel deglycosylated strictosidine analogs*

LCMS analysis showed that SGD was able to deglycosylate all the indole substituted strictosidine **1** analogs shown in Figure 2-8, as well as 10-fluoro- α -methyl

strictosidine **1-u** and α -dimethyl strictosidine **1-v**. This result contrasts with that of strictosidine synthase, the enzyme acting before SGD, which does not accept 5-methyl tryptamine **18-h**, 5-methoxy tryptamine **18-s**, or α -dimethyl tryptamine **18-v**^{70,86,88}. SGD is apparently more tolerant than strictosidine synthase for substitutions at the C-5 and C-10 positions. That all indole substituted strictosidine **1** analogs are accepted by SGD is exciting for the prospect of producing novel downstream TIAs with improved biological activities. Fluorination, for example, is reported to improve metabolic stability by making nearby moieties less susceptible to oxidation by cytochrome P450s⁴⁸. Fluorination, chlorination, bromination, and methylation are all reported to increase the lipophilicity of compounds, facilitating the penetration of membranes. Hydroxylation and methoxylation can improve the water solubility of compounds, facilitating diffusion in the cytosol.

Pentynyl-ester strictosidine **1-t** was also accepted, indicating that the SGD active site can tolerate much larger groups than a methyl ester. I used pentynyl-ester strictosidine **1-t** in crosslinking studies, which are described in Chapter 4.

SGD could deglycosylate strictosidine analogs containing alternate heterocyclic moieties: 9-aza strictosidine **1-w**, 12-aza strictosidine **1-x**, benzo strictosidine **1-a**, and thio strictosidine **1-b** (Figure 2-12) were all accepted by SGD. I assayed 9-aza strictosidine **1-w**, 12-aza strictosidine **1-x**, benzo strictosidine **1-a**, and thio strictosidine **1-b** in order to explore what effect, if any, the decreased electron density of the analogs would have on deglycosylation. Numerous compounds containing aza, benzofuran, and benzothiophene moieties have been reported to have intriguing biological properties^{53,54,55-57}, including the drugs raloxifene⁵⁸, zileuton⁵⁹, and sertaconazole⁶⁰. If the aza **1-w** and **1-x**, benzo **1-a**, and thio **1-b** strictosidine analogs are accepted by SGD and

by enzymes farther downstream, perhaps novel TIAs with altered biological properties could be produced. For example, aza compounds are reported to have high water solubility and unique hydrogen-bonding properties⁶¹.

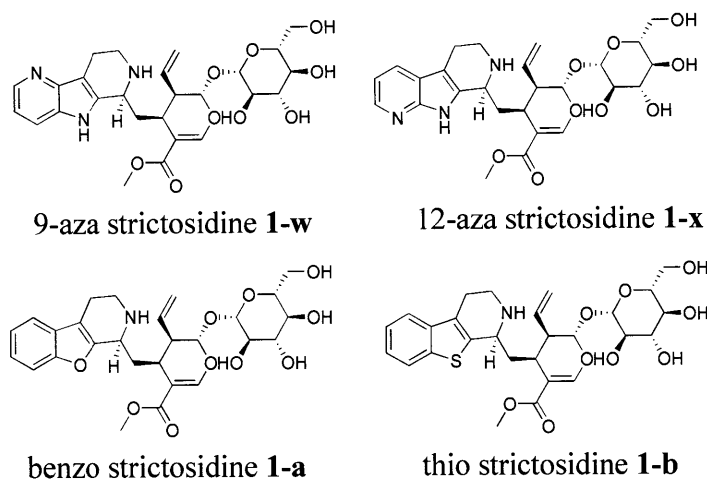


Figure 2-12: Structures of 9-aza strictosidine **1-w**, 12-aza strictosidine **1-x**, benzo strictosidine **1-a**, and thio strictosidine **1-b**.

The mixture of isomers of deacetylpecosides **45-1** are also accepted by SGD; LCMS analysis clearly showed the formation of deglycosylated deacetylpecoside isomers, along with the disappearance of the starting material (Figure 2-13). Deacetylpecosides **45-1** are produced enzymatically by deacetylpecoside synthase and deacetylisoipecoside synthase⁷¹, two of the few enzymes currently known to be functionally related to strictosidine synthase⁷². Deacetylpecoside synthase and deacetylisoipecoside synthase catalyze the condensation of tryptamine **18** and dopamine **44**, leading to the family of monoterpene tetrahydroisoquinoline alkaloids. I investigated deacetylpecosides **45-1** as potential substrates for deglycosylation by SGD because of the potential of using deglycosylated deacetylpecosides as substrates for later

TIA biosynthetic enzymes⁷⁰. Because SGD was able to deglycosylate various deacetylpecoside isomers **45-1**, perhaps later biosynthetic enzymes can produce novel TIA analogs from these substrates.

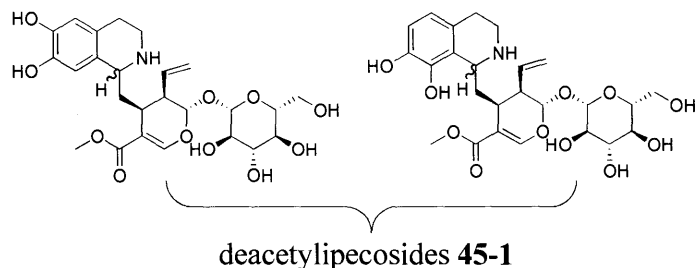


Figure 2-13: Structure of deacetylpecosides **45-1**.

SGD from *C. roseus* also deglycosylates vincoside **43**, the C-3 diastereomer of strictosidine **1**, and d₄-vincoside **43-1** (Figure 2-14). This is intriguing, because vincoside **43** is not accepted by SGD from *R. serpentina*⁷⁴. To verify this surprising finding, a glucose-detection assay was also used in addition to LCMS analysis. This finding is encouraging because it suggests that downstream alkaloids containing alternate stereochemistries can be produced. Different stereoisomers can have different pharmacological profiles⁶², and perhaps downstream alkaloids containing *R* stereochemistry at the C-3 position will have different pharmacological properties than the natural alkaloids with *S* stereochemistry at the C-3 position.

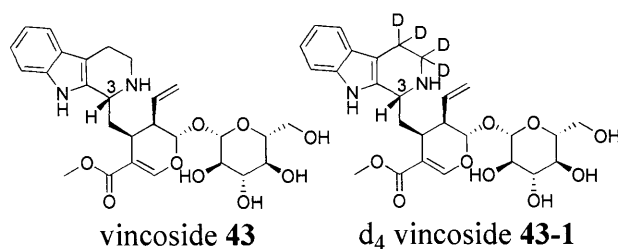


Figure 2-14: Structures of vincoside **43** and d₄ vincoside **43-1**.

I performed additional analysis of strictosidine **1** analogs with alternate stereochemistry using a mixture of des-vinyl strictosidine isomers **1-y** synthesized by Dr. Peter Bernhardt (Figure 2-15)⁹⁷. Using LCMS, this mixture was separated into six peaks. A single diastereomer of des-vinyl strictosidine analog **1-z** was also synthesized enzymatically using strictosidine synthase. This enzymatically synthesized analog **1-z** co-elutes with peak 3 of the des-vinyl strictosidine mixture **1-y** (Figure 2-15 and Figure 2-16).

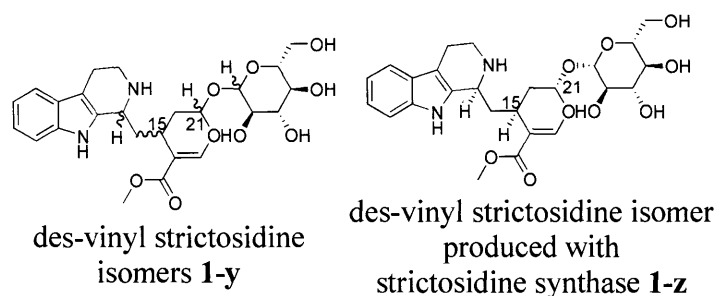


Figure 2-15: Structure of des-vinyl strictosidine isomers **1-y** and of the enzymatically produced des-vinyl strictosidine isomer **1-z**, with the C-15 and C-21 positions labeled in blue.

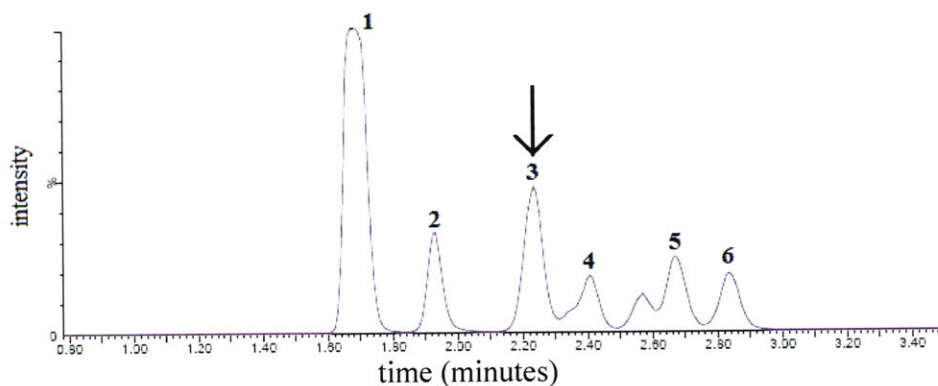


Figure 2-16: LCMS trace of the des-vinyl strictosidine mixture **1-y**. Peak 3 (indicated with an arrow) co-elutes with the des-vinyl strictosidine analog **1-z** produced enzymatically with strictosidine synthase.

When SGD was incubated with the des-vinyl strictosidine mixture **1-y**, LCMS analysis of the starting material showed a decrease in area of only two of the separable six peaks, peaks 1 and 3 (Figure 2-16). Peak 3 co-elutes with the strictosidine synthase-formed des-vinyl strictosidine analog **1-z**, suggesting that the compound with natural C15/21 *trans* stereochemistry is turned over by SGD. The observed deglycosylation of various des-vinyl strictosidine isomers indicates that SGD does not require a vinyl moiety on strictosidine **1** for turnover.

To fully explore the stereochemical promiscuity of downstream enzymatic reactions, however, complete deglycosylation of the des-vinyl strictosidine mixture **1-y** is required. (Figure 2-16 and Figure 2-17). Because it has been previously shown that strictosidine **1** can be deglycosylated by bacterial glucosidases⁹⁸, I examined whether two commercially available glucosyl hydrolases, *Bacillus stearothermophilus* α -glucosidase and almond β -glucosidase, display different deglycosylation patterns than SGD does. Both an α -glucosidase and a β -glucosidase were chosen because the mixture of des-vinyl

strictosidine isomers **1-y** contains both α and β anomers, and complete deglycosylation of the mixture was desired. *B. stearothermophilus* α -glucosidase is specific for terminal α -1,4 bonds of maltosaccharides and α -glucans⁹⁹. Almond- β -glucosidase is a well-studied¹⁰⁰ retaining glucosidase that has a broad substrate specificity; it is often assayed with aryl-glucosides^{100,101}.

Almond- β -glucosidase was considerably more permissive than SGD, consuming four out of the six peaks in the chromatogram, peaks 1, 3, 5, and 6 (Figure 2-17). *B. stearothermophilus* α -glucosidase facilitated the consumption of two peaks that were not converted by either β -glucosidase, peaks 2 and 4 (Figure 2-17). Based on these data, we hypothesize that peak 1, peak 3, and peak 6 contain mainly β -anomers, while peaks 2 and 4 contain mainly α -anomers. Peak 5 appears to contain both α - and β -anomers. SGD therefore appears to be more specific for its substrate strictosidine **1**, while the two commercially available glucosidases likely have active sites that allow a greater diversity of substrates to be accepted. By using glucosidases from different metabolic pathways, it is possible to bypass the native biosynthetic pathway to fully deglycosylate the des-vinyl strictosidine mixture **1-y**.

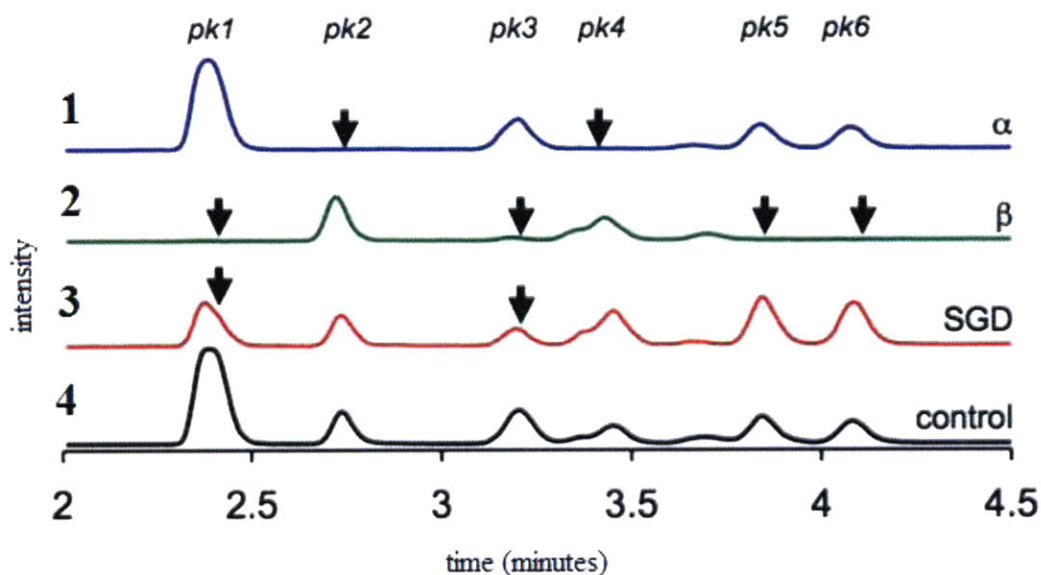


Figure 2-17: Chromatogram 1: Des-vinyl strictosidine mixture **1-y** subjected to deglycosylation by *B. stearothermophilus* α -glucosidase (blue trace). Chromatogram 2: Des-vinyl strictosidine mixture **1-y** subjected to deglycosylation by almond β -glucosidase (green trace). Chromatogram 3: Des-vinyl strictosidine mixture **1-y** subjected to deglycosylation by *C. roseus* SGD (red trace). Chromatogram 4: Des-vinyl strictosidine mixture **1-y** without glucosidase (black trace). Black downward arrows indicate peaks that have decreased in area due to consumption by the glucosidase.

B. Steady state kinetic analysis

Not all substrate analogs are incorporated into the TIA pathway with equal efficiency⁸⁷. If substrate specificity of individual biosynthetic enzymes correlates with rate-limiting steps *in vivo*, then enzymes having a low catalytic efficiency for a nonnatural substrate could be reengineered to improve turnover of the analog. Therefore, evaluation of enzyme substrate specificity is crucial for biosynthetic engineering efforts. To determine quantitatively whether SGD acts as a bottleneck for the production of

various indole-substituted TIA analogs or TIA analogs with altered stereochemistry, I performed steady state kinetic analysis studies with the indole substituted strictosidine analogs **1-d**, **1-e**, **1-g**, **1-h**, **1-i**, **1-j**, **1-r**, and **1-s**, d₄ strictosidine **1-1**, and the C-3 diastereomer of d₄ strictosidine **1-1**, d₄ vincoside **43-1**. The indole substituted strictosidine analogs were chosen as representative examples to determine the effects of indole substituents on strictosidine deglycosylation by SGD.

To assess the catalytic efficiency of SGD, I incubated strictosidine **1** analogs with SGD in 0.15 M citrate phosphate buffer, pH 6. I determined kinetic constants by monitoring strictosidine **1** analog deglycosylation by HPLC or LCMS. Substrate disappearance was measured instead of product formation because of the many rapidly interconverting isomers that are produced by strictosidine **1** analogs upon deglycosylation. These rapidly interconverting isomers prevented accurate quantification of the product.

Since all steady state kinetic data (Table 2-1) appeared to fit a sigmoidal rather than a Michaelis-Menten curve, kinetic constants (half-saturation value $K_{0.5}$, maximum velocity V_{\max})¹⁰² were obtained from a sigmoidal fit to the data. SGD from *C. roseus* has been reported to form aggregates consisting of 4-12 monomers; although a sigmoidal fit has not been previously reported for *C. roseus* SGD, the oligomeric state of the enzyme is compatible with the cooperative mechanism suggested by the sigmoidal curve. Hill coefficients were also obtained for each analog; however, no correlation between the substitution and the Hill coefficient was observed (Table 2-1).

With indole substituted strictosidine analogs **1-d**, **1-e**, **1-g**, **1-h**, **1-i**, **1-j**, **1-r**, and **1-s**, the catalytic efficiencies ($V_{\max}/K_{0.5}$) varied by less than an order of magnitude from naturally occurring strictosidine **1** (Table 2-1). Strictosidine analogs with methyl groups in the 9, 10, 11, and 12 positions **1-g** through **1-j** demonstrated that steric effects did not disrupt enzyme activity dramatically. Not surprisingly, replacement of methyl groups with larger methoxy substituents **1-r** and **1-s** resulted in a small increase in the $K_{0.5}$ values. Electronic perturbations did not appear to impact the turnover profoundly; the catalytic efficiencies of the fluorinated strictosidine analogs **1-d** and **1-e** (relative $V_{\max}/K_{0.5}$ of 0.7 for both 10-fluoro strictosidine **1-d** and 11-fluoro strictosidine **1-e**) did not vary significantly from that of naturally occurring strictosidine **1**.

Strictosidine Substrate	$K_{0.5}$ (mM)	V_{\max} (mM/min)	Relative $V_{\max}/K_{0.5}$	Hill coefficient
strictosidine 1	0.22 ± 0.009	0.078 ± 0.002	1	1.8 ± 0.1
9-methyl 1-g	0.22 ± 0.02	0.018 ± 0.0003	0.2	3.3 ± 0.9
10-methyl 1-h	0.071 ± 0.002	0.016 ± 0.0005	0.6	7.9 ± 2.0
11-methyl 1-i	0.092 ± 0.003	0.017 ± 0.0001	0.5	3.3 ± 0.2
12-methyl 1-j	0.14 ± 0.01	0.016 ± 0.0007	0.3	2.0 ± 0.4
10-methoxy 1-r	0.37 ± 0.03	0.035 ± 0.001	0.3	4.3 ± 1.5
11-methoxy 1-s	0.43 ± 0.05	0.037 ± 0.003	0.2	2.3 ± 0.7
10-fluoro 1-d	0.15 ± 0.01	0.038 ± 0.002	0.7	2.2 ± 0.4
11-fluoro 1-e	0.12 ± 0.01	0.032 ± 0.001	0.7	2.4 ± 0.6

Table 2-1: Kinetic data and Hill coefficients of the indole substituted strictosidine **1** analogs deglycosylated by SGD.

d_4 Strictosidine **1-1** had a catalytic efficiency ($V_{\max}/K_{0.5}$) 6-fold higher than that of d_4 vincoside **43-1** (Table 2-2). The crystal structure of SGD from *R. serpentina* shows that the C-3 of strictosidine **1** is located near the surface of SGD⁷³. We speculate that the orientation of the glucose **50** moiety, which is in the interior of SGD, remains unchanged

during turnover, while the binding pocket for more distal regions of the substrate, such as the C-3 position, can accommodate vincoside **43**.

Substrate	$K_{0.5}$ (mM)	V_{\max} (mM/min)	Hill coefficient
d_4 vincoside 43-1	0.19 ± 0.10	0.012 ± 0.002	0.9 ± 0.3

Table 2-2: Kinetic data for d_4 vincoside **43-1** deglycosylation by SGD.

III. Discussion

Substrate specificity studies:

I assayed numerous strictosidine **1** analogs with SGD (Figure 2-8, Figure 2-9), and all were deglycosylated: this indicates that SGD is promiscuous in regard to substrate turnover. The analogs tested included substitutions at the indole positions (C-9, C-10, C-11, C-12), the α position (C-5), the C-3 position, the N-1 position, the vinyl position (C-20), the methyl ester, and the anomeric position (C-21).

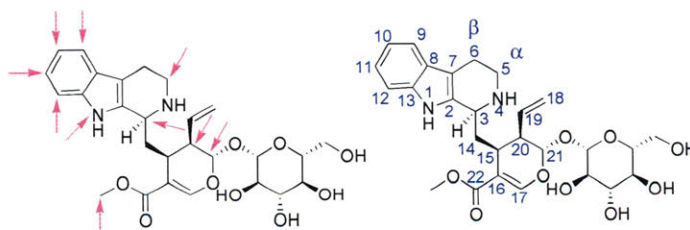


Figure 2-18: Strictosidine **1**, with pink arrows indicating positions at which strictosidine **1** was modified and with the numbering system shown in blue⁹⁵.

All C-9 through C-12 indole substituted strictosidine **1** analogs were accepted by SGD. The recently reported crystal structure of SGD from *R. serpentina* indicates that whereas the glucose **50** moiety of strictosidine **1** is buried within the enzyme active site,

the indole portion of strictosidine **1** is located near the surface of the enzyme (Figure 2-19). Although the crystal structure of SGD is static, and does not show strictosidine **1** movement in the active site, the crystallographic data were consistent with the observed turnover of all indole substituted strictosidine **1** analogs tested by SGD. The finding that all indole substituted strictosidine **1** analogs are accepted by SGD agrees with the results of a precursor directed biosynthesis study performed in which fluorinated, chlorinated, brominated, methylated, and methoxylated indole substituted tryptamine **18** or strictosidine **1** analogs were co-cultured with hairy root cultures³⁶. In the study, alkaloids downstream of SGD were observed for all analogs, indicating that each analog is deglycosylated by SGD *in vivo*^{34,36}.

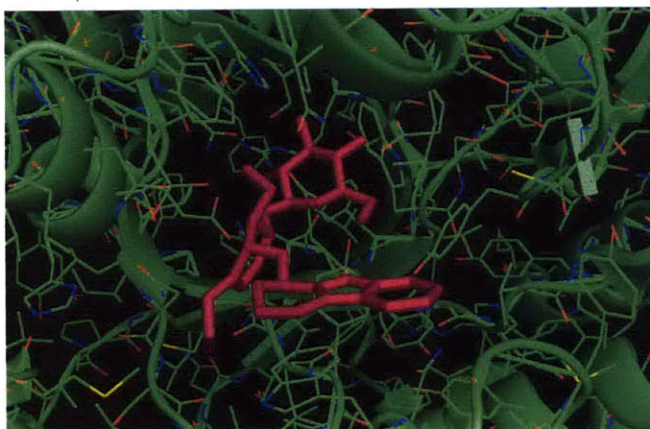


Figure 2-19: Structure of SGD (green) with strictosidine **1** (pink) bound in the active site⁷⁶.

Steady state kinetic analysis of indole substituted strictosidine **1** analogs revealed that the methylated strictosidine analogs **1-g** through **1-j** each had relative catalytic efficiencies (V_{\max}/K_m) between 0.2 and 0.6 (with the catalytic efficiency of strictosidine **1** normalized to 1), with 10-methyl **1-h** and 11-methyl **1-i** strictosidine analogs having

catalytic efficiencies of 0.6 and 0.5, respectively. The 10-methoxy **1-r** and 11-methoxy **1-s** strictosidine analogs had catalytic efficiencies of 0.3 and 0.2, respectively, and 10-fluoro **1-d** and 11-fluoro **1-e** strictosidine analogs each had catalytic efficiencies of 0.7. These results indicate that for C-10 and C-11 substituted strictosidine **1** analogs, the size of the substituent at the C-10 and C-11 positions was directly correlated to the catalytic efficiency: the largest substituent, the methoxy moiety, was accepted less efficiently than the methyl moiety, which was accepted less efficiently than the smallest substituent, the fluorine moiety.

SGD could also deglycosylate strictosidine **1** analogs containing substitutions at the C-5, or α , position. The finding that strictosidine **1** analogs containing substitutions at the C-5 position can be accepted by SGD also agrees with the results of a previous precursor directed biosynthesis study. Bernhardt *et al.*⁸⁵ report that *C. roseus* hairy root cultures co-cultured with (5*R*)-hydroxymethyl strictosidine **1-u-1** produced (5*R*)-hydroxymethyl isositsirikine **7-u-1**, which shows that (5*R*)-hydroxymethyl strictosidine **1-u-1** is deglycosylated by SGD *in vivo*.

SGD can also deglycosylate a strictosidine analog **1-t** in which the methyl ester is replaced by a pentynyl ester. The finding that pentynyl-ester strictosidine **1-t** can be deglycosylated by SGD *in vitro* agrees with an *in vivo* precursor directed biosynthesis study in which pentynyl-ester secologanin **54** co-cultured with hairy root cultures produced pentynyl-ester serpentine, which indicates that pentynyl-ester strictosidine **1-t** is deglycosylated by SGD *in vivo*⁸⁷. In the precursor directed biosynthesis study, however, a significant accumulation of pentynyl-ester strictosidine **1-t** was observed⁸⁷. Strictosidine **1** is not normally a major product in hairy root cultures, and thus an accumulation of

pentynyl-ester strictosidine **1-t** indicates that pentynyl-ester strictosidine **1-t** is not being deglycosylated by SGD at the usual rate. I confirmed this finding when I attempted a steady state kinetic analysis of SGD with pentynyl-ester strictosidine **1-t**. I did not observe any turnover of pentynyl-ester strictosidine **1-t** with the conditions used for the steady state kinetic analysis of strictosidine analogs **1-d**, **1-e**, **1-g**, **1-h**, **1-i**, **1-j**, **1-r**, and **1-s**, in which the SGD concentration was approximately 0.6 nM. I observed deglycosylation only when the SGD concentration was increased from approximately 0.6 nM to 50 μ M, an increase of more than ten-thousand fold. This slow deglycosylation is most likely caused by steric clashes of the pentynyl group with the surrounding enzyme residues.

Benzo strictosidine **1-a** and thio strictosidine **1-b** were also accepted by SGD, indicating that SGD is able to turn over substrates containing alternate heterocycles. Examination of the crystal structure of SGD from *R. serpentina*⁷⁶ reveals that the indole nitrogen of strictosidine **1** is located approximately 6.5 Å from Leu-475, 4.3 Å from Tyr-481, and 7 Å from Tyr-345 (Figure 2-20). The van der Waals radii of oxygen and sulfur are 1.50 Å and 1.80 Å, respectively¹⁰³; thus there is sufficient space in the active site both to accommodate the heteroatom oxygen, which has a slightly smaller van der Waals radius than nitrogen, and also to accommodate the heteroatom sulfur, which has a van der Waals radius that is approximately 15% larger than that of nitrogen. The closest residue to the indole nitrogen is Tyr-481, and the 4.3 Å distance between the Tyr-481 hydroxyl and the indole nitrogen of strictosidine is sufficient to accommodate replacement of the indole nitrogen with the larger sulfur heteroatom. The electronic perturbations of the alternate heterocycles do not appear to affect deglycosylation. The turnover of these

analogs **1-a** and **1-b** also suggests that there is no hydrogen bonding interaction between the enzyme and the indole nitrogen that is critical for substrate turnover. The compounds 9-aza strictosidine **1-w** and 12-aza strictosidine **1-x** were also accepted by SGD. Nitrogen has a smaller van der Waals radius than carbon, and thus steric effects should not prevent turnover of 9-aza strictosidine **1-w** and 12-aza strictosidine **1-x** by SGD. Although alternate electronic properties could potentially prevent turnover, this was not observed: both 9-aza strictosidine **1-w** and 12-aza strictosidine **1-x** were deglycosylated by SGD. Although rates were not quantified for these particular substrates, the turnover of these substrates agrees with precursor directed biosynthesis studies showing that 9-aza strictosidine **1-w**, 12-aza strictosidine **1-x**, and benzo strictosidine **1-a** are all deglycosylated by SGD; in the precursor directed biosynthesis study, 12-aza strictosidine **1-x** and benzo strictosidine **1-a** were incorporated to form 12-aza isositsirikine **7-x** and benzo isositsirikine **7-a**^{36,104}.

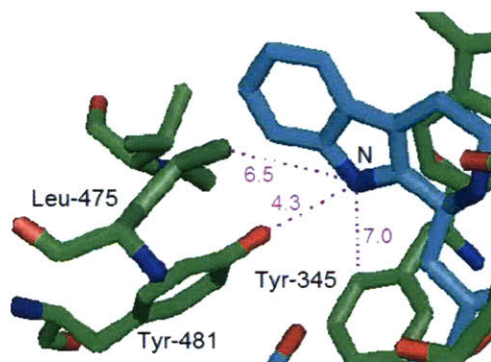


Figure 2-20: The crystal structure of *R. serpentina* SGD⁷⁶, with the indole nitrogen of strictosidine **1** (dark blue) and the residues Leu-475, Tyr-481, and Tyr-345 labeled. Distances (Å) between the indole nitrogen and the various residues are shown in purple.

Strictosidine synthase is absolutely stereoselective. The vincoside **43** diastereomer is not formed enzymatically in any known TIA pathway. Although SGD from *R. serpentina* is not reported to turn over the vincoside **43** diastereomer⁷⁴, SGD from *C. roseus* does in fact turn over the “nonnatural” vincoside **43**, as evidenced by consumption of starting material and detection of the glucose **50** product. Inspection of the SGD sequence from *R. serpentina* did not reveal any obvious differences in the strictosidine **1** binding site, so the structural basis for the difference in diastereoselectivity between the two enzymes remains to be determined⁷⁶.

In contrast to the relaxed substrate specificity observed for strictosidine analogs **1-a** through **1-x**, strictosidine isomers containing an α glucose linkage were not accepted by SGD; the β anomer was found to be absolutely required for turnover by SGD. When SGD was incubated with the mixture of des-vinyl strictosidine isomers **1-y**, LCMS analysis of the starting material showed a decrease in area of only two of the separable six peaks, peaks 1 and 3 (Figure 2-16). Peak 3 co-elutes with naturally occurring strictosidine **1**, suggesting that the compound with natural C15/21 *trans* stereochemistry is turned over. SGD does not appear to be able to deglycosylate any α anomers of strictosidine **1**.

SGD could deglycosylate various isomers in the deacetylipecoside mixture **45-1**; several deglycosylated products were observed by LCMS. Detailed characterization of the starting material and deglycosylated products was difficult, since despite extensive efforts, the isomers of the deacetylipecoside mixture could not be separated. Nevertheless, it was clear that deacetylipecoside isomers **45-1** were consumed by SGD and thus the deglycosylation of various deacetylipecoside isomers **45-1** by SGD is further

evidence that the indole moiety of strictosidine **1** is not an important recognition element for turnover by SGD. The finding that deacetylpecoside isomers **45-1** can be deglycosylated by SGD is encouraging, for perhaps downstream TIAs can be produced containing this altered structure. Downstream TIAs produced from deacetylpecoside isomers **45-1** could potentially have excellent solubility and hydrogen bonding-properties.

Conclusions

Strictosidine **1**, the central intermediate of TIA biosynthesis, is deglycosylated by SGD to produce a reactive hemiacetal intermediate that can enter numerous biosynthetic pathways. For a novel TIA to be produced from a strictosidine **1** analog, the strictosidine **1** analog must be deglycosylated by SGD. My studies show that SGD does not appear to be a bottleneck in the production of novel TIAs. SGD deglycosylated all indole strictosidine **1** analogs assayed, as well as C-5 substituted analogs, 10-fluoro- α -methyl strictosidine **1-u**, and α -dimethyl strictosidine **1-v**. SGD can also deglycosylate strictosidine **1** analogs such as benzo strictosidine **1a** and thio strictosidine **1b** that contain alternate heterocycles such as benzofuran and benzothiophene moieties, respectively. Atoms can be removed from the strictosidine structure, as in des-vinyl strictosidine **1-y-z**, or can be added, as in pentynyl-ester strictosidine **1-t**. SGD is also not selective for the natural stereoisomer; the C-3 diastereomer of strictosidine, vincoside **43**, is accepted by SGD. The primary recognition element appeared to be the β glucose linkage. This broad substrate specificity is promising for the development of novel TIAs with improved or altered biological properties. A number of serpentine **5**, ajmalicine **4**, isositsirikine **7**, and akuammicine **63** analogs produced from the TIA pathway are

currently undergoing screening for cytotoxic activity (Usera, Lee, O'Connor, unpublished).

IV. *Materials and Methods*

A. *Synthesis of strictosidine analogs*

Secologanin **17** was purified by procedures developed by the O'Connor laboratory¹⁰⁵. Briefly, *Lonicera tatarica* leaves (100g, stored at -80°C) were ground in methanol and filtered through cheesecloth. The filtrate was then pre-absorbed onto silica gel and dried under vacuum overnight. Column chromatography was then performed using a gradient of methanol and dichloromethane. Secologanin **17** elutes at a ratio of approximately 10% methanol to 90% dichloromethane, and was concentrated *in vacuo*. Secologanin **17** was then further purified by reverse-phase chromatography using a methanol and water gradient. Secologanin **17** elutes at approximately 30% methanol: 70% water. Purified secologanin **17** was then frozen at -80°C and lyophilized. For every 100 g of leaves, approximately 1 g of secologanin **17** was obtained. Reverse-phase chromatography is necessary in the secologanin **17** purification to separate secologanin **17** from the compound sweroside **71** (Figure 2-21). Sweroside **71** elutes closely to secologanin¹⁰⁶.

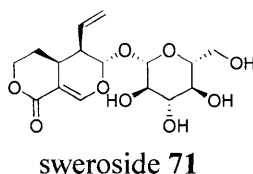


Figure 2-21: Structure of sweroside **71**¹⁰⁶.

All tryptamine **18** analogs used for the synthesis of strictosidine analogs in the substrate specificity study were obtained from Sigma, with the exception of 4-methyl, 7-methyl, 4-fluoro, 7-fluoro, 4-chloro, 7-chloro, 4-bromo, and 5-isopropyl tryptamines,

which were provided by Dr. Elizabeth McCoy³⁶, and d₄-tryptamine, which was obtained from CDN Isotopes.

Indole substituted strictosidine **1** analogs were synthesized by incubating secologanin **17** and tryptamine **18** in an enzymatic reaction with strictosidine synthase for approximately 3 hours at 30°C in pH 6, 0.15 M citrate phosphate buffer (Figure 2-22). As previously described^{85,86}, strictosidine synthase was expressed in *E. coli* BL21(DE3) cells with a C-terminal hexa-histidine tag and purified with cobalt-nickel resin. The resulting strictosidine **1** analogs were purified by preparatory HPLC. A 15-minute method with a 10 to 40% gradient of acetonitrile in 0.1% formic acid was used, with detection at 238 nm. The strictosidine **1** analogs typically eluted at approximately 30% acetonitrile.

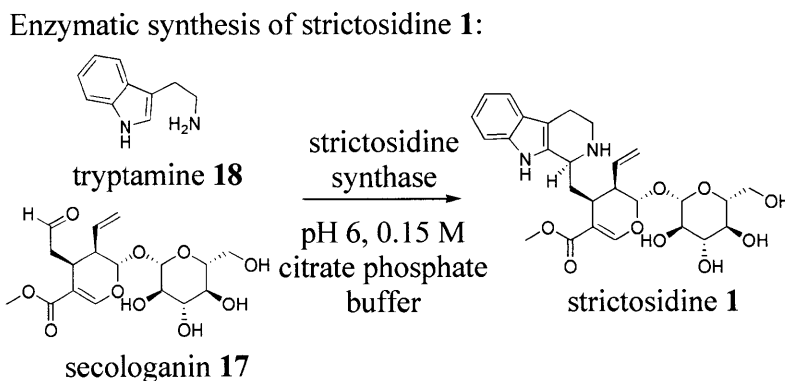


Figure 2-22: Strictosidine **1** is produced enzymatically with strictosidine synthase by incubating secologanin **17** and tryptamine **18** in 0.15 M citrate phosphate buffer, pH 6.

A chemical, nonenzymatic reaction was used for those tryptamine **18** substrates that are known not to be accepted by strictosidine synthase or that are turned over slowly^{85,86} (Figure 2-23). Substrates made via the chemical reaction include vincoside **43**, d₄-vincoside **43-1**, and 10-methyl **1-h**, 11-methyl **1-i**, 10-fluoro **1-d**, 11-fluoro **1-e**, 9-

chloro **1-k**, 10-chloro **1-l**, 12-chloro **1-m**, 9-bromo **1-n**, 10-bromo **1-o**, 10-hydroxy **1-p**, 10-isopropyl **1-q**, 10-methoxy **1-r**, 11-methoxy **1-s**, 10-fluoro- α -methyl **1-u**, and α -dimethyl **1-v** strictosidine. In the chemical reaction, secologanin **17** and the tryptamine **18** analog were incubated in pH 2, 0.1 M maleic acid at 30°C overnight. Both strictosidine **1** and its C-3 diastereomer vincoside **43** (Figure 2-23) are produced in the chemical reaction. Strictosidine **1** has *S* stereochemistry at the C-3 position, and vincoside **43** has *R* stereochemistry at the C-3 position. The resulting strictosidine **1** analogs could be purified and separated from the vincoside **43** analogs by preparatory HPLC. A 15-minute method with a 10 to 40% gradient of acetonitrile in 0.1% formic acid was used, with detection at 238 nm. The strictosidine **1** analogs typically eluted at approximately 30% acetonitrile. The vincoside **43** analogs typically eluted at approximately 35% acetonitrile.

Chemical synthesis of strictosidine **1**:

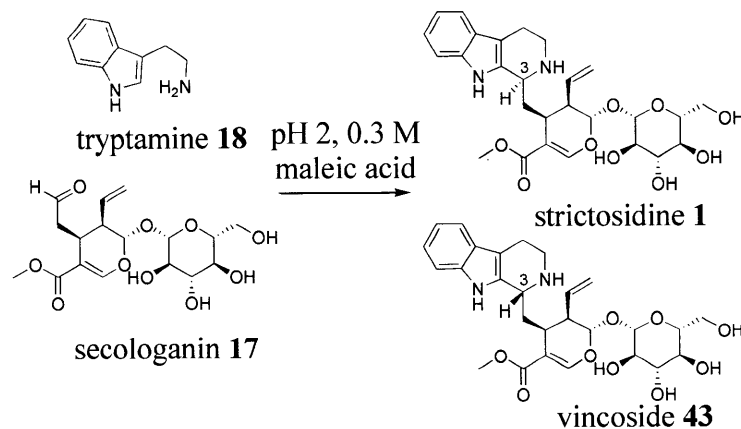


Figure 2-23: In the chemical reaction to form strictosidine **1**, tryptamine **18** and secologanin **17** are incubated in 0.3 M maleic acid, pH 2. Strictosidine **1** and its C-3 diastereomer vincoside **43** are formed from the chemical reaction. Strictosidine **1** has *S* stereochemistry at the C-3 position, and vincoside **43** has *R* stereochemistry at the C-3 position. The C-3 position of strictosidine **1** and vincoside **43** are labeled in blue.

The resulting strictosidine **1** analogs were purified by preparatory HPLC. A 15-minute method with a 10 to 40% gradient of acetonitrile in 0.1% formic acid was used, with detection at 238 nm. The strictosidine **1** analogs typically eluted at approximately 30% acetonitrile.

Pentynyl-ester strictosidine **1-t** was synthesized enzymatically by incubating pentynyl-ester secologanin **54** and tryptamine **18** with strictosidine synthase. Pentynyl-ester secologanin **54** was synthesized according to previously published procedures^{87,105}. Pentynyl-ester strictosidine **1-t** was purified by preparatory HPLC using the same method as for indole strictosidine **1** analog purification.

The compounds 9-aza strictosidine **1-w**, 12-aza strictosidine **1-x**, benzo strictosidine **1-a**, and thio strictosidine **1-b** were all made in an enzymatic reaction with strictosidine synthase. The compounds 9-aza strictosidine **1-w** and 12-aza strictosidine **1-x** were synthesized by Dr. Hyang-Yeol Lee by incubation of strictosidine synthase, secologanin **17**, and 4-aza tryptamine or 7-aza tryptamine, respectively¹⁰⁴. Benzo strictosidine **1-a** was synthesized enzymatically with strictosidine synthase, secologanin **17**, and 2-benzofuran-3-yl-ethylamine **61** (Figure 2-24). Thio strictosidine **1-b** was synthesized enzymatically with strictosidine synthase, secologanin **17**, and 2-benzo[*b*]thiophen-3-yl-ethylamine **62** (Figure 2-24). The compound 2-benzofuran-3-yl-ethylamine **61** was synthesized by reducing benzofuran-3-acetonitrile with LiAlH₄ in THF⁸⁶. The compound 2-benzo[*b*]thiophen-3-yl-ethylamine **62** was synthesized by reducing benzo(B)thiophene-3-acetonitrile with LiAlH₄ in THF⁸⁶. Benzo strictosidine **1-a** and thio strictosidine **1-b** were purified by preparatory HPLC using the same method as described for indole strictosidine **1** analog purification.

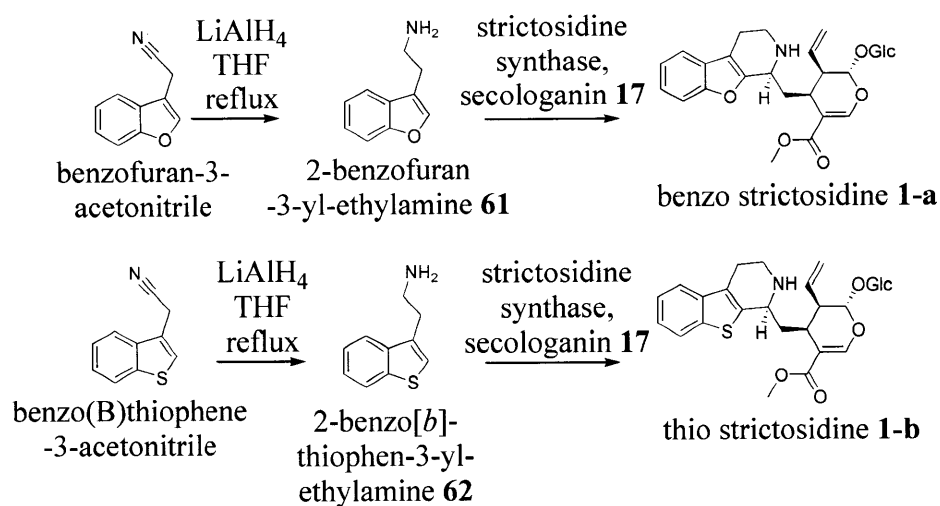


Figure 2-24: Benzofuran-3-acetonitrile and benzo(B)thiophene-3-acetonitrile are reduced with LiAlH_4 in THF to produce 2-benzofuran-3-yl-ethylamine **61** and 2-benzo[b]-thiophen-3-yl-ethylamine **62**, respectively, which are incubated with secologanin **17** and strictosidine synthase to form benzo strictosidine **1-a** and thio strictosidine **1-b**, respectively⁸⁶.

Deacetylipecosides **45-1** were produced in a chemical reaction by incubating dopamine **44** and secologanin **17** in pH 2, 0.1 M maleic acid. The mixture of isomers was purified by preparatory HPLC using the same method as for indole strictosidine **1** analog purification. The different isomers of the mixture could not be separated, and the resulting mixture was referred to as “deacetylipecosides **45-1**”.

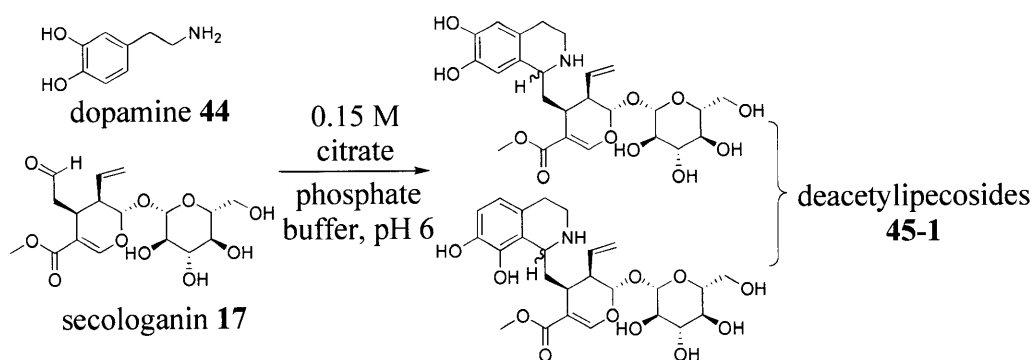


Figure 2-25: Dopamine **44** and secologanin **17** condense in a nonenzymatic reaction to form a mixture of deacetylpecoside isomers, called “deacetylpecosides **45-1**.”

The mixture of des-vinylated strictosidine analogs **1-y** and the des-vinyl strictosidine analog produced with strictosidine synthase **1-z** (Figure 2-9) were both synthesized and characterized by Dr. Peter Bernhardt⁹⁷.

All strictosidine **1** analogs purified were characterized by high-resolution mass spectrometry. Most were also previously characterized by ¹H NMR, as previously reported^{36,85,87,104} and described below. Deglycosylated strictosidine **49** analogs were characterized by high-resolution mass spectrometry; characterization by ¹H NMR was impeded because deglycosylated strictosidine **49** exists as a mixture of isomers that interconvert rapidly and are difficult to separate.

B. LCMS analysis

Ultra-performance LC analysis was performed on an Acquity Ultra Performance BEH C18 column with a 1.7 μm particle size, a 2.1 \times 100 mm dimension, and a flow rate of 0.5 mL min⁻¹ in tandem with a Micromass LCT Premier TOF Mass Spectrometer with an ESI Source (Waters Corporation). The capillary and sample cone voltages were 3000V and 30V, respectively. The desolvation and source temperatures were 300°C and

100°C, respectively. The cone and desolvation gas-flow rates were 60 l hr⁻¹ and 8000 l hr⁻¹. Analysis was performed with MassLynx 4.1.

C. NMR characterization

Proton nuclear magnetic resonance (¹H NMR) spectra were recorded on a Varian 300 MHz spectrometer. Chemical shifts (δ) were referenced to residual protium in the NMR solvent. ¹H NMR data has been previously reported for strictosidine analogs **1-a** through **1-v**³⁶, **1-w** and **1-x**¹⁰⁴, and **1-y** and **1-z**⁹⁷.

D. High-resolution mass spectrometry data

High-resolution mass spectrometry data were obtained using either the O'Connor lab LCMS or the MIT DCIF mass spectrometry equipment. Samples were diluted in methanol and then ionized by ESI using a Micromass LCT Premier TOF Mass Spectrometer. The LC was performed on an Acquity Ultra Performance BEH C18 column. MassLynx 4.1 was used for analysis, and accurate mass measurements were obtained in W-mode, with reserpine as a reference. With the MIT DCIF mass spectrometry equipment, the samples were diluted in methanol and then ionized by ESI/FT-MS in the positive ion mode.

Secologanin analogs

pentynyl-ester secologanin **54**: [M+H]⁺ expected 441.1761, observed 441.1787

Strictosidine analogs

strictosidine **1**: [M+H]⁺ expected 531.2343, observed 531.2327

d₄ strictosidine **1-1**: [M+H]⁺ expected 535.2588, observed 535.2569

benzo strictosidine **1-a**: $[M+H]^+$ expected 532.2177, observed 532.2186

thio strictosidine **1-b**: $[M+H]^+$ expected 548.1949, observed 548.1943

9-fluoro strictosidine **1-c**: $[M+H]^+$ expected 549.2248, observed 549.2259

10-fluoro strictosidine **1-d**: $[M+H]^+$ expected 549.2248, observed 549.2220

11-fluoro strictosidine **1-e**: $[M+H]^+$ expected 549.2248, observed 549.2240

12-fluoro strictosidine **1-f**: $[M+H]^+$ expected 549.2248, observed 549.2232

9-methyl strictosidine **1-g**: $[M+H]^+$ expected 545.2499, observed 545.2482

10-methyl strictosidine **1-h**: $[M+H]^+$ expected 545.2499, observed 545.2474

11-methyl strictosidine **1-i**: $[M+H]^+$ expected 545.2499, observed 545.2482

12-methyl strictosidine **1-j**: $[M+H]^+$ expected 545.2499, observed 545.2498

9-chloro strictosidine **1-k**: $[M+H]^+$ expected 565.1947, 565.1986

10-chloro strictosidine **1-l**: $[M+H]^+$ expected 565.1947, observed 565.1918

12-chloro strictosidine **1-m**: $[M+H]^+$ expected 565.1947, observed 565.1953

9-bromo strictosidine **1-n**: $[M+H]^+$ expected 609.1442, 609.1458

10-bromo strictosidine **1-o**: $[M+H]^+$ expected 609.1442, observed 609.1450

10-hydroxy strictosidine **1-p**: $[M+H]^+$ expected 367.1652, observed 367.1648

10-isopropyl strictosidine **1-q**: $[M+H]^+$ expected 393.2173, observed 393.2181

10-methoxy strictosidine **1-r**: [M+H]⁺ expected 561.2448, observed 561.2452

11-methoxy strictosidine **1-s**: [M+H]⁺ expected 561.2448, observed 561.2430

pentynyl-ester strictosidine **1-t**: [M+H]⁺ expected 583.2656, observed 583.2687

10-fluoro- α -methyl strictosidine **1-u**: expected 563.2399, observed 563.2412

α -dimethyl strictosidine **1-v**: expected 559.2650, observed 559.2637

enzymatically formed des-vinyl strictosidine **1-z**: [M+H]⁺ expected 505.2181, observed 505.2180

vincoside **43**: [M+H]⁺ expected 531.2343, observed 531.2356

deacetylpecosides **45-1**: [M+H]⁺ expected 524.2126, 524.2113

Deglycosylated strictosidine analogs

deglycosylated strictosidine **49**: [M+H]⁺ expected 351.1709, observed 351.1711

deglycosylated d₄ strictosidine **49-1**: [M+H]⁺ expected 355.1954, observed 355.1939

deglycosylated benzo strictosidine **49-a**: [M+H]⁺ expected 352.1543, observed 352.1546

deglycosylated thio strictosidine **49-b**: [M+H]⁺ expected 368.1315, observed 368.1324

deglycosylated 9-fluoro strictosidine **49-c**: [M+H]⁺ expected 369.1614, observed 369.1612

deglycosylated 10-fluoro strictosidine **49-d**: [M+H]⁺ expected 369.1614, observed 369.1623

deglycosylated 11-fluoro strictosidine **49-e**: $[M+H]^+$ expected 369.1614, observed 369.1623

deglycosylated 12-fluoro strictosidine **49-f**: $[M+H]^+$ expected 369.1614, observed 369.1603

deglycosylated 9-methyl strictosidine **49-g**: $[M+H]^+$ expected 365.1865, observed 365.1887

deglycosylated 10-methyl strictosidine **49-h**: $[M+H]^+$ expected 365.1865, observed 365.1887

deglycosylated 11-methyl strictosidine **49-i**: $[M+H]^+$ expected 365.1865, observed 365.1863

deglycosylated 12-methyl strictosidine **49-j**: $[M+H]^+$ expected 365.1865, observed 365.1885

deglycosylated 9-chloro strictosidine **49-k**: $[M+H]^+$ expected 385.1313, observed 385.1346

deglycosylated 10-chloro strictosidine **49-l**: $[M+H]^+$ expected 385.1313, observed 385.1300

deglycosylated 12-chloro strictosidine **49-m**: $[M+H]^+$ expected 385.1313, observed 385.1325

deglycosylated 9-bromo strictosidine **49-n**: $[M+H]^+$ expected 429.0808, observed 429.0795

deglycosylated 10-bromo strictosidine **49-o**: $[M+H]^+$ expected 429.0808, observed 429.0808

deglycosylated 10-hydroxy strictosidine **49-p**: $[M+H]^+$ expected 367.1652, observed 367.1648

deglycosylated 10-isopropyl strictosidine **49-q**: $[M+H]^+$ expected 573.2807, observed 573.2822

deglycosylated 10-methoxy strictosidine **49-r**: $[M+H]^+$ expected 381.1814, observed 381.1823

deglycosylated 11-methoxy strictosidine **49-s**: $[M+H]^+$ expected 381.1814, observed 381.1802

deglycosylated pentynyl-ester strictosidine **49-t**: $[M+H]^+$ expected 403.2022, observed 403.2047

deglycosylated 10-fluoro- α -methyl strictosidine **49-u**: expected 383.1765, observed 383.1750

deglycosylated α -dimethyl strictosidine **49-v**: expected 379.2016, observed 379.2016

deglycosylated deacetylipecosides **49-45-1**: $[M+H]^+$ expected 344.1492, observed 344.1496.

deglycosylated vincoside: $[M+H]^+$ expected 351.1709, observed 351.1722.

E. Assay conditions

SGD was expressed in *E. coli* as an N-terminal maltose-binding protein (MBP) or as a C-terminal hexa-His-tag fusion using a codon-optimized synthetic gene. The MBP fusion was used for the determination of all kinetic constants. In assays to detect SGD activity, strictosidine analogs were incubated at 30°C in pH 6, 0.15 M citrate phosphate buffer for 5 to 10 minutes. Three methods of detection were used: LCMS, HPLC, and a glucose **50** detection kit.

In the LCMS assay, aliquots from the enzymatic reaction were quenched with methanol, centrifuged (13,000g, 1 min) to remove particulates, and then analyzed by LCMS. The starting material and products were separated using a gradient of 10-40% acetonitrile in water with 0.1% formic acid over a period of 5 minutes.

In the HPLC assay, cathenamine **49** formation and strictosidine **1** disappearance were both observed. Aliquots from the assay were quenched with methanol, centrifuged (13,000g, 1 min) to remove particulates, and then analyzed by HPLC. The starting material and products were separated using a gradient of 10-90% acetonitrile in water with 0.1% trifluoroacetic acid over a period of 15 minutes, with detection at 238 nm.

A glucose **50** detection assay was used as further verification that vincoside **43** is deglycosylated by SGD. The glucose detection assay monitored the formation of glucose **50**, one of the products of strictosidine deglycosylation by SGD. In the glucose detection assay, the Amplex® Red Glucose/Glucose Oxidase Assay Kit from Invitrogen was used (Figure 2-26). Glucose formation was monitored at 560 nm using a reaction solution made from glucose oxidase, horseradish peroxidase, and Amplex® Red according to the

manufacturer's instructions (Figure 2-26). Upon deglycosylation, glucose was released. A coupled assay reaction with glucose oxidase and horseradish peroxidase converted Amplex® Red to a fluorescent compound, resorufin¹⁰⁷.

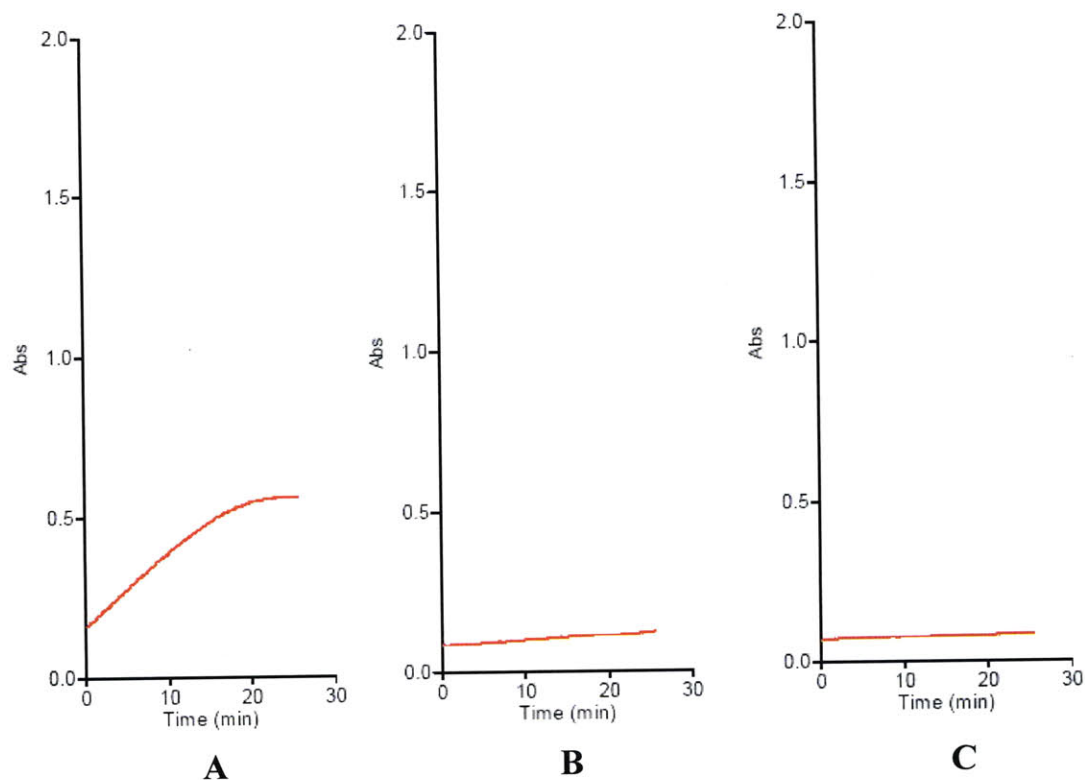


Figure 2-26: Representative UV-visible time courses at 560 nm of the glucose **50** detection assay. **A:** Vincoside **43** incubated with SGD and all components of the Amplex® Red assay. **B:** Vincoside **43** and all components of the enzyme assay without SGD. **C:** Vincoside **43** and SGD without components of the Amplex® Red assay (Amplex® Red, glucose oxidase, and horseradish peroxidase).

F. *Steady state kinetic analysis conditions*

Steady state kinetic analysis conditions for indole substituted strictosidine analogs 1, 1-d, 1-e, 1-g, 1-h, 1-i, 1-j, 1-r, and 1-s

Quantitative steady state kinetic analysis assays for SGD with indole substituted strictosidine analogs **1**, **1-d**, **1-e**, **1-g**, **1-h**, **1-i**, **1-j**, **1-r**, and **1-s** were performed at pH 6, the optimal pH of the enzyme^{73,74}, in 0.15 M citrate phosphate buffer. Assays were conducted at 37°C in the presence of 0.61 nM SGD. Nine or more substrate concentrations were used for each analog, and six time points were measured for each substrate concentration. An HPLC assay was used to monitor strictosidine **1** consumption at 238 nm with naphthalene acetic acid as an internal standard. The concentration of all strictosidine **1** analogs was determined with a standard curve. A logistic curve using OriginPro 7 (OriginLab, Northampton, MA) was used to fit the data, and R^2 values ranged from 0.979 to 0.999. A sigmoidal curve was observed for SGD expressed both as an N-terminal maltose-binding protein fusion and as a C-terminal His-tag fusion, indicating that a specific affinity tag does not significantly alter the kinetic parameters.

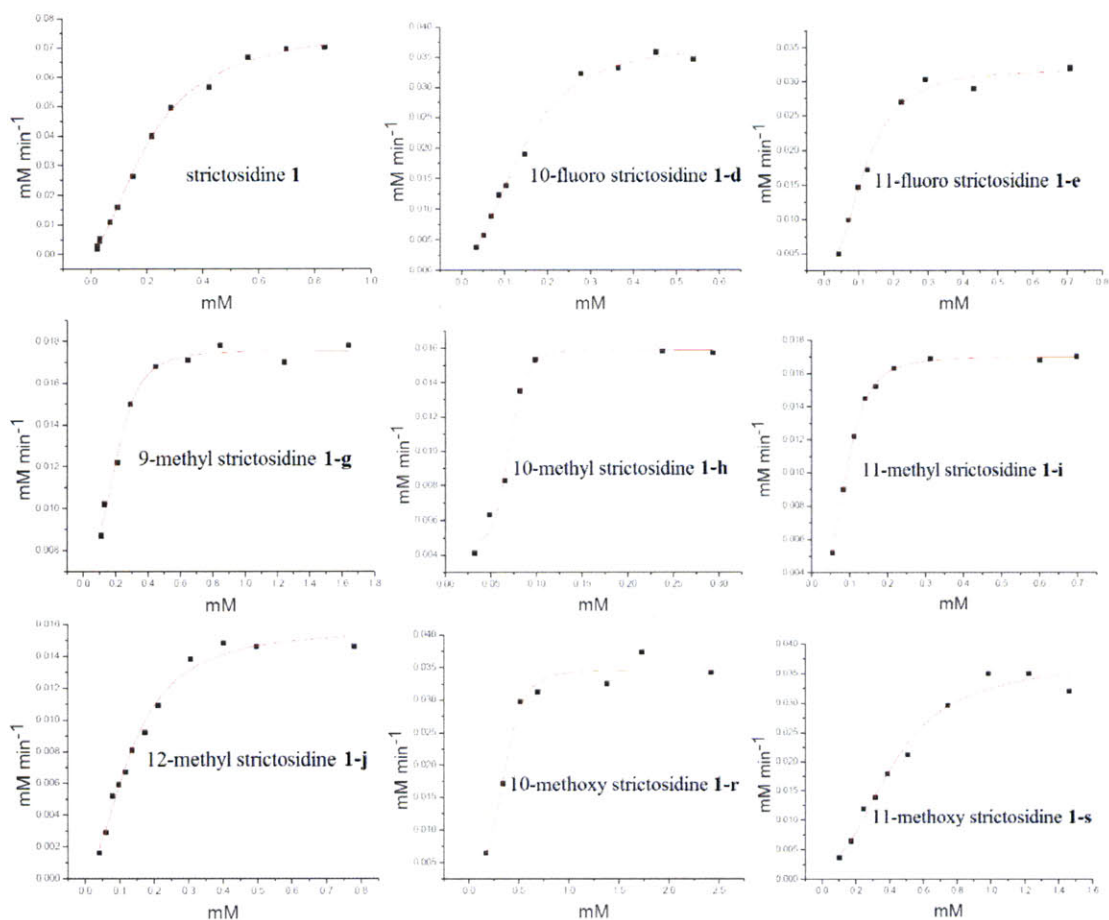


Figure 2-27: Data fit for steady state kinetic analysis of SGD with indole substituted strictosidine analogs **1**, **1-d**, **1-e**, **1-g**, **1-h**, **1-i**, **1-j**, **1-r**, and **1-s**. The unit for the x-axis is mM strictosidine analog, and the unit for the y-axis is mM strictosidine analog deglycosylated per minute.

Steady state kinetic analysis conditions for d₄ vincoside 43-1

Steady state kinetic analysis of d₄ vincoside **43-1** was performed in 0.15 M citrate phosphate buffer, pH 6, at 30°C in a 0.2 mL reaction volume with SGD concentrations appropriate for measuring the initial rate of the reaction (0.005-0.2 μM). Aliquots (10 μL) were quenched in 1 mL methanol, containing yohimbine **6** (500 nM) as an internal

standard, at appropriate time points. The samples were centrifuged (13,000g, 1 min) to remove particulates and then analyzed by LCMS. The starting material and products were separated using a 5-minute method with a gradient of 10-40% acetonitrile in 0.1% formic acid. The disappearance of d_4 vincoside **43-1** was monitored by peak integration and normalized to the internal standard. Seven substrate concentrations were tested, and the amount of d_4 vincoside **43-1** remaining was correlated to peak area by standard curves. Each concentration was assayed at least three times. The data were fitted (Figure 2-28) with a logistic curve using OriginPro 7 (OriginLab, Northampton, MA). The unit for the x -axis is mM d_4 vincoside **43-1**, and the unit for the y -axis is mM d_4 vincoside **43-1** deglycosylated per minute.

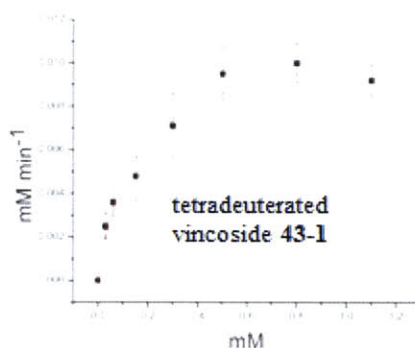


Figure 2-28: Data fit for steady state kinetic analysis of SGD with d_4 vincoside **43-1**. The unit for the x -axis is mM d_4 vincoside **43-1**, and the unit for the y -axis is mM d_4 vincoside **43-1** deglycosylated per minute.

Deglycosylation conditions for des-vinyl strictosidine isomers 1-y

Deglycosylation of the des-vinyl strictosidine isomers **1-y** (0.24 mM final concentration) was carried out in 0.15 M citrate phosphate buffer, pH 6, at 30°C in the presence of SGD (20 μ M), almond β -glucosidase (5 U), or *B. stearothermophilus* α -

glucosidase (15 U) in a 0.145 mL reaction volume. Aliquots (5 μ L) were quenched at appropriate time points and treated as described above. Peaks corresponding to starting material were integrated and normalized to the yohimbine **6** internal standard present in the methanol quench solution.

V. *Acknowledgments*

I had helpful discussions with Dr. Elizabeth McCoy, Dr. Peter Bernhardt, Dr. Shi Chen, Dr. Aimee Usera, and William Hillmann. Weslee Glenn provided assistance with PyMol. Dr. Elizabeth McCoy showed me how to express and purify SGD and also provided 4-methyl, 7-methyl, 4-fluoro, 7-fluoro, 4-chloro, 7-chloro, 4-bromo, and 5-isopropyl tryptamine **18** analogs. Dr. Elizabeth McCoy and Dr. Carmen Galan performed the precursor directed biosynthesis study in which pentynyl-ester strictosidine **1-t** was fed to hairy roots. Dr. Peter Bernhardt synthesized the des-vinyl strictosidine isomers **1-y** and **1-z** and assisted with ^1H NMR analysis. An undergraduate student Jia Xin (Joann) Wu assisted in the synthesis of various strictosidine **1** analogs. Dr. Hyang-Yeol Lee synthesized 4-aza tryptamine and 7-aza tryptamine, which were used to make 9-aza strictosidine **1-w** and 12-aza strictosidine **1-x**, respectively. Dr. L. Li of the MIT Department of Chemistry Instrumentation Facility performed high-resolution mass analysis.

VI. *References*

- (1) O'Connor, S. E.; Maresh, J. J. Chemistry and biology of monoterpene indole alkaloid biosynthesis. *Natural Products Reports* **2006**, *23*, 532-47.
- (2) Geerlings, A.; Ibanez, M. M.; Memelink, J.; van Der Heijden, R.; Verpoorte, R. Molecular cloning and analysis of strictosidine beta-D-glucosidase, an enzyme in terpenoid indole alkaloid biosynthesis in *Catharanthus roseus*. *The Journal of Biological Chemistry* **2000**, *275*, 3051-56.
- (3) Gerasimenko, I.; Sheludko, Y.; Ma, X.; Stockigt, J. Heterologous expression of a *Rauvolfia* cDNA encoding strictosidine glucosidase, a biosynthetic key to over 2000 monoterpene indole alkaloids. *European Journal of Biochemistry* **2002**, *269*, 2204-13.
- (4) Warzecha, H.; Gerasimenko, I.; Kutchan, T.M.; Stoeckigt, J. Molecular cloning and functional bacterial expression of a plant glucosidase specifically involved in alkaloid biosynthesis. *Phytochemistry* **2000**, 657-66.
- (5) Barleben, L.; Panjikar, S.; Ruppert, M.; Koepke, J.; Stockigt, J. Molecular architecture of strictosidine glucosidase: the gateway to the biosynthesis of the monoterpene indole alkaloid family. *The Plant Cell* **2007**, *19*, 2886-97.
- (6) van der Heijden, R.; Jacobs, D. I.; Snoeijer, W.; Hallard, D.; Verpoorte, R. The *Catharanthus* alkaloids: pharmacognosy and biotechnology. *Current Medicinal Chemistry* **2004**, *11*, 607-28.
- (7) Kjær, A.; Thomsen, H. Isothiocyanate-producing glucosides in species of Capparidaceae. *Phytochemistry* **1963**, *2*, 29-32.
- (8) Jonczyk, R.; Schmidt, H.; Osterrieder, A.; Fiesselmann, A.; Schullehner, K.; Haslbeck, M.; Sicker, D.; Hofmann, D.; Yalpani, N.; Simmons, C.; Frey, M.; Gierl, A. Elucidation of the final reactions of DIMBOA-glucoside biosynthesis in maize: characterization of Bx6 and Bx7. *Plant Physiology* **2008**, *146*, 1053-63.
- (9) Zagobelny, M.; Bak, S.; Moller, B.L. Cyanogenesis in plants and arthropods. *Phytochemistry* **2008**, *69*, 1457-68.
- (10) Nomura, T.; Quesada, A. L.; Kutchan, T. M. The new beta-D-glucosidase in terpenoid-isoquinoline alkaloid biosynthesis in *Psychotria ipecacuanha*. *The Journal of Biological Chemistry* **2008**, *283*, 34650-59.
- (11) Tsuji, Y.; Chen, F.; Yasuda, S.; Fukushima, K. Unexpected behavior of coniferin in lignin biosynthesis of *Ginkgo biloba* L. *Planta* **2005**, *222*, 58-69.
- (12) McCoy, E.; Galan, M.C.; O'Connor, S.E. Substrate specificity of strictosidine synthase. *Bioorganic and Medicinal Chemistry Letters* **2006**, *16*, 2475-78.
- (13) McCoy, E. Substrate analogs to investigate alkaloid biosynthesis in *C. roseus*. Ph.D. dissertation, Massachusetts Institute of Technology, 2009.
- (14) Galan, M.C., McCoy, E.; O'Connor, S.E. Chemoselective derivatization of alkaloids in periwinkle. *Chemical Communications* **2007**, 3249-51.
- (15) McCoy, E., O'Connor, S.E. Directed biosynthesis of alkaloid analogs in the medicinal plant *Catharanthus roseus*. *Journal of the American Chemical Society* **2006**, *128*, 14276-77.
- (16) Szabo, L.F. Rigorous biogenetic network for a group of indole alkaloids derived from strictosidine. *Molecules* **2008**, *13*, 1875-96.

- (17) Helmuth, R.; Manske, F.; Holmes, H.L.; Ridrigo, R.G.A. *The alkaloids: chemistry and physiology*; Academic Press: New York, New York, 1981; Vol. 5.
- (18) Ma, X.; Panjikar, S.; Koepke, J.; Loris, E.; Stockigt, J. The structure of Rauvolfia serpentina strictosidine synthase is a novel six-bladed beta-propeller fold in plant proteins. *The Plant Cell* **2006**, *18*, 907-20.
- (19) Loris, E. A.; Panjikar, S.; Ruppert, M.; Barleben, L.; Unger, M.; Schubel, H.; Stockigt, J. Structure-based engineering of strictosidine synthase: auxiliary for alkaloid libraries. *Chemistry and Biology* **2007**, *14*, 979-85.
- (20) Muller, K.; Faeh, C.; Diederich, F. Fluorine in pharmaceuticals: looking beyond intuition. *Science* **2007**, *317*, 1881-86.
- (21) Albanese-Walker, J.; Rossen, K.; Reamer, R.A.; Volante, R.P.; Reider, P.J. Synthesis of benzofuroquinoline for alpha-2 adrenoceptor antagonist MK-912: an O-analogue of the Pictet-Spengler reaction. *Tetrahedron Letters* **1999** *40*, 4917-20.
- (22) Kawakubo, H.; Okazaki, K.; Nagatani, T.; Takao, K.; Hasimoto, S.; Sugihara, T. Potent anticonflict activity and lessening of memory impairment with a series of novel [1]benzothieno[2,3-C]pyridines and 1,2,3,4-tetrahydro[1]benzothieno[2,3-C]pyridines. *Journal of Medicinal Chemistry* **1990** *33*, 3110-16.
- (23) Perry, N.B.; Ettouati, L.; Litaudon, M.; Blunt, J.W.; Munro, M.H.H. Alkaloids from the antarctic sponge kirkpatrickia-varialosa. 1. Variolin-b, a new antitumor and antiviral compound. *Tetrahedron* **1994**, *50*, 3987-92.
- (24) Schumacher, R.W.; Davidson, B.S. Didemnolines a-d, new N9-substituted beta-carbolines from the marine ascidian Didemnum sp. *Tetrahedron* **1995**, *51*, 10125-30.
- (25) Trimurtulu, G.; Faulker, D.J.; Perry, N.B.; Ettouati, L.; Litaudon, M.; Blunt, J.W.; Munro, M.H.G.; Jameson, G.B. Alkaloids from the antarctic sponge Kirkpatrickia-varialosa. 2. variolin-a and N(3')-methyl tetrahydrovariolin-b. *Tetrahedron* **1994**, *50*, 3993-4000.
- (26) Schafer, J.I.M.; Liu, H.; Tonetti, D.A.; Jordan, V.C. The interaction of raloxifene and the active metabolite of the antiestrogen EM-800 (SC 5705) with the human estrogen reporter. *Cancer Research* **1999**, *59*, 4308-13.
- (27) Lu, P.; Schrag, M.L.; Slaughter, D.E.; Raab, C.E.; Shou, M.; Rodrigues, A.D. Mechanism-based inhibition of human liver microsomal cytochrome P450 1A2 by zileuton, a 5-lipoxygenase inhibitor. *Drug Metabolism and Disposition* **2003**, *31*, 1352-60.
- (28) Croxtall, J.D.; Plosker, G.L. Sertaconazole: a review of its use in the management of superficial mycoses in dermatology and gynaecology. *Drugs* **2009**, *69*, 339-59.
- (29) Merour, J.Y.; Joseph, B. Synthesis and reactivity of 7-azaindoles (1H-pyrrolo[2,3-b]pyridine). *Current Organic Chemistry* **2001**, *5*, 471-506.
- (30) De-Eknankul, W.; Suttipanta, N.; Kutchan, T.M. Purification and characterization of deacetylpecoside synthase from Alangium lamarckii Thw. *Phytochemistry* **2000**, *55*, 177-81.
- (31) Samanani, N.; Facchini, P.J. Purification and characterization of norcoclaurine synthase, the first committed enzyme in benzyloquinoline alkaloid biosynthesis in plants. *The Journal of Biological Chemistry* **2002**, *277*, 33878-83.

- (32) De Camp, W.H. The FDA perspective on the development of stereoisomers. *Chirality* **1989**, *1*, 2-6.
- (33) Bernhardt, P.; Yerkes, N.; O'Connor, S. E. Bypassing stereoselectivity in the early steps of alkaloid biosynthesis. *Organic and Biomolecular Chemistry* **2009**, *7*, 4166-68.
- (34) Zhengwu, S.; Eisenreich, W.; Kutchan, T.M. Bacterial biotransformation of 3-alpha-S-strictosidine to the monoterpene indole alkaloid vallesiachotamine. *Phytochemistry* **1998**, *48*, 293-96.
- (35) Takii, Y.; Takahashi, K.; Yamamoto, K.; Sogabe, Y.; Suzuki, Y. Bacillus stearothermophilus ATCC12016 alpha-glucosidase specific for alpha-1,4 bonds of maltosaccharides and alpha-glucans shows high amino acid sequence similarities to seven alpha-D-glucohydrolases with different substrate specificity. *Applied Microbiology and Biotechnology* **1996**, *44*, 629-34.
- (36) He, S.; Withers, S.G. Assignment of sweet almond beta-glucosidase as a family 1 glycosidase and identification of its active site nucleophile. *The Journal of Biological Chemistry* **1997**, *272*, 24864-67.
- (37) Golden, E.B.; Byers, L.D. Methyl glucoside hydrolysis catalyzed by beta-glucosidase. *Biochimica et Biophysica Acta* **2009**, *11*, 1643-47.
- (38) Niemeyer, H.; de la Luz Cárdenas, M.; Rabajille, E.; Ureta, T.; Clark-Turri, L.; Peñaranda J. Sigmoidal kinetics of glucokinase. *Enzyme* **1975**, *20*, 321-23.
- (39) Bernhardt, P.; McCoy, E.; O'Connor, S. E. Rapid identification of enzyme variants for reengineered alkaloid biosynthesis in periwinkle. *Chemistry and Biology* **2007**, *14*, 888-97.
- (40) Anslyn, E.V.; Dougherty, D.A. *Modern Physical Organic Chemistry*; University Science Books: Sausalito, California, 2006.
- (41) Lee, H. Y.; Yerkes, N.; O'Connor, S. E. Aza-tryptamine substrates in monoterpene indole alkaloid biosynthesis. *Chemistry and Biology* **2009**, *16*, 1225-29.
- (42) Galan, M. C.; O'Connor, S.E. Semi-synthesis of secologanin analogues. *Tetrahedron Letters* **2006**, *47*, 1563-65.
- (43) Hamilton, R.G.; McLean, S. The conversion of sweroside to secologanin. *Canadian Journal of Chemistry* **1981**, *59*, 215-16.
- (44) Zhou, M.; Diwu, Z.; Panchuk-Voloshina, N.; Haugland, R. A stable nonfluorescent derivative of resorufin for the fluorometric determination of trace hydrogen peroxide: applications in detecting the activity of phagocyte NADPH oxidase and other oxidases. *Analytical Biochemistry* **1997**, *253*, 162-68.

Chapter 3: Partial purification and substrate specificity of ajmalicine synthase and isositsirikine synthase

I. Introduction

- A. Previous reports
- B. Plant enzyme purification techniques

II. Results

- A. Assay development for detection of ajmalicine synthase and isositsirikine synthase activity
- B. Partial purification protocol for ajmalicine synthase and isositsirikine synthase
- C. Additional purification methods
 - i. Dye-ligand chromatography
 - ii. Ammonium sulfate precipitation
 - iii. Protein pulldown experiment with strictosidine- β -glucosidase
- D. Novel ajmalicine and isositsirikine analogs
 - i. Novel indole substituted, heterocyclic, and ester analogs
 - ii. Novel des-vinyl analogs
 - iii. Steady state kinetic analysis studies

III. Discussion

IV. Materials and Methods

- A. *C. roseus* hairy root cultures
- B. *C. roseus* cell suspension cultures

- C. Preparation of strictosidine analogs
 - D. High-resolution mass spectrometry data
 - E. NMR characterization
 - F. Partial purification procedure
 - G. LCMS data
 - H. Steady state kinetic analysis conditions
 - I. Radioactive enzyme assay
 - J. Chemical reduction of deglycosylated strictosidine with NaCNBH_3
- V. Acknowledgments
- VI. References

The results in this chapter have been reported in the following publications:

- Peter Bernhardt*, Nancy Yerkes*, Sarah E. O'Connor. Bypassing stereoselectivity in the early steps of alkaloid biosynthesis. *Organic and Biomolecular Chemistry* 7 (2009) 4166-68. (*co-first authors)
- Hyang-Yeol Lee, Nancy Yerkes, Sarah E. O'Connor. Aza-tryptamine substrates in natural product biosynthesis. *Chemistry and Biology* 16 (2009) 1225-29.

The results in this chapter will also be reported in a manuscript currently in preparation:

- Aimee R. Usera*; Nancy Yerkes*; Elizabeth McCoy*; David K. Liscombe; Nathan E. Nims; Anne C. Friedrich; Sarah E. O'Connor. Crosslinking strategies

to isolate a new *C. roseus* enzyme. *Manuscript in preparation*, 2010. (* co-first authors)

I. *Introduction*

Upon deglycosylation by strictosidine- β -glucosidase (SGD), strictosidine **1** is converted into a reactive hemiacetal that rearranges into numerous isomers¹. These isomers are channeled into various TIA pathway branches, resulting in the formation of hundreds of different TIAs. Numerous pathways, such as the biosynthetic pathway to vinblastine **2**, involve many enzymes catalyzing diverse reactions such as oxidations, reductions, hydroxylations, and methylations. Other pathways, such as the biosynthetic pathways to the heteroyohimbine class alkaloids ajmalicine **4** and isositsirikine **7**, are proposed to be significantly shorter, involving only one or two reduction reactions¹.

The reductases producing ajmalicine **4** and isositsirikine **7** isomers from deglycosylated strictosidine **49** have never been isolated or cloned (Figure 3-1). Because strictosidine synthase and SGD have previously been cloned, identification of these reductases would complete the biosynthetic pathway from secologanin **17** and tryptamine **18** to ajmalicine **4** and isositsirikine **7**. The reductases producing ajmalicine **4** and isositsirikine **7** will herein be referred to as “ajmalicine synthase” and “isositsirikine synthase.”

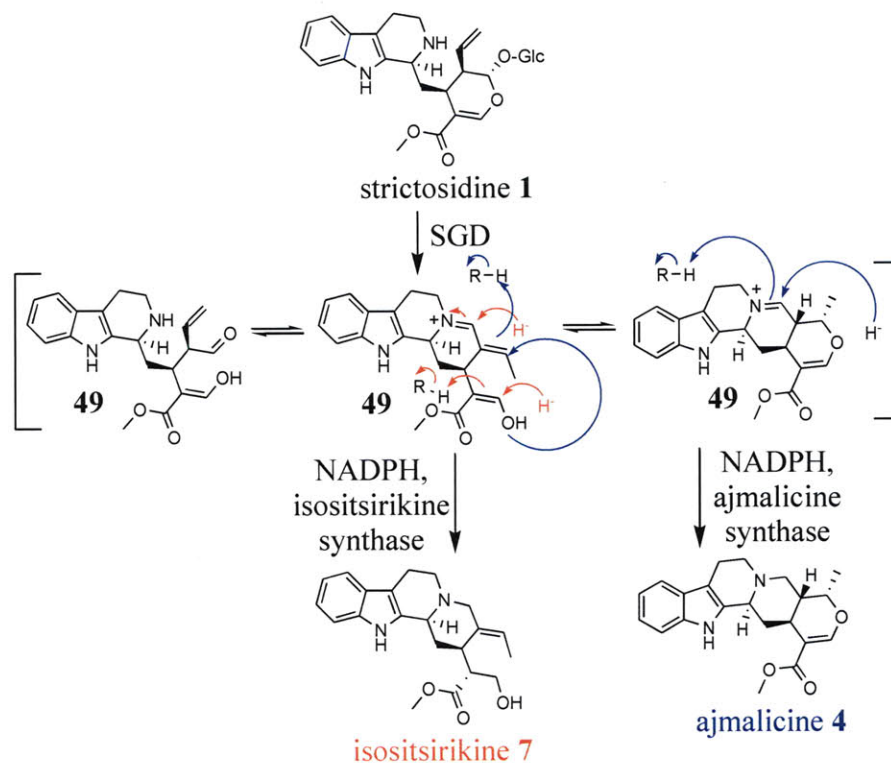


Figure 3-1: Ajmalicine synthase is proposed to produce ajmalicine **4** from deglycosylated strictosidine **49** and NADPH (blue arrows). Isositsirikine synthase is proposed to produce isositsirikine **7** from deglycosylated strictosidine **49** and NADPH (red arrows). “Glc” is an abbreviation for the glucose moiety of strictosidine **1**, and “SGD” is an abbreviation for strictosidine- β -glucosidase.

Ajmalicine **4** is reported to be a major product in *C. roseus* cultures; one report indicates that ajmalicine **4** constituted 13.5% of the total alkaloid content of a *C. roseus* hairy root culture¹⁰⁸. In the proposed mechanism of ajmalicine **4** formation¹⁰⁹, an imine is formed after strictosidine **1** deglycosylation, which is reduced by the *pro*-R hydride of NADPH (Figure 3-1). Ajmalicine synthase has been shown to be able to accept deglycosylated strictosidine analogs **49** *in vivo*. In one precursor directed biosynthesis study, numerous indole substituted tryptamine analogs – 5-fluoro tryptamine **18-d**, 6-

fluoro tryptamine **18-e**, 7-methyl tryptamine **18-j**, and 5-hydroxy tryptamine **18-p** – each formed the corresponding ajmalicine **4** analogs when co-cultured with *C. roseus* hairy root culture³⁴.

In contrast to ajmalicine **4**, isositsirikine **7** is produced in only small amounts in *C. roseus* cultures. For a *C. roseus* culture in which ajmalicine **4** constituted 13.5% of the total alkaloid content, isositsirikine **7** constituted only 0.75%¹⁰⁸. However, isositsirikine **7** analogs have been observed as major products in *C. roseus* precursor directed biosynthesis studies. For example, in one precursor directed biosynthesis study, it was found that *C. roseus* cell suspension cultures co-cultured with 12-aza-strictosidine **1-x** (Figure 3-2) produced 16*R*, 19*E* isositsirikine **7-x** as the major product (Figure 3-2)⁸⁵. In additional precursor directed biosynthesis studies, *C. roseus* cell suspension cultures co-cultured with (5*R*)-hydroxymethyl strictosidine **1-u-1** and benzo strictosidine **1-a** produced (5*R*)-hydroxymethyl isositsirikine **7-u-1** and benzo isositsirikine **7-a**, respectively, as the major products (Figure 3-2)^{104,36}. When co-cultured with benzo strictosidine **1-a**, *C. roseus* hairy roots produced benzo isositsirikine **7-a** as approximately 58% of the total amount of furan-derived alkaloids produced, whereas benzo ajmalicine **4-a** and benzo serpentine **5-a**, which is formed via a peroxidase-catalyzed oxidation of ajmalicine **4**¹, constituted 0% and 10%, respectively, of the total amount of furan-derived alkaloids produced (Figure 3-3)³⁶. As will be addressed in this chapter, the reason for the predominance of isositsirikine **7** analogs derived from these substrates is the substrate specificity of isositsirikine synthase.

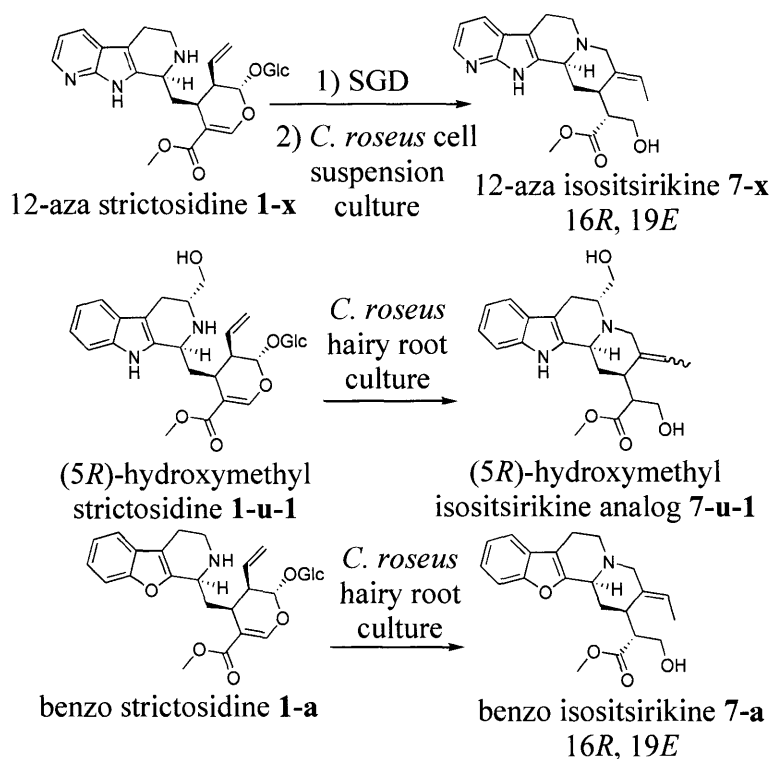


Figure 3-2: A major product isolated from *C. roseus* cell suspension cultures incubated with deglycosylated 7-aza strictosidine **1-x** was 12-aza isositsirikine **7-x**¹⁰⁴. A (5*R*)-hydroxymethyl isositsirikine analog **7-u-1** was the major product of a *C. roseus* hairy root culture incubated with (5*R*)-hydroxymethyl strictosidine **1-u-1**⁸⁵. Benzo isositsirikine **7-a** was the major product of a *C. roseus* hairy root culture incubated with benzo strictosidine **1-a**³⁶.

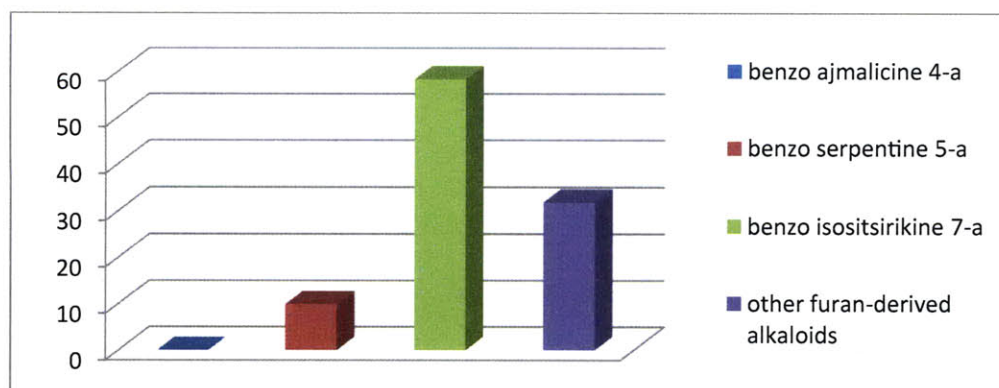


Figure 3-3: Results of a precursor directed biosynthesis study in which benzo strictosidine **1-a** was co-cultured with *C. roseus* hairy root cultures. Benzo ajmalicine **4-a**, benzo serpentine **5-a**, and benzo isositsirikine **7-a** constituted 0%, 10%, and 58%, respectively, of the furan-derived alkaloids produced³⁶.

A. Previous reports of reductase activity

The two known ajmalicine **4** isomers produced by *C. roseus* are tetrahydroalstonine **73** and 19-epi-ajmalicine **75** (Figure 3-5). Ajmalicine **4** has C-19 *S*, C-20 *R* stereochemistry, tetrahydroalstonine **73** has C-19 *S*, C-20 *S* stereochemistry, and 19-epi-ajmalicine **75** has C-19 *R*, C-20 *R* stereochemistry. Gerasimenko *et al.*⁷⁴ have reported the chemical formation of tetrahydroalstonine **73**, the C-20 *S* diastereomer of ajmalicine **4**, and two isositsirikine **7** isomers by reacting deglycosylated strictosidine **49** with sodium cyanoborohydride (NaCNBH₃). In their study, Gerasimenko *et al.*⁷⁴ formed tetrahydroalstonine **73** by incubating 225 nmol deglycosylated strictosidine **49** with 450 nmol NaCNBH₃ (Figure 3-4). When the NaCNBH₃ concentration was increased to a two-thousand-fold excess over strictosidine **1**, two isositsirikine **7** isomers were observed (Figure 3-4)⁷⁴.

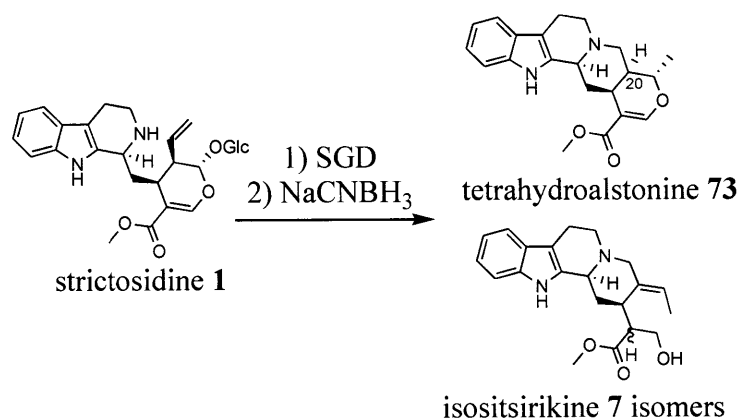


Figure 3-4: Gerasimenko *et al.*⁷⁴ reported that tetrahydroalstonine **73**, the C-20 *S* diastereomer of ajmalicine **4**, formed when deglycosylated strictosidine **49** was incubated 1:2 with NaCNBH₃. Two isositsirikine **7** isomers formed when deglycosylated strictosidine **49** was incubated with a two-thousand-fold excess of NaCNBH₃⁷⁴. The C-20 position of tetrahydroalstonine **73** is indicated in blue.

There has been only one report in the literature of a partial purification of a reductase leading to tetrahydroalstonine **73**. In 1985, Hemscheidt *et al.*¹¹⁰ reported a 33-fold partial purification of an 81 kDa NADPH-dependent reductase that converted cathenamine **49** into tetrahydroalstonine **73**; Hemscheidt also reported a second reductase activity from a *C. roseus* cell culture with a different alkaloid profile that converted cathenamine **49** into ajmalicine **4** and 19-epi-ajmalicine **75**. However, minimal data is reported about this reductase activity¹¹⁰. No further studies on this enzyme have been reported.

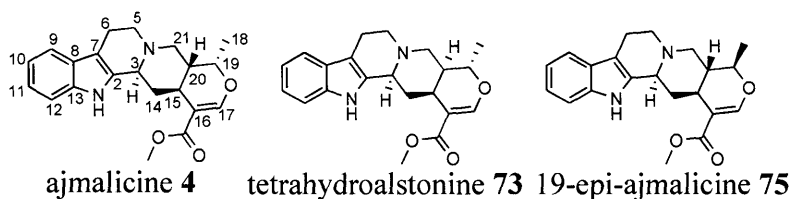


Figure 3-5: Structures of ajmalicine **4**, tetrahydroalstonine **73**, and 19-epi-ajmalicine **75**.

The numbering system is shown for ajmalicine **4**^{1,111}.

In Hemscheidt's partial purification procedure¹¹⁰, a *C. roseus* cell line that produced tetrahydroalstonine **73** and no other heteroyohimbine alkaloids such as ajmalicine **4** and 19-epi-ajmalicine **75** was cultured for seven days, filtered, frozen with liquid nitrogen, and stored at -18°C . The cells were then thawed in 0.1 M borate buffer, pH 7.6, containing 20 mM β -mercaptoethanol, and then centrifuged 20 minutes at 27,000g. An ammonium sulfate precipitation was next performed, with the enzymatic activity retained in the 40-70% fraction. The protein precipitate was resuspended in 50 mM potassium phosphate buffer, pH 7, and then applied to a gel filtration column followed by an ion exchange column. Overall, a mere 33-fold purification was attained. The authors reported that gel filtration chromatography suggested that the molecular weight of the native enzyme was 81 ± 2.4 kDa. It was found that only NADPH, and not NADH, could serve as a reducing cofactor in the reaction. No inhibition was observed in the presence of EDTA, Mg^{2+} , Mn^{2+} , or Co^{2+} , though irreversible inhibition was observed in the presence of 10 mM Fe^{2+} , Cu^{2+} , Hg^{2+} , and Zn^{2+} . The optimum pH and temperature were found to be 6.6 and 30°C , respectively. A 5.7 mM cathenamine **49** in DMSO solution was used in the assays. DMSO was used because of the low solubility of cathenamine **49** in water¹¹⁰.

Hemscheidt also reported a partial enzyme purification from a cell line that produced ajmalicine **4** and 19-epi-ajmalicine **75** in addition to tetrahydroalstonine **73**. In this purification, when an ammonium sulfate precipitation fraction was applied to a DEAE-cellulose column after gel filtration chromatography, two additional enzyme activities were observed, one forming ajmalicine **4** and one forming 19-epi-ajmalicine **75**. Collectively, these data suggest that there are three different reductases that produce ajmalicine **4** isomers¹¹⁰.

There are no literature reports demonstrating *in vitro* reductase activity that results in formation of an isositsirikine **7** isomer. Because more than one isositsirikine **7** isomers has been reported (Figure 3-6)¹¹², it is possible that there are multiple reductases that produce isositsirikine **7** isomers. Alternatively, a single nonspecific reductase could produce all diastereomers. In a precursor directed biosynthesis study performed by Dr. Elizabeth McCoy using *C. roseus* hairy root cultures, formation of multiple isositsirikine **7** analogs was observed for various indole substituted strictosidine **1** analogs³⁶. Isositsirikine **7** may form directly from deglycosylated strictosidine **49** or 4,21-dehydrogeissoschizine **64** via a double reduction. Alternatively, one reductase may form geissoschizine **64-1**¹¹³ (Figure 3-6), which then goes on to form isositsirikine **7**. A total synthesis of geissoschizine **64-1** has recently been completed in the O'Connor laboratory (Usera, O'Connor, unpublished) and will be used to further explore these questions.

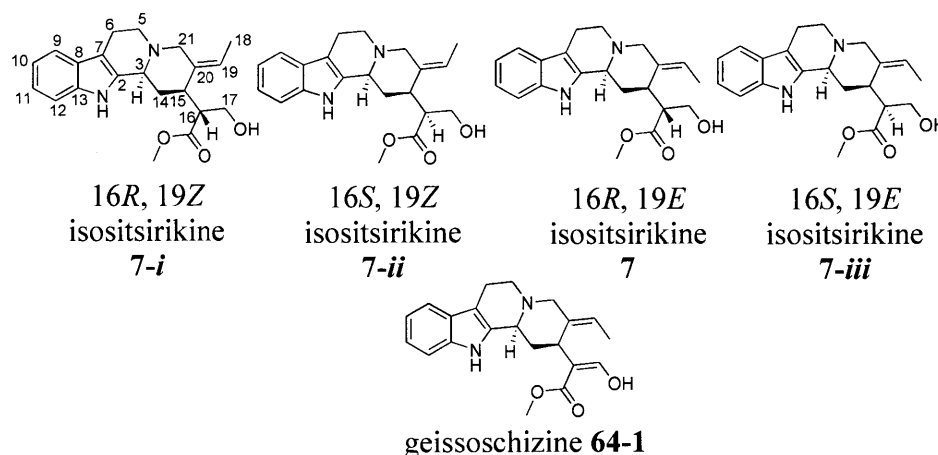


Figure 3-6: Structures of geissoschizine **64-1**¹¹³ and the naturally occurring isositsirikine **7** isomers, with the numbering system shown on 16*R*, 19*Z* isositsirikine **7-i**¹¹².

B. Plant enzyme purification techniques

Lysis

Plant tissues require harsh methods such as blending with stainless steel blades to break the cellulose cell wall. The solution used for lysis needs to be adequately buffered, since acidic plant cell vacuoles break during lysis, lowering the pH of the protein extract. Proteolysis is another concern when purifying enzymes from the native organism, and plant cells are no exception. Proteases are released upon cell lysis, so a variety of protease inhibitors are included throughout the purification procedure. Phenylmethanesulfonyl fluoride **76** (PMSF) (Figure 3-7), which inhibits serine proteases, and ethylenediaminetetraacetic acid **77** (EDTA) (Figure 3-7), which deactivates metal-dependent proteases by scavenging metal ions, are two commonly used proteolysis inhibitors^{114,115}.

If oxygen is present during lysis, phenolic compounds present in plant cells are converted to polymeric pigments by phenol oxidases, which can bind to and damage proteins in the extract. To prevent formation of these polymeric pigments, a reducing agent such as β -mercaptoethanol **78** (Figure 3-7) is added to inhibit the phenol oxidases. Additionally, polymers such as polyvinylpyrrolidone **79** (PVP) (Figure 3-7) are added to the mixture to adsorb phenolic polymers¹¹⁴. PVP forms insoluble complexes with phenolics via hydrogen bonding¹¹⁶. Borate buffer is frequently used for lysis because borate buffer forms complexes with compounds that have *cis* hydroxyl groups, such as phenolics^{115,116}.

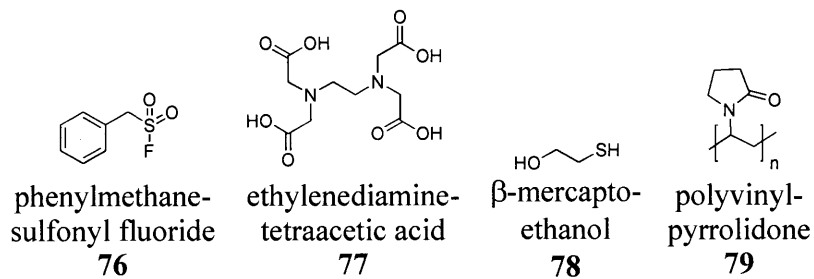


Figure 3-7: Structures of phenylmethanesulfonyl fluoride **76** (PMSF), ethylenediaminetetraacetic acid **77** (EDTA), β -mercaptoethanol **78**, and polyvinylpyrrolidone **79** (PVP).

Protein Precipitation

Precipitation is a commonly used partial purification method for proteins. Protein precipitation enables a protein to be simultaneously concentrated and purified from contaminant proteins typically directly after lysis. Difficulties with protein precipitation include irreversible denaturation and failure to re-solubilize the precipitated proteins¹¹⁴. One commonly used method of precipitation for protein purification is ammonium sulfate

precipitation,¹¹⁵ which is called “salting out” or “high salt precipitation.” Protein solubility is affected by the ionic strength of the solution. At high salt concentrations, the solubility of proteins generally decreases with increasing salt concentration by disrupting the solvation of the protein residues. At different salt concentrations, certain proteins will aggregate more than others because of the presence of more hydrophobic surface residues such as phenylalanine, valine, and leucine. Thus, some proteins precipitate at low salt concentrations, and others precipitate only at high salt concentrations. Additionally, larger proteins typically precipitate earlier than smaller proteins^{114,115}. One advantage of ammonium sulfate precipitation is low heat of solubilization, which helps prevent denaturation of proteins.^{114,115}

Acetone precipitation is another commonly used protein precipitation method. Acetone, an organic solvent with a small dielectric constant, also causes protein molecules to aggregate. Acetone is miscible with water, and when acetone is added to an enzyme extract, the dielectric constant of the acetone-extract mixture is lowered. This lower dielectric constant lowers protein solubility and induces protein precipitation^{114,115}. Solvents with large dielectric constants, on the other hand, such as water and DMSO, help stabilize the interaction between solvent and protein molecules, which favors the dissolution of the protein molecules^{114,115}. Acetone has a lower tendency to denature proteins than other organic solvents such as methanol or ethanol do because lower concentrations of acetone are necessary to cause comparable amounts of precipitation. Acetone is also more volatile than methanol or ethanol, enabling acetone to be removed easily from resolubilized precipitates¹¹⁷. As in ammonium sulfate precipitation, in acetone precipitation, larger proteins typically precipitate earlier than smaller proteins¹¹⁷.

Ion exchange chromatography

Enzyme mixtures are often subjected to column chromatography after a crude purification step such as protein precipitation. Ion exchange chromatography utilizes an electrostatic interaction between oppositely charged adsorbent and protein. There are two basic types of exchangers, positive (anion) and negative (cation). In anion exchange chromatography, the immobilized functional group is positively charged, and the binding ions are negative. Q-anion (“Q” for quaternary amine) and DEAE-anion (“DEAE” for diethylaminoethane) are two commonly used anion exchange resins (Figure 3-8). In cation exchange chromatography, the immobilized functional group is negatively charged, and the binding ions are positive. S-cation (“S” for sulfate) and CM-cation (“CM” for carboxymethyl) are two commonly used cation exchange resins (Figure 3-8). Resins are classified as either weak or strong exchangers. Weak exchangers, which include DEAE-anion and CM-cation resins, have groups that titrate in the neutral pH range at which enzymes are likely to function (Figure 3-8). Strong exchangers, which include Q-anion and S-cation resins, stay fully charged throughout the pH range used in the chromatography (Figure 3-8)^{114,115}.

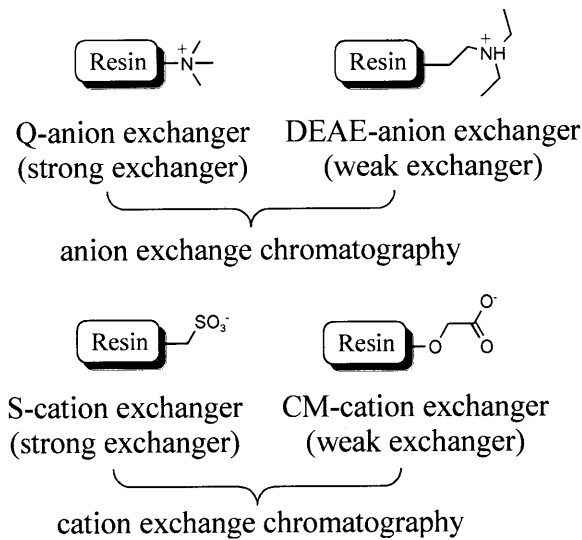


Figure 3-8: Examples of resins used in anion exchange chromatography and cation exchange chromatography. Q-anion and DEAE-anion are commonly used anion exchange resins. S-cation and CM-cation are commonly used cation exchange resins. DEAE-anion and CM-cation are weak exchangers, and Q-anion and S-cation are strong exchangers^{114,115}.

Ion exchange chromatography achieves protein separation because the amount of salt needed to release proteins bound to the resin varies based on the pI of each protein^{114,115}. Ion exchange chromatography is a resolution-based technique, and therefore works most effectively when used with fast performance liquid chromatography (FPLC). Most ion exchange chromatography for protein purification is performed at a slightly alkaline pH (8 to 8.5) using anion exchangers such as DEAE^{114,115}, since most proteins are stable at those pH ranges.

Size exclusion chromatography

Size exclusion, or gel filtration, chromatography uses bead particles with pores that can be penetrated only by small proteins, while larger proteins are excluded from the beads. Large proteins therefore pass through the column most rapidly, typically emerging in a fraction about 25-35% of the column volume. Medium-sized molecules typically elute in a fraction about 35-90% of the column volume, while the smallest proteins, which enter the beads and thus take much longer to pass through the column, typically elute in a fraction about 90-100% of the column volume. The separation achieved by gel filtration chromatography is due to differences in size between proteins, or, more precisely, on the Stokes radius, which is the radius of an equivalent spherical molecule^{114,115}. The formula for the Stokes radius, r , of a particle is $r = f / (6\pi\eta)$, where f is the frictional coefficient of the particle, and η is the viscosity of the solution²³.

Affinity chromatography

Affinity chromatography utilizes specific interactions between a protein of interest and an immobilized ligand for purification. A wide variety of ligands have been successfully immobilized on a solid support to be employed in protein purification efforts. Both proteins, such as an antibody, and small molecules can be used as immobilized ligands. Unlike ion exchange chromatography, in which selectivity is achieved through resolution, affinity chromatography achieves selectivity at the adsorption stage^{114,115}.

The goal in affinity chromatography is for the target protein to selectively bind the immobilized ligand. After an incubation period with crude protein and resin, the adsorbent is washed to remove the undesired proteins that, theoretically, should not bind

to the resin. Ideally, the protein of interest is then selectively eluted via a change in buffer designed to disrupt the specific ligand-protein interaction. However, affinity chromatography does not always work as well as expected. For instance, the lack of a tight binding interaction between the ligand and the protein of interest, as well as nonspecific interactions between contaminant proteins and the immobilized ligand, can prevent successful affinity chromatography^{114,115}.

Dye-ligand chromatography is a widely used type of affinity chromatography for NADPH-binding enzymes, which are the focus of this chapter. Dye-ligand chromatography was developed after the discovery that many textile dyes strongly bind proteins, particularly enzymes that bind nucleotides¹¹⁴. Since this initial discovery, many dyes have been designed to bind biological materials such as cellulose and proteins. In some cases this interaction occurs at the ligand binding site; alternatively, the interaction may be nonspecific, with the dye binding at various sites on the protein surface. A range of immobilized dyes have been reported to bind between 5 and 60% of proteins in crude cell extracts. It is difficult to predict which dye will interact most effectively with a given NADPH-binding protein, so typically many dyes are screened in the development of a protein purification protocol. The dye used most in protein purification is Cibacron Blue (Figure 3-11)¹¹⁸, which interacts with enzymes containing ATP- or NAD-binding sites, and has been found to bind competitively with ATP- and NAD-nucleotides¹¹⁸. A similar dye, Reactive Red, has also been used for the isolation of NADP-dependent dehydrogenases. Other commonly used dyes include Reactive Green, Reactive Brown, and Reactive Yellow (Figure 3-9 – Figure 3-13)¹¹⁸. All of these dyes are available immobilized to agarose.

Reactive Red Agarose

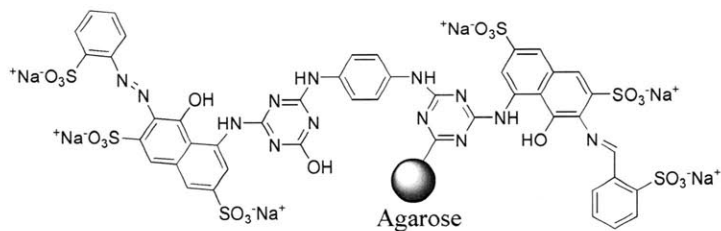


Figure 3-9: Structure of Reactive Red Agarose¹¹⁸.

Reactive Green Agarose

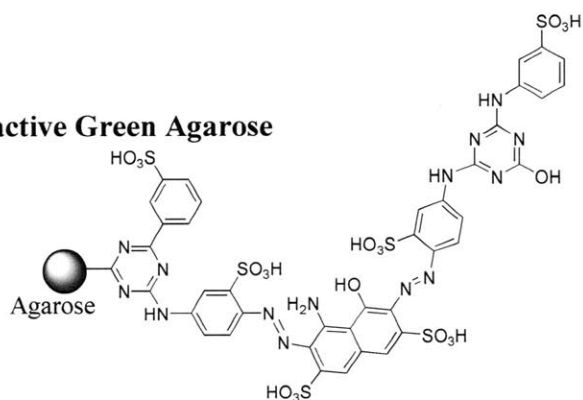


Figure 3-10: Structure of Reactive Green Agarose¹¹⁸.

Cibacron Blue Agarose

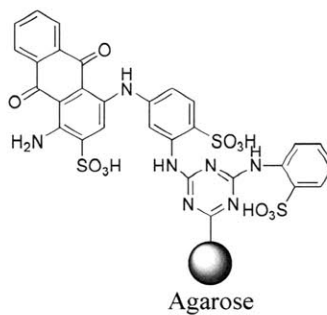
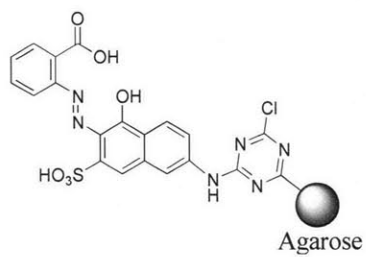
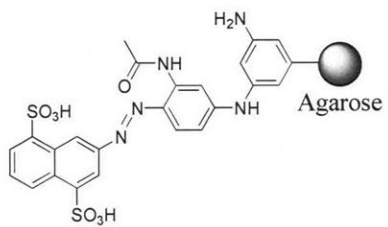


Figure 3-11: Structure of Cibacron Blue Agarose¹¹⁸.

Reactive Brown AgaroseFigure 3-12: Structure of Reactive Brown Agarose¹¹⁸.**Reactive Yellow 3**Figure 3-13: Structure of Reactive Yellow Agarose¹¹⁸.

II. Results

A. Assay development for detection of ajmalicine synthase and isositsirikine synthase activity

To successfully characterize and purify an enzyme, a robust assay for enzymatic activity must be developed. In the assay to detect ajmalicine synthase and isositsirikine synthase reductase activity, I incubated strictosidine **1** or strictosidine **1** analogs with SGD, NADPH, and a partially purified enzyme fraction (Figure 3-14). A 200 μL reaction volume was used, with 0.25 mM strictosidine **1** or strictosidine **1** analog, 750 nM SGD (typically), 5 mM NADPH, and 180 μL partially purified reductase fraction (typically at a concentration of 1 to 3 total mg protein mL^{-1}). The reaction was incubated at 30°C, 5 μL aliquots were quenched with methanol, and product formation was subjected to analysis by LCMS. A description of the synthesis and characterization of the strictosidine **1** analogs used is provided in the Materials and Methods section. Strictosidine **1** analogs were often used instead of strictosidine **1** in assays to ensure that no trace amounts of ajmalicine **4** and isositsirikine **7** present in the partially purified enzyme fraction would interfere with detection of reductase activity. Control experiments revealed that NADPH was absolutely necessary for reduction to occur; no reduction was observed when NADH was used as a cofactor.

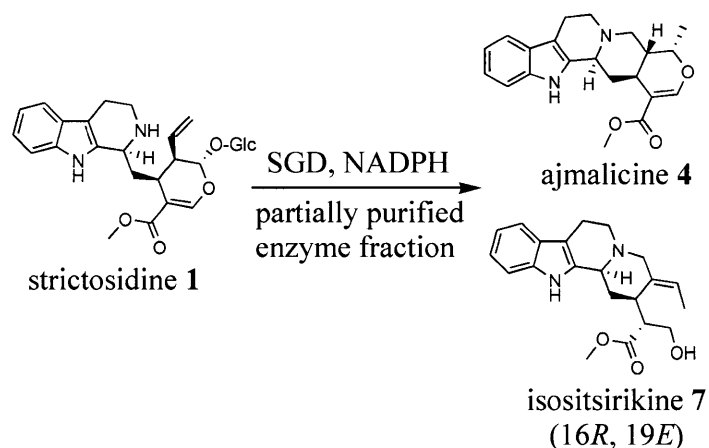


Figure 3-14: In the assay to detect ajmalicine synthase and isositsirikine synthase activity, strictosidine **1** (or strictosidine **1** analogs) was incubated with SGD, NADPH, and a partially purified enzyme fraction.

Co-elution studies with authentic standards demonstrated that ajmalicine **4** and 16*R*, 19*E* isositsirikine **7** are enzymatically produced in these assays. When d_4 strictosidine **1-1** was incubated with SGD, NADPH, and a partially purified enzyme fraction, a product with m/z 357 ($353 + 4$) eluted with the same LCMS retention time as ajmalicine **4** (Figure 3-15). When benzo strictosidine **1-a** was incubated with SGD, NADPH, and a partially purified enzyme fraction, a product with m/z 356 eluted with the same LCMS retention time as 16*R*, 19*E* benzo isositsirikine **7-a** (m/z 356) (Figure 3-16). Benzo isositsirikine **7-a** was used as an authentic standard instead of natural isositsirikine **7** because no authentic standard of natural isositsirikine **7** was available for co-elution: the quantities at which natural isositsirikine **7** are produced in *C. roseus* culture are too small. The 16*R*, 19*E* benzo isositsirikine **7-a** standard had been obtained from a precursor directed biosynthesis study in which benzo strictosidine **1-a**, which produces

comparatively more of the isositsirikine **7** product, was co-cultured with *C. roseus* hairy root cultures³⁶.

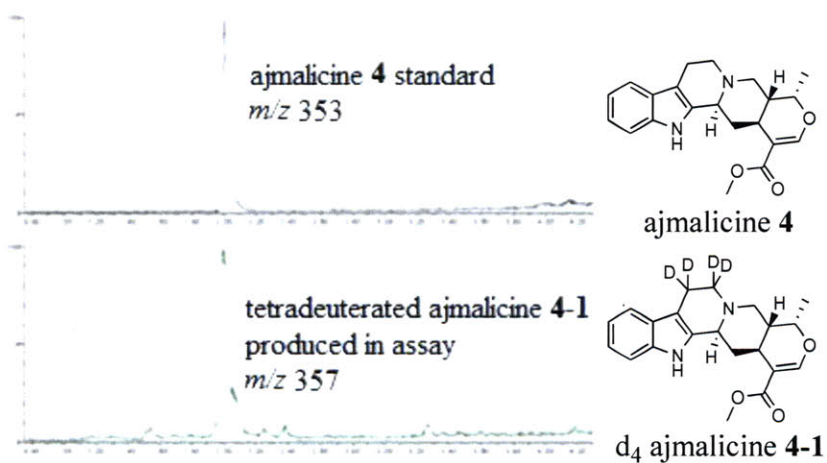


Figure 3-15: In an enzymatic assay of ajmalicine synthase, the d₄ ajmalicine **4-1** enzymatically produced (bottom chromatogram, m/z 357) has the same retention time on LCMS as an ajmalicine **4** standard (top chromatogram, m/z 353). An LCMS gradient of 10-60% acetonitrile in water with 0.1% formic acid over a period of 5 minutes was used. The x -axis is time in minutes and the y -axis is intensity.

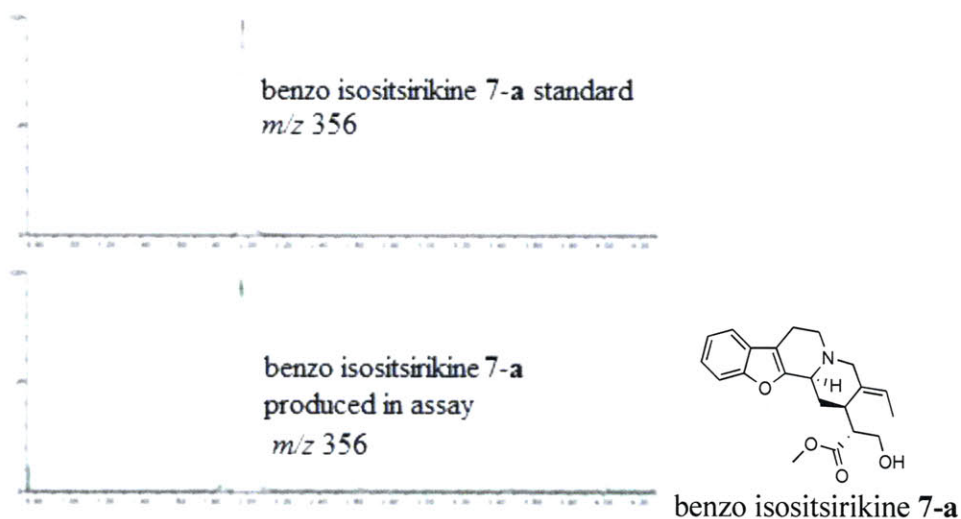


Figure 3-16: In an enzymatic assay of isositsirikine synthase, the benzo isositsirikine **7-a** enzymatically produced (bottom chromatogram, *m/z* 356) has the same retention time on LCMS as a *16R*, *19E* benzo isositsirikine **7-a** standard (top chromatogram, *m/z* 356). An LCMS gradient of 10-60% acetonitrile in water with 0.1% formic acid over a period of 5 minutes was used. The *x*-axis is time in minutes and the *y*-axis is intensity.

A radioactivity assay utilizing *R* ³H-NADPH also confirmed ajmalicine synthase activity by monitoring ³H-ajmalicine formation. *R* NADPH had been previously reported in enzymatic production of ajmalicine **4**¹⁰⁹. In my assay, I incubated deglycosylated strictosidine **49** with *R* ³H-NADPH and a partially purified enzyme fraction containing ajmalicine synthase activity. Aliquots from the reaction mixture were spotted and run on thin liquid chromatography (TLC) plates. The silica in the area of the plate with the same *R_f* value as an ajmalicine **4** standard was removed with a scalpel, and suspended in scintillation fluid, and the radioactivity was measured with a scintillation counter. One drawback of this assay, however, was that it required synthesis of the labeled NADPH cofactor; thus I did not routinely use this assay. Further details are available in the

Materials and Methods section. A spectrophotometric assay that measured the change of NADPH-NADP⁺ at 340 nm was also tested. However, the LCMS assay proved to be both faster and more sensitive.

B. Partial purification protocol for ajmalicine synthase and isositsirikine synthase

All active fractions contained both ajmalicine synthase activity and isositsirikine synthase activity, and the two enzyme activities were never separated during the purification procedure. Ajmalicine synthase activity was always approximately tenfold higher than isositsirikine synthase activity. The purification procedure is described below, and further details are provided in the Materials and Methods section.

In the partial purification procedure, hairy root or cell suspension cultures were subcultured for two weeks, stored at -80°C or used fresh, and then lysed by blending in borate buffer. After a brief centrifugation, an acetone precipitation was performed on the supernatant, with three precipitation fractions collected. Each protein precipitate pellet was resuspended in 50 mM sodium phosphate buffer, pH 7.5, containing 10% glycerol. The first precipitate (25% v/v acetone) was discarded (Figure 3-17) because it did not contain ajmalicine synthase or isositsirikine synthase activity. The second (40% v/v acetone) and third (57% v/v acetone) precipitates contained ajmalicine synthase and isositsirikine synthase activity; the specific activities of ajmalicine synthase and isositsirikine synthase in $\mu\text{M min}^{-1}$ per mg protein mL^{-1} for the two precipitates are shown below. The third acetone precipitate was subjected to analysis by 1D and 2D SDS-PAGE (Figure 3-17, Figure 3-18).

Acetone fraction	Ajmalicine synthase activity ($\mu\text{M min}^{-1} / \text{mg protein mL}^{-1}$)	Isositsirikine synthase activity ($\mu\text{M min}^{-1} / \text{mg protein mL}^{-1}$)
fraction two (40% v/v acetone)	0.068	0.003
fraction three (57% v/v acetone)	0.094	0.044

Table 3-1: The specific activities of ajmalicine synthase and isositsirikine synthase in $\mu\text{M min}^{-1}$ per $\text{mg protein mL}^{-1}$ for acetone precipitation fractions two and three.

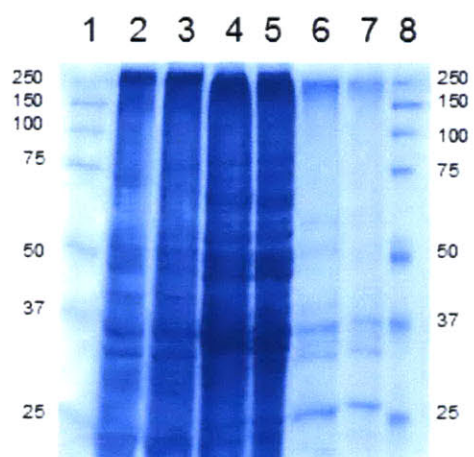


Figure 3-17: A 1D SDS-PAGE of acetone precipitation fractions one, two, and three of a typical partial purification procedure. Lanes 1 and 8: Protein ladder (Bio-Rad Precision Plus Protein Prestained Standard, Dual Color), with weights marked in kDa. Lanes 2 and 3: Acetone precipitation fraction one. Lanes 4 and 5: Acetone precipitation fraction two. Lanes 6 and 7: Acetone precipitation fraction three.

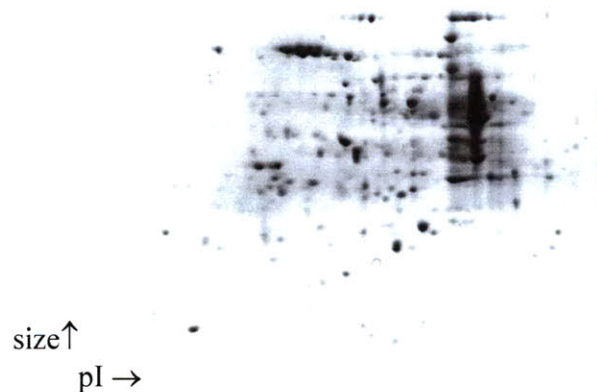


Figure 3-18: A 2D SDS-PAGE of fraction three of an acetone precipitation of *C. roseus* lysate.

The third fraction from the acetone precipitation was then applied to a DEAE column on an FPLC system. A gradient of 400–800 mM NaCl in 50 mM sodium phosphate buffer, pH 7.5, containing 10% glycerol with a flow rate of 5 mL min⁻¹ was used, and the absorbance at 280 nm was monitored (Figure 3-19). Fractions were often combined from two or three DEAE chromatographic steps, concentrated, and then assayed for activity (Table 3-2). Fractions B8-9 (Figure 3-19) of the DEAE column were consistently found to have the highest ajmalicine synthase specific activity and isositsirikine synthase specific activity (Figure 3-20).

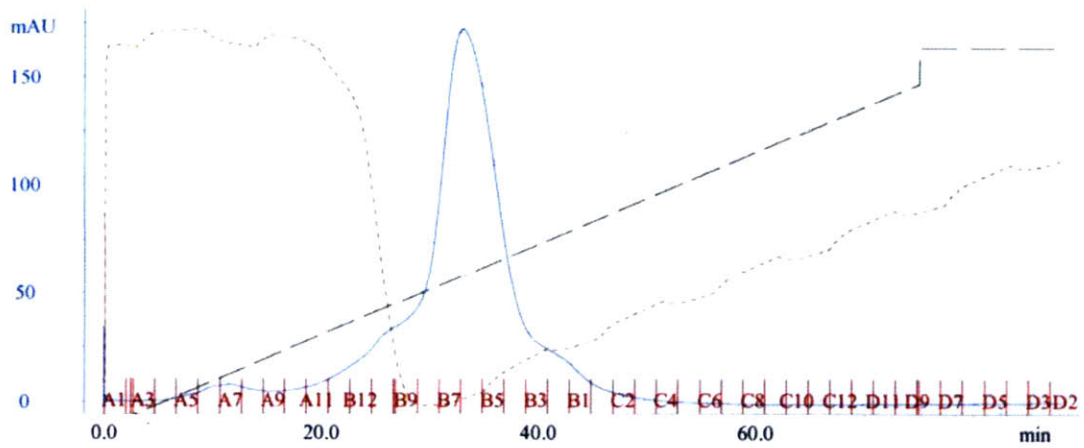


Figure 3-19: Chromatogram of the third fraction of an acetone precipitation subjected to ion exchange (DEAE) chromatography.

DEAE fraction	Ajmalicine synthase activity ($\mu\text{M min}^{-1} / \text{mg protein mL}^{-1}$)	Isositsirikine synthase activity ($\mu\text{M min}^{-1} / \text{mg protein mL}^{-1}$)
A11-12 (490-510 mM NaCl, 100-120 mL buffer)	0.120	0.004
B10-12 (510-530 mM NaCl, 120-140 mL buffer)	0.273	0.017
B8-9 (530-550 mM NaCl, 140-160 mL buffer)	0.333	0.019
B6-7 (550-570 mM NaCl, 160-180 mL buffer)	0.200	0.011
B4-5 (570-590 mM NaCl, 180-200 mL buffer)	0.146	0.009
B2-3 (590-610 mM NaCl, 200-220 mL buffer)	0.048	0.004

Table 3-2: Ajmalicine synthase specific activity and isositsirikine synthase specific activity of each DEAE fraction, in $\mu\text{M min}^{-1}$ per mg protein mL^{-1} . The DEAE fraction numbers are shown in Figure 3-19. For each fraction, the approximate concentration of mM NaCl at which the enzymes in the fraction eluted and the total number of mL buffer used by the FPLC at that point are given.

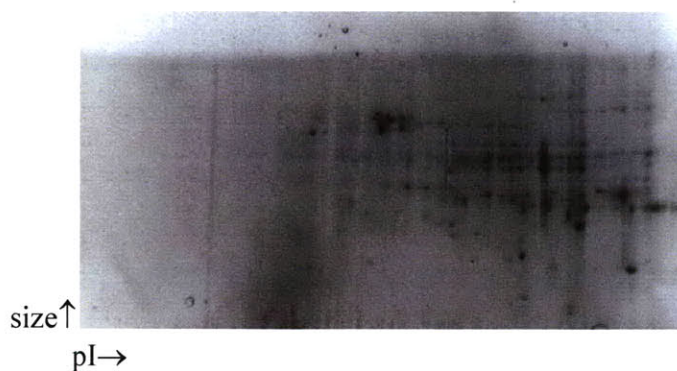


Figure 3-20: A 2D SDS-PAGE of DEAE fractions B8-9 (Figure 3-19) of a typical purification procedure.

Fractions B8-9 from the DEAE column were then applied to a size 200 gel filtration column on an FPLC system. For the size 200 gel filtration column, a 50 mM sodium phosphate buffer, pH 7.5, containing 10% glycerol with a flow rate of 1 mL min^{-1} was used, and the absorbance at 280 nm was monitored (Figure 3-21, Figure 3-22). Fractions were collected, concentrated, and assayed for activity. Fractions C9-12 and D9-12 (Figure 3-21) of the size 200 gel filtration column consistently showed the best ajmalicine synthase specific activities and isositsirikine synthase specific activities, though unfortunately a decrease in specific activity occurred compared to the previous purification step, which exemplified the lability of this enzyme activity. Nevertheless, fractions C9-12 were subjected to separation by 2D SDS-PAGE, stained with SYPRO Ruby protein gel stain (Sigma), and observed with a UV transilluminator (254 nm, Bio-Rad). The major protein spots from this 2D SDS-PAGE (Figure 3-22) were excised and sent to the Donald Danforth Plant Science Center (St. Louis, Missouri) for sequencing by mass spectrometry. The peptide sequences obtained from spots 1 through 8 of the 2D SDS-PAGE shown in Figure 3-22 were subjected to a BLAST (Basic Local Alignment Search Tool) search against the available *C. roseus* expressed sequence tag (EST)

database. ESTs are short sub-sequences of transcribed cDNA sequences that are used in gene discovery efforts to identify gene transcripts¹¹⁹. The ESTs that had the highest sequence identity to spots (proteins) 1 through 8 are listed in Table 3-4.

Of the 8 proteins listed in Table 3-4, protein 3 appears to be the most promising in terms of potential ajmalicine synthase and isositsirikine synthase activity, because it exhibits 61% sequence identity to a cinnamyl alcohol dehydrogenase. Cinnamyl alcohol dehydrogenases, which are discussed further in Chapter 4, are NADPH-dependent enzymes that catalyze the reduction of *p*-hydroxycinnamyl aldehyde and *p*-hydroxycinnamyl aldehyde analogs into the corresponding *p*-hydroxycinnamyl alcohols¹²⁰. Although 61% sequence identity to a cinnamyl alcohol dehydrogenase suggests that the enzyme is likely to be an NADPH-dependent dehydrogenase, the sequence identity is not so high as to suggest that the enzyme is definitively a cinnamyl alcohol dehydrogenase. Notably, there is precedence for cinnamyl alcohol dehydrogenase homologs that act on TIAs; for example, as will be further discussed in Chapter 4, perakine reductase reduces the aldehyde moiety of the TIA perakine. Notably, perakine reductase also reduces the aldehyde moiety of cinnamaldehyde, even though perakine and cinnamaldehyde have vastly different structures¹²¹. Even if protein 3 exhibits cinnamyl aldehyde dehydrogenase activity, it could potentially also reduce an imine to an amine, as is required for ajmalicine **4** or isositsirikine **7** formation. Only the 3' fragment of this gene is available in the public database, which impedes functional characterization. Future efforts will involve the cloning and expression of the full length protein 3.

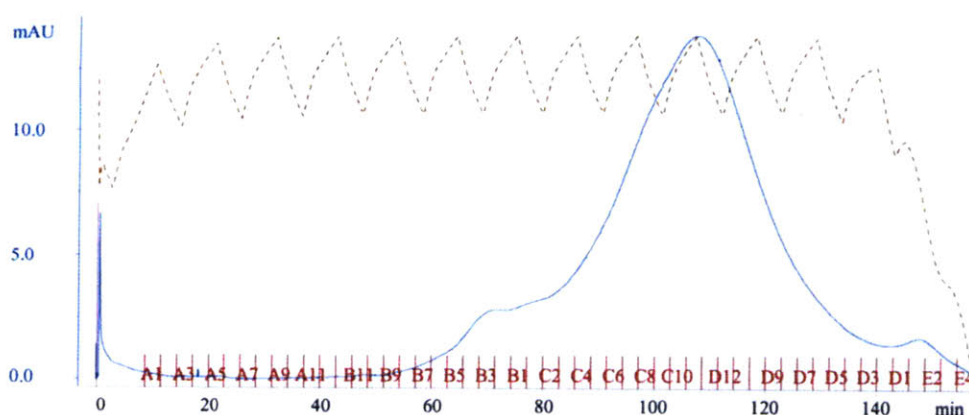


Figure 3-21: Chromatogram of the DEAE B8-9 fractions subjected to size 200 gel filtration chromatography.

Size 200 gel filtration fraction	Ajmalicine synthase activity ($\mu\text{M min}^{-1} / \text{mg protein mL}^{-1}$)	Isositsirikine synthase activity ($\mu\text{M min}^{-1} / \text{mg protein mL}^{-1}$)
C1-4 (48-56 mL buffer)	0	0
C5-8 (56-64 mL buffer)	0.014	0
C9-12 (64-72 mL buffer)	0.033	0.003
D9-12 (72-80 mL buffer)	0.031	0.010
D5-8 (80-88 mL buffer)	0	0
D1-4 (88-96 mL buffer)	0	0

Table 3-3: Ajmalicine synthase specific activity and isositsirikine synthase specific activity of each size 200 gel filtration FPLC fraction, in $\mu\text{M min}^{-1}$ per mg protein mL^{-1} . The size 200 gel filtration fraction numbers are shown in Figure 3-21. For each fraction the total number of mL buffer used by the FPLC at that point are given.

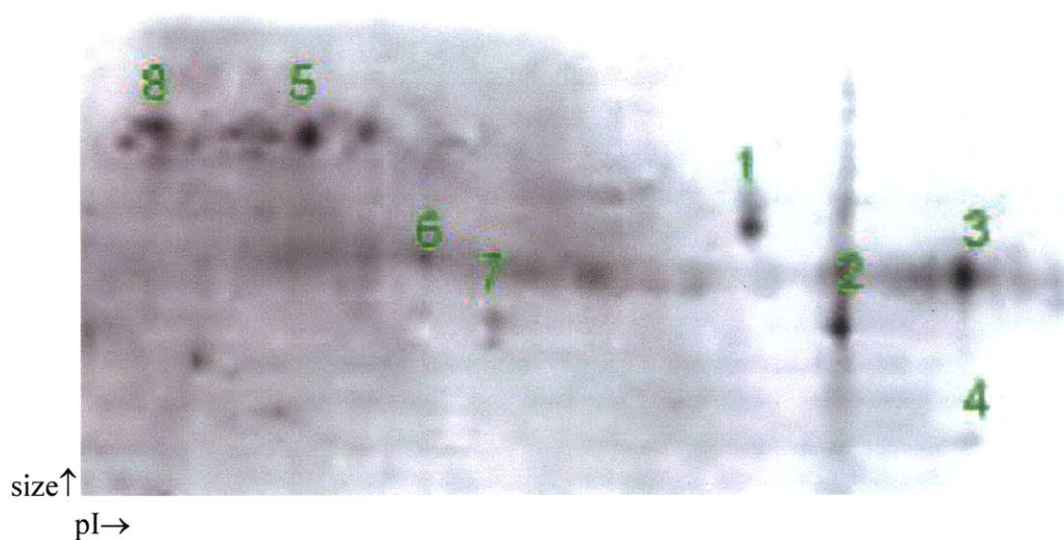


Figure 3-22: A 2D SDS-PAGE of fractions C9-12 from a size 200 gel filtration column. Major proteins (“spots”) labeled 1 through 8 in green were excised and sequenced.

Spot	EST accession number	Enzyme type
1	RT00026R_T3_026_B11_02JUNE2004_093_ab1 CR03015E07 1 SM-JB_R1-F04_T3_F04_3100168_12_ab1	peroxidase peroxidase peroxidase
2	CR02028A05 CR02026D12	malate dehydrogenase malate dehydrogenase
3	LB00039R_T3_039_D07_21JUN2004_057_ab1	cinnamyl alcohol dehydrogenase
4	1_SM-JB_L11-H03_T3_H03_3100405_15_ab1	triosphosphate isomerase
5	no protein match	no protein match
6	CR01010C11	succinyl-CoA ligase
7	CR01020F03	cysteine synthase
8	CR02002F08	S-adenosyl-L-homocysteine hydrolase

Table 3-4: Table of *C. roseus* ESTs that correspond to the peptide sequence data obtained for each spot from the 2D SDS-PAGE shown in Figure 3-22. When more than one EST accession number is listed, this indicates that the protein sequence matched equally well to each of the listed ESTs.

C. *Additional purification methods*

i. *Dye-ligand chromatography*

As Figure 3-22 shows, numerous proteins in addition to ajmalicine synthase and isositsirikine synthase are present in the partially purified enzyme fraction even after the third step in the purification protocol, the size 200 gel filtration FPLC step. The goal of the protein purification procedure is to obtain ajmalicine synthase and/or isositsirikine synthase in a fraction containing as few enzymes as possible. In an attempt to find other purification methods, I used dye-ligand chromatography. Cibacron Blue Agarose, Reactive Red Agarose, Reactive Brown Agarose, Reactive Green Agarose, and Reactive Yellow Agarose (Figure 3-9–Figure 3-13) were all tested to see if they could be used as a purification step. If a particular dye were able to partially purify ajmalicine synthase or isositsirikine synthase, the dye could be incorporated into future purification procedures.

I obtained the most promising results by using Reactive Red Agarose. An acetone precipitation fraction (1.5 mL, 1.9 mg protein mL⁻¹) was added to 2.5 mL Reactive Red Agarose (pre-packed column from Sigma Aldrich) pre-equilibrated with 10 mM Tris buffer, pH 7.5, containing 0 M NaCl and 10% glycerol. The supernatant and wash were collected, and 1500 mM NaCl was added to the Tris buffer for elution. The supernatant, wash, and elution were assayed for ajmalicine synthase specific activity (Table 3-5). Encouragingly, the highest ajmalicine synthase specific activity was seen in the elution fraction. Similar results were obtained when I used a purer ajmalicine synthase fraction (0.7 mg protein mL⁻¹) obtained after purification from acetone precipitation, DEAE, and size 200 gel filtration chromatography steps (Table 3-6); the best ajmalicine synthase

specific activity was also seen in the elution fraction. The specific activity was modestly improved by a factor of ten.

Reactive Red Agarose	Ajmalicine synthase specific activity ($\mu\text{M min}^{-1} / \text{mg protein mL}^{-1}$)
Supernatant	0.010
Wash	0.051
Elution	0.158

Table 3-5: Ajmalicine synthase specific activity ($\mu\text{M min}^{-1}$ per mg protein mL^{-1}) for the fractions from a Reactive Red Agarose column using an acetone precipitation fraction.

Reactive Red Agarose	Ajmalicine synthase specific activity ($\mu\text{M min}^{-1} / \text{mg protein mL}^{-1}$)
Supernatant	0
Wash	0.058
Elution	0.215

Table 3-6: Ajmalicine synthase specific activity ($\mu\text{M min}^{-1}$ per mg protein mL^{-1}) for the fractions from a Reactive Red Agarose column using a size 200 gel filtration fraction.

The procedure was then performed using Reactive Green Agarose and an acetone precipitation fraction ($1.2 \text{ mg protein mL}^{-1}$). As with Reactive Red Agarose, ajmalicine synthase specific activity correlated with increasing NaCl concentration used for elution (Table 3-7).

mM NaCl fraction	Ajmalicine synthase specific activity ($\mu\text{M min}^{-1} / \text{mg protein mL}^{-1}$)
0	0.020
150	0.039
300	0.037
500	0.077
1500	0.090

Table 3-7: Ajmalicine synthase specific activity ($\mu\text{M min}^{-1}$ per mg protein mL^{-1}) for the fractions from a Reactive Green Agarose column using an acetone precipitation fraction.

Reactive Brown Agarose, Cibacron Blue Agarose, and Reactive Yellow Agarose were also assayed. An acetone precipitation fraction ($1.6 \text{ mg protein mL}^{-1}$) was used. Unlike Reactive Red and Reactive Green Agarose, however, decreasing ajmalicine synthase specific activity was observed with increasing NaCl concentration (Table 3-8). Reactive Brown Agarose, Cibacron Blue Agarose, and Reactive Yellow Agarose are thus not suitable for purifying ajmalicine synthase.

mM NaCl fraction	Reactive Brown ($\mu\text{M min}^{-1} / \text{mg protein mL}^{-1}$)	Cibacron Blue ($\mu\text{M min}^{-1} / \text{mg protein mL}^{-1}$)	Reactive Yellow ($\mu\text{M min}^{-1} / \text{mg protein mL}^{-1}$)
0	0.169	0.154	0.201
150	0.228	0.128	0.166
300	0.134	0.105	0.139
500	0.084	0.053	0.095
1500	0.055	0.033	0.083

Table 3-8: Ajmalicine synthase specific activity ($\mu\text{M min}^{-1}$ per mg protein mL^{-1}) for each fraction using Reactive Brown Agarose, Cibacron Blue Agarose, and Reactive Yellow Agarose.

In future ajmalicine synthase purification procedures, Reactive Red Agarose or Reactive Green Agarose could be used to supplement the purification procedure. Ajmalicine synthase is eluted from both Reactive Red Agarose and Reactive Green Agarose in fractions with high NaCl concentrations, which shows that ajmalicine synthase is able to bind to Reactive Red Agarose and Reactive Green Agarose. The specific activity was higher in the elution fractions, indicating that ajmalicine synthase is partially purified by Reactive Red Agarose and Reactive Green Agarose. Additional purification strategies such as the use of Reactive Red Agarose and Reactive Green Agarose are necessary for the enrichment of ajmalicine synthase and isositsirikine synthase, and efforts must also be made to ensure that no loss of specific activity occurs during the additional purification steps.

ii. Ammonium sulfate precipitation

In my initial purification attempts I performed an ammonium sulfate precipitation after the lysis step with borate buffer. I used ammonium sulfate precipitation because it is much more commonly performed than acetone precipitation. I found that activity was retained in the 40-70% ammonium sulfate fraction.

I switched to acetone precipitation because acetone precipitation can be done much more quickly than ammonium sulfate precipitation, thus lowering the chance of enzyme activity loss over time. A typical ammonium sulfate precipitation followed by desalting and concentration lasted approximately four hours, whereas an acetone precipitation followed by resuspension can be performed in approximately 15 minutes. Importantly, protein obtained from acetone precipitation had higher specific activities for ajmalicine synthase and isositsirikine synthase than did protein obtained with ammonium

sulfate precipitation. Notably, isositsirikine synthase activity was observed only after acetone precipitations, and not after ammonium sulfate precipitations. Perhaps isositsirikine synthase loses its activity during the lengthy ammonium sulfate procedure, or perhaps, for some unknown reason, isositsirikine synthase is able to tolerate acetone precipitation better than ammonium sulfate precipitation.

iii. Protein pulldown experiment with strictosidine- β -glucosidase

I performed a protein pulldown experiment (Figure 3-23) with strictosidine- β -glucosidase (SGD). Because the intermediates produced by the action of SGD are extremely reactive and have low solubility in water⁷⁶, it can be hypothesized that ajmalicine synthase and isositsirikine synthase interact with SGD, which is believed to be associated with the endoplasmic reticulum (ER)⁷³. Protein complex, or “metabolon” formation has been known to occur in *Arabidopsis thaliana*¹²²⁻¹²⁵; much of phenylpropanoid and flavonoid metabolism is hypothesized to occur in metabolons on the cytosolic side of the ER¹²⁶. I performed a pulldown experiment (Figure 3-23) to determine whether ajmalicine synthase and isositsirikine synthase associate with SGD. In the pulldown experiment, a maltose binding protein (MBP) fusion of SGD was immobilized onto an amylose resin. The resin with SGD was then incubated with extracts from *C. roseus* seedlings. Proteins not interacting with SGD were eluted by washing the resin with buffer. Finally, SGD, along with any potential interacting partners of SGD, was eluted from the resin with maltose. Because of the large size of the MBP, an alternative pulldown procedure was also performed. In the alternative procedure, the MBP of SGD was first cleaved with thrombin. SGD was then crosslinked to an Affigel

resin via the surface amines of SGD. Extracts from *C. roseus* seedlings were then added, and non-interacting proteins were eluted by washing. After washing, proteins bound to SGD were eluted by heat denaturation.

After elution, SDS-PAGE was used to analyze the wash and elution fractions. Protein bands that appeared in the elution but not in the wash fractions were excised from the gel and sequenced via nano-LCMS at the protein core facility of the University of Arizona. Unfortunately, no proteins were found that had homology to known reductases; many of the proteins sequenced had high sequence identity to methionine synthases. Additionally, interacting proteins that were eluted with maltose were also found to have no ajmalicine synthase activity.

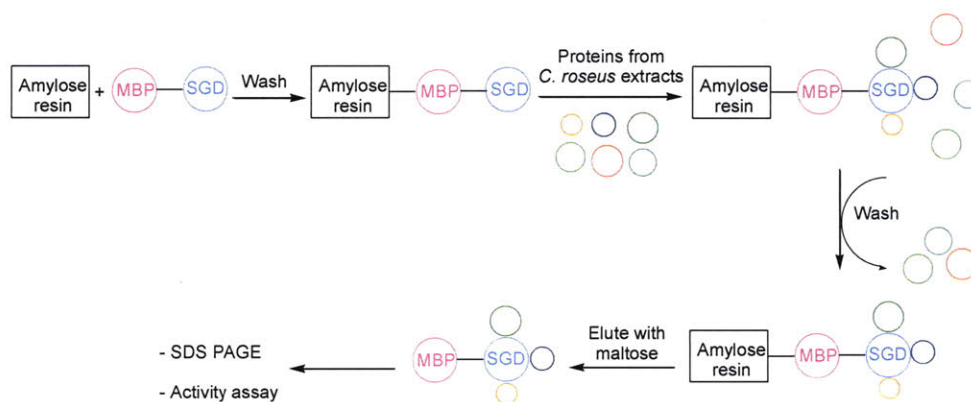


Figure 3-23: Design of protein pulldown experiment with SGD.

These experiments do not exclude the possibility of SGD-ajmalicine synthase and SGD-isositsirikine synthase metabolons, however. Most protein-protein interactions have low affinities, and enzyme interactions in secondary metabolism are particularly difficult to detect. Winkel-Shirley^{126,127} speculates that enzyme interactions that occur in primary metabolism, such as the metabolons involved in the tryptophan synthase, the pyruvate

dehydrogenase, the citric acid and Calvin cycles, the proteasome, and the glycine decarboxylase systems, may be relatively stable when compared to many interactions that occur in secondary metabolism pathways. For example, whereas the primary metabolism enzymes of the citric acid cycle can be co-purified, attempts to co-purify the secondary metabolism enzymes of the phenylpropanoid pathway have failed^{126,127}.

D. Novel ajmalicine and isositsirikine analogs

Novel ajmalicine **4** and isositsirikine **7** analogs can be produced if deglycosylated strictosidine **49** analogs are accepted by ajmalicine synthase and isositsirikine synthase, respectively. Previous work has explored the substrate specificity of strictosidine synthase^{36,85,86}, and as described in Chapter 2, numerous strictosidine **1** analogs are accepted by SGD. These strictosidine **1** analogs include indole substituted strictosidine analogs **1-c** through **1-s**, strictosidine containing alternate heterocycles **1-a** and **1-b** and esters **1-t**, and des-vinyl strictosidine isomers **1-y** and **1-z**. If these unnatural biosynthetic intermediates are accepted by downstream enzymes, novel alkaloids with potentially improved biological properties can be made.

i. Novel indole substituted, heterocyclic, and ester analogs

Numerous strictosidine **1** analogs that were found to be deglycosylated by SGD *in vitro* (Chapter 2) were assayed with a partially purified enzyme fraction containing ajmalicine synthase and isositsirikine synthase activity (Figure 3-24 and Table 3-9). In the assays, strictosidine **1** analogs were first incubated with SGD for 5 minutes, followed by addition of NADPH and a partially purified enzyme fraction containing ajmalicine synthase and isositsirikine synthase activity. After two hours, an aliquot was quenched and subjected to LCMS analysis. Gratifyingly, all strictosidine **1** analogs tested (**1-c**, **1-g**, **1-h**, **1-k**, **1-n**, **1-o**, and **1-p**) (Table 3-9) except for α -dimethyl strictosidine **1-u** were found to form compounds with exact masses matching the corresponding ajmalicine **4** isomers. Co-elution with authentic standards in the LCMS assay further confirmed the identity of some of the ajmalicine **4** and isositsirikine **7** analogs produced in the assays (as shown in Figure 3-15 and in Figure 3-37 and Figure 3-38 in the Materials and

Methods section) as well as the identity of the benzo isositsirikine compound **7-a** (Figure 3-16). The standards were produced and characterized by Dr. Elizabeth McCoy³⁶ and Dr. Hyang-Yeol Lee¹⁰⁴. Enzymatic products were also characterized by high-resolution mass spectrometry (Materials and Methods section). Indole substituted strictosidine analogs **1-1** and **1-a**, **1-b**, **1-d**, **1-e**, **1-f**, **1-i**, **1-j**, **1-m**, **1-q**, **1-r**, **1-s**, and **1-t** (Table 3-9) were also consumed by this enzyme preparation and were observed by LCMS to form the corresponding ajmalicine **4** (Figure 3-39 in the Materials and Methods section) and isositsirikine **7** analogs (Figure 3-40 in the Materials and Methods section), and d₄ vincoside **43-1** appeared to form an isomer of ajmalicine, presumably the C-3 *R* ajmalicine **85**. However, because no standards are currently available for co-elution studies, these enzymatic products were characterized only by high-resolution mass spectrometry. Efforts to obtain the products from these partially purified enzyme assays in sufficient quantities for more rigorous characterization by NMR unfortunately proved unsuccessful. For a number of substrates, numerous products corresponding to the isositsirikine **7** analog were observed, suggesting that this enzyme activity produced a variety of isomers with identical molecular formulae upon reduction of certain substrate analogs (Figure 3-40). In summary, for many of these analogs, rigorous structural identification could not be performed. However, consumption of the starting material, along with the formation of a product with an exact mass corresponding to the ajmalicine **4** and isositsirikine **7** analog strongly suggests that the substrate analogs are turned over.

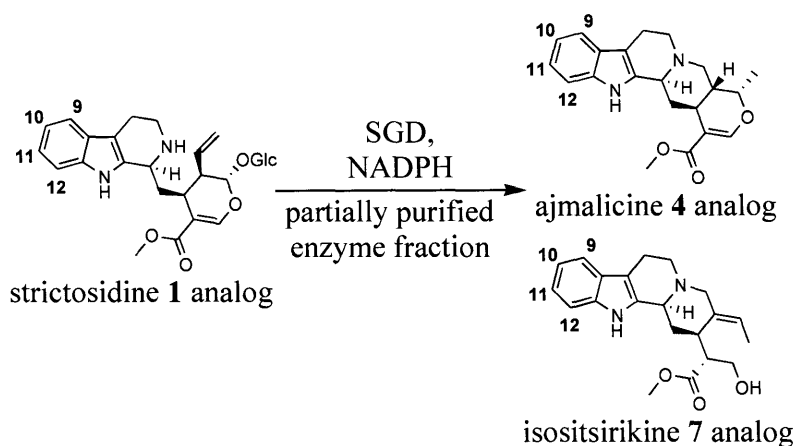


Figure 3-24: Indole substituted strictosidine analogs **1-1** and **1-a** through **1-t** were accepted by ajmalicine synthase and isositsirikine synthase to form the corresponding ajmalicine **4** and isositsirikine **7** analogs.

d_4 strictosidine 1-1	9-chloro strictosidine 1-k
benzo strictosidine 1-a	10-chloro strictosidine 1-l
thio strictosidine 1-b	12-chloro strictosidine 1-m
9-fluoro strictosidine 1-c	9-bromo strictosidine 1-n
10-fluoro strictosidine 1-d	10-bromo strictosidine 1-o
11-fluoro strictosidine 1-e	10-hydroxy strictosidine 1-p
12-fluoro strictosidine 1-f	10-isopropyl 1-q
9-methyl strictosidine 1-g	10-methoxy strictosidine 1-r
10-methyl strictosidine 1-h	11-methoxy strictosidine 1-s
11-methyl strictosidine 1-i	pentynyl-ester strictosidine 1-t
12-methyl strictosidine 1-j	

Table 3-9: Indole substituted strictosidine **1** analogs that were found to form the corresponding ajmalicine **4** and isositsirikine **7** analogs.

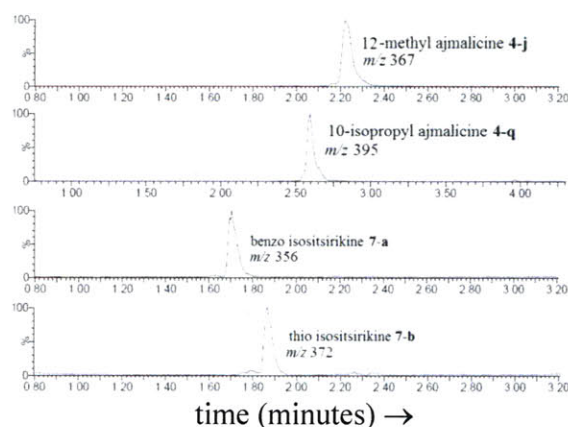


Figure 3-25: Representative LCMS chromatograms of enzymatically produced ajmalicine **4** and isositsirikine **7** analogs. The *x*-axis is time in minutes, and the *y*-axis is intensity.

ii. Novel des-vinyl analogs

In collaboration with Dr. Peter Bernhardt, 18,19-des-vinyl strictosidine **1-z** was enzymatically synthesized from tryptamine **18**, des-vinyl secologanin, and strictosidine synthase. This strictosidine analog was deglycosylated with SGD to produce 18,19-des-vinyl strictosidine aglycone **49-z** (as described in Chapter 2), which was then converted by a partially purified ajmalicine synthase fraction into a compound with a ^1H NMR spectrum and mass (m/z 327) consistent with reduced 18,19-des-vinyl strictosidine aglycone **4-z** (Figure 3-26).

A mixture of 18,19-des-vinyl strictosidine isomers **1-y** that were synthesized chemically from tryptamine **18** and des-vinyl secologanin was completely deglycosylated upon addition of a mixture of α - and β -glucosidases (SGD, β -glucosidase from almonds, and α -glucosidase from *B. stearothermophilus*) to form 18,19-des-vinyl strictosidine aglycone isomers **49-y** (Figure 3-26 and chromatogram 1 of Figure 3-27). When NADPH and a partially purified enzyme fraction were added to 18,19-des-vinyl strictosidine

aglycone isomers **49-y**, two separable reduced isomers formed (**4-y**); one product co-eluted with the reduced product of 18,19-des-vinyl strictosidine aglycone **4-z** (Figure 3-28). The reduced products **4-y** contain two stereogenic centers, C-3 and C-15, and only two sets of diastereomers are expected to separate under the chromatographic conditions. Because all 18,19-des-vinyl strictosidine aglycone isomers **49-y** were completely consumed upon addition of the reductase activity, we conclude that the reductase(s) present in the partially purified enzyme fraction turn(s) over all secologanin dihydropyran configurations. The reductase(s) that generate heteroyohimbine alkaloids appear(s) to be capable of acting upon a wide variety of substrates. This suggests that this reductase(s) will have broad applications in chemoenzymatic synthesis after efforts to clone the enzyme are successful. Synthetic installation of the vinyl group at the C-20 position will allow access to an even broader range of alkaloid structures.

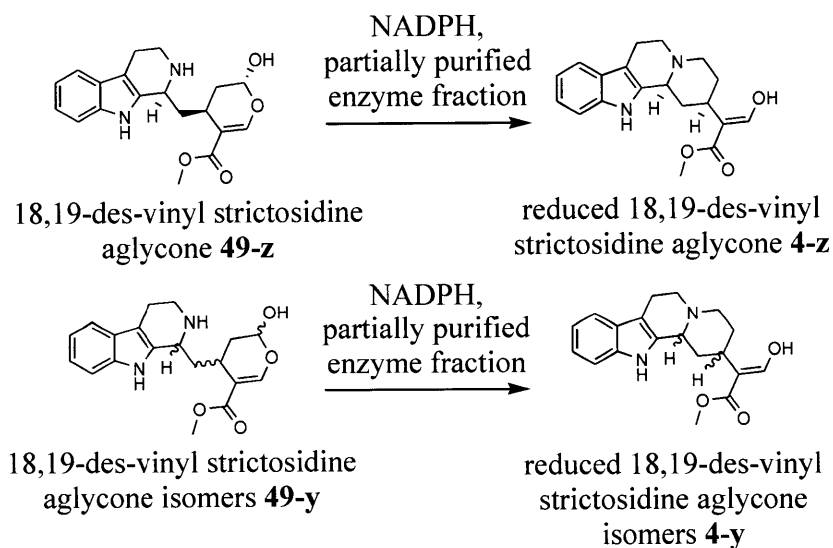


Figure 3-26: 18,19-des-vinyl strictosidine aglycone **49-z** is reduced by NADPH and a partially purified enzyme fraction to produce a compound with a ^1H NMR spectrum and mass consistent with reduced 18,19-des-vinyl strictosidine aglycone **4-z** (m/z 327). The

mixture of 18,19-des-vinyl strictosidine aglycone isomers **49-y** is reduced to two different diastereomers **4-y** (m/z 327) upon addition of NADPH and a partially purified enzyme fraction.

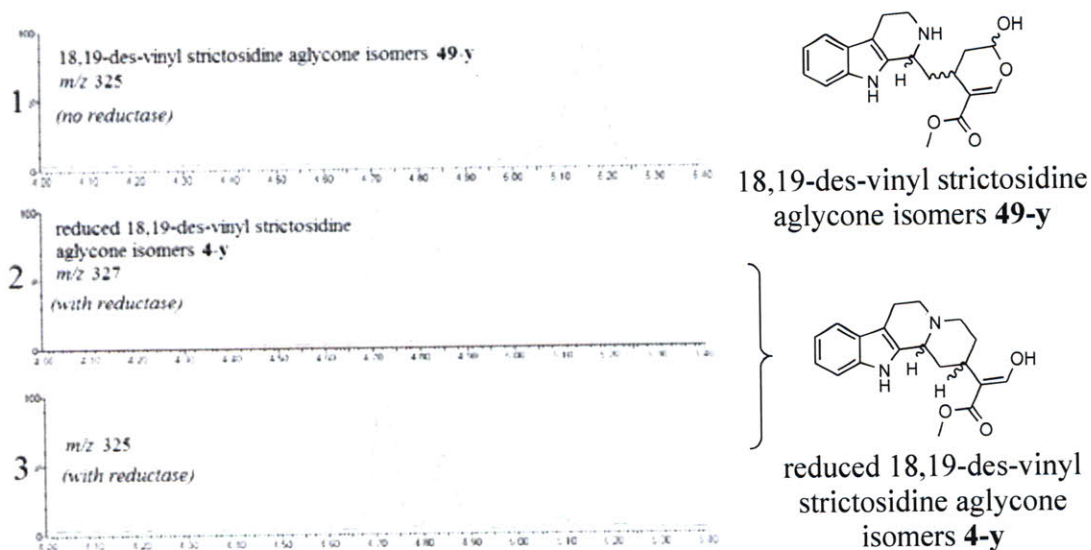


Figure 3-27: 18,19-des-vinyl strictosidine aglycone isomers **49-y** (m/z 325) (chromatogram 1) are completely converted by the reductase activity to reduced 18,19-des-vinyl strictosidine aglycone isomers **4-y** (m/z 327) (chromatogram 2). The two peaks with m/z 325 observed in chromatogram 3 correspond to the isotope peaks of m/z 327; all 18,19-des-vinyl strictosidine aglycone isomers **49-y** have been consumed by reductase(s) present in the partially purified enzyme fraction. Chromatogram 1 shows the product **49-y** of incubation of 18,19-des-vinyl strictosidine **1-y** with *B. stearrowophilus* α -glucosidase, almond β -glucosidase, and *C. roseus* strictosidine- β -glucosidase, without reductase. Chromatograms 2 and 3 are extracted masses from the same reaction, where reductase has been added. The x -axis is time in minutes, and the y -axis is intensity.

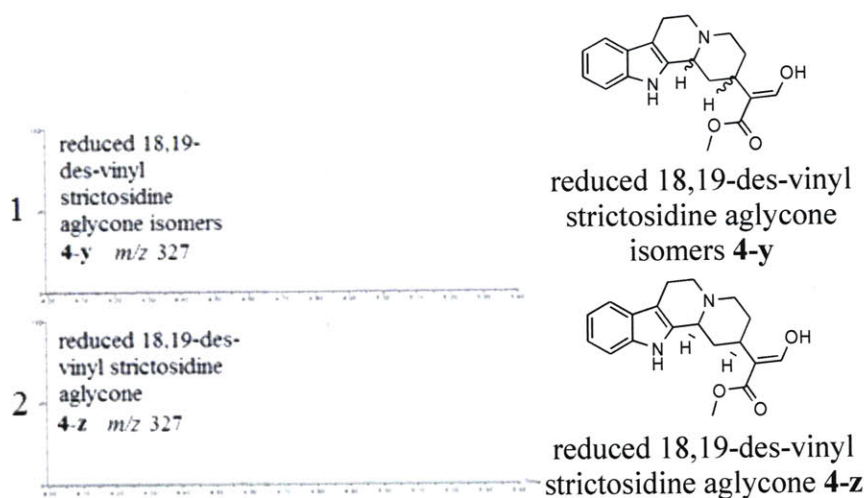


Figure 3-28: Chromatogram 1: Reduction of 18,19-des-vinyl strictosidine aglycone isomers **49-y** yields two separable isomers **4-y** with m/z 327. Chromatogram 2: Reduction of 18,19-des-vinyl strictosidine aglycone **49-z** yields a single product **4-z** with m/z 327. The x -axis is time in minutes, and the y -axis is intensity.

iii. Steady state kinetic analysis studies

Steady state kinetic analysis studies on the reduction of representative deglycosylated strictosidine **49** analogs by ajmalicine synthase and isositsirikine synthase were performed to quantify the effects of substrate specificity. However, since despite extensive efforts, neither ajmalicine synthase nor isositsirikine synthase has been purified to homogeneity, we cannot rigorously exclude the involvement of additional reductases in the turnover of the deglycosylated strictosidine **49** analogs described herein.

The steady state kinetic analysis for the reduction catalyzed by ajmalicine synthase of deglycosylated d_4 strictosidine **49-1** to d_4 ajmalicine **4-1** (Figure 3-29) was performed (Table 3-10). Partially purified ajmalicine synthase formed d_4 ajmalicine **4-1** with a catalytic efficiency (V_{\max}/K_m) of $1.61 \times 10^{-2} \text{ min}^{-1}$. The deuterium atoms of d_4

strictosidine **1-1** are not expected to interfere with the catalytic efficiency of ajmalicine synthase. d_4 strictosidine **1-1** was used instead of natural strictosidine **1** to ensure that no trace amounts of ajmalicine **4** present in the partially purified enzyme fraction would interfere with detection of reductase activity.

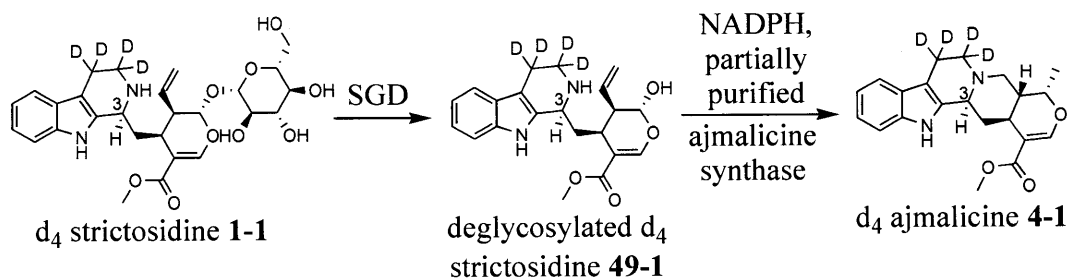


Figure 3-29: d_4 Strictosidine **1-1** is deglycosylated by SGD to form deglycosylated d_4 strictosidine **49-1**, which is then reduced by NADPH and partially purified ajmalicine synthase to d_4 ajmalicine **4-1**.

Strictosidine analog	V_{\max} ($\mu\text{M}/\text{min}$)	K_m (μM)	V_{\max}/K_m (min^{-1})
d_4 strictosidine 1-1	1.09 ± 0.06	67.9 ± 11.5	1.61×10^{-2}

Table 3-10: The steady state kinetic data of partially purified ajmalicine synthase. d_4 Strictosidine **1-1** is deglycosylated by SGD and then reduced by partially purified ajmalicine synthase to d_4 ajmalicine **4-1**.

To explore the effects of steric substitution on the indole ring, steady state kinetic analysis was performed on 9-methyl **1-g**, 10-methyl **1-h**, 11-methyl **1-i**, and 12-methyl **1-j** strictosidine (Table 3-11). The catalytic efficiency of ajmalicine synthase does not appear to be significantly altered by indole substitution: V_{\max}/K_m values for the four methyl strictosidine analogs **1-g** through **1-j** did not differ by more than an order of magnitude. Similarly, in a precursor directed biosynthesis study³⁶ with 9-methyl **1-g**, 10-

methyl **1-h**, 11-methyl **1-i**, and 12-methyl **1-j** strictosidine, the percentages of methylated ajmalicine **4** analogs and methylated serpentine **5** analogs, which are formed via a peroxidase-catalyzed oxidation of ajmalicine **4**¹, did not vary significantly. Specifically, the percentages of methylated ajmalicine **4** analogs and methylated serpentine **5** analogs produced as part of the total amounts of alkaloids produced were 21%, 34%, 22%, and 6% for 9-methyl **1-g**, 10-methyl **1-h**, 11-methyl **1-i**, and 12-methyl **1-j** strictosidine, respectively.

Strictosidine analog	V_{\max} ($\mu\text{M}/\text{min}$)	K_m (μM)	V_{\max} / K_m (min^{-1})	Relative V_{\max} / K_m	% in precursor study
9-methyl 1-g	0.49 ± 0.01	69.2 ± 5.3	7.08×10^{-3}	0.61	21
10-methyl 1-h	0.46 ± 0.01	70.6 ± 5.7	6.52×10^{-3}	0.56	34
11-methyl 1-i	0.69 ± 0.02	58.9 ± 6.6	1.17×10^{-2}	1	22
12-methyl 1-j	0.67 ± 0.02	95.5 ± 10.6	7.01×10^{-3}	0.6	6

Table 3-11: Steady state kinetic data of partially purified ajmalicine synthase. Methylated strictosidine analogs **1-g** through **1-j** were deglycosylated by SGD and then reduced by partially purified ajmalicine synthase to form methylated ajmalicine analogs **4-g** through **4-j**, respectively. The relative V_{\max}/K_m values are listed, with the V_{\max}/K_m value for 11-methyl strictosidine **1-i** normalized to 1. The percentages of methylated ajmalicine **4** analogs and methylated serpentine **5** analogs formed as part of the total amounts of methylated alkaloids produced in a previous precursor directed biosynthesis study³⁶ are also listed.

To quantitatively measure the capacity of this reductase for alternate stereoisomers, the steady state kinetics for ajmalicine synthase with deglycosylated d₄ vincoside **84** were also determined (Table 3-12 and Figure 3-43). Partially purified

ajmalicine synthase formed a compound with an exact mass corresponding to an isomer of ajmalicine, presumably d_4 C-3 *R* ajmalicine **85**. Partially purified ajmalicine synthase reduced deglycosylated d_4 vincoside **84** with a catalytic efficiency (V_{\max}/K_m) of $1.13 \times 10^{-4} \text{ min}^{-1}$. The preference for deglycosylated d_4 strictosidine **49-1** compared to deglycosylated d_4 vincoside **84** suggests that the reductase activity derives from the monoterpene indole alkaloid pathway; vincoside **43**, the C-3 *R* diastereomer of strictosidine **1**, is not produced by strictosidine synthase, and no alkaloids downstream of strictosidine **1** are naturally observed with C-3 *R* stereochemistry. Ajmalicine synthase, which has evolved to catalytically prefer its natural substrate, can nevertheless reduce the nonnatural stereoisomer.

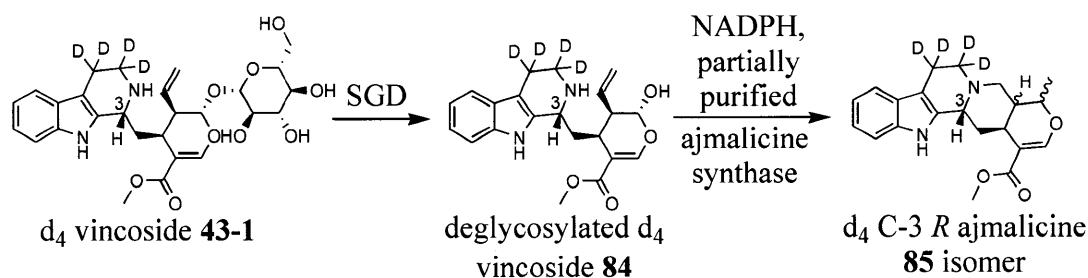


Figure 3-30: d_4 vincoside **43-1** is deglycosylated by SGD to form deglycosylated d_4 vincoside **84**, which is then reduced by NADPH and partially purified ajmalicine synthase to form a compound with an exact mass corresponding to an ajmalicine isomer, presumably d_4 C-3 *R* ajmalicine **85**. The C-3 position is indicated in blue.

Strictosidine analog	V_{\max} ($\mu\text{M}/\text{min}$)	K_m (μM)	V_{\max}/K_m (min^{-1})
d_4 vincoside 43-1	0.079 ± 0.004	701.5 ± 91.7	1.13×10^{-4}

Table 3-12: Steady state kinetic data of partially purified ajmalicine synthase. d_4 vincoside **43-1** is deglycosylated by SGD and then reduced by partially purified ajmalicine synthase.

In all of the substrate specificity assays using indole substituted strictosidine analogs **1-c** through **1-s**, the ajmalicine **4** analog was the major product and the isositsirikine **7** analog was a minor product. For benzo strictosidine **1-a** and thio strictosidine **1-b**, however, the ratio of ajmalicine **4** analog to isositsirikine **7** analog was reversed. Moreover, more than one product corresponding to the ajmalicine **4** product analog was formed for benzo strictosidine **1-a** and thio strictosidine **1-b**; all other strictosidine **1** analogs only produced a single ajmalicine **4** isomer product. Again, the difficulties of obtaining milligram quantities of enzymatic product from these enzymatic preparations unfortunately precluded more detailed analysis of these products. Nevertheless, intrigued by this finding, I determined the steady state kinetics for the reduction of deglycosylated d_4 strictosidine **49-1**, deglycosylated benzo strictosidine **49-a**, and deglycosylated thio strictosidine **49-b** by partially purified isositsirikine synthase (Table 3-13). Isositsirikine synthase showed a 25-fold catalytic preference (V_{\max}/K_m) for deglycosylated benzo strictosidine **49-a** over deglycosylated d_4 strictosidine **49-1**, and a 37-fold catalytic preference for deglycosylated thio strictosidine **49-b** over deglycosylated d_4 strictosidine **49-1**³⁴.

Strictosidine analog	V_{\max} ($\mu\text{M}/\text{min}$)	K_m (μM)	V_{\max}/K_m (min^{-1})
d₄ 1-1	0.16 ± 0.02	98.9 ± 36.4	1.63×10^{-3}
benzo 1-a	1.23 ± 0.09	36.6 ± 9.5	3.36×10^{-2}
thio 1-b	1.04 ± 0.04	17.2 ± 2.1	6.03×10^{-2}

Table 3-13: Steady state kinetic data of partially purified isositsirikine synthase. d₄ Strictosidine **1-1**, benzo strictosidine **1-a**, and thio strictosidine **1-b** were deglycosylated by SGD and then reduced by partially purified isositsirikine synthase to form d₄ isositsirikine **7-1**, benzo isositsirikine **7-a**, and thio isositsirikine **7-b**, respectively.

We wanted to investigate whether the inherent electronic difference in the indole **35**, benzofuran **37**, and benzothiophene **38** moieties may have affected the product ratio of ajmalicine **4** to isositsirikine **7**. A chemical reduction of deglycosylated d₄ strictosidine **49-1**, deglycosylated benzo strictosidine **49-a**, and deglycosylated thio strictosidine **49-b** with NaCNBH₃ was performed for comparison with the enzymatic reaction (Figure 3-31). A 400- or 6,000-fold excess of NaCNBH₃ was added to deglycosylated d₄ strictosidine **49-1**, deglycosylated benzo strictosidine **49-a**, or deglycosylated thio strictosidine **49-b** in 50 mM sodium phosphate buffer, pH 7.5, and the reaction mixture was incubated at 30°C. Aliquots were quenched in methanol, and the starting materials and products were analyzed via LCMS using a five minute, 10-90% acetonitrile in 0.1% formic acid gradient. With this LCMS method, d₄ ajmalicine **4-1** and d₄ isositsirikine **7-1** are typically observed at 2.0 and 1.8 minutes, respectively; benzo ajmalicine **4-a** and isositsirikine **7-a** are typically observed at 2.3 and 1.7 minutes, respectively; and thio ajmalicine **4-b** and isositsirikine **7-b** are typically observed at 2.3 and 1.8 minutes, respectively. For all time points, from 1 minute to 2 hours, the ajmalicine **4** isomers were the major product observed by LCMS; virtually no isositsirikine **7** products were observed (Figure 3-32).

We therefore conclude that the faster reduction of deglycosylated benzo **49-a** and deglycosylated thio **49-b** strictosidine to the corresponding isositsirikine **7** analogs in the assay with partially purified isositsirikine synthase is the result of enzymatic, and not chemical, effects.

Intriguingly, an additional reduced product **80** (Figure 3-32 and Figure 3-33) with the same mass as isositsirikine **7** was produced for all three strictosidine **1** analogs in this chemical reaction. This product **80** has the same retention time as ajmalicine **4**, and we hypothesize that this product results from reduction of the double bond of the α , β unsaturated ester of the ajmalicine **4** isomer (Figure 3-33). This product is not formed in the enzymatic reaction, it is not found in *C. roseus* hairy root or cell suspension culture, and we do not believe it to be an isositsirikine **7** isomer its LCMS retention time is significantly later than that of isositsirikine **7**. Efforts to isolate and characterize the product by ^1H NMR proved unsuccessful.

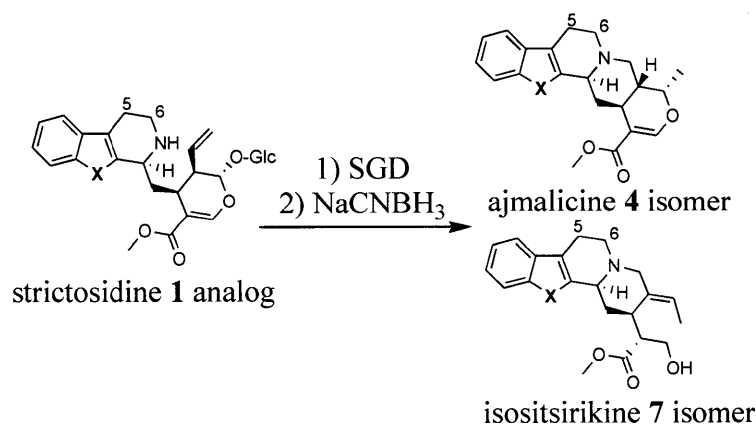


Figure 3-31: The d₄ **1-1**, benzo **1-a**, and thio **1-b** strictosidine analogs were deglycosylated and then incubated with sodium cyanoborohydride (NaCNBH₃). The ajmalicine **4** isomer was the major product produced for all three analogs; virtually no

detectable isositsirikine **7** isomer product was observed. X means NH for d₄ strictosidine **1-1** and d₄ ajmalicine isomers **4-1** (and two deuteriums at each of the C-5 and C-6 positions, which are labeled in blue), X means O for benzo strictosidine **1-a** and benzo ajmalicine **4-a** isomers, and X means S for thio strictosidine **1-b** and thio ajmalicine **4-b** isomers.

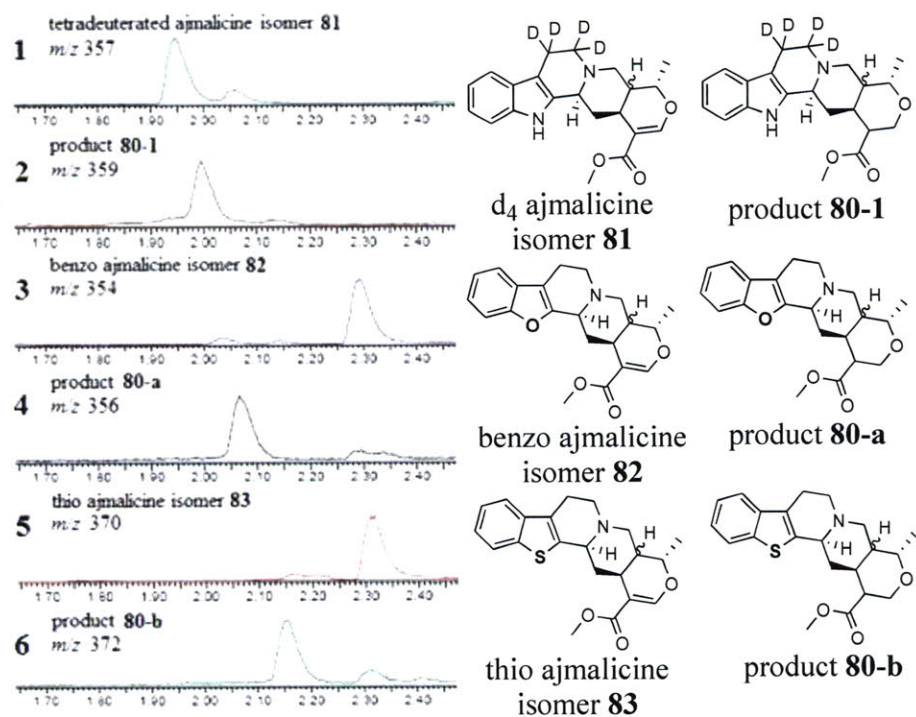


Figure 3-32: LCMS chromatograms of NaCNBH₃ reaction with strictosidine analogs **1-1**, **1-a**, and **1-b**. The chemical structure of each peak is shown. A gradient of 10-90% acetonitrile in water with 0.1% formic acid over 5 minutes was used. Chromatogram 1: d₄ ajmalicine isomer **81** elutes at 1.95 minutes. Chromatogram 2: No d₄ isositsirikine isomer is observed at 1.8 minutes. The peak at 2 minutes is the d₄ reduction product **80-1** that we hypothesize is produced via reduction of the double bond of the α , β unsaturated ester of the ajmalicine isomer. Chromatogram 3: Benzo ajmalicine isomer **82** elutes at 2.3

and second (40% v/v acetone) acetone precipitations. The third acetone precipitation (57% v/v acetone) contains the majority of the ajmalicine synthase activity; ajmalicine synthase specific activities of 0, 0.068, and 0.094 $\mu\text{M min}^{-1}$ per mg protein mL^{-1} are observed for the first, second, and third acetone precipitations, respectively. The third acetone precipitation contains virtually all of the isositsirikine synthase activity; isositsirikine synthase specific activities of 0, 0.003, and 0.044 $\mu\text{M min}^{-1}$ per mg protein mL^{-1} are observed for the first, second, and third acetone precipitations, respectively (Table 3-1). The switch from ammonium sulfate precipitation, which I performed in my early purification attempts, to acetone precipitation resulted in the discovery of isositsirikine synthase activity; isositsirikine synthase activity had never been detected from preparations using ammonium sulfate precipitation. There are no reports to date in the literature for isositsirikine synthase; thus the switch from ammonium sulfate to acetone precipitation was particularly fortuitous.

After the acetone precipitation step, I performed an anion exchange FPLC step using a DEAE matrix. As Figure 3-19 and Table 3-2 show, the two groups of fractions with the highest ajmalicine synthase specific activity and isositsirikine synthase specific activity, B8-9 and B10-12, have lower UV_{280} absorbencies and thus lower protein concentrations than fractions such as B6-7 and B4-5. Fractions B6-7 and B4-5 have higher UV_{280} absorbencies yet lower ajmalicine synthase specific activity and isositsirikine synthase specific activity than fractions B8-9 and B10-12. Thus, DEAE FPLC chromatography successfully enriched the specific activity of ajmalicine synthase and isositsirikine synthase.

The size 200 gel filtration FPLC step following DEAE FPLC was partially successful in purification (Figure 3-21). Unfortunately, however, low specific activities are observed after this step, and ajmalicine synthase and isositsirikine synthase are spread out over many fractions. The extreme lability of these reductases was an extraordinarily challenging aspect of this purification. It is possible that ajmalicine synthase and isositsirikine synthase exist as multimeric enzymes, and the decrease in activity could perhaps be explained by separation of the subunits during the size 200 gel filtration FPLC step. A 2D SDS-PAGE of fractions from the size 200 gel filtration step shows numerous proteins (Figure 3-21). Additional purification strategies are necessary for enrichment of ajmalicine synthase and isositsirikine synthase, but these efforts are complicated by the loss in specific activity throughout the purification process.

Reactive Red Agarose, a dye affinity chromatography strategy, was shown to elute ajmalicine synthase in high salt fractions while eluting the majority of the proteins in wash fractions (Table 3-5). A purification step using Reactive Red Agarose could potentially be performed after the DEAE FPLC step. However, 2D gel analysis did not show significant purification of a fraction from size exclusion chromatography after elution from Reactive Red Agarose, indicating that many more chromatography steps are still required.

Nevertheless, protein sequences of the eight major proteins present after acetone precipitation, DEAE, and size exclusion chromatography were subjected to protein sequencing for identification after separation by 2D SDS-PAGE. One of the eight proteins in Table 3-4, protein 3 exhibits 61% sequence identity to a cinnamyl alcohol dehydrogenase, an enzyme that reduces an aldehyde to an alcohol¹²⁰. One cinnamyl

alcohol dehydrogenase homolog, perakine reductase, has also been reported to reduce the aldehyde moiety of the TIA perakine. It is possible, based on the sequence homology, that protein 3 could reduce an imine to an amine, such as in the reduction of the iminium moiety of cathenamine **49** to ajmalicine **4** (Figure 3-34). Only a partial sequence of protein 3 is known and deposited in a *C. roseus* EST database (747 nucleotides). Because cloning full length cDNA is difficult and time consuming, we defer further characterization of this protein until a transcriptome sequencing project now underway is completed: the completion is scheduled for July 2010.

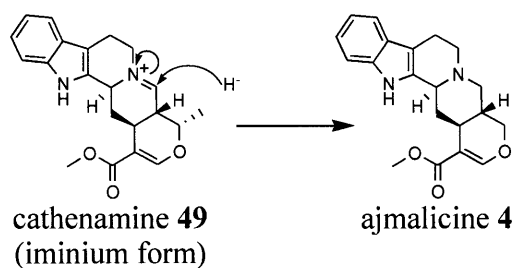


Figure 3-34: An enzyme like cinnamyl alcohol dehydrogenase could potentially reduce the iminium of cathenamine **49** to form the amine in ajmalicine **4**.

Preliminary expression data obtained from the Illumina sequencing of *C. roseus* seedling cDNA currently shows that the transcript for the EST for protein 3 in Table 3-4 is up-regulated in elicited seedlings along with all other alkaloid biosynthetic genes. Elicitation of *C. roseus* seedlings by the plant hormone methyl jasmonate has been reported to increase both alkaloid production and expression of TIA biosynthetic genes¹²⁸. Although the up-regulation observed in the preliminary expression data from the transcriptome sequencing is modest (1.5-fold), it is similar to the levels of elicitation observed in known vindoline **28** biosynthetic enzymes (1.5-1.9-fold) (R. Buell, Michigan

State University, unpublished). Therefore, the levels of up-regulation of this gene are consistent with those of an enzyme involved in alkaloid biosynthesis.

Substrate specificity and steady state kinetic studies

Ajmalicine synthase and isositsirikine synthase were shown to have broad substrate specificity, reducing deglycosylated strictosidine **49** analogs containing altered indole, ester, and heterocyclic moieties. This finding qualitatively agreed with previous precursor directed biosynthesis studies^{34,36}. All deglycosylated indole substituted strictosidine analogs, which included fluoro (**49-c** through **49-f**), chloro (**49-k** through **49-m**), bromo (**49-n** and **49-o**), and methyl (**49-g** through **49-j**) substitutions, were accepted by ajmalicine synthase and isositsirikine synthase to form products with exact masses corresponding to ajmalicine **4** and isositsirikine **7** analogs, indicating that the active sites of both enzymes are able to tolerate substitutions on the indole moiety. Deglycosylated pentynyl-ester strictosidine **49-t** was also reduced by both enzymes to form products with exact masses corresponding to pentynyl-ester ajmalicine **4-t** and pentynyl-ester isositsirikine **7-t**, indicating that a large alkyl ester chain does not prevent turnover. Deglycosylated benzo strictosidine **49-a** and deglycosylated thio strictosidine **49-b** are turned over as well, indicating that ajmalicine and isositsirikine synthase are able to tolerate strictosidine **1** analogs with altered electron densities. Additionally, deglycosylated d₄ vincoside **84** was reduced by ajmalicine synthase to form an isomer of ajmalicine, presumably d₄ C-3 *R* ajmalicine **85**, thus indicating that ajmalicine synthase does not require a specific stereoisomer for turnover. The reduction of 18,19-des-vinyl strictosidine aglycone isomers **49-y** (Figure 1-35) further demonstrates that altered stereochemical configurations are tolerated.

The broad substrate specificity observed is promising for the development of novel analogs with improved therapeutic activities. Ajmalicine **4** is used clinically as an anti-hypertensive agent, and isositsirikine **7** has been reported to have anti-neoplastic activities. The introduction of halogens as indole substitutions could increase the lipophilicity of the ajmalicine **4** and isositsirikine **7** analogs, improving their ability to traverse membranes. The introduction of a hydroxy moiety at the C-10 position could improve the water solubility of ajmalicine **4** and isositsirikine **7** analogs, improving their ability to diffuse through the cytosol. The introduction of altered stereochemical configurations could drastically alter the biological properties of ajmalicine **4** and isositsirikine **7** analogs.

Steady state kinetic studies also showed that 9-methyl **1-g**, 10-methyl **1-h**, 11-methyl **1-i**, and 12-methyl **1-j** strictosidine all had catalytic efficiencies within an order of magnitude. This finding indicates that ajmalicine synthase is able to tolerate substituents at each indole position approximately equally. In a precursor directed biosynthesis study performed by Dr. Elizabeth McCoy³⁶, 9-methyl **1-g**, 10-methyl **1-h**, 11-methyl **1-i**, and 12-methyl **1-j** strictosidine were each incorporated to form methylated analogs of ajmalicine **4** and serpentine **5**, the downstream product of ajmalicine **4**. The percentages of ajmalicine **4** and serpentine **5**, which is formed via a peroxidase-catalyzed oxidation of ajmalicine **4**¹, in the methylated alkaloid profiles varied from 6 to 34%³⁶. Thus both in the steady state kinetic analysis study of methylated strictosidine analogs and in the precursor directed biosynthesis study, the presence of a methyl moiety at a given indole position of strictosidine **1** did not have drastic effects either on the turnover by ajmalicine synthase or on the partitioning of a given strictosidine **1** analog into the different biosynthetic

pathways. The differences were more pronounced *in vivo*, suggesting that factors in addition to enzyme substrate specificity direct the product partitioning.

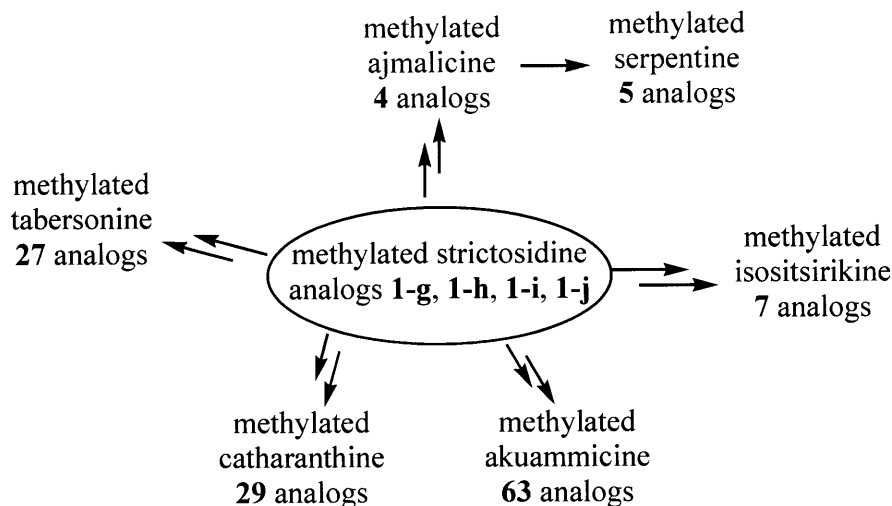


Figure 3-35: In a precursor directed biosynthesis study performed by Dr. Elizabeth McCoy³⁶, 9-methyl **1-g**, 10-methyl **1-h**, 11-methyl **1-i**, and 12-methyl **1-j** strictosidine analogs were co-cultured with *C. roseus* hairy root cultures for two weeks, and the resulting methylated alkaloid profile was measured. The percentages of methylated ajmalicine **4** and methylated serpentine **5** analogs (blue) produced from the 9-methyl **1-g**, 10-methyl **1-h**, 11-methyl **1-i**, and 12-methyl **1-j** strictosidine analogs varied from 6 to 34% of the total amount of methylated alkaloids produced³⁶.

In steady state kinetic studies with partially purified ajmalicine synthase, the slower rate of reduction of deglycosylated d₄ vincoside **84** compared to reduction of deglycosylated d₄ strictosidine **49-1** suggests that the reductase activity derives from the monoterpene indole alkaloid pathway. Vincoside **43**, the C-3 *R* diastereomer of strictosidine **1**, is not produced by strictosidine synthase, and no downstream TIAs with C-3 *R* stereochemistry are observed. Thus it is perhaps not unexpected that ajmalicine

synthase reduces d_4 deglycosylated strictosidine **49-1**, its natural substrate, more efficiently than it does the unnatural substrate, deglycosylated d_4 vincoside **84**.

Steady state kinetic analysis of isositsirikine synthase with deglycosylated d_4 strictosidine **49-1**, deglycosylated benzo strictosidine **49-a**, and deglycosylated thio strictosidine **49-b** showed that isositsirikine synthase reduces deglycosylated benzo strictosidine **49-a** and deglycosylated thio strictosidine **49-b** approximately 25- and 37-fold faster, respectively, than it does deglycosylated d_4 strictosidine **49-1**. The reason for this is currently unclear, though one hypothesis is that isositsirikine synthase is better able to tolerate substituents with altered electron densities than ajmalicine synthase.

Chemical reduction of deglycosylated strictosidine analogs **49-1**, **49-a**, and **49-b** with NaCNBH_3 demonstrated that ajmalicine **4** isomers were the major product, with virtually no isositsirikine **7** products formed. The mechanism of reduction by isositsirikine synthase is also unknown; unlike ajmalicine **4** formation, in which one NADPH-dependent reduction is required, two NADPH-dependent reduction steps are required for the formation of isositsirikine **7** from deglycosylated strictosidine **49**. It is unknown whether one or two reductases catalyze these reactions (Figure 3-1). Further studies are required to determine the mechanism of isositsirikine synthase. The availability of the potential reaction intermediate geissoschizine **64-1** will allow us to further explore these questions.

IV. *Materials and Methods*

A. *C. roseus* hairy root cultures

Catharanthus roseus hairy root cultures (Figure 3-36) were obtained from Professor Carolyn Lee Parsons of Northeastern University, Boston, MA. The hairy root cultures were grown in the dark at 125 rotations per minute (rpm) at 26°C in 100 mL of Gamborg's B5 media (half strength basal salts, full strength vitamins, 30 g sucrose L⁻¹, pH 5.7) and recultured every two weeks.



Figure 3-36: *C. roseus* hairy root cultures.

B. *C. roseus* cell suspension cultures

Catharanthus roseus PC510 cell suspension cultures were obtained from Deutsche Sammlung von Mikroorganismen und Zellkulturen GmbH (DSMZ) in Germany. The cell suspension cultures were grown at 125 rpm at room temperature (25°C) on a 12-hour light, 12-hour dark cycle. In each flask, 100 mL AM1B media (*PhytoTechnology* Laboratories, Shawnee Mission, Kansas) was used, and the cultures were recultured every two weeks.

C. Preparation of strictosidine analogs

Strictosidine **1** analogs were synthesized both chemically and enzymatically as described in the Materials and Methods section of Chapter 2.

D. High-resolution mass spectrometry data

All compounds were diluted in methanol to approximately 1 nM concentration and then ionized by ESI/FT-MS in the positive ion mode.

Ajmalicine analogs

d₄ ajmalicine **4-1**: [M+H]⁺ Expected: 357.2111. Observed: 357.2116

benzo ajmalicine **4-a**: [M+H]⁺ Expected: 354.1700. Observed: 354.1704

thio ajmalicine **4-b**: [M+H]⁺ Expected: 370.1471. Observed: 370.1463

9-fluoro ajmalicine **4-c**: [M+H]⁺ Expected: 371.1765. Observed: 371.1751

10-fluoro ajmalicine **4-d**: [M+H]⁺ Expected: 371.1765. Observed: 371.1771

11-fluoro ajmalicine **4-e**: [M+H]⁺ Expected: 371.1765. Observed: 371.1750

12-fluoro ajmalicine **4-f**: [M+H]⁺ Expected: 371.1765. Observed: 371.1756

9-methyl ajmalicine **4-g**: [M+H]⁺ Expected: 367.2016. Observed: 367.2014

10-methyl ajmalicine **4-h**: [M+H]⁺ Expected: 367.2016. Observed: 367.2006

11-methyl ajmalicine **4-i**: [M+H]⁺ Expected: 367.2016. Observed: 367.2001

12-methyl ajmalicine **4-j**: [M+H]⁺ Expected: 367.2016. Observed: 367.2025

9-chloro ajmalicine **4-k**: [M+H]⁺ Expected: 387.1470. Observed: 387.1485

10-chloro ajmalicine **4-l**: [M+H]⁺ Expected: 387.1470. Observed: 387.1456

12-chloro ajmalicine **4-m**: [M+H]⁺ Expected: 387.1470. Observed: 387.1479

9-bromo ajmalicine **4-n**: [M+H]⁺ Expected: 431.0965. Observed: 431.0967

10-bromo ajmalicine **4-o**: [M+H]⁺ Expected: 431.0965. Observed: 431.0968

10-hydroxy ajmalicine **4-p**: [M+H]⁺ Expected: 369.1809. Observed: 369.1802

10-isopropyl ajmalicine **4-q**: [M+H]⁺ Expected: 395.2329. Observed: 395.2328

10-methoxy ajmalicine **4-r**: [M+H]⁺ Expected: 383.1965. Observed: 383.1952

11-methoxy ajmalicine **4-s**: [M+H]⁺ Expected: 383.1965. Observed: 383.1963

pentynyl-ester ajmalicine **4-t**: [M+H]⁺ Expected: 405.2173. Observed: 405.2159

Isositsirikine analogs

d₄ isositsirikine **7-1**: [M+H]⁺ Expected: 359.2267. Observed: 359.2276

benzo isositsirikine **7-a**: [M+H]⁺ Expected: 356.1856. Observed: 356.1861

thio isositsirikine **7-b**: [M+H]⁺ Expected: 372.1628. Observed: 372.1620

9-fluoro isositsirikine **7-c**: [M+H]⁺ Expected: 373.1922. Observed: 373.1923

10-fluoro isositsirikine **7-d**: [M+H]⁺ Expected: 373.1922. Observed: 373.1932

11-fluoro isositsirikine **7-e**: [M+H]⁺ Expected: 373.1922. Observed: 373.1921

12-fluoro isositsirikine **7-f**: [M+H]⁺ Expected: 373.1922. Observed: 373.1925

9-methyl isositsirikine **7-g**: [M+H]⁺ Expected: 369.2173. Observed: 369.2188

10-methyl isositsirikine **7-h**: [M+H]⁺ Expected: 369.2173. Observed: 369.2173

11-methyl isositsirikine **7-i**: [M+H]⁺ Expected: 369.2173. Observed: 369.2191

12-methyl isositsirikine **7-j**: [M+H]⁺ Expected: 369.2173. Observed: 369.2211

9-chloro isositsirikine **7-k**: [M+H]⁺ Expected: 389.1626. Observed: 389.1454

10-chloro isositsirikine **7-l**: [M+H]⁺ Expected: 389.1626. Observed: 389.1624

12-chloro isositsirikine **7-m**: [M+H]⁺ Expected: 389.1626. Observed: 389.1444

9-bromo isositsirikine **7-n**: [M+H]⁺ Expected: 433.1122. Observed: 433.0929

10-bromo isositsirikine **7-o**: [M+H]⁺ Expected: 433.1122. Observed: 433.0946

10-hydroxy isositsirikine **7-p**: [M+H]⁺ Expected: 371.1965. Observed: 371.1961

10-isopropyl isositsirikine **7-q**: [M+H]⁺ Expected: 397.2486. Observed: 397.2129

10-methoxy isositsirikine **7-r**: [M+H]⁺ Expected: 385.2122. Observed: 385.2112

11-methoxy isositsirikine **7-s**: [M+H]⁺ Expected: 385.2122. Observed: 385.2127

pentynyl-ester isositsirikine **7-t**: [M+H]⁺ Expected: 407.2329. Observed: 407.2325

E. NMR characterization

¹H NMR data for reduced 18,19-des-vinyl strictosidine aglycone **4-z** are described by Bernhardt *et al.*⁹⁷ ¹H-NMR data for authentic standards of strictosidine **1** and selected

ajmalicine **4** and isositsirikine **7** analogs are described by Dr. Elizabeth McCoy³⁶ and Dr. Hyang-Yeol Lee¹⁰⁴.

F. *Partial purification procedure*

Hairy root or cell suspension cultures were subcultured for two weeks, and then lysed by blending in borate buffer. Hairy roots (75 g) or filtered cell suspension cultures (300 g) were blended in 200 mL of 0.1 M borate buffer, pH 7.5, containing 20 mM β -mercaptoethanol, 0.1% PVP, 1 mM EDTA, and 10% glycerol. The hairy root or cell suspension cultures were lysed in a blender at 4°C for 5 minutes. The mixture was then centrifuged at 3,000g. The precipitate was discarded because it did not contain ajmalicine synthase or isositsirikine synthase activity.

I then performed acetone precipitation on the supernatant. For the first precipitation, 100 mL acetone was added to a total of 400 mL supernatant. The mixture was stirred at 80 rpm at 4°C for 5 minutes, and then centrifuged at 4,000g for 3 minutes. This first precipitate was discarded because it did not contain ajmalicine synthase or isositsirikine synthase activity. An additional 100 mL acetone was then added to the supernatant, and the mixture was stirred at 80 rpm at 4°C for 5 minutes, and then centrifuged at 4,000g for 3 minutes. The second precipitate was resuspended in 50 mM sodium phosphate buffer, pH 7.5, containing 10% glycerol (7 mL). A third precipitation was then performed by adding 200 mL acetone to the supernatant, stirring at 80 rpm at 4°C for 5 minutes, and centrifuging at 4,000g for 3 minutes. The third precipitate was also resuspended in 50 mM sodium phosphate buffer, pH 7.5, containing 10% glycerol (7 mL). I performed enzyme activity assays with resolubilized precipitate to assess ajmalicine synthase or isositsirikine synthase activity.

I applied the third acetone precipitation fraction to a DEAE column (DEAE Sepharose Fast Flow, GE Healthcare) on FPLC (GE Healthcare). Approximately 2 mg of protein was eluted with a gradient of 400-800 mM NaCl in 50 mM sodium phosphate buffer, pH 7.5, containing 10% glycerol. The flow rate was 5 mL min⁻¹, and the absorbance at 280 nm was monitored. Fractions were concentrated using Amicon Ultra 15 tubes (Millipore) with a 10 kDa membrane, and were then assayed for activity. Fractions B8-9 (Figure 3-19), which eluted at approximately 530-550 mM NaCl, consistently had the best ajmalicine synthase and isositsirikine synthase activity.

I then applied fractions B8-9 to a size 200 gel filtration column (HiLoad 16/60 Superdex 200 prep grade, GE Biosciences) on FPLC (GE Biosciences) using 50 mM sodium phosphate buffer, pH 7.5, containing 10% glycerol. The flow rate was 1 mL min⁻¹, and the absorbance at 280 nm was monitored. Fractions were collected and concentrated using Amicon Ultra 15 tubes (Millipore) with a 10 kDa membrane, and were then assayed for activity. Fractions C9-12 and D9-12 (Figure 3-21), which eluted at 64-72 mL and 72-80 mL, respectively, consistently had the best ajmalicine synthase and isositsirikine synthase activity.

To measure specific activity, I incubated strictosidine **1** or strictosidine **1** analogs with SGD, NADPH, and a partially purified enzyme fraction. A 200 μ L reaction volume was used, with 0.25 mM strictosidine **1** or strictosidine **1** analog, 750 nM SGD (typically), 5 mM NADPH, and 180 μ L partially purified reductase fraction (typically at a concentration of 1-3 total mg protein mL⁻¹). The reaction was incubated at 30°C, and 5 μ L aliquots were quenched with 950 μ L MeOH containing 500 nM yohimbine **6** as an internal standard. The samples were centrifuged (13,000g, 1 min) to remove particulates

and then analyzed by LCMS. The starting material and products were separated using a gradient of 10-90% acetonitrile in water with 0.1% formic acid over a period of 5 minutes. The increase in the area of the product peak was used to obtain the initial rates of the reduction reaction. The formation of ajmalicine **4** isomers was monitored by peak integration, normalized to an internal standard (yohimbine **6**), and correlated to peak area using a standard curve of ajmalicine **4**. The rate of ajmalicine **4** formation was divided by the protein concentration to obtain the specific activity in units of $\mu\text{M min}^{-1} / \text{mg protein mL}^{-1}$.

G. LCMS data

In Figure 3-37 and Figure 3-38 below, LCMS chromatograms for ajmalicine analogs **4-c**, **4-g**, **4-h**, **4-k**, **4-n**, **4-o**, and **4-p** and isositsirikine analog **7-c** are shown, with the top chromatograms showing the products of enzymatic assays, and the bottom chromatograms showing the standards provided by Dr. Elizabeth McCoy³⁶.

Ajmalicine analogs 4-c, 4-k, 4-n, 4-o

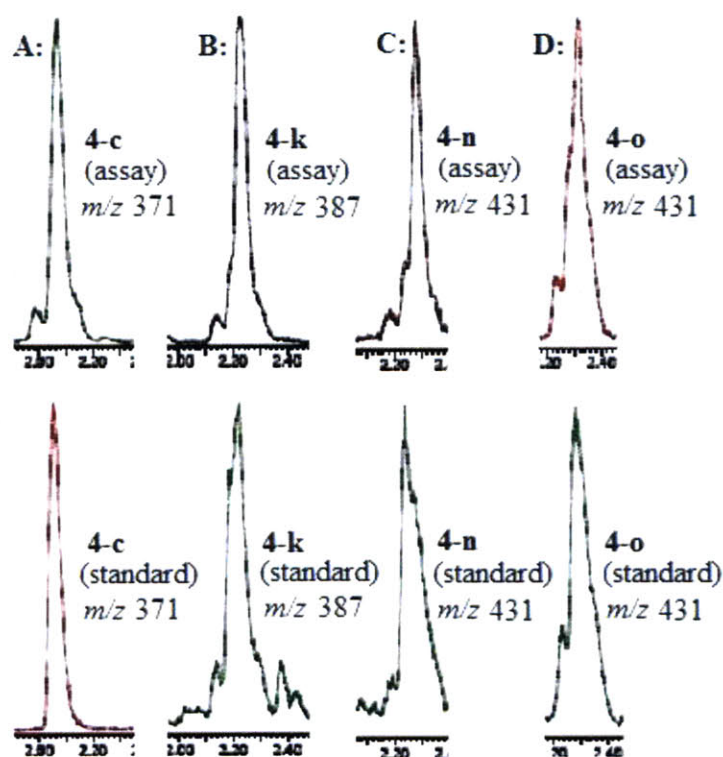


Figure 3-37: **A:** 9-fluoro ajmalicine **4-c** produced in assay (top chromatogram) and 9-fluoro ajmalicine **4-c** standard (bottom chromatogram). **B:** 9-chloro ajmalicine **4-k** produced in assay (top chromatogram) and 9-chloro ajmalicine **4-k** standard (bottom chromatogram). **C:** 9-bromo ajmalicine **4-n** produced in assay (top chromatogram) and 9-bromo ajmalicine **4-n** standard (bottom chromatogram). **D:** 10-bromo ajmalicine **4-o** produced in assay (top chromatogram) and 10-bromo ajmalicine **4-o** standard (bottom chromatogram). All standards are provided by Dr. Elizabeth McCoy³⁶. The x -axis is time in minutes, and the y -axis is intensity.

Ajmalicine analogs 4-g, 4-h, 4-p, 4-t and isositsirikine analog 7-c

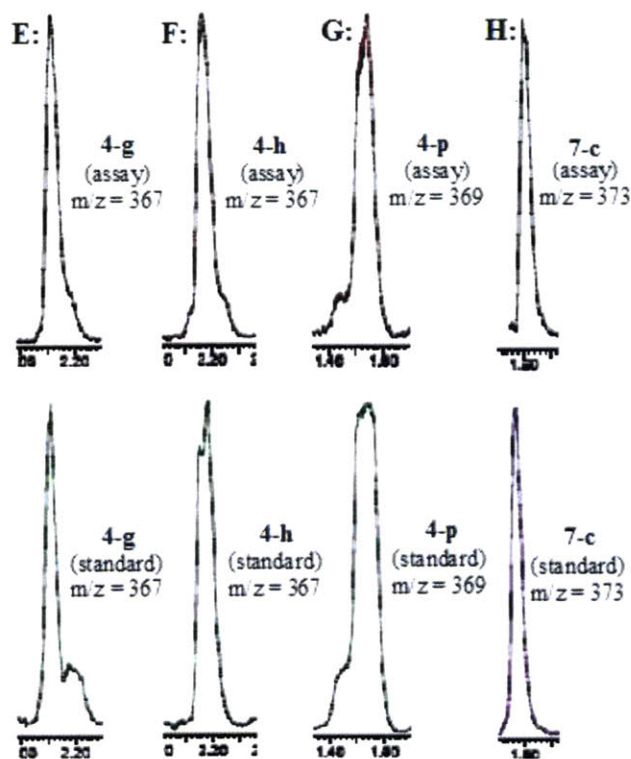


Figure 3-38: **E**: 9-methyl ajmalicine **4-g** produced in assay (top chromatogram) and 9-methyl ajmalicine **4-g** standard (bottom chromatogram). **F**: 10-methyl ajmalicine **4-h** produced in assay (top chromatogram) and 10-methyl ajmalicine **4-h** standard (bottom chromatogram). **G**: 10-hydroxy ajmalicine **4-p** produced in assay (top chromatogram) and 10-hydroxy ajmalicine **4-p** standard (bottom chromatogram). **H**: 9-fluoro isositsirikine **7-c** produced in assay (top chromatogram) and 9-fluoro isositsirikine **7-c** standard (bottom chromatogram). All standards are provided by Dr. Elizabeth McCoy³⁶. The *x*-axis is time in minutes, and the *y*-axis is intensity.

The LCMS retention times in minutes of standards of isositsirikine **7** analogs and isositsirikine **7** analogs produced in assays are listed below. All standards are provided by Dr. Elizabeth McCoy³⁶.

9-methyl isositsirikine **7-g**: 1.83 (standard), 1.83 (assay)

9-chloro isositsirikine **7-k**: 2.03 (standard), 2.02 (assay)

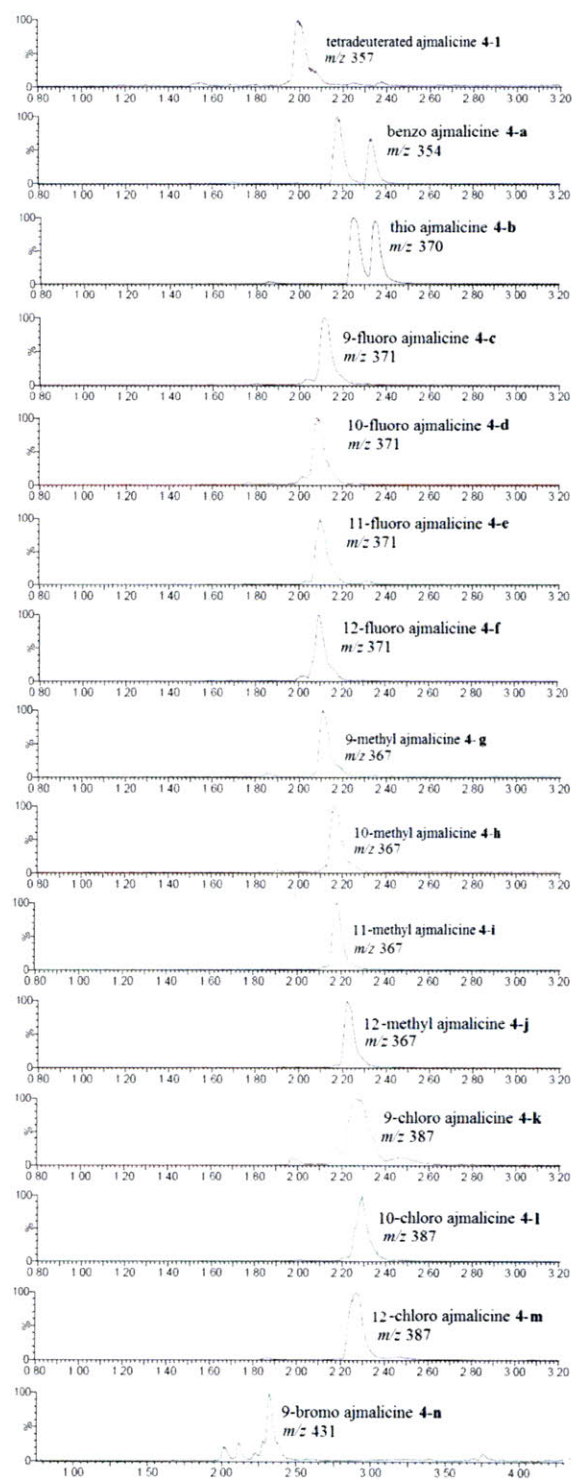
9-bromo isositsirikine **7-n**: 2.03 (standard), 2.04 (assay)

10-bromo isositsirikine **7-o**: 2.04 (standard), 2.04 (assay)

10-hydroxy isositsirikine **7-p**: 1.18 (standard), 1.17 (assay)

pentynyl-ester isositsirikine **7-t**: 2.12 (standard), 2.12 (assay)

Figure 3-39 and Figure 3-40 below show LCMS chromatograms of all ajmalicine analogs **4-1** and **4-a** through **4-t** and isositsirikine analogs **7-1** and **7-a** through **7-t** produced in assays.

Ajmalicine analogs 4-1 and 4-a through 4-t produced in assays

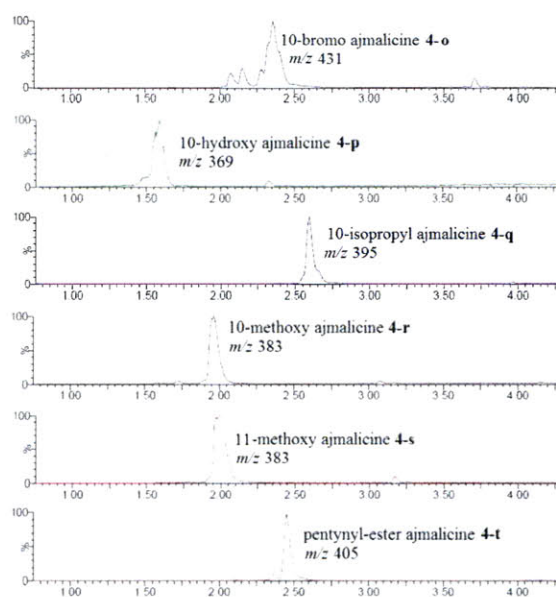
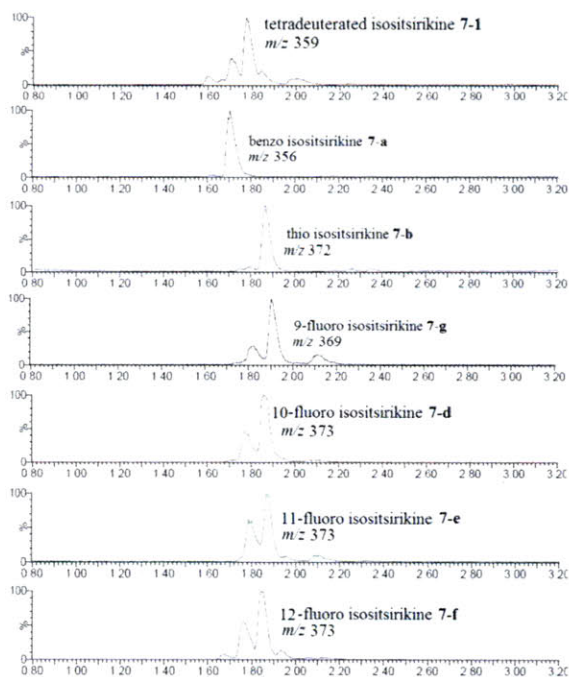


Figure 3-39: LCMS chromatograms of ajmalicine analogs **4-1** and **4-a** through **4-t** produced in assays. The *x*-axis is time in minutes, and the *y*-axis is intensity.

Isositsirikine analogs 7-1 and 7-a through 7-t produced in assays



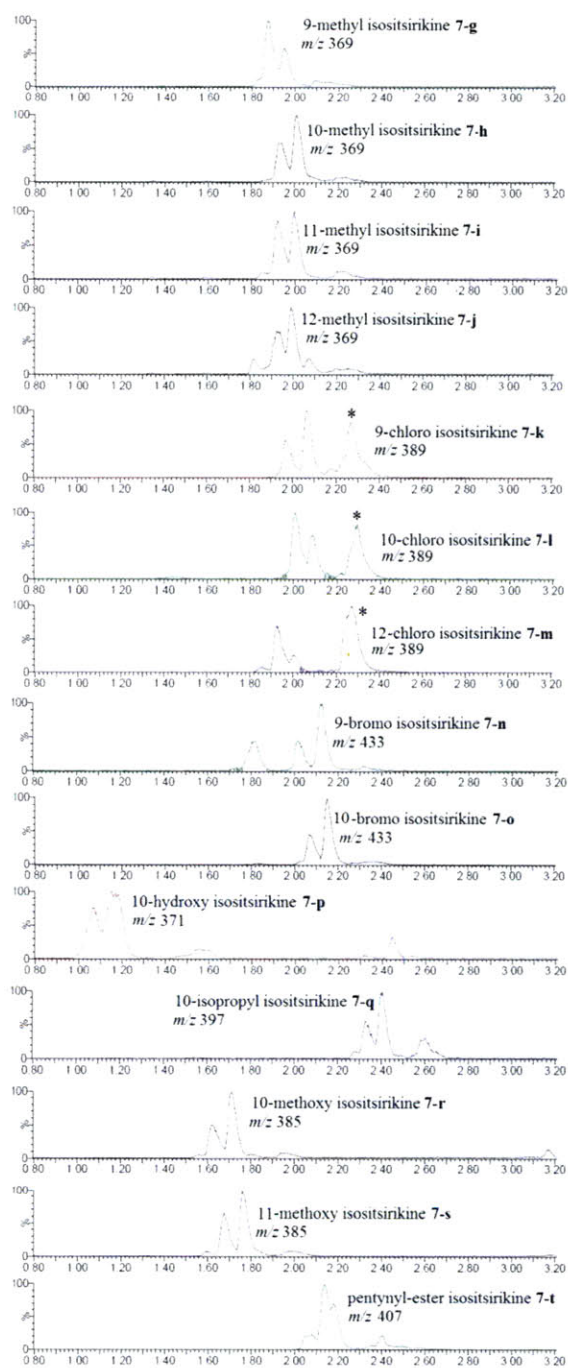


Figure 3-40: LCMS chromatograms of isositsirikine analogs 7-1 and 7-a through 7-t produced in assays. The x -axis is time in minutes, and the y -axis is intensity.

H. *Steady state kinetic analysis conditions*

I performed steady state kinetic analysis of ajmalicine synthase to determine substrate specificity with either a 40-70% ammonium sulfate fraction or, in later studies, an acetone precipitation fraction. In the steady state kinetic study with d₄ strictosidine **1-1**, d₄ strictosidine **1-1** (10-400 μM) was first incubated with 5 μM SGD. Under these conditions, the reactions with the highest concentrations of d₄ strictosidine **1-1** are completely deglycosylated after 5 minutes at 30°C. After this time, deglycosylated d₄ strictosidine **49-1** was added to a solution of NADPH (5 mM), partially purified enzyme fraction from an acetone precipitation (0.9 mg protein mL⁻¹), and 50 mM sodium phosphate buffer, pH 7.5, containing 400 mM sodium chloride and 10% glycerol, for a total reaction volume of 200 μL. The reaction mixture was incubated at 30°C, and each concentration was assayed at least twice. The aliquots were quenched with 950 μL MeOH containing 500 nM yohimbine **6** as an internal standard. The samples were centrifuged (13,000g, 1 min) to remove particulates and then analyzed by LCMS. The starting material and products were separated using a gradient of 10-40% acetonitrile in water with 0.1% formic acid over a period of 5 minutes. The increase in the area under the product peak was used to obtain the initial rates of the reduction reaction. The formation of ajmalicine **4** isomers was monitored by peak integration, normalized to an internal standard (yohimbine **6**), and correlated to peak area using a standard curve of ajmalicine **4**. The data were fitted by the same method as described for SGD kinetics with d₄ strictosidine **1-1** and d₄ vincoside **43-1** (Chapter 2, Materials and Methods).

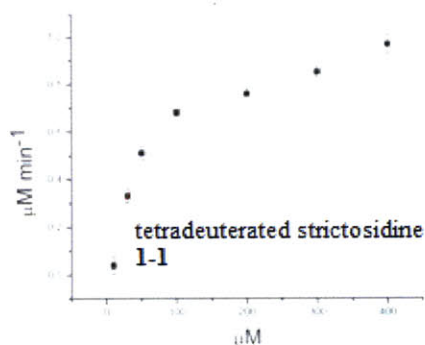


Figure 3-41: Data fit for the steady state kinetic analysis of ajmalicine synthase with d_4 strictosidine **1-1**, with the x -axis in μM d_4 strictosidine **1-1**, and the y -axis in μM d_4 ajmalicine **4-1** formed per minute.

For the steady state kinetic analysis of ajmalicine synthase with 9-methyl **1-g**, 10-methyl **1-h**, 11-methyl **1-i**, and 12-methyl **1-j** strictosidine, a 75 μL reaction was performed involving NADPH (4 mM), SGD (5 μM), a partially purified enzyme fraction from an ammonium sulfate precipitation (3.4 mg mL^{-1} protein), and 9-methyl **1-g**, 10-methyl **1-h**, 11-methyl **1-i**, and 12-methyl **1-j** strictosidine (0.005-1.4 mM). The reaction was incubated at 37°C, and 10 μL aliquots were taken every minute. Each concentration was assayed at least three times. The LCMS conditions and data fitting methods described above for the steady state kinetic analysis of d_4 strictosidine **1-1** were used.

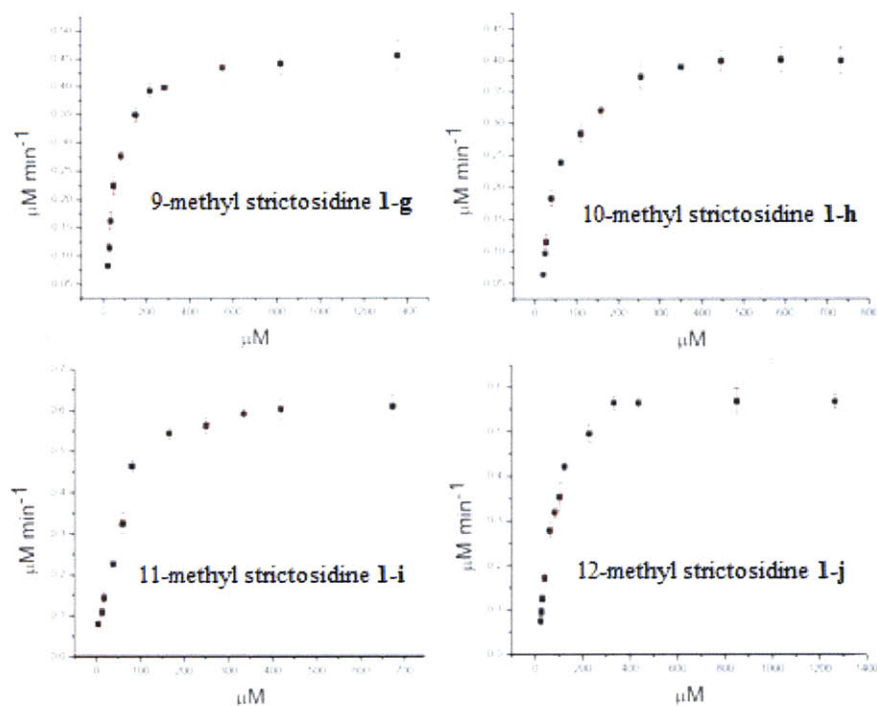


Figure 3-42: Data fit for the steady state kinetic analysis of ajmalicine synthase with 9-methyl **1-g**, 10-methyl **1-h**, 11-methyl **1-i**, and 12-methyl **1-j** strictosidine, with the *x*-axis in μM 9-methyl **1-g**, 10-methyl **1-h**, 11-methyl **1-i**, or 12-methyl **1-j** strictosidine, and the *y*-axis in μM 9-methyl **4-g**, 10-methyl **4-h**, 11-methyl **4-i**, or 12-methyl **4-j** ajmalicine formed per minute.

For the steady state kinetic analysis of ajmalicine synthase with d_4 vincoside **43-1**, d_4 vincoside **43-1** (38-2885 μM) was diluted in 0.15 M citrate phosphate buffer (pH 6, 0.05 mL final volume), and SGD (7.3 μM final concentration) was added. Under these conditions, the reactions with the highest concentrations of d_4 vincoside **43-1** are completely deglycosylated after 30 minutes at 30°C. After this time deglycosylated d_4 vincoside **84** was added to a solution containing NADPH (2.4 mM) and a partially purified enzyme fraction from an ammonium sulfate precipitation (3.3 mg protein mL^{-1}).

The reaction mixture was incubated at 30°C, and 5 μL aliquots were quenched at appropriate time points. Each concentration was assayed at least three times. The LCMS conditions and data fitting methods described above for the steady state kinetic analysis of d_4 strictosidine **1-1** were used.

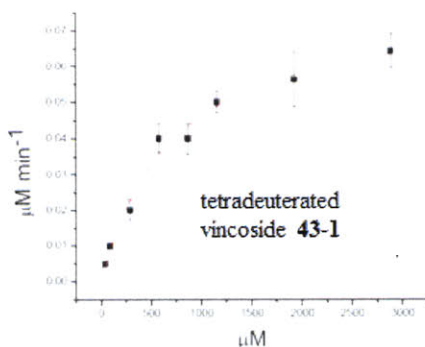


Figure 3-43: Data fit for the steady state kinetic analysis of ajmalicine synthase with d_4 vincoside **43-1**, with the x -axis in μM d_4 vincoside **43-1**, and the y -axis in μM ajmalicine isomer, presumably d_4 C-3 *R* ajmalicine **85**, formed per minute.

For the steady state kinetic analysis of isositsirikine synthase with d_4 strictosidine **1-1**, benzo strictosidine **1-a**, and thio strictosidine **1-b**, the three strictosidine analogs (10–400 μM) were first incubated with 5 μM SGD. Under these conditions, the reactions with the highest concentrations of d_4 strictosidine **1-1**, benzo strictosidine **1-a**, or thio strictosidine **1-b** are completely deglycosylated after 5 minutes at 30°C. After this time, deglycosylated d_4 strictosidine **49-1**, deglycosylated benzo strictosidine **49-a**, or deglycosylated thio strictosidine **49-b** was added to a solution of NADPH (5 mM), partially purified enzyme fraction from an acetone precipitation (0.9 mg protein mL^{-1}), and 50 mM sodium phosphate buffer, pH 7.5, containing 400 mM sodium chloride and 10% glycerol, for a total reaction volume of 200 μL . The reaction mixture was incubated

at 30°C. Each concentration was assayed at least two times. The LCMS conditions and data fitting methods described above for the steady state kinetic analysis of d_4 strictosidine **1-1** were used. The formation of isositsirikine **7** was monitored by peak integration and normalized to the internal standard.

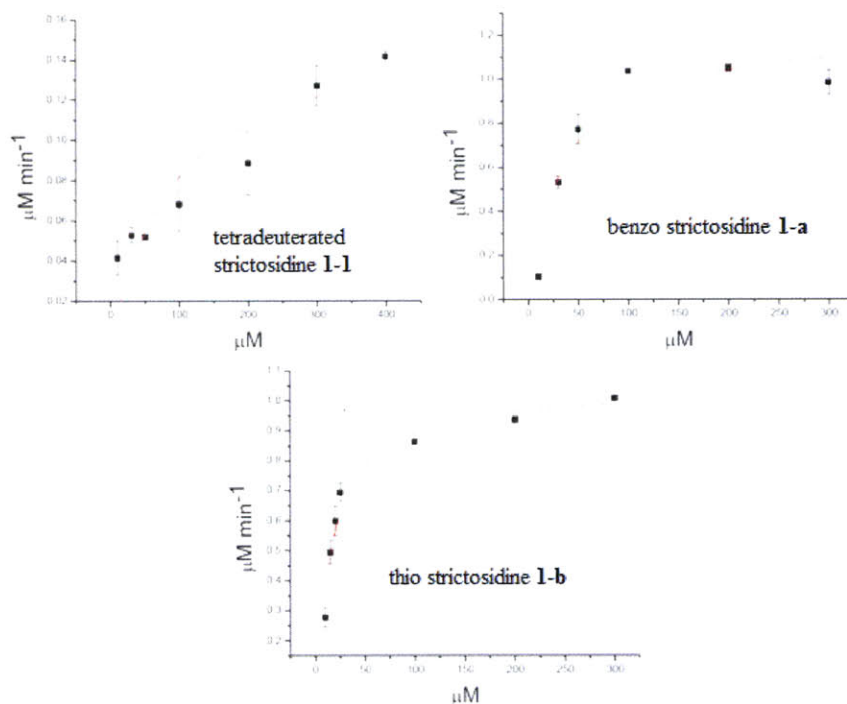


Figure 3-44: Data fit for the steady state kinetic analysis of isositsirikine synthase with d_4 strictosidine **1-1**, benzo strictosidine **1-a**, and thio strictosidine **1-b**, with the x -axis in μM d_4 strictosidine **1-1**, benzo strictosidine **1-a**, or thio strictosidine **1-b**, and the y -axis in μM d_4 isositsirikine **7-1**, benzo isositsirikine **7-a**, or thio isositsirikine **7-b** formed per minute.

I. Radioactive enzyme assay

I synthesized tritiated R NADPH according to a previously published procedure¹²⁹; R NADPH had been previously reported in enzymatic production of ajmalicine¹⁰⁹. All reagents were obtained from Sigma Aldrich. Tritiated R NADPH was

made from tritiated *S* NADPH (Figure 3-45). To synthesize tritiated *S* NADPH, 100 mM potassium phosphate buffer, pH 8, with 1 mM EDTA (300 μ L) was added to 10 mM NADP⁺ (300 μ L) and 0.2 mCi [1-³H]D-glucose (10 nmol). Glucose dehydrogenase (GDH) (40 μ L) was then added, and the reaction was incubated at 37°C for 15 minutes. Afterwards, 10 mM [1-¹H]D-glucose (3 μ L, 30 nmol) was added to the reaction solution and the reaction proceeded for another 5 minutes; then 10 mM [1-¹H]D-glucose (3 μ L, 30 nmol) was added. The reaction was then incubated for an additional 10 minutes. The specific radioactivity of the final product obtained was estimated to be 2.7 Ci/mmol.

To the solution of *S* ³H-NADPH, acetone (20 μ L) and *tb*ADH (alcohol dehydrogenase from *Thermoanaerobium brockii*) (100 μ L) were added, and the mixture was incubated at 37°C for 12 minutes. The solution was then filtered through an Amicon Ultra 15 tube with a 30 kDa filter and centrifuged at 4,500g at 4°C for 10 minutes. After 10 minutes, ¹H-glucose (300 μ L) and GDH (40 μ L) were added, and the reaction was incubated at 37°C for 15 minutes to yield *R* ³H-NADPH. The crude *R* ³H-NADPH was used immediately in assays.

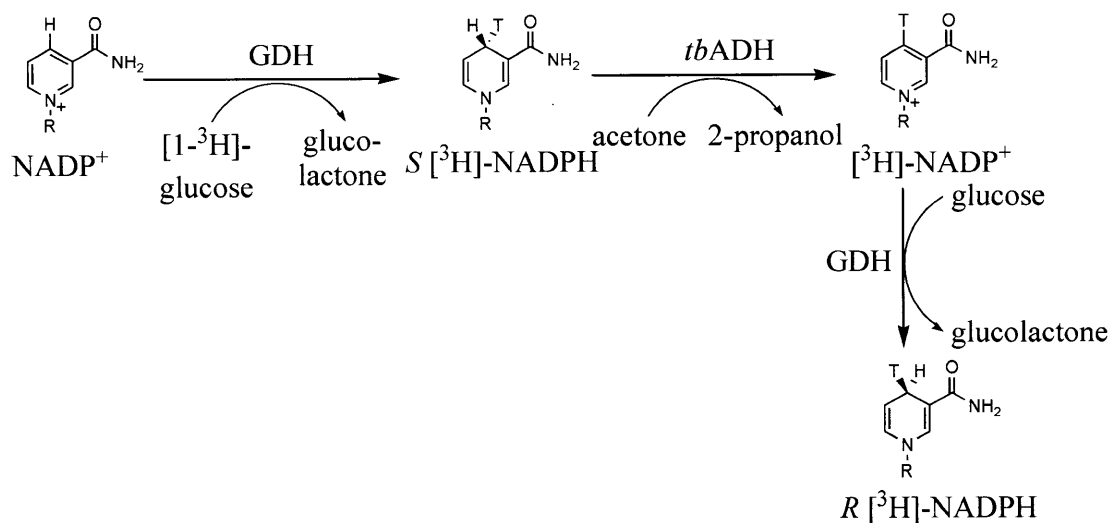


Figure 3-45: Synthesis of R - ^3H -NADPH¹²⁹.

The relative activities of a series of gel filtration fractions was further confirmed using an enzyme assay that utilized R - ^3H -NADPH (Figure 3-46, Table 3-14). In this assay, deglycosylated strictosidine **49** was incubated with R - ^3H -NADPH and gel filtration fractions containing ajmalicine synthase activity. At various time points, aliquots from the reaction mixture were spotted on thin liquid chromatography (TLC) plates, vacuum dried, and run in 15% methanol to 85% dichloromethane. The silica in the area of the plate with the same R_f value as an ajmalicine **4** standard was then removed with a scalpel and suspended in scintillation fluid, and the radioactivity was measured with a scintillation counter. The results confirmed previous experiments: the fractions with the highest ajmalicine synthase activity (C7-8) as measured by LCMS also had the highest activity as measured by the scintillation counter. Fractions D11-12 had a slightly higher slope than fractions D2-3. Assays with no extract or no NADPH had the lowest slopes as measured by the scintillation counter.

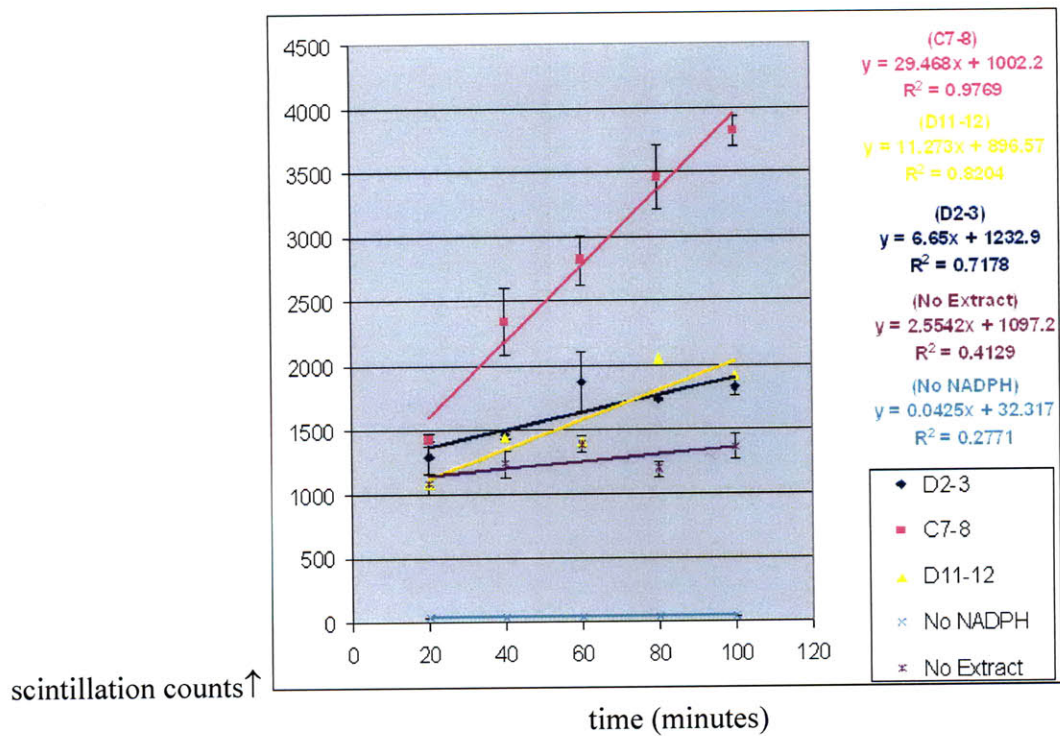


Figure 3-46: Rates of tritiated ajmalicine formation using various gel filtration fractions, strictosidine **1-1**, SGD, and $R^3\text{H-NADPH}$. The x -axis is in minutes, and the y -axis is in scintillation counts.

Graph symbol color	Fraction	Equation	R ²
Pink (■)	Most active gel filtration fractions (C7-8)	$y = 29.5x + 1002.2$	0.98
Yellow (▲)	Moderately active gel filtration fractions (D3-4)	$y = 11.3x + 896.6$	0.82
Dark blue (◆)	Moderately active gel filtration fractions (D11-12)	$y = 6.7x + 1232.9$	0.72
Purple (*)	No extract control	$y = 2.5x + 1097.2$	0.41
Cyan (*)	No NADPH control	$y = 0.04x + 32.3$	0.28

Table 3-14: Tritiated NADPH assay using various gel filtration fractions.

J. *Chemical reduction of deglycosylated strictosidine with NaCNBH₃*

To chemically reduce deglycosylated d₄ strictosidine **49-1**, deglycosylated benzo strictosidine **49-a**, and deglycosylated thio strictosidine **49-b** with NaCNBH₃, d₄ strictosidine **1-1**, benzo strictosidine **1-a**, and thio strictosidine **1-b** (0.2 μmol each) were first deglycosylated with SGD in 0.15 M citrate phosphate buffer, pH 6. Upon deglycosylation, the pH of the buffer was raised to 7.5, and 80 or 1200 μmol NaCNBH₃ was added. The reaction mixture was incubated at 30°C, and aliquots (5 μL) were quenched at appropriate time points in 950 μL methanol. The starting materials and products were separated using a gradient of 10-90% acetonitrile in water with 0.1% formic acid over a period of 5 minutes.

V. Acknowledgments

I had helpful discussions with Dr. Aimee Usera, Dr. Elizabeth McCoy, and Dr. Peter Bernhardt. Dr. Aimee Usera assisted in the synthesis of benzo strictosidine **1-a** and thio strictosidine **1-b**. Dr. Elizabeth McCoy provided the 4-fluoro **18-c**, 7-fluoro **18-f**, 4-methyl **18-g**, 7-methyl **18-j**, 4-chloro **18-k**, 7-chloro **18-m**, 4-bromo **18-n**, and 5-isopropyl tryptamine **18-q** analogs that I used to make the corresponding strictosidine **1** analogs. Dr. Elizabeth McCoy taught me how to reculture hairy root cultures. Dr. Peter Bernhardt synthesized 18,19-des-vinyl strictosidine **1-z** and the mixture of 18,19-des-vinyl strictosidine isomers **1-y**. Dr. Peter Bernhardt also assisted me with ¹H NMR analysis. An undergraduate student, Jia Xin (Joann) Wu, assisted in the synthesis of various strictosidine **1** analogs. Dr. Justin Maresh initially provided me with cell suspension cultures, and also taught me how to reculture cell suspension cultures.

Professor Catherine Drennan allowed me to use the FPLC in her laboratory. Many members of her laboratory assisted me at various times. These laboratory members include Yan Kung, Rebekah Bjork, Peter Goldman, Marcus Gibson, Christina Stock, Dr. Danny Yun, Dr. Hector Hernandez, Dr. Katherine Ryan, Dr. Leah Blasiak, and Dr. C. Ainsley Davis.

Dr. L. Li of the MIT Department of Chemistry Instrumentation Facility performed the high-resolution mass studies. Professor John Essigmann allowed me to use the scintillation counter in his laboratory. Professor Carolyn Lee Parsons of Northeastern University provided the initial *C. roseus* hairy root cultures. Dr. Leslie Hicks and Dr. Sophia Alvarez at the proteomics and mass spectrometry facility of the Donald Danforth

Plant Science Center (St. Louis, Missouri) performed MS/MS analysis on the enzymes sent.

VI. *References*

- (1) O'Connor, S. E.; Maresh, J. J. Chemistry and biology of monoterpene indole alkaloid biosynthesis. *Natural Products Reports* **2006**, *23*, 532-47.
- (2) Kutney, J.P.; Choi, L.S.L.; Kolodziejczyk; Sleigh, S.K.; Stuart, K.L.; Worth, B.R.; Kurz, W.G.W.; Chatson, K.B.; Constabel, F. Alkaloid production in *Catharanthus roseus* cell cultures. V. Alkaloids from the 76G, 299Y, 340Y, and 951G cell lines. *Journal of Natural Products* **1981**, *44*, 536-40.
- (3) Stockigt, J.; Hemscheidt, T.; Hofle, G.; Heinsteinst, P.; Formacek, V. Steric course of hydrogen transfer during enzymatic formation of 3 α -heteroyohimbine alkaloids. *Biochemistry* **1983**, *22*, 3448-52.
- (4) McCoy, E., O'Connor, S.E. Directed biosynthesis of alkaloid analogs in the medicinal plant *Catharanthus roseus*. *Journal of the American Chemical Society* **2006**, *128*, 14276-77.
- (5) Bernhardt, P.; McCoy, E.; O'Connor, S. E. Rapid identification of enzyme variants for reengineered alkaloid biosynthesis in periwinkle. *Chemistry and Biology* **2007**, *14*, 888-97.
- (6) Lee, H. Y.; Yerkes, N.; O'Connor, S. E. Aza-tryptamine substrates in monoterpene indole alkaloid biosynthesis. *Chemistry and Biology* **2009**, *16*, 1225-29.
- (7) McCoy, E. Substrate analogs to investigate alkaloid biosynthesis in *C. roseus*. Ph.D. dissertation, Massachusetts Institute of Technology, 2009.
- (8) Gerasimenko, I.; Sheludko, Y.; Ma, X.; Stockigt, J. Heterologous expression of a *Rauvolfia* cDNA encoding strictosidine glucosidase, a biosynthetic key to over 2000 monoterpene indole alkaloids. *European Journal of Biochemistry* **2002**, *269*, 2204-13.
- (9) Heimscheidt, T.; Zenk, M.H. Partial purification and characterization of a NADPH dependent tetrahydroalstonine synthase from *Catharanthus roseus* cell suspension cultures. *Plant Cell Reports* **1985**, *4*, 216-219.
- (10) Stockigt, J.; Hofle, G.; Pfitzner, A. Mechanism of the biosynthetic conversion of geissoschizine to 19-epi-ajmalicine in *Catharanthus roseus*. *Tetrahedron Letters* **1980**, *21*, 1925-26.
- (11) Lounasmaa, M.; Jokela, R.; Hanhinen, P.; Miettinen, J. Salo, J. Preparation and conformational study of Z-isositsirikine and E-isositsirikine epimers and model compounds: determination of their C-16 configurations. *Tetrahedron* **1994**, *50*, 9207-22.
- (12) Martin, S.F.; Chen, K.X.; Eary, C.T. An enantioselective total synthesis of (+)-geissoschizine. *Organic Letters* **1999**, *1*, 79-81.
- (13) Price, E.N. *Proteins LabFax*; BIOS Scientific Publishers Limited: Oxford, United Kingdom, 1996.
- (14) Cutler, P. *Methods in Molecular Biology: Protein Purification Protocols*; 2 ed.; Humana Press: Totowa, New Jersey, 2004; Vol. 244.
- (15) King, E.E. Extraction of cotton leaf enzymes with borate. *Phytochemistry* **1971**, *10*, 2337-41.
- (16) Scopes, R.K. *Protein Purification: Principles and Practice*; 3 ed.; Springer-Verlag: New York, New York, 1994.

- (17) Voet, D; Voet, J.G *Biochemistry*; John Wiley & Sons: Danvers, Massachusetts, 2004.
- (18) Sigma Product Information. Reactive Dye Resins. http://www.sigmaaldrich.com/etc/medialib/docs/Sigma/Product_Information_Sheet/c8321pis.Par.0001.File.tmp/c8321pis.pdf, accessed May 2, 2010.
- (19) Adams, M.D.; Kelley, J.M.; Gocayne, J.D.; Dubnick, M.; Polymeropoulos, M.H.; Xiao, H.; Merrill, C.R.; Wu, A.; Olde, B.; Moreno, R.F. Complementary DNA sequencing: expressed sequence tags and human genome project. *Science* **1991**, *252*, 1651-56.
- (20) Youn, B.; Camacho, R.; Mounuddin, S.G.A.; Lee, C.; Davin, L.B.; Lewis, N.G.; Kang, C. Crystal structures and catalytic mechanism of the Arabidopsis cinnamyl alcohol dehydrogenases AtCAD5 and AtCAD4. *Organic and Biomolecular Chemistry* **2006**, *4*, 1687-97.
- (21) Rosenthal, C.; Mueller, U.; Panjekar, S.; Sun, L.; Ruppert, M.; Zhao, Y.; Stockigt, J. Expression, purification, crystallization and preliminary X-ray analysis of perakine reductase, a new member of the aldo-keto reductase enzyme superfamily from higher plants. *Acta Crystallographica Section F Structural Biology and Crystallization Communications* **2006**, *F62*, 1286-89.
- (22) Barleben, L.; Panjekar, S.; Ruppert, M.; Koepke, J.; Stockigt, J. Molecular architecture of strictosidine glucosidase: the gateway to the biosynthesis of the monoterpenoid indole alkaloid family. *The Plant Cell* **2007**, *19*, 2886-97.
- (23) Geerlings, A.; Ibanez, M. M.; Memelink, J.; van Der Heijden, R.; Verpoorte, R. Molecular cloning and analysis of strictosidine beta-D-glucosidase, an enzyme in terpenoid indole alkaloid biosynthesis in *Catharanthus roseus*. *The Journal of Biological Chemistry* **2000**, *275*, 3051-56.
- (24) Burbulis, I. E.; Winkel-Shirley, B. Interactions among enzymes of the Arabidopsis flavonoid biosynthetic pathway. *Proceedings of the National Academy of Sciences USA* **1999**, *96*, 12929-34.
- (25) Jorgensen, K.; Rasmussen, A. V.; Morant, M.; Nielsen, A. H.; Bjarnholt, N.; Zagrobelny, M.; Bak, S.; Moller, B. L. Metabolon formation and metabolic channeling in the biosynthesis of plant natural products. *Current Opinion in Plant Biology* **2005**, *8*, 280-91.
- (26) Nielsen, K.A.; Tattersall, D.B.; Jones, P.R.; Moller, B.L. Metabolon formation in dhurrin biosynthesis. *Phytochemistry* **2008**, *69*, 88-98.
- (27) Panicot, M.; Minguet, E.; Ferrando, C.; Alcázar, R.; Blázquez, M.A.; Carbonell, J.; Altabella, T.; Koncz, C.; Tiburcio, A.F. A polyamine metabolon involving aminopropyl transferase complexes in Arabidopsis. *The Plant Cell* **2002**, *14*, 2539-51.
- (28) Winkel-Shirley, B. Evidence for enzyme complexes in the phenylpropanoid and flavonoid pathways. *Physiologia Plantarum* **1999**, *107*, 142-49.
- (29) Winkel, B.S.J. Metabolic channeling in plants. *Annual Review of Plant Biology* **2004**, *55*, 85-107.
- (30) McCoy, E.; Galan, M.C.; O'Connor, S.E. Substrate specificity of strictosidine synthase. *Bioorganic and Medicinal Chemistry Letters* **2006**, *16*, 2475-78.
- (31) Lee-Parsons, C.W.T.; Royce, A.J. Precursor limitations in methyl jasmonate-induced *Catharanthus roseus* cell cultures. *Plant Cell Reports* **2006**, *25*, 607-12.

(32) Bernhardt, P.; Yerkes, N.; O'Connor, S. E. Bypassing stereoselectivity in the early steps of alkaloid biosynthesis. *Organic and Biomolecular Chemistry* **2009**, *7*, 4166-68.

(33) McCracken, J.A.; Wang, L.; Kohen, A. Synthesis of R and S tritiated reduced B-nicotinamide adenine dinucleotide 2' phosphate. *Analytical Biochemistry* **2004**, *324*, 131-36.

Chapter 4: Cloning and characterization of novel *C. roseus* enzymes

- I. Introduction
 - A. Enzyme isolation via crosslinking
 - B. Cinnamyl / sinapyl alcohol dehydrogenases, malate / mannitol dehydrogenases, and 10-hydroxy geraniol oxidoreductase
- II. Results
 - A. Crosslinking experiments
 - B. Characterization of enzymes isolated via crosslinking experiments
- III. Discussion
- IV. Materials and Methods
 - A. Crosslinking experiments conditions
 - B. Cloning of crosslinked enzymes
 - C. Heterologous expression and purification of crosslinked enzymes
 - D. DNA and amino acid sequences of crosslinked enzymes
 - E. Assay conditions
 - F. Steady state kinetic analysis conditions
 - G. LCMS conditions
 - H. High-resolution mass spectrometry data
- V. Acknowledgments
- VI. References

The results in this chapter will be reported in a manuscript currently in preparation:

- Aimee R. Usera*; Nancy Yerkes*; Elizabeth McCoy*; David K. Liscombe; Nathan E. Nims; Anne C. Friedrich; Sarah E. O'Connor. Crosslinking strategies to isolate a new *C. roseus* enzyme. *Manuscript in preparation*, 2010. (* co-first authors)

I. *Introduction*

A. *Enzyme isolation via crosslinking*

In addition to the traditional, chromatography-based strategies described in Chapter 3, unknown enzymes can be isolated by crosslinking, or photoaffinity labeling. In crosslinking, a substrate or inhibitor of an enzyme is modified with a photo-reactive group. Upon photo-activation, the modified substrate, which is presumably bound to the enzyme active site, is able to covalently modify the active site of the enzyme of interest. Aryl azides **86**, diazirines **87**, and benzophenones **88** are all commonly employed photo-reactive groups to modify enzymes (Figure 4-1)¹³⁰. When aryl azides **86** are photo-activated, a reactive nitrene **89** (Figure 4-1) is generated, whereas when diazirines **87** or benzophenones **88** are photo-activated, a reactive carbene **90** (Figure 4-1) is generated. Nitrenes **89** and carbenes **90** are highly reactive, and once formed they will covalently modify nearby active site residues of the enzyme. One advantage of aryl azides **86** and diazirines **87** over benzophenones **88** is that the azide **86** and diazirine **87** moieties are significantly smaller than the benzophenone **88** moiety, making the presence of these groups less likely to disrupt the ligand-protein interaction. One disadvantage of aryl

azides **86** is that the reactive nitrene **89** species can be generated only by using short wavelength light, which can damage the enzyme of interest. Another disadvantage is that the N-X bonds formed by nitrenes **89** are not always as stable as the C-X linkages formed by carbenes **90**¹³⁰.

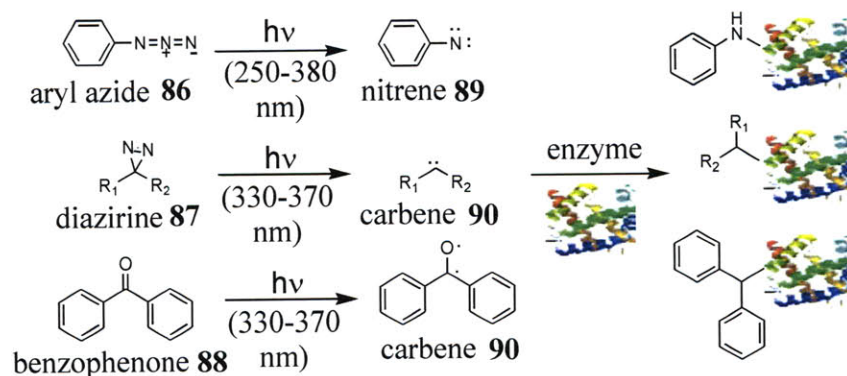


Figure 4-1: Commonly used photo-reactive groups in crosslinking studies include aryl azides **86**, diazirines **87**, and benzophenones **88**. A nitrene **89** is a reactive species generated by photo-activation of an aryl azide **86**¹³¹; a carbene **90** is a reactive species generated by photo-activation of a diazirine **87** or benzophenone **88**^{130,132}. Nitrenes **89** and carbenes **90** can react with active site residues of an enzyme.

In affinity based protein profiling (ABPP), multifunctional probes that contain a bio-orthogonal handle and an electrophilic or photo-active group are used to isolate an enzyme of interest. The electrophilic or photo-active group is used to modify the enzyme, and the bio-orthogonal handle is used for detection¹³³. The bio-orthogonal handle is in many cases an alkyne which can be functionalized via Huisgen 1,3-dipolar cycloaddition, or “click chemistry.” In “click chemistry” a terminal alkyne and an alkyl-azide react to form a triazole **91** (Figure 4-2). Rhodamine azides **92** or biotin azides **93** are often used to

facilitate detection of the proteins by fluorescence spectroscopy or streptavidin binding, respectively (Figure 4-3)¹³⁴.

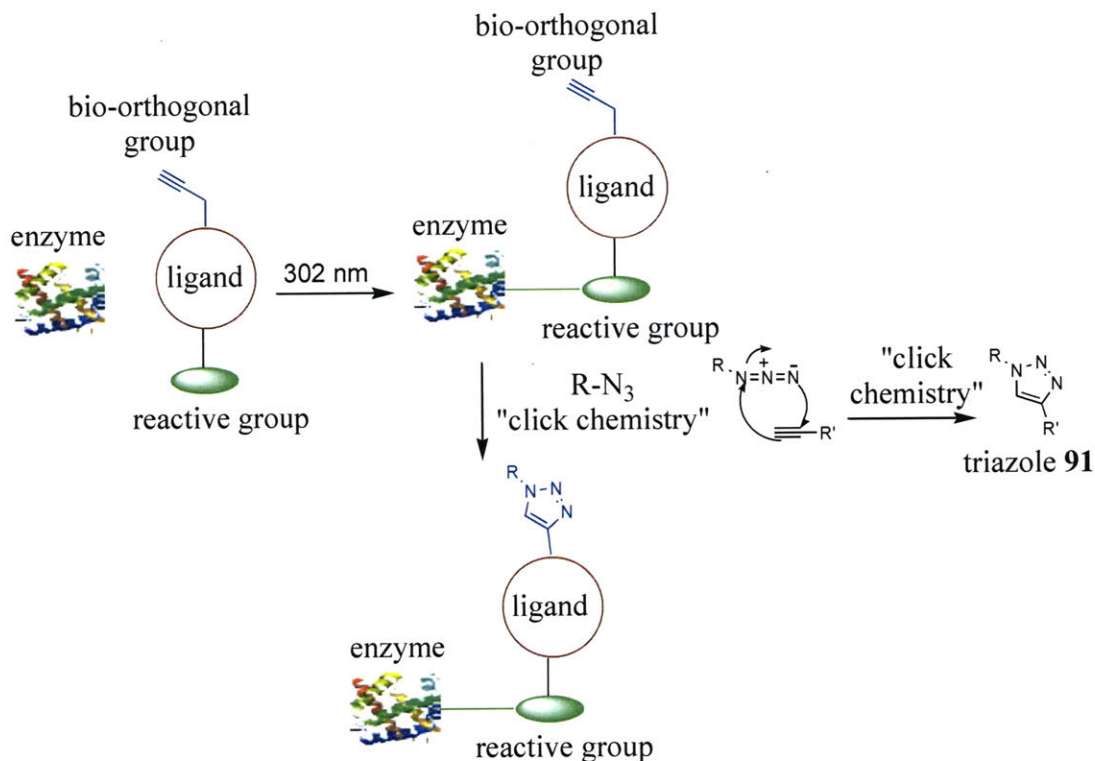


Figure 4-2: In affinity based protein profiling, a ligand is modified with both a reactive electrophilic or photo-active group (green) and a bio-orthogonal handle (blue). Upon irradiation, the photo-active group covalently modifies the enzyme. "Click chemistry" using an alkyl azide ($R-N_3$), typically either rhodamine azide **92** or biotin azide **93**, is then used for detection.

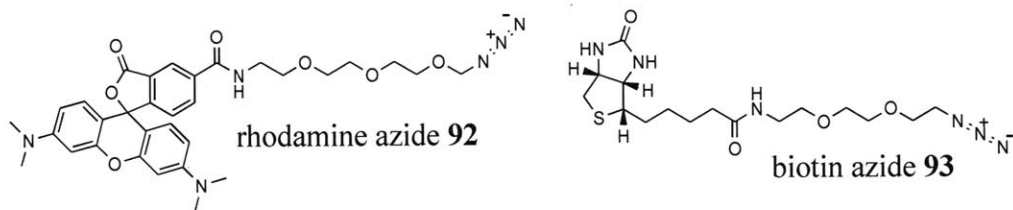


Figure 4-3: The structures of rhodamine azide **92** and biotin azide **93**.

B. *Cinnamyl / sinapyl alcohol dehydrogenases, malate / mannitol dehydrogenases, and 10-hydroxy geraniol oxidoreductase*

For the experiments described in this chapter, partially purified *C. roseus* lysate containing ajmalicine and isositsirikine synthase activity were subjected to crosslinking. After crosslinking, proteins were separated on 2D SDS-PAGE and labeled proteins were then identified by mass spectrometry. The peptide fragments obtained from the mass spectrometry analysis were used to search a protein sequence database consisting of expressed sequence tags (ESTs) of *C. roseus* to identify potential ajmalicine synthase and isositsirikine synthase candidates. Dr. David Liscombe and Dr. Nathan Ezekiel Nims (O'Connor group) then used a cDNA library to clone and express in *E. coli* four candidates that displayed sequence identity to a variety of known NADPH-binding enzymes. The four candidates, which were named Cr-2141, Cr-12, Cr-318, and Cr-611, had high sequence identity to cinnamyl / sinapyl alcohol dehydrogenases, malate / mannitol dehydrogenases, and 10-hydroxy geraniol oxidoreductase¹³⁵. A brief description of each type of enzyme is provided below.

Cinnamyl / sinapyl alcohol dehydrogenases

Cinnamyl alcohol dehydrogenases are NADPH-dependent enzymes that catalyze reduction of *p*-hydroxycinnamyl aldehyde and *p*-hydroxycinnamyl aldehyde analogs **94** into the corresponding *p*-hydroxycinnamyl alcohols **95** (Figure 4-4)¹²⁰. Sinapyl alcohol dehydrogenase is a type of cinnamyl alcohol dehydrogenase that reduces sinapyl aldehyde, or sinapaldehyde **96**, to sinapyl alcohol **97** (Figure 4-4). The alcohols serve as precursors for both lignin and lignan. Lignin is a structural, heterogeneous biopolymer found in all vascular plants¹³⁶. Lignans are a class of phytoestrogens derived from

phenylalanine that are formed via dimerization of substituted cinnamyl alcohols. Lignans have important roles in both human health and plant defense¹³⁷. One medicinal lignan is the anti-viral agent podophyllotoxin **98**, which is used in the semi-synthesis of the anti-cancer compounds etoposide **99** (Eposin®, Vepesid®, VP-16®), etoposide phosphate **100** (Etopophos®), and teniposide **101** (Vumon®) (Figure 4-5). Podophyllotoxin **98** is produced by the *Podophyllum* species, which is also known as the American Mayapple¹³⁸.

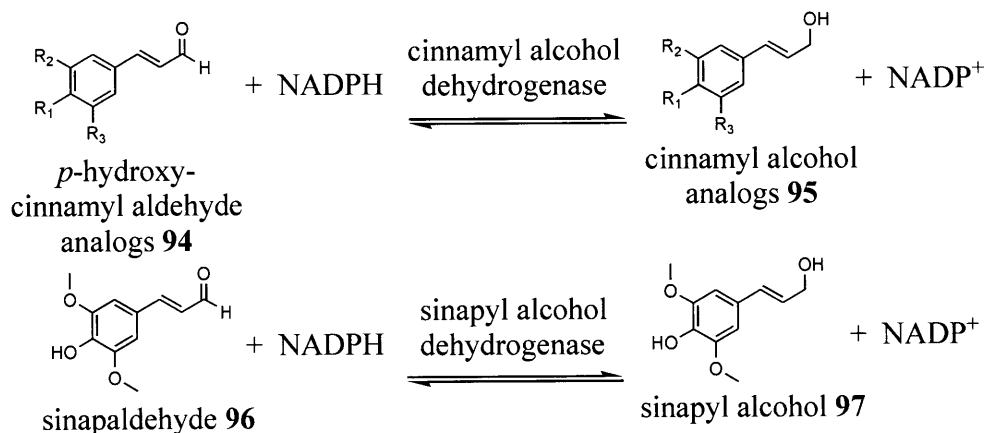


Figure 4-4: Cinnamyl alcohol dehydrogenases are NADPH-dependent enzymes that catalyze the reductions of *p*-hydroxycinnamyl aldehyde ($R_1 = \text{OH}$; $R_2 = R_3 = \text{H}$) and *p*-hydroxycinnamyl aldehyde analogs **94** into the corresponding cinnamyl alcohol analogs **97**¹²⁰. Sinapyl alcohol dehydrogenases are NADPH-dependent enzymes that catalyze the reduction of sinapaldehyde **96** to sinapyl alcohol **97**.

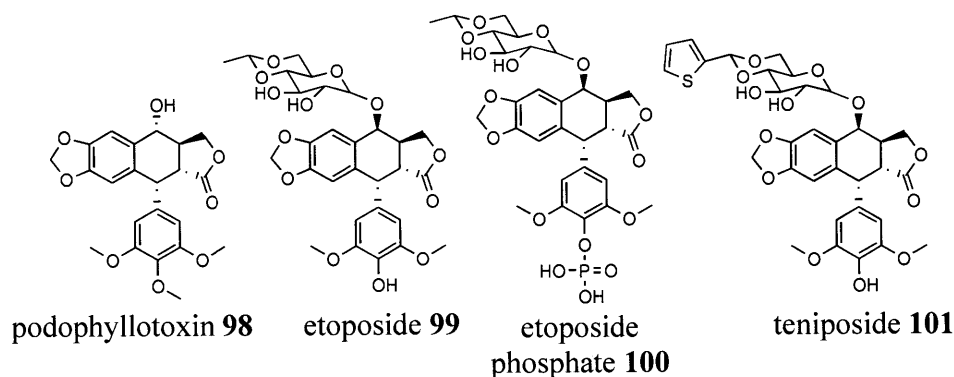


Figure 4-5: Structures of podophyllotoxin **98**, etoposide **99**, etoposide phosphate **100**, and teniposide **101**¹²⁰.

Other lignans include matairesinol **102** and secoisolariciresinol **103**, which serve as precursors to enterolactone **104** and enterodiol **105** (Figure 4-6)¹²⁰. Intestinal bacteria form enterolactone **104** and enterodiol **105** in the gut from matairesinol **102** and secoisolariciresinol **103** following ingestion of food high in fiber^{137,139}. Enterolactone **104** and enterodiol **105** are believed to help protect against colon, prostate, and breast cancers.

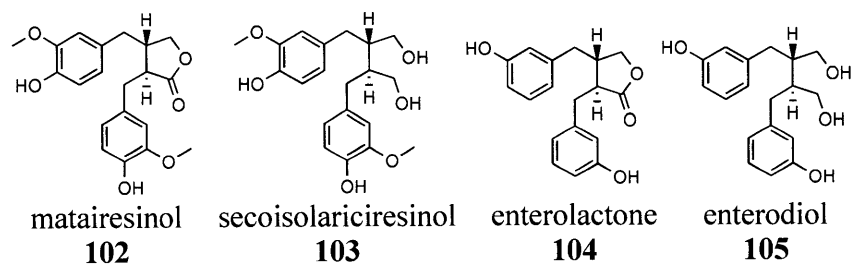


Figure 4-6: Structures of matairesinol **102**, secoisolariciresinol **103**, enterolactone **104**, and enterodiol **105**¹²⁰.

Many cinnamyl alcohol dehydrogenases are reported to be zinc-dependent¹²⁰. For example, in a cinnamyl alcohol dehydrogenase from *Arabidopsis thaliana* shown below

in Figure 4-7, the catalytic Zn^{2+} ion (shown in red) is coordinated to the carbonyl oxygen of the cinnamyl aldehyde analog substrate (shown in black) and facilitates the reduction of the aldehyde to an alcohol¹²⁰.

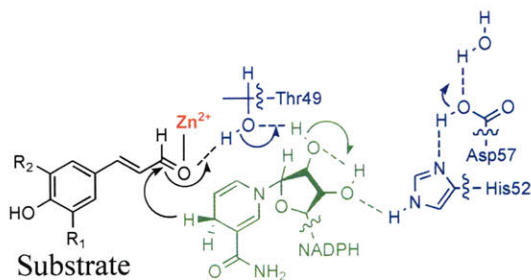


Figure 4-7: Cinnamyl alcohol dehydrogenases are zinc-dependent. This figure is taken from Youn *et al.*¹²⁰

Five of the most frequently observed cinnamyl aldehyde analogs **94** utilized in lignin and lignan biosynthesis are *p*-coumaryl aldehyde **106**, caffeyl aldehyde **107**, coniferyl aldehyde **108**, 5-hydroxy coniferyl aldehyde **109**, and sinapaldehyde **96** (Figure 4-8)^{140,141}. Cinnamyl alcohol dehydrogenases typically do not display absolute specificity for a given cinnamyl aldehyde analog **94**¹⁴⁰. For example, in a study of six cinnamyl alcohol dehydrogenases from *A. thaliana*, all six cinnamyl alcohol dehydrogenases were able to reduce each of the five aldehydes shown in Figure 4-8.

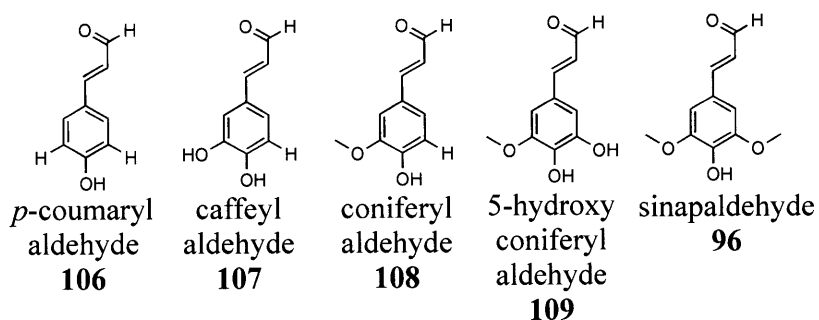


Figure 4-8: Structures of common lignin and lignan precursors *p*-coumaryl aldehyde **106**, caffeoyl aldehyde **107**, coniferyl aldehyde **108**, 5-hydroxy coniferyl aldehyde **109**, and sinapaldehyde **96**^{140,141}.

Malate dehydrogenase and mannitol dehydrogenase

Malate dehydrogenase, an enzyme in the citric acid cycle, catalyzes the reversible NADP⁺-dependent conversion of malate **110** to oxaloacetate **111** (Figure 4-9)¹⁴². Additionally, in gluconeogenesis, malate dehydrogenase facilitates the transport of oxaloacetate **111** out of the mitochondria by reducing oxaloacetate **111** to malate **110**. Once malate **110** has reached the cytosol, it is oxidized back to oxaloacetate **111** by malate dehydrogenase¹⁴².

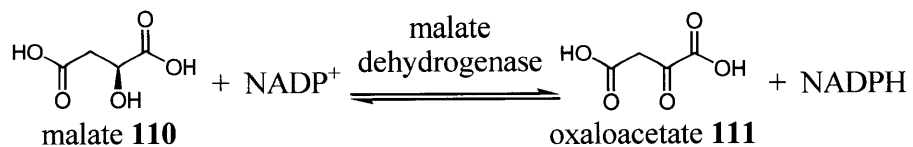


Figure 4-9: Malate dehydrogenase catalyzes the reversible NADP⁺-dependent conversion of malate **110** to oxaloacetate **111**¹⁴².

Mannitol dehydrogenase catalyzes the reversible NADP⁺-dependent conversion of D-mannitol **112** to D-mannose **113** (Figure 4-10), the first step in the catabolism of D-

mannitol **112**¹⁴³. Mannitol **112** is a six-carbon acyclic alcohol present in more than 70 higher plant families¹⁴³.

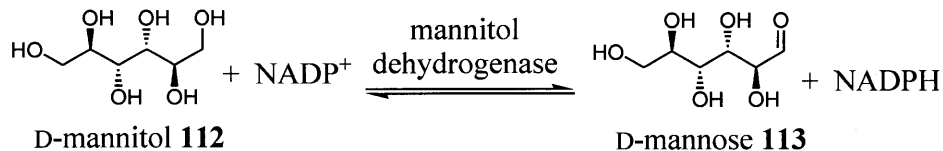


Figure 4-10: Mannitol dehydrogenase catalyzes the reversible NADP⁺-dependent conversion of D-mannitol **112** to D-mannose **113**¹⁴³.

10-hydroxy geraniol oxidoreductase

10-hydroxy geraniol oxidoreductase catalyzes the conversion of 10-hydroxy geraniol **23** to 10-oxo geraniol **72** (Figure 4-11). A protein that catalyzes this reaction has been isolated and characterized from *C. roseus*, though because this enzyme reduces a variety of unsaturated aldehydes, it is not certain whether this is the physiological function (personal communication, Professor Thomas McKnight, Texas A&M University). This protein is 360 amino acids, is 38,937 Da^{144,145}, and has 79% identity with a cinnamyl alcohol dehydrogenase from *Nicotiana tabacum* (common tobacco)^{135,146}.

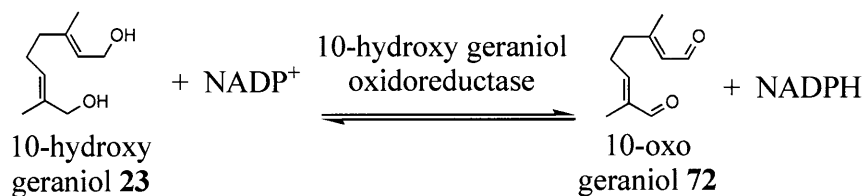


Figure 4-11: 10-hydroxy geraniol oxidoreductase catalyzes the NADP⁺-dependent conversion of 10-hydroxy geraniol **23** to 10-oxo geraniol **72**^{144,145,147-149}.

In the biosynthesis of loganic acid **42**, a precursor to secologanin **17**, from geraniol **22** (Figure 4-12), geraniol-10-hydroxylase and 10-hydroxy geraniol oxidoreductase are the only two enzymes that have been isolated. The enzymes converting 10-oxo geraniol **72** to loganic acid **42** remain to be identified¹⁹⁻²².

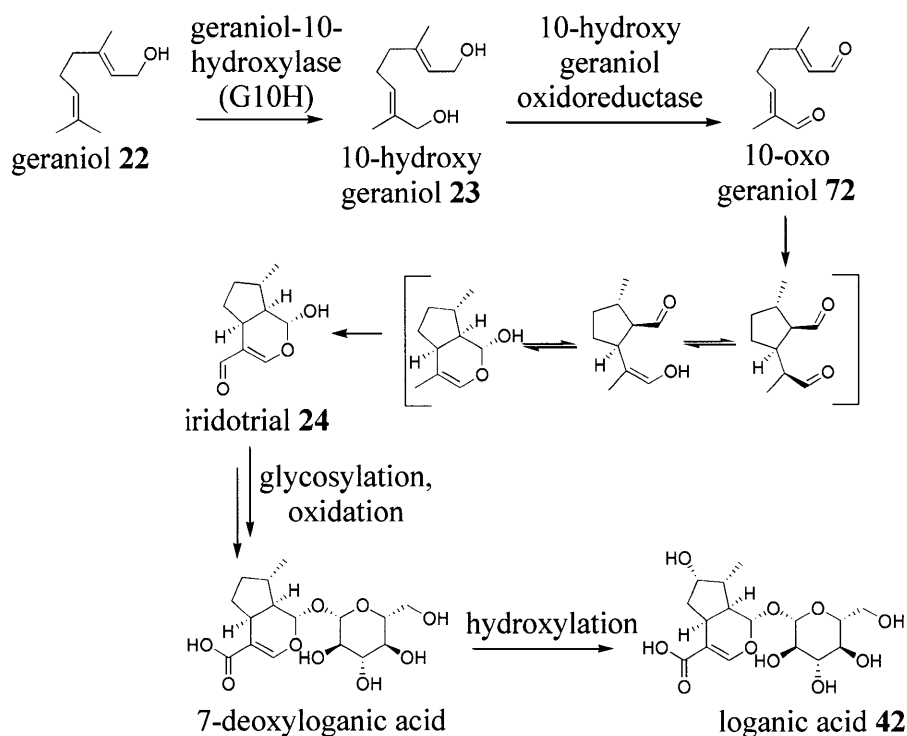


Figure 4-12: In the biosynthesis of loganic acid **42**, geraniol **22** is hydroxylated by geraniol-10-hydroxylase to form 10-hydroxy geraniol **23**, which is then oxidized by 10-hydroxy geraniol oxidoreductase to form 10-oxo geraniol **72**. The conversion of 10-oxo geraniol **72** to loganic acid **42** involves a number of enzymes that have not been isolated¹⁹⁻²².

II. *Results*

A. *Crosslinking experiments*

Ajmalicine synthase and isositsirikine synthase have proven difficult to purify to homogeneity using traditional protein purification methods, as described in Chapter 3. As an alternative approach, in collaboration with Dr. Elizabeth McCoy and Dr. Aimee Usera, I performed a crosslinking experiment in an attempt to isolate ajmalicine synthase. Initial crosslinking experiments were performed by Dr. Elizabeth McCoy³⁶, and these efforts were continued by Dr. Aimee Usera and me. In the crosslinking experiments, I used a bifunctional probe, 11-azido-pentynyl-ester strictosidine **114** (Figure 4-13)¹⁵⁰; Dr. Aimee Usera concurrently performed an identical experiment using 12-azido-pentynyl-ester strictosidine **115**. The indole azide moiety served as the photoaffinity label. Indole azides have been reported to label a wide variety of proteins after irradiation at 280-300 nm to generate the reactive nitrene species. For example, tryptophan synthase has been labeled by 6-azidotryptophan¹⁵¹, and 5-azido-indole-3-acetic acid, an analog of the plant auxin indole-3-acetic acid, was shown to covalently modify its auxin receptor¹⁵². An indole azide was also chosen because 4-, 5-, 6-, and 7-azidotryptamines had been previously synthesized and shown through precursor directed biosynthesis studies to be accepted by downstream enzymes in *C. roseus*¹⁵⁰. Therefore, it seemed reasonable that downstream enzymes would bind the azido-derivatized substrate analogs. Similarly, a pentynyl ester was used because a previous study showed that *C. roseus* hairy root cultures co-cultured with pentynyl-ester strictosidine **1-t** produced ajmalicine **4**, serpentine **5**, and isositsirikine **7** analogs containing pentynyl esters, thus indicating that downstream enzymes can accept substrates containing a pentynyl ester^{87,105,150}.

In the crosslinking experiment that I performed (Figure 4-13), 11-azido-pentynyl-ester strictosidine **114** served as a bifunctional substrate designed to covalently modify and label ajmalicine synthase. In this experiment, 11-azido-pentynyl-ester strictosidine **114** was first incubated with SGD to form deglycosylated 11-azido-pentynyl-ester strictosidine **116**. Upon deglycosylation, I added NADPH and a partially purified *C. roseus* cell culture lysate containing ajmalicine synthase activity. The reaction mixture was then irradiated with 302 nm light to generate the reactive nitrene moiety from the indole azide (Figure 4-13). The alkyne was then modified with rhodamine azide **92** via Huisgen 1,3-dipolar cycloaddition, or “click chemistry” (Figure 4-13), and the labeled proteins were separated by 2D SDS-PAGE and identified by fluorescence. Since 12-azido-pentynyl-ester strictosidine **115** appeared to label fewer proteins than 11-azido-pentynyl-ester strictosidine **114**, proteins labeled by 12-azido-pentynyl-ester strictosidine **115** were subjected to sequencing (Figure 4-14). The genome of *C. roseus* has not been sequenced, and so the peptides identified via mass spectrometry were used to probe the EST database of *C. roseus*. Potential candidates for ajmalicine synthase and isositsirikine synthase were thus identified. The results from a BLAST (Basic Local Alignment Search Tool) search of the amino acid sequences obtained from each spot are shown in Table 4-1¹³⁵.

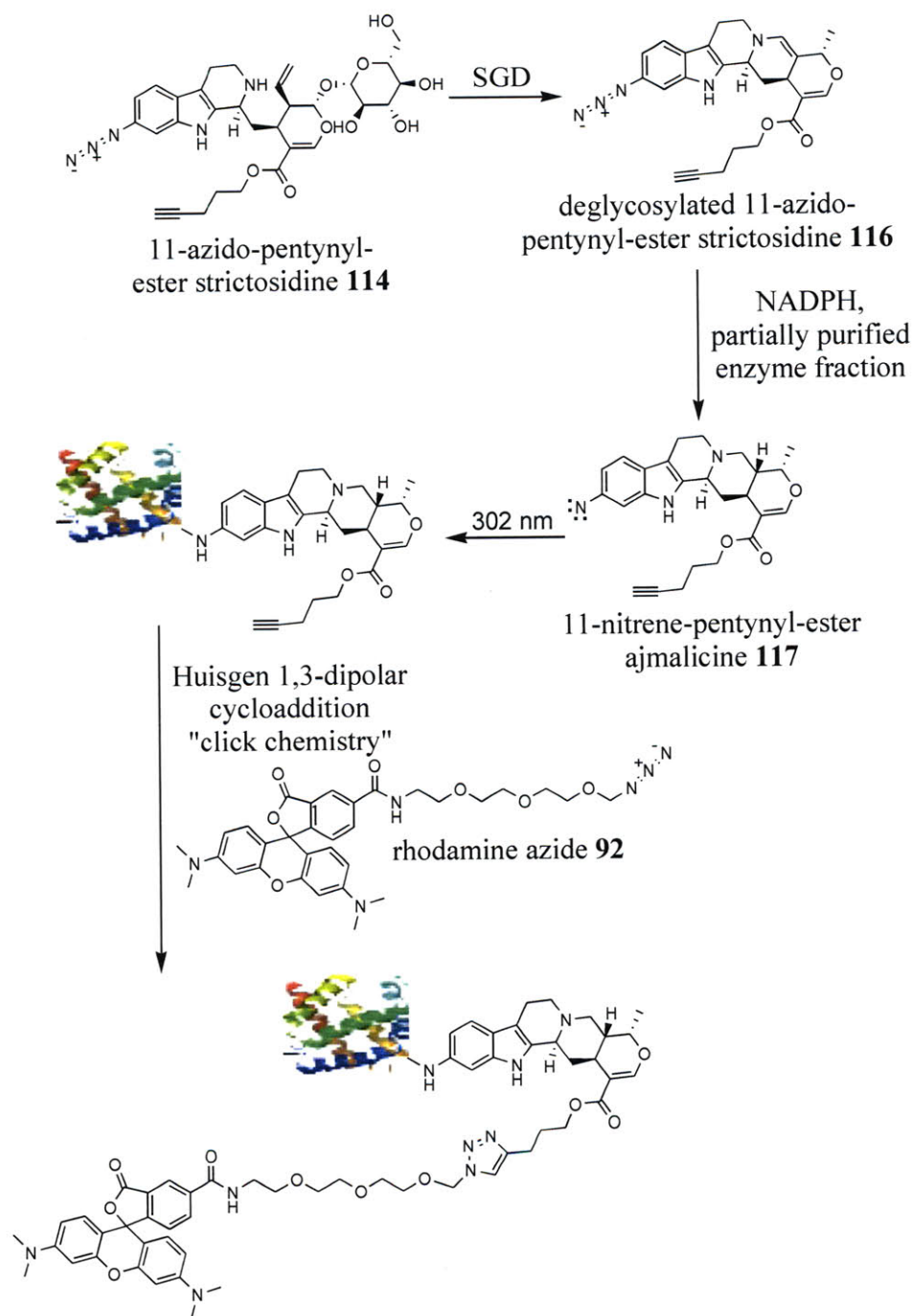


Figure 4-13: In the crosslinking experiments of *C. roseus* enzymes, the probe 11-azido-pentynyl-ester strictosidine **114** was incubated with SGD, followed by NADPH and a partially purified enzyme fraction containing ajmalicine synthase activity. The reaction

mixture was then irradiated with 302 nm light to generate the reactive nitrene moiety, and the alkyne was then derivatized with rhodamine azide **92**.

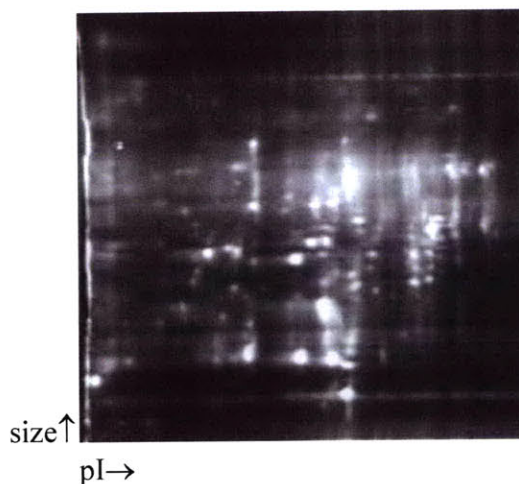


Figure 4-14: A 2D SDS-PAGE of crosslinked enzymes using 11-azido-pentynyl-ester strictosidine **114**. The 2D SDS-PAGE was observed with a UV transilluminator at 254 nm (Bio-Rad).



Figure 4-15: A 2D SDS-PAGE of crosslinked enzymes using 12-azido-pentynyl-ester strictosidine **115**, with the enzymes that were excised and sent for sequencing labeled in green. The 2D SDS-PAGE was observed with a UV transilluminator at 254 nm.

Spot	EST accession number	Enzyme type
1	CR02026D12 CR02028A05 RT00013R_T3_013_B06_27_MAY2004_046_ab1 CR03023A01 _SM-JB_R14-G08_T3_G08_3100401_14_ab1 CROLF1NG_EX2_165_G01_25AUG2006_003	malate dehydrogenase malate dehydrogenase fructose-bisphosphate aldolase sinapyl alcohol dehydrogenase fructose-bisphosphate aldolase 10-hydroxy geraniol oxidoreductase
2	CR02028A05 CR02026D12 LB00003R_T3_003_A03_04JUN2004_031_ab1 G08_T3_G08_3100401_14_ab1 CR01002H09 CROLF1NG_EX2_110_C06_23AUG2004_04 CR01012B09	malate dehydrogenase malate dehydrogenase malate dehydrogenase fructose-bisphosphate aldolase fructose-bisphosphate aldolase malate dehydrogenase fructose-bisphosphate aldolase
3	CR02028A05 RT00013R_T3_013_B06_27MAY2004_046_ab1 1_SM-JB_R14-G08-T3_G08_3100401_14_ab1 LB00003T_T3_003_A03_04JUN2004_031_ab1 CR03023A01 CR04012D03 CR02024C06 CROLF1NG_EX2_101_B09_17AUG2006_077	malate dehydrogenase fructose-bisphosphate aldolase fructose-bisphosphate aldolase malate dehydrogenase sinapyl alcohol dehydrogenase 10-hydroxy geraniol oxidoreductase 4-diphosphocytidyl-2-C-methyl-D-erythritol kinase caffeic acid O-methyltransferase
4	CR02028A05 CR01002H09 CR01015D08 CROLF1NG_EX2_110_C06_23AUG2006_04 CR01011B01	malate dehydrogenase fructose-bisphosphate aldolase malate dehydrogenase malate dehydrogenase malate dehydrogenase
5	CR02023A01 LB00003R_T3_003_A03_04JUN2004_031_ab1 CR02012A04 RT00014R_T3_014_F11_28MAY2004_085_ab1 CR04016D01	sinapyl alcohol dehydrogenase malate dehydrogenase 10-hydroxy geraniol oxidoreductase 3-phosphoglycerate kinase alcohol dehydrogenase
6	RT00015R_T3_015_C09_28MAY2004_075_ab1 LB00035R_T3_035_B11_21JUN2004_093_ab1 CR02028A05 CROLF1NG_EX2_110_C06_23AUG2006_044 CR02026D12 LB00003R_T3_003_A03_04JUN2004_031_ab1 CRS1008B12	fructose-bisphosphate aldolase fructose-bisphosphate aldolase malate dehydrogenase malate dehydrogenase malate dehydrogenase malate dehydrogenase formate dehydrogenase
7	RT00015R_T3_015_C09_28MAY2004_075_ab1 G08_T3_G08_3100401_14_ab1 CR01031D11 CR02028A05 LB00003R_T3_003_A03_04JUN2004_031_ab1 CROLF1NG_EX2_110_C06_23AUG2006_04 CRS1008B12	fructose-bisphosphate aldolase fructose-bisphosphate aldolase fructose-bisphosphate aldolase malate dehydrogenase malate dehydrogenase malate dehydrogenase formate dehydrogenase
8	CR03023H01 RT00015R_T3_015_C09_28MAY2004_075_ab1 1_SM-JB_R14-G08_T3_G08_3100401_14_ab1 LB00035R_T3_035_H03_21JUN2004_017_ab1 CR03022C07 CR04015E12	serine protease fructose-bisphosphate aldolase fructose-bisphosphate aldolase fructose-bisphosphate aldolase mitochondrial chaperonin mitochondrial chaperonin
9	CR04015E12 LB00007R_T3_007_B05_15JUN2004_045_ab1	mitochondrial chaperonin mitochondrial chaperonin

	<p>CR02019F11 CR03023H01 CR03022C07 CR01020A03 CR02028B05 1 SM-JB S4-B01 T3 B01 3100192 03 ab1</p>	<p>mitochondrial F1-ATPase beta subunit serine protease serine protease alanine aminotransferase alanine aminotransferase alanine aminotransferase</p>
10	<p>CR01020E07 LB00007R_T3_007_B05_15JUN2004_045_ab1 RT00038R_T3_038_D05_01JUN2004_-41_ab1 RT00019R_T3_019_G12_31MAY2004_084_ab1 CR01010C11 1 SM-JB R6-E09 T3 E09 3100310 09 ab1</p>	<p>aldehyde dehydrogenases mitochondrial chaperonin pyruvate dehydrogenase alcohol dehydrogenase, class V succinyl CoA-ligase aspartyl protease</p>
11	<p>1RT00028R_T3_028_B09_01JUN2004_077_ab1 1 SM-JB S4-B01 T3 B01 3100192 03 ab1 LB00002R_T3_002_D07_04JUN2004_057_ab1 RT00038R_T3_038_D05_01JUN2004_041_ab1 CR03023A01 CR01010C11 CR02023D04 CR02028B05 CR03023H01 LB00007R_T3_007_B05_15JUN2004_045_ab1 1 SM-JB R6-E09 T3 E09 3100310 09 ab1</p>	<p>alcohol dehydrogenase, class V alanine aminotransferase enolase pyruvate dehydrogenase sinapyl alcohol dehydrogenase succinyl-CoA-ligase enolase alanine aminotransferase serine protease mitochondrial chaperonin aspartyl protease</p>
12	<p>RT00028R_T3_028_B09_01JUN2004_077_ab1 1 SM-JB S4-B01 T3 B01 3100192 03 ab1 CR03023A01 RT00014R_T3_014_F11_28MAY2004_085_ab1 CR02028B05 CR01010C11 LB00002R_T3_002_D07_04JUN2004_057_ab1 CR03023H01 Cr02031B05 CR01012B04</p>	<p>alcohol dehydrogenase, class V alanine aminotransferase sinapyl alcohol dehydrogenase 3-phosphoglycerate kinase alanine aminotransferase succinyl-CoA-ligase enolase serine protease alanine aminotransferase enolase</p>
13	<p>RT00027R_T3_027_F12_01JUN2004_086_ab1 1 SM-JB S4-B01 t3 B01 3100192 03 ab1 CR01012B04 CR02010G03 CR02028B05 RT0028R_T3_028_B09_01JUN2004_077_ab1 CR03023A01</p>	<p>enolase alanine aminotransferase enolase enolase alanine aminotransferase alcohol dehydrogenase, class V sinapyl alcohol dehydrogenase</p>
14	<p>RT00038R_T3_038_D05_01JUN2004_041_ab1 CR02028A05</p>	<p>pyruvate dehydrogenase</p>
15	<p>RT00013R_T3_-13_B06_27MAY2004_046_ab1 CR02026D12 RT00003R_T3_003_D11_18MAY2004_089_ab1 1 SM-JB R14-G08 T3 G08 3100401 14 ab1 CROLF1NG_EX2_165_G01_25AUG2006_003 RT00038R_T3_038_D05_01JUN2004_041_ab1</p>	<p>malate dehydrogenase fructose-bisphosphate aldolase malate dehydrogenase enoyl-[acyl-carrier-protein] fructose-bisphosphate aldolase 10-hydroxy geraniol oxidoreductase pyruvate dehydrogenase</p>
16	<p>RT00028R_T3_028_B09_01JUN2004_077_ab1 1 SM-JB R14-G08 T3 G08 3100401 14 ab1 CR01012B04 CR01004C04 CROLF1NG_EX2_110_C06_23AUG2006_044</p>	<p>alcohol dehydrogenase, class V fructose-bisphosphate aldolase enolase sinapyl alcohol dehydrogenase malate dehydrogenase</p>

Table 4-1: Protein candidates 1-16 sequenced from the 2D SDS-PAGE shown in Figure 4-15. The identities of the proteins, as determined by a BLAST search of the mass spectrometry data against the *C. roseus* EST database, are shown¹³⁵. When the peptide sequence matched to more than one EST sequence, all matching EST sequences are shown. The ESTs are listed in order of likely match.

From the crosslinking study described above and from a preliminary crosslinking study previously performed by Dr. Elizabeth McCoy³⁶, four enzymes – Cr-2141, Cr-12, Cr-318, and Cr-611 – have been successfully cloned by Dr. David Liscombe and Dr. Nathan Ezekiel Nims. Dr. Liscombe, Dr. Nims, and I heterologously expressed and purified to homogeneity each gene in *E. coli*. The four enzymes were chosen for further analysis because all have high sequence identity to NADP-dependent dehydrogenases, and thus could potentially display the desired reductase activity. Cr-2141 and Cr-12 were each identified from protein 1 (Table 4-1) in this study, Cr-611 was identified from protein 5 (Table 4-1) in this study, and Cr-318 was identified in a preliminary crosslinking study performed by Dr. McCoy³⁶. Descriptions of the cloning, expression, and purification procedures are provided in the Materials and Methods section, and were performed with Dr. Liscombe and Dr. Nims. Additional enzymes identified in the crosslinking study will continue to be cloned and functionally characterized.

All four enzymes were assayed for ajmalicine synthase and isositsirikine synthase activity as described in Chapter 3. Unfortunately, no ajmalicine synthase and isositsirikine synthase activity was observed for any of the four enzymes. Nonetheless, efforts were made to determine the function of these novel *C. roseus* enzymes, and we

uncovered an enzyme that displays sinapyl alcohol dehydrogenase activity and is presumably involved in lignin biosynthesis.

B. *Characterization of enzymes isolated via crosslinking experiments*

Cr-2141 characterization

Based on the amino acid sequence, the calculated pI and molecular weight of Cr-2141 are 6.86 and 38,411 Da, respectively¹⁴⁶. A BLAST search of the Cr-2141 amino acid sequence shows that Cr-2141 has the highest sequence identity to cinnamyl / sinapyl alcohol dehydrogenases and 10-hydroxy geraniol oxidoreductase¹³⁵. The top ten results in the BLAST search of Cr-2141 against the protein database are shown below (Table 4-2)¹³⁵. Table 4-2 below shows the score, protein ID probability, accession number, entry name, and species for each cinnamyl alcohol dehydrogenase or 10-hydroxy geraniol oxidoreductase. The score is calculated based on the substitutions and gaps associated with the aligned sequences. A higher score indicates a better alignment, with a score of 600 indicating a perfect alignment. The protein ID probability indicates the percentage of identical amino acids between Cr-2141 and the given enzyme in the table¹³⁵.

Score	Protein ID probability	Accession number	Entry name	Species
501	79%	B9IIT8	Sinapyl alcohol dehydrogenase	<i>Populus trichocarpa</i> (Western balsam poplar)
501	79%	B2Z6P7	Cinnamyl alcohol dehydrogenase	<i>Populus trichocarpa</i> (Western balsam poplar)
499	79%	Q5I6D6	Sinapyl alcohol dehydrogenase-like protein	<i>Populus tremula x Populus tremuloides</i>
498	78%	Q94G59	Sinapyl alcohol dehydrogenase	<i>Populus tremuloides</i> (Quaking aspen)
491	77%	B9H9N8	Cinnamyl alcohol dehydrogenase-like protein	<i>Populus trichocarpa</i> (Western balsam poplar)
490	80%	Q7XAB2	10-hydroxy geraniol oxidoreductase	<i>Camptotheca acuminata</i> (Happy tree)
486	78%	Q6V4H0	10-hydroxy geraniol oxidoreductase	<i>Catharanthus roseus</i> (Madagascar periwinkle) <i>(Vinca rosea)</i>
485	78%	B9T7R7	Alcohol dehydrogenase, putative	<i>Ricinus communis</i> (Castor bean)
485	76%	B9IIG5	Cinnamyl alcohol dehydrogenase-like protein	<i>Populus trichocarpa</i> (Western balsam poplar)
484	78%	B9P5A5	Cinnamyl alcohol dehydrogenase-like protein	<i>Populus trichocarpa</i> (Western balsam poplar)

Table 4-2: BLAST results of Cr-2141. The 10 enzymes with the highest sequence identity to Cr-2141 are shown¹³⁵.

Because of the high sequence identity of Cr-2141 to cinnamyl alcohol dehydrogenases, I assayed cinnamyl aldehyde analogs with this enzyme. In the assays, the cinnamyl aldehyde analogs were incubated with Cr-2141 and NADPH, and product formation was monitored via LCMS. The commercially available cinnamyl aldehyde

analogs sinapaldehyde **96** and coniferyl aldehyde **108** were reduced by Cr-2141 and NADPH to form sinapyl alcohol **97** and coniferyl alcohol **118**, respectively (Figure 4-16). Sinapaldehyde **96** and coniferyl aldehyde **108** are known to be turned over by cinnamyl alcohol dehydrogenases from *Arabidopsis*, and are known substrates in lignan and lignin biosynthesis (Figure 4-8)¹⁴⁰. Although *p*-coumaryl aldehyde **106**, caffeoyl aldehyde **107**, and 5-hydroxy coniferyl aldehyde **109** are also natural substrates for cinnamyl aldehyde dehydrogenases (Figure 4-8)¹⁴⁰, they are not commercially available, and so they were not assayed in this screen. Authentic sinapyl alcohol **97** and coniferyl alcohol **118** standards were used to confirm the identities of the products.

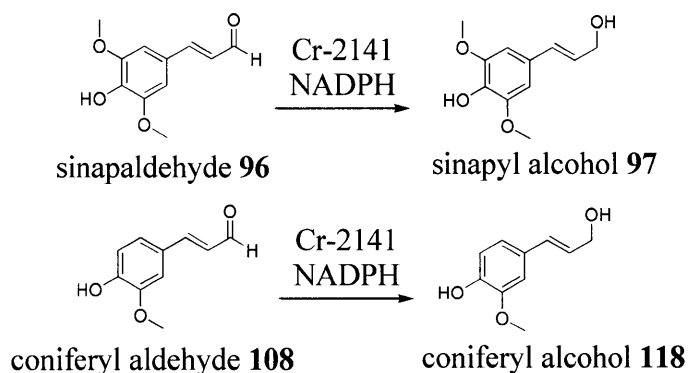


Figure 4-16: Sinapaldehyde **96** and coniferyl aldehyde **108** were reduced by Cr-2141 and NADPH to form sinapyl alcohol **97** and coniferyl alcohol **118**, respectively.

Cr-2141 was also tested with nonnatural cinnamyl aldehyde derivatives. None of these substrates, which included α -methyl-*trans*-cinnamaldehyde **119**, 6-hydroxychrome-3-carboxaldehyde **120**, sinapic acid **121**, 3,4,5-trimethoxy sinapic acid **122**, and cinnamide **123** (Figure 4-17) was accepted by Cr-2141.

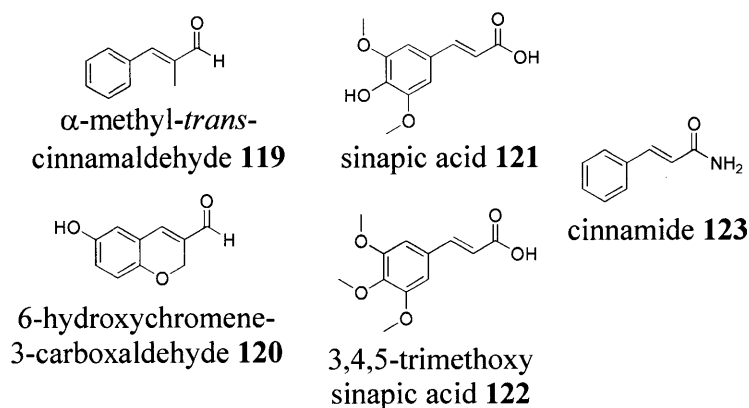


Figure 4-17: Cinnamyl aldehyde derivatives not reduced by Cr-2141 and NADPH include α -methyl-*trans*-cinnamaldehyde **119**, 6-hydroxychromene-3-carboxaldehyde **120**, sinapic acid **121**, 3,4,5-trimethoxy acid **122**, and cinnamide **123**.

Steady state kinetic analysis of Cr-2141 was performed to determine if Cr-2141 has kinetic parameters similar to those of other reported cinnamyl alcohol dehydrogenases. Kim *et al.*¹⁴⁰ have reported the kinetic parameters for five cinnamyl alcohol dehydrogenases from *A. thaliana* with the substrates shown in Figure 4-8. K_m values ranging from 13 to 3,685 μM and k_{cat} values ranging from 3 to 871 min^{-1} were observed¹⁴⁰. In the steady state kinetic analysis of Cr-2141, I chose sinapaldehyde **96** as the substrate instead of coniferyl aldehyde **108** (Table 4-3) because Kim *et al.*¹⁴⁰ had reported that sinapaldehyde **96** had higher k_{cat} values on average than coniferyl aldehyde **108**. Qualitative analysis with Cr-2141 also revealed this preference for sinapaldehyde **96**. Though sinapaldehyde **96** showed K_m values consistent with those reported by Kim *et al.*¹⁴⁰, I observed lower k_{cat} values. Nevertheless, the kinetic parameters are consistent with Cr-2141 playing a role in lignin biosynthesis in *C. roseus*.

Substrate	K_m (μM)	V_{max} ($\mu\text{M min}^{-1}$)	k_{cat} (min^{-1})	k_{cat}/K_m ($\mu\text{M}^{-1} \text{min}^{-1}$)
Sinapaldehyde 96	335.66 \pm 87.35	0.13 \pm 0.01	0.092 \pm 0.01	2.74×10^{-4}

Table 4-3: Steady state kinetic values for sinapaldehyde **96** NADPH-dependent reduction by Cr-2141.

Cr-2141 was assayed for sinapaldehyde dehydrogenase activity based on the sequence identity of this enzyme to known enzymes in lignin biosynthesis. However, although Cr-2141 turns over the appropriate substrates *in vitro*, this does not prove that Cr-2141 plays a role in lignin biosynthesis in *C. roseus*. Additional experiments, described in the Discussion section of this chapter, are required to validate the function of this gene *in planta*.

Cr-12 characterization

Based on the amino acid sequence, the calculated pI and molecular weight of Cr-12 are 6.21 and 38,870 Da, respectively¹⁴⁶. Cr-12 has the highest sequence identity to cinnamyl / sinapyl alcohol dehydrogenases, and has high sequence identity to 10-hydroxy geraniol **23** from *Camptotheca acuminata*, as well as to mannitol dehydrogenase from *Apium graveolens* (celery) (Table 4-4). The first ten results from a BLAST search are shown below (Table 4-4)¹³⁵.

Score	Protein ID probability	Accession number	Entry name	Species
435	73%	B2Z6P7	Cinnamyl alcohol dehydrogenase	<i>Populus trichocarpa</i> (Western balsam poplar)
434	73%	Q5I6D6	Sinapyl alcohol dehydrogenase-like protein	<i>Populus tremula x Populus tremuloides</i>
432	72%	Q94G59	Sinapyl alcohol dehydrogenase	<i>Populus tremuloides</i> (Quaking aspen)
432	73%	B9IIT8	Sinapyl alcohol dehydrogenase	<i>Populus trichocarpa</i> (Western balsam poplar)
432	73%	Q7XAB2	10-hydroxy geraniol oxidoreductase	<i>Camptotheca acuminata</i> (Happy tree)
429	72%	B9H9N8	Cinnamyl alcohol dehydrogenase-like protein	<i>Populus trichocarpa</i> (Western balsam poplar)
427	70%	A5CA75	Putative uncharacterized protein	<i>Vitis vinifera</i> (Grape)
426	72%	B9IIG5	Cinnamyl alcohol dehydrogenase-like protein	<i>Populus trichocarpa</i> (Western balsam poplar)
425	72%	B9HNN3	Cinnamyl alcohol dehydrogenase-like protein	<i>Populus trichocarpa</i> (Western balsam poplar)
425	73%	Q38707	Mannitol dehydrogenase	<i>Apium graveolens</i> (Celery)

Table 4-4: BLAST results of Cr-12. The 10 proteins with the highest sequence identity to Cr-12 are shown¹³⁵.

Cr-12 failed to show dehydrogenase activity when incubated with sinapaldehyde **96** and NADPH. Given that Cr-12 also displayed sequence similarity to 10-hydroxy geraniol oxidoreductase, Cr-12 could potentially be an enzyme involved in secologanin **17** biosynthesis, such as one of the enzymes converting 10-oxo geraniol **72** to loganic acid **42** (Figure 4-12)¹⁹⁻²². Future efforts could involve synthesizing or isolating the intermediates between 10-oxo geraniol **72** and loganic acid **42** for use in activity assays to

determine the function of Cr-12. Additionally, disrupting the function of the gene *in vivo* could also provide clues to its function.

Cr-318 characterization

The calculated pI and molecular weight of Cr-318 are 6.09 and 38,770 Da, respectively, based on the predicted amino acid sequence¹⁴⁶. Cr-318 has the highest sequence identity to cinnamyl / sinapyl alcohol dehydrogenases (Table 4-5). The first ten results from a BLAST search are shown below (Table 4-5)¹³⁵. However, as with Cr-12, assays performed with sinapaldehyde **96** did not show sinapyl alcohol dehydrogenase activity. The function of Cr-318 remains to be determined.

Score	Protein ID probability	Accession number	Entry name	Species
392	67%	B2Z6P7	Cinnamyl alcohol dehydrogenase	<i>Populus trichocarpa</i> (Western balsam poplar)
392	67%	Q516D6	Sinapyl alcohol dehydrogenase-like protein	<i>Populus tremula x Populus tremuloides</i>
390	67%	Q94G59	Sinapyl alcohol dehydrogenase	<i>Populus tremuloides</i> (Quaking aspen)
390	67%	B9IIT8	Sinapyl alcohol dehydrogenase	<i>Populus trichocarpa</i> (Western balsam poplar)
385	66%	B9IIG5	Cinnamyl alcohol dehydrogenase-like protein	<i>Populus trichocarpa</i> (Western balsam poplar)
385	66%	A5CA75	Putative uncharacterized protein	<i>Vitis vinifera</i> (Grape)
383	66%	A9PJN2	Putative uncharacterized protein	<i>Populus trichocarpa x Populus deltoides</i>
381	66%	B9P5A5	Cinnamyl alcohol dehydrogenase-like protein	<i>Populus trichocarpa</i> (Western balsam poplar)
381	66%	B9HNN3	Cinnamyl alcohol dehydrogenase-like protein	<i>Populus trichocarpa</i> (Western balsam poplar)
380	66%	B9HNN0	Cinnamyl alcohol dehydrogenase-like protein	<i>Populus trichocarpa</i> (Western balsam poplar)

Table 4-5: BLAST results of Cr-318; the 10 enzymes with the highest sequence identity to Cr-318 are shown¹³⁵.

Cr-611 characterization

The calculated pI and molecular weight of Cr-611 are 6.02 and 35,593 Da, respectively¹⁴⁶. Cr-611 has the highest sequence identity to malate dehydrogenases (Table 4-6). The first ten results from a BLAST search are shown below (Table 4-6)¹³⁵. The high score (588-596) and protein ID probabilities (91-93%) shown in Table 4-6

indicate that Cr-611 is most likely a malate dehydrogenase. After validating that this enzyme did not exhibit ajmalicine synthase or isositsirikine synthase activity, functional characterization of this enzyme was not pursued further.

Score	Protein ID probability	Accession number	Entry name	Species
596	93%	<u>Q9FSF0</u>	Malate dehydrogenase	<i>Nicotiana tabacum</i> (Common tobacco)
595	92%	<u>D2D318</u>	Malate dehydrogenase	<i>Gossypium hirsutum</i> (Upland cotton)
593	93%	<u>P57106</u>	Malate dehydrogenase, cytoplasmic 2	<i>Arabidopsis thaliana</i> (Mouse-ear cress)
593	91%	<u>B9NBW3</u>	Malate dehydrogenase	<i>Populus trichocarpa</i> (Western balsam poplar)
592	93%	<u>Q8LA78</u>	Malate dehydrogenase	<i>Arabidopsis thaliana</i> (Mouse-ear cress)
592	92%	<u>Q08062</u>	Malate dehydrogenase, cytoplasmic	<i>Zea mays</i> (Maize)
592	92%	<u>C4IZW9</u>	Malate dehydrogenase	<i>Zea mays</i> (Maize)
591	93%	<u>B6SLL8</u>	Malate dehydrogenase	<i>Zea mays</i> (Maize)
590	92%	<u>Q2PYY8</u>	Malate dehydrogenase	<i>Solanum tuberosum</i> (Potato)
588	92%	<u>C5WYF2</u>	Malate dehydrogenase	<i>Sorghum bicolor</i> (Sorghum)

Table 4-6: BLAST results of Cr-611; the 10 enzymes with the highest sequence identity to Cr-611 are shown¹³⁵.

III. Discussion

Although Cr-2141, Cr-12, Cr-318, and Cr-611 do not exhibit the desired ajmalicine synthase or isositsirikine synthase activity, these proteins undoubtedly perform other metabolic functions in *C. roseus*. I discovered that Cr-2141 exhibits sinapyl dehydrogenase activity, reducing sinapaldehyde **96** to sinapyl alcohol **97** with a k_{cat}/K_m value of $2.74 \times 10^{-4} \mu\text{M}^{-1} \text{min}^{-1}$ (Table 4-3). Cr-2141 may also exhibit dehydrogenase activity with other substrates. Sinapyl alcohol dehydrogenases often have broad substrate specificities; Kim *et al.*¹⁴⁰ reported that six cinnamyl alcohol dehydrogenases from *A. thaliana* reduce five different cinnamyl aldehyde analogs (**96** and **106-109**) (Figure 4-8) with similar catalytic efficiency. Intriguingly, the *R. serpentina* alkaloid biosynthetic enzyme perakine reductase shows cinnamyl alcohol dehydrogenase activity in addition to perakine reductase activity; it reduces cinnamaldehyde **126** to cinnamyl alcohol **127** and reduces perakine **124** to raucaffrinoline **125** (Figure 4-18)¹²¹. Notably, perakine reductase reduces cinnamaldehyde **126** to cinnamyl alcohol **127** with a 31% higher relative activity than when it reduces perakine **124** to raucaffrinoline **125** (Figure 4-18)¹²¹. Therefore *in vitro* enzymatic activity assays do not always provide a definitive answer for the metabolic function of an enzyme.

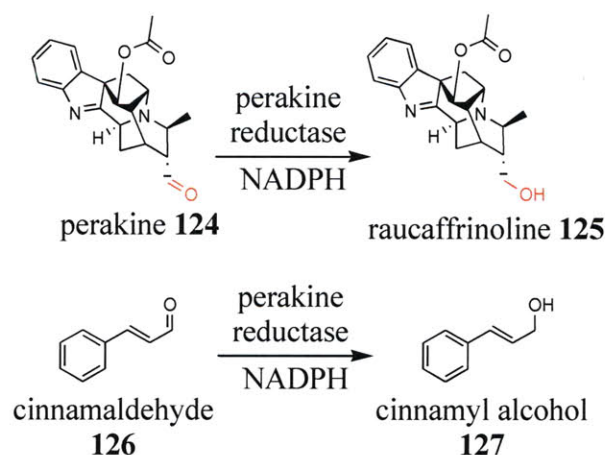


Figure 4-18: NADPH-dependent perakine reductase reduces the TIA perakine **124** to raucaffrinoline **125**; the aldehyde that is reduced is shown in red. Perakine reductase also reduces cinnamaldehyde **126** to cinnamyl alcohol **127**¹²¹.

The relatively high sequence similarity of Cr-2141 to known cinnamyl / sinapyl alcohol dehydrogenases led us to test Cr-2141 for this activity. The activity is clear, but the catalytic efficiency is slightly lower than those reported for cinnamyl / sinapyl alcohol dehydrogenases identified from *A. thaliana*. Whereas Cr-2141 has a k_{cat} of 0.092 min^{-1} for sinapaldehyde **96**, six cinnamyl alcohol dehydrogenases from *A. thaliana* have k_{cat} values from 3 to 871 min^{-1} ; this lower k_{cat} value may simply indicate that Cr-2141 is a less efficient enzyme, or that it is not expressed in a highly functional form under heterologous expression conditions. It is also possible that Cr-2141 plays some additional role in *C. roseus* metabolism, and the sinapyl alcohol dehydrogenase activity is adventitious. The function of Cr-2141 can be more definitively assessed by examining its expression *in vivo*. Future work will examine the expression levels of Cr-2141 by measuring Cr-2141 mRNA levels by Northern blot or qPCR, and evaluating whether the expression levels are comparable in level and location to other known lignin biosynthesis

genes. Moreover, the function of Cr-2141 can be disrupted in *C. roseus* using RNAi³⁵. After disruption of this gene, the resulting phenotype or metabolic profile can be compared with wild-type tissue to provide more information about the role of this enzyme in the plant.

We note that Cr-2141 also exhibits 80% sequence identity to 10-hydroxy geraniol oxidoreductase from *Camptotheca acuminata*, an enzyme that also catalyzes the interconversion of an aldehyde and an alcohol. It is possible that Cr-2141 may also act on one of the geraniol **22** derived substrates of the secologanin **17** pathway. The substrates of the enzymes that convert 10-oxo geraniol **72** to loganic acid **42** (Figure 4-12) could be synthesized or isolated and then assayed with Cr-2141 *in vitro*. If Cr-2141 plays a role in secologanin **17** biosynthesis, disruption of Cr-2141 production through RNAi could disrupt secologanin **17** biosynthesis *in vivo*.

The functions of Cr-12, Cr-318, and Cr-611 have not been established. Again, disruption of these genes in *C. roseus* using RNAi followed by comparison of the resulting phenotype or metabolic profile with that of wild-type tissue could facilitate determination of the functions of these genes.

Crosslinking as a method to identify *C. roseus* enzymes has proven partially successful. Unfortunately, no recombinant enzyme exhibiting ajmalicine synthase or isositsirikine synthase activity was isolated. However, we did isolate one enzyme that exhibited dehydrogenase activity with a substrate utilized in lignin biosynthesis. Although the sinapaldehyde **96** substrate is not structurally identical to the deglycosylated 11-azido-pentynyl-ester strictosidine **116** probe (Figure 4-19), there are nevertheless

some similar structural recognition elements, such as the aromatic moiety, that could perhaps allow the probe to bind to this sinapaldehyde dehydrogenase. These results highlight the advantages and pitfalls of a crosslinking strategy. Obviously, our data indicates that crosslinking to non-targeted enzymes occurs, but nevertheless, this strategy allowed us to identify a new enzyme involved in *C. roseus* secondary metabolism.

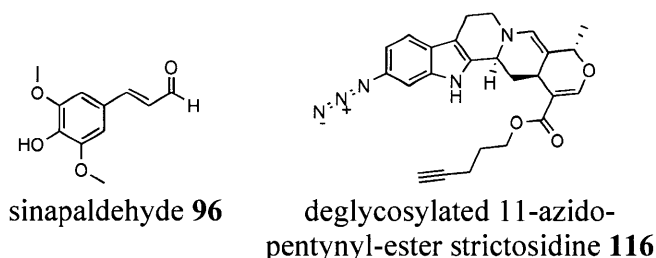


Figure 4-19: The structures of sinapaldehyde **96** and deglycosylated 11-azido-pentynyl-ester strictosidine **116**.

IV. *Materials and Methods*

A. *Crosslinking experiments conditions*

The probe 11-azido-pentynyl-ester strictosidine **114** (0.7 mg, 1.6 μmol) was incubated with SGD (7 μM) at room temperature for 30 minutes in 50 mM sodium phosphate buffer, pH 7.5. NADPH (3 mM) was then added, followed by ajmalicine synthase partially purified by acetone precipitation (1 mg total protein). The reaction mixture was wrapped in aluminum foil to prevent photolysis of the azide and was incubated at 25°C for 30 minutes. After 30 minutes, the aluminum foil was removed, and the reaction mixture was irradiated at 302 nm for 5 minutes, followed by the addition of 1 mM TCEP, CuSO_4 , rhodamine azide, and *t*BuOH. After an incubation period of 75

minutes, the sample was prepared for 2D SDS-PAGE using the Perfect-FOCUS (G-Biosciences) protocol.

For 2D SDS-PAGE analysis, 200 μ L rehydration/sample buffer (BioRad) was added to the labeled protein pellet obtained using the Perfect-FOCUS kit. The reaction mixture was vortexed and centrifuged to remove particulates, and the sample was then put in the 2D gel tray. An 11 cm pH 4-7 IPG strip (Biorad) was laid over the sample. The sample and IPG strip were incubated for 15 minutes, after which time 2 mL mineral oil was added. The 2D gel was run for 17 hours, and then incubated for 10 minutes with 1.6 mL of equilibration buffer I (Biorad), followed by another 10 minutes with equilibration buffer II (Biorad), and then separated in the second dimension on a Criterion Precast Gel (12.5% Tris HCl, 11 cm, IPG+1, Biorad). The 2D SDS-PAGE was observed with a UV transilluminator (254 nm).

B. *Cloning of crosslinked enzymes*

The plant growth and cloning procedures were performed by Dr. David Liscombe and Dr. Nathan Ezekiel Nims. Briefly, *C. roseus* seeds were purchased from Horizon Herbs (Williams, Oregon). Sterile seedlings were cultured and elicited with the plant hormone methyl jasmonate as described previously by Aerts *et al.*¹⁵³ Total RNA was isolated from mature *C. roseus* leaves, as well as from unelicited and methyl jasmonate-elicited seedlings, using the Plant RNeasy kit (QIAGEN). First-strand cDNA was obtained using M-MuLV Reverse Transcriptase (New England Biolabs) and oligo d(T) primer. Leaf, unelicited seedling, and methyl jasmonate-elicited seedling cDNA were combined (1:1:1) and used as a template for PCR.

The full-length open reading frames of Cr-2141, Cr-12, Cr-318, and Cr-611 were each amplified by PCR using a sense primer, an antisense primer, and Platinum Taq High Fidelity (Invitrogen) (Table 4-7). Each amplicon was cloned into pGEM-T Easy shuttle vector, and the gene products were confirmed by DNA sequencing. The ORF was then reamplified using primers containing the appropriate restriction sites and cloned into pET28a (Novagen).

Enzyme	Sense primer
Cr-2141	5'-ATGGCCGGAAAATCACCAGAAGAG-3'
Cr-12	5'-AAAGGATCCATGAAAGATCAACACCCCGTGAAGG-3'
Cr-318	5'-ATGGCTGGAAAATCACCAGAAGAGCAAC-3'
Cr-611	5'-ATGGCTGGAAAATCACCAGAAGAGCAAC-3'
Enzyme	Antisense primer
Cr-2141	5'-TTAAGGAGCTTTCAAGTCTTTGCAACG-3'
Cr-12	5'-TTTCTCGAGTAGGCTTAAGACTCCGGTGGAGG-3'
Cr-318	5'-AGACTCCGGTGGAGGAGTTAAAGTGTTC-3'
Cr-611	5'-AGACTCCGGTGGAGGAGTTAAAGTGTTC-3'

Table 4-7: Sense and antisense primers used to clone Cr-2141, Cr-12, Cr-318, and Cr-611.

C. Heterologous expression and purification of crosslinked enzymes

E. coli Rosetta 2 (DE3) pLysS cells harboring the pET28 expression constructs were grown in 500 mL of Luria-Bertani medium supplemented with antibiotic at 37°C with shaking (220 rpm) to an absorbance at 600 nm of 0.6, and then induced with 1 mM IPTG. After 4 hours of growth at 37°C, the cells were collected by centrifugation at 3000g, and stored at -80°C. Pelleted cells were resuspended in buffer A (100 mM Tris-HCl, pH 7.5, 100 mM KCl, 10% glycerol, 20 mM β-mercaptoethanol) and lysed by sonication. Cell debris was removed by centrifugation (10,000g) for 30 minutes at 4°C, and the supernatant was bound to Talon cobalt affinity resin (bed volume of 300 μL;

Clontech, <http://www.clontech.com>), which was then washed with buffer A and eluted with buffer A containing increasing concentrations (10, 50, 100, and 200 mM) of imidazole. Under these conditions, the largest amount of pure recombinant protein is typically recovered in the 100 mM imidazole fraction. Figure 4-20 below shows 1D SDS-PAGE of purified Cr-2141, Cr-12, Cr-318, and Cr-611.

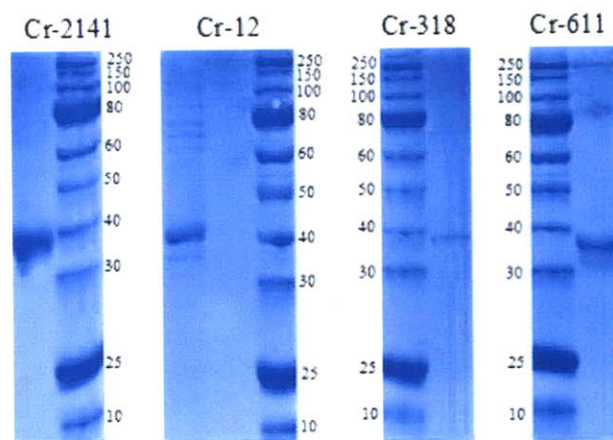


Figure 4-20: A 1D SDS-PAGE of purified Cr-2141, Cr-12, Cr-318, and Cr-611.

D. DNA and amino acid sequences of crosslinked enzymes

The DNA and amino acid sequences of Cr-2141, Cr-12, Cr-318, and Cr-611 are listed below.

Cr-2141 DNA sequence:

```
ATGCCCGGAAAATCACCAGAAGAGGAGCACCCAGTCAAGACCTATGGATTGGCTGCTCATGA
TTCATCTGGGGTTTTATCTCCGTTCAAATTCTCCAGGAGGGCAACTCTTGAGGATGATGTGAG
GTTCAAGGTGCTATATTGTGGGATTTGTCATACTGACCTTCATTTGCTAAGAATGAGTGGGGT
ATTCGACCTATCCTCTTGTACCAGGACATGAAATCGTAGGGGAAGTTACAGAGGTCGGCGGC
AAAGTTACAAAGGTCAAGGTTGGAGATAAAGTTGGTGTGGCTGCTTGGTTGGTTCATGCCGC
ACTTGTGATAATTGTCGTGCAGATCTTGAGAACTATTGTCCAAAATGGTGCTAACCTATGCA
AGTCCAAACGTTGATGGAACGATTACCTATGGAGGCTATTCCAATGAGATGGTATGCAACGA
ACACTTTATTGTTTCGTTTCCCAGAGAACCTACCACTTGATGGTGGGGCACCATTGCTTTGTGCC
GGTATTACTGTGTACAGTCCAATGAAATACTATGGCTTCGCCAAACCCGGGAGCCACATAGCT
GTTAATGGTCTTGGTGGACTTGGCCATGTGGCTGTTAAGTTTGCAAAGGCCATGGGAGCAAAA
GTGACAGTTATAAGTACATCTGAGGGCAAGAAAGACGATGCCCTCAATCGTTTGGGTGCAGA
TGCATTTTTGTTGAGCAGTAATCCAGAAGCACTGCAGGCTGCAACAGGCACATTTGATGGCAT
```


ACTTAATACTATTTCTGCTAAGCAGCTATTATCCCATTGCTTGGTCTACTAAAGTCTCATGGC
 AAGCTTGTTCTTCTTGGGGCACCCCCGGAACCACTTGATCTTCACTCTGCTCCTTTGCTTATGG
 GGAGGAAGATGGTTGCTGGAAGTAGCATTGGAGGATTGAAGGAGACCCAAGAGATGCTTGAT
 TTTGCCGGAAGCATAACATTACTGCAGATATAGAACTCATTTCCGCGGACAATATCAACACA
 GCTTTGGAGCGTCTGGCCAAGGGTATGTTAGATATCGCTTTGTCCTTGACGTTGCAAAGACC
 TTGAAAGCTCCTTAA

Cr-2141 amino acid sequence:

MAGKSPREEHPVKTYGLAAHDSSGVLSPFKFSRRATLEDDVRFKVLVYCGICHTDLHFAKNEWGIS
 TYPLVPGHEIVGEVTEVGGKVKVKVGDVKVGVGCLVGSRTCDCNCRADLENYCPKMVLTYASPN
 VDGTYGGYSNEMVCNEHFIVRFPENLPLDGGAPLLCAGITVYSPMKYYGFAKPGSHIAVNGLG
 GLGHVAVKFAKAMGAKVTVISTSEGKDDALNRLGADAFLLSNPEALQAATGTFDGLNTISAK
 HAIPLLGLLKSHGKLVLLGAPPEPLDLHSAPLLMGRKMVAGSSIGGLKETQEMLDFAGKHNITAD
 IELISADNINTALERLAKGDVRYRFVLDVAKTLKAP

Cr-12 DNA sequence:

ATGAAAGATCAACACCCCGTGAAGGCTTATGGATGGGCAGCTAGAGACACATCTGGGATTCT
 TTCTCCTTCAAGTTTTCCAGAAGGGCAACAGGGGATCATGATGTAAGAGTAAAGATTCTCTA
 CTGTGGTATTTGCCATTCTGACCATCAAGCTGCCACGAACTTAATGGGCTTTTATACATATCCT
 ATGTGCCCCGGGTTGAGACAGTACGGGTAGCATCTGAAGTTGGAAGCAAGGTCACAAAAGT
 GAAAGTTGGTGATAAAGTTGCCACGGGGATCATTGTGGGATCATGTGGCGAATGTAATGAGT
 GTATCAATGACCGTGATTGTTATTGCCCTAAGATGACCGCAGCTTATGGTTCGGTAGACCGTG
 ATGGAACTCCCAATTATGGAGGTTTCTCCAATGAGACAGTAGTAAATGAGAATTTTGTCTTTC
 GTTTCCTGAAAACCTTCTCTTCTGCTGGTGTCTCCACTGCTCAATGCTGGAATAACTGTGTA
 CAGTCCCATGAGATTTTATGGCCTGGACAAACCAGGAATGCACTTGGGAGTTGTTGGCCTAGG
 TGGACTTGGTCATTTAGCTGTGAAGTTTGGCAAGGCTTTTGGGGCCAAAGTCACTGTGATTAG
 TACCTCTCCAAGCAAGAAAGACGAAGCTGTCAATTTTCTTGGTGCGGATGGCTTCTTGGTCAG
 CAGTGATGCTGAACAAATGAAGGCTGCTGCTGGAACCTTGGATGGGATTATTGATACCGTGCC
 TGTTGTCCATCCTATTGAGCCCTTGCTATGGCTTCTGAAGAATCATTCAAAGCTTGTTTGGTT
 GGAGCTACAGGTGGTTCATTTGATTTGCCAATTCTTCTTTAGCATTGGGCAGGAGAAGTGTG
 GCTTCAAGCATTGGTGAAGTACAAAGGAGGCTCAAGAGATGCTCGATTTTGCAGCTGAGCA
 CAATATCACTGCAAACGTTGAGATTATTCCAATGGACTATGCGAATACAGCAATGGAACGCAT
 TGACAAGAGTGATGTTTCGATACCGATTTGTGATTGATATTTGGGAACACTTAACTCCTCCACC
 GGAGTCTTAAGCCTATAG

Cr-12 amino acid sequence:

MKDQHPVKAYGWAARDTSGILSPFKFSRRATGDHDVVRVKILYCGICHSDHQAATNLMGFYTYPIV
 PGFETVRVASEVGSKVKVKVGDKVATGIIVSCGECNECINDRDCYCPKMTAA YGSVDRDGT
 PNYGGFSNETVNNENFVFRFPENLSLPGGAPLLNAGITVYSPMRFYGLDKPGMHLGVVGLGGLGHLA
 VKFGKAFGAKVTVISTSPSKKDEAVNFLGADGFLVSSDAEQMKAAGTLDGIIDTVPVHPIEPL
 WLLKNHSKLVLVGATGGSFDLPILPLALGRRTVASSIGGSTKEAQEMLDFAAEHNITANVEIIPMD
 YANTAMERIDKSDVRYRFVIDIWEHFNSSTGVLSL

Cr-318 DNA sequence:

ATGGCTGGAATAACACCAGAAGAGCAACACCCAGTGAAGGCCTATGGATGGGCAGCAAGAG
 ATTCTTCTGGGATTCTTTCTCCCTTCAAGTTTCTAGAAGGGTTACAGGTGATTATGATGTCAG
 AGTAAAATTCTTTACTGTGGTATTTGTCATTCTGACCTTCAAATTGCCAAGAATGAAATGGGC
 TTTTCCACATATCCTCTTGTCCCTGGGTTTGGAGACGGTAGGGATAGCAACTGAAGTTGGAAGC
 AAGGTCACAAAAGTGAAAGTTGGTGACAAAGTTGCAGTGGGAGCCATTGTGGGATCATGCGG
 TAAATGTGATGAGTGTGTGAATGACCGTGATTGTTATTGCCCTAGGCTTATCACGGCTTATGG
 CGGAATAGACCATGATGGAACCTCCACTTATGGAGGGTTTTCCAATGAGACAGTAGCAAATG

AGAATTATGTTTTTCGTTTCCCTGAAAATCTTCCGCTTGCTGCTGGTGCTCCACTACTCAATGC
 TGGACTCACGGTATACAGTCCAATGAGATTTTATGGTCTAGATAAACCCAGGCACGAGGATGCA
 CTTGGGAGTTGTTGGTCTAGGTGGACTTGGTCATTTAGCTGTGAAGTTTGGCAAGGCTTTTGGG
 GCCAAAGTCACTGTGATTAGTACCTCTCCAAGCAAGAAAGACGAAGCTGTCAATTTTCTTGGT
 GCGGATGGCTTCTTGGTCAAGCAGTGTGCTGAACAAATGAAGGCTGCTGCTGGAACCTTGGAT
 GGGATTATTGATACCGTGCCTGTTGTCCATCCTATTGAGCCCTTGCTATGGCTTCTGAAGAATC
 ATTCAAAGCTTGTGTTTGGTGGAGCTACAGGTGGTTCATTTGATTTGCCAATTCCTCCTTAGC
 ATTGGGCAGGAGAACTGTGGCTTCAAGCATTGGTGGAAGTACAAAGGAGGCTCAAGAGATGC
 TCGATTTTGCAGCTGAGCACAATACACTGCAAACGTTGAGATTATTCCAATGGACTATGTGA
 ATACAGCAATGGAACGCATTGACAAGAGTGTGTTTCGATACCGATTTGTGATTGATATTGGGA
 ACACCTTAACCTCCACCGGAGTCTTAA

Cr-318 amino acid sequence:

MAGKSPEEQHPVKAYGWAARDSSGILSPFKFSRRVTGDYDVRVKILYCGICHSDLQIAKNEMGFS
 TYPLVPGFETVGIATEVGSVKVTKVKVGDKVAVGAIVSGCGKCECVNDRDCYCPRLITAYGGIDH
 DGTPTYGGFSNETVANENYVFRFPENLPLAAGAPLLNAGLTVYSPMRFYGLDKPGTRMHLGVVG
 LGGLGHLAVKFGKAFGAKVTVISTSPSKKDEAVNFLGADGLVSSDAEQMKAAGTLDDIHDTPV
 VHPIPELLWLLKNHSLVVGATGGSFDPILPLALGRRTVASSIGGSTKEAQEMLDFAAEHNITAN
 VEIIPMDYVNTAMERIDKSDVRYRFVIIGNTLTPPPES

Cr-611 DNA sequence:

ATGGCAAAGAGCCCGTTTCGTGTTCTCGTCACCGGTGCCGCAGGGCAAATCGGTTATGCTCTC
 GTTCCCATGATTGCCAGGGGAGTTATGTTGGGTGCTGATCAACCTGTTATCCTCCACATGCTAG
 ATATTCTCCTGCTGCAGAGGCATTGAATGGGGTTAAGATGGAATTGGTTGATGCTGCTTTTCC
 TCTACTTAAAGGTGTTGTGCTACAACCTGATGTTGCTGAGGCTTGTGCTGGTGTAAACATTGCT
 GTGATGGTTGGTGGGTCCCAAGGAAAGAGGGAATGGAGCGGAAAGATGTAATGTCAAAGAA
 TGTATCTATTTACAAGTCCCAAGCTTCTGCACCTGAGCAATATGCTGCCCTAACTGCAAGGTT
 TTGTTTGTGCTAACCCAGCCAACACCAATGCATTGATTCTGAAGGAATTTGCACCATCTATTC
 CTGCAAAAAATGTTACTTGTGTTGACAAGATTGGACCACAACAGGGCCCTTGGTCAAATCTCAG
 AGAGATTGAACGTTCCAGTTTCTGAGGTTAAAAATGTCATAATTTGGGGAAATCACTCCTCAA
 CACAATATCCTGATGTCAACCATGCCACTGTAAAACATCAGCTGGAGAAAAGCCTGTGCGGG
 AGCTAGTTAAAGATGATGAATGGTTGAATGGGGAGTTCATAACTACTGTCCAGCAACGTGGTG
 CTGCAATTATTAAGCCAGGAAGCTTTCTAGTGCACCTTCTGCTGCTAGTGCTGCATGTGACCA
 CATTCTGACTGGGTCCCTTGGAACTCCTGAGGGCACTTGGGTCTCCATGGGTGTATACTCAGA
 TGGCTCCTACAATGTCCCTGCTGGTCTTATTTACTCCTTCCCAGTTACATGTAAAAATGGAGAA
 TGGACTGTTGTTCAAGGACTTCCAATTGACGAGTTATCAAGAAAGAAGATGGACTCAACAGCT
 GAAGAACTCTCTGAGGAAAAGGCTTTGGCATACTCATGTCTTACTTAA

Cr-611 amino acid sequence:

MAKEPVRVLVTGAAGQIGYALVPMIARGVMLGADQPVILHMLDIPPAEALNGVKMELVDAAFP
 LLKGVVATTDVAEACAGVNIAVMVGGFPRKEGMRKDVMSKNVSIYKSQASALEQYAAPNCKV
 LFVANPANTNALILKEFAPSIPAKNVTCLTRLDHNRALGQISERLNVVSEVKNVIIWGNHSSTQYP
 DVNHATVKTSAGEKPVRELVKDDEWLNGEFITTQQRGAIIKARKLSSALSASAACDHIRDWV
 LGTPEGTWVSMGVYSYDGSYNVPAGLIYSFPVTCKNGEWTVVQGLPIDELSRKKMDSTAEELSEEK
 ALAYSCLT

E. Assay conditions

In sinapaldehyde dehydrogenase assays of Cr-2141, I incubated Cr-2141 (30 μ M) with 2.3 mM substrate and 7.8 mM NADPH in a 128 μ L reaction volume. All substrates were purchased from Sigma Aldrich, and product formation was monitored by LCMS. Sinapyl alcohol **97** and coniferyl alcohol **118** produced in assays with Cr-2141 and NADPH had the same LCMS retention time and mass as sinapyl alcohol **97** and coniferyl alcohol **118** standards (Sigma Aldrich) (Figure 4-21). In the LCMS analysis of the assays, the starting material and products were separated using a 5-minute method with a gradient of 10-90% acetonitrile in 0.1% formic acid.

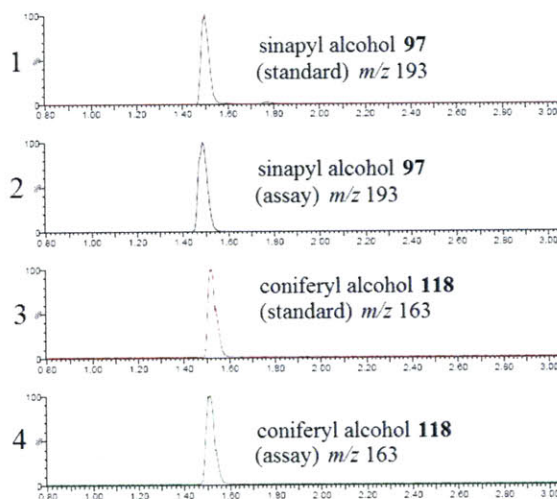


Figure 4-21: A sinapyl alcohol **97** standard (chromatogram **1**) has the same LCMS retention time and mass as sinapyl alcohol **97** produced in an assay with Cr-2141, sinapaldehyde **96**, and NADPH (chromatogram **2**). A coniferyl alcohol **118** standard (chromatogram **3**) has the same LCMS retention time and mass as coniferyl alcohol **118** produced in an assay with Cr-2141, coniferyl aldehyde **108**, and NADPH (chromatogram **4**). Sinapyl alcohol **97** and coniferyl alcohol **118** both lost one unit of H₂O under the mass

spectrometry ionization conditions. The *x*-axis is time in minutes, and the *y*-axis is intensity.

Assays to determine whether Cr-2141, Cr-12, Cr-318, or Cr-611 contained ajmalicine synthase or isositsirikine synthase activity were performed as described in the Materials and Methods section of Chapter 3; Cr-2141, Cr-12, Cr-318, or Cr-611 was used in place of a partially purified enzyme fraction.

F. *Steady state kinetic analysis conditions*

I performed steady state kinetic analysis assays for Cr-2141 with sinapaldehyde **96** in 50 mM sodium phosphate buffer, pH 7.5, at 30°C. Six substrate concentrations were used, and three time points were measured for each substrate concentration. A 135 μ L reaction volume was used, and 5 μ L aliquots were taken at minute intervals. Aliquots were quenched with 950 μ L MeOH containing 500 nM yohimbine **6** as an internal standard, and centrifuged (13,000g, 1 min) to remove particulates. Sinapaldehyde **96** (67-1481 μ M) was incubated with Cr-2141 (1.41 μ M) and NADPH (11.1 mM)¹⁴⁰. Sinapaldehyde **96** disappearance was measured. A logistic curve using OriginPro 7 (OriginLab, Northampton, MA) was used to fit the data, and R^2 value of 0.94 was obtained for the sinapaldehyde **96** data fit (Figure 4-22).

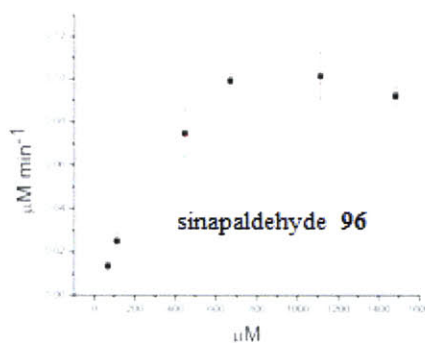


Figure 4-22: Data fit for steady state kinetics of Cr-2141 with sinapaldehyde **96**. The unit for the x -axis is μM sinapaldehyde **96**, and the unit for the y -axis is μM sinapaldehyde **96** reduced per minute.

G. LCMS conditions

Ultra-performance LC analysis was performed on an Acquity Ultra Performance BEH C18 column with a $1.7 \mu\text{m}$ particle size, a $2.1 \times 100 \text{ mm}$ dimension, and a flow rate of 0.5 mL min^{-1} in tandem with a Micromass LCT Premier TOF Mass Spectrometer with an ESI Source (Waters Corporation). The capillary and sample cone voltages were 3000V and 30V , respectively. The desolvation and source temperatures were 300°C and 100°C , respectively. The cone and desolvation gas-flow rates were 60 l hr^{-1} and 8000 l hr^{-1} . Analysis was performed with MassLynx 4.1.

H. High-resolution mass spectrometry data

High-resolution mass spectrometry data were obtained using the MIT DCIF mass spectrometry equipment. Samples were diluted in methanol and then ionized by ESI/FT-MS in the positive ion mode.

sinapyl alcohol **97**: $[\text{M}+\text{H}]^+$ expected 211.0965, observed 211.0961

coniferyl alcohol **118**: $[M+H]^+$ expected 181.0859, observed 181.0851

V. *Acknowledgments:*

I had helpful discussions with Dr. Aimee Usera, Dr. David Liscombe, Dr. Nathan Ezekiel Nims, and Dr. Elizabeth McCoy. I collaborated with Dr. Aimee Usera and Dr. Elizabeth McCoy for the crosslinking studies. Dr. Aimee Usera synthesized the 11-azido-pentynyl-ester strictosidine **114**. Dr. David Liscombe cloned the Cr-2141 and Cr-12 enzymes, and Dr. Nathan Ezekiel Nims cloned the Cr-318 and Cr-611 enzymes from *C. roseus* cDNA. Sequence and database searches were performed by Dr. Sophie Alvarez and Dr. Leslie Hicks at the Donald Danforth Plant Science Center proteomics and mass spectrometry facility (St. Louis, Missouri). Dr. L. Li of the MIT Department of Chemistry Instrumentation Facility performed the high-resolution mass studies. Professor Thomas McKnight of Texas A&M University generously provided information about research done in his laboratory on 10-hydroxy geraniol oxidoreductase.

VI. *References:*

- (1) Sadakane, Y.; Hatanaka, Y. Photochemical fishing approaches for identifying target proteins and elucidating the structure of a ligand-binding region using carbene-generating photoreactive probes. *Analytical Sciences* **2006**, *22*, 209-18.
- (2) Lakshmi, S.; Kumar, S.S.P.; Jayakrishnan, A. Bacterial adhesion onto azidated poly(vinyl chloride) surfaces. *Journal of Biomedical Materials Research Part A* **2002**, *61*, 26-32.
- (3) Thermo Scientific Pierce Protein Research Products, <http://www.piercenet.com/products/browse.cfm?fldID=DB013E61-5056-8A76-4EC4-473A6F2468A1>, accessed June 5, 2010.
- (4) Cravatt, B.F.; Wright, A.T.; Kozarich, J.W. Activity-based protein profiling: from enzyme chemistry to proteomic chemistry. *Annual Review of Biochemistry* **2008**, *77*, 383-414.
- (5) Rostovtsev, V.V.; Green, L.G.; Fokin, V.V.; Sharpless, K.B. A stepwise Huisgen cycloaddition process: copper(I)-catalyzed regioselective "ligation" of azides and terminal alkynes. *Angewandte Chemie International Edition English* **2002**, *41*, 2596-99.
- (6) Swiss Institute of Bioinformatics. SIB BLAST Network Service. ExpASY Proteomics Server. <http://ca.expasy.org/tools/blast>, accessed May 10, 2010.
- (7) Youn, B.; Camacho, R.; Moinuddin, S.G.A.; Lee, C.; Davin, L.B.; Lewis, N.G.; Kang, C. Crystal structures and catalytic mechanism of the Arabidopsis cinnamyl alcohol dehydrogenases AtCAD5 and AtCAD4. *Organic and Biomolecular Chemistry* **2006**, *4*, 1687-97.
- (8) McCrady, E. <http://cool.conservation-us.org/byorg/abbey/ap/ap04/ap04-4/ap04-402.html>, accessed May 22, 2010.
- (9) Moinuddin, S. G.; Youn, B.; Bedgar, D. L.; Costa, M. A.; Helms, G. L.; Kang, C.; Davin, L. B.; Lewis, N. G. Secoisolariciresinol dehydrogenase: mode of catalysis and stereospecificity of hydride transfer in *Podophyllum peltatum*. *Organic and Biomolecular Chemistry* **2006**, *4*, 808-16.
- (10) Lata, H.; Mizuno, C.S.; Moraes, R.M. The role of biotechnology in the production of the anticancer compound podophyllotoxin. *Methods in Molecular Biology* **2009**, *547*, 387-402.
- (11) Carreau, C.; Flouriot, G.; Bennetau-Pelissero, C.; Potier, M. Enterodiol and enterolactone, two major diet-derived polyphenol metabolites have different impact on ER α transcriptional activation in human breast cancer cells *The Journal of Steroid Biochemistry and Molecular Biology* **2008**, *110*, 176-85.
- (12) Kim, S. J.; Kim, M. R.; Bedgar, D. L.; Moinuddin, S. G.; Cardenas, C. L.; Davin, L. B.; Kang, C.; Lewis, N. G. Functional reclassification of the putative cinnamyl alcohol dehydrogenase multigene family in Arabidopsis. *Proceedings of the National Academy of Sciences USA* **2004**, *101*, 1455-60.
- (13) Davin, L. B.; Jourdes, M.; Patten, A.M.; Kim, K.-W.; Vassao, D.G.; Lewis, N.G. Dissection of lignan macromolecular configuration and assembly: comparison to related biochemical processes in allyl/propenyl phenol and lignan biosynthesis. *Natural Products Reports* **2008**, *25*, 1015-90.

- (14) Devlin, T.M. *Textbook of biochemistry with clinical correlations*; 6 ed.; John Wiley & Sons: Hoboken, NJ, 2006.
- (15) Stoop, J.M.H.; Williamson, J.D.; Conkling, M.A.; Pharr, D.M. Purification of NAD-dependent mannitol dehydrogenase from celery suspension cultures. *Plant Physiology* **1995**, *108*, 1219-25.
- (16) Teoh, K.H.; Gorman, E.B.; McKnight, T.D. Origin of 10-hydroxygeraniol oxidoreductase. Sequence Q6V4H0. *EMBL/GenBank/DDBJ databases* **2003**.
- (17) Teoh, K.H.; Gorman, E.; McKnight, T.D. In *American Society of Plant Biologists: Plant Biology 2000* San Diego, CA, 2000.
- (18) Swiss Institute of Bioinformatics. Compute pI/Mw tool. ExPASy Proteomics Server. http://ca.expasy.org/tools/pi_tool.html, accessed May 10, 2010.
- (19) Gorman, E.B.; McKnight, T.D. The origin of 10-hydroxygeraniol oxidoreductase. Q7XAB2. *EMBL/GenBank/DDBJ databases* **2003**.
- (20) Balsevich, J.; Constabel, F.; Kurz, W.G. Efficient incorporation of 10-hydroxygeraniol and 10-hydroxyneryl into indole alkaloids by a cell suspension culture of *Catharanthus roseus*. *Planta Medica* **1982**, *44*, 231-33.
- (21) Balsevich, J.; Kurz, W.G. The role of 9- and/or 10-oxygenated derivatives of geraniol, geranial, nerol, and neral in the biosynthesis of loganin and ajmalicine. *Planta Medica* **1983**, *49*, 79-84.
- (22) El-Sayed, M.; Verpoorte, R. *Catharanthus* terpenoid indole alkaloids: biosynthesis and regulation. *Phytochemistry Reviews* **2007**, *6*, 277-305.
- (23) Collu, G.; Garcia, A.A.; Heijden, R.; Verpoorte, R. Activity of the cytochrome P450 enzyme geraniol 10-hydroxylase and alkaloid production in plant cell cultures. *Plant Science* **2002**, *162*, 165-72.
- (24) Collu, G.; Unver, N.; Peltenburg-Looman, A.M.G.; Heijden, R.; Verpoorte, R.; Memelink, J. Geraniol 10-hydroxylase, a P450 enzyme involved in terpenoid indole alkaloid biosynthesis. *FEBS Letters* **2001**, *508*, 215-20.
- (25) Contin, A.; van der Heijden, R.; Lefeber, A. W.; Verpoorte, R. The iridoid glucoside secologanin is derived from the novel triose phosphate/pyruvate pathway in a *Catharanthus roseus* cell culture. *FEBS Letters* **1998**, *434*, 413-16.
- (26) McCoy, E. Substrate analogs to investigate alkaloid biosynthesis in *C. roseus*. Ph.D. dissertation, Massachusetts Institute of Technology, 2009.
- (27) Friedrich, A.; Bräse, S.; O'Connor, S.E. Synthesis of 4-, 5-, 6-, and 7-azidotryptamines. *Tetrahedron Letters* **2009**, *50*, 75-76.
- (28) Miles, E.W.; Phillips, R.S. Photoinactivation and photoaffinity labeling of tryptophan synthase alpha-2-beta-2 complex by the product analogue 6-azido-L-tryptophan. *Biochemistry* **1985**, *24*, 4694-4703.
- (29) Jones, A.M.; Venis, M.A. Photoaffinity labeling of indole-3-acetic acid binding proteins in maize. *Proceedings of the National Academy of Sciences USA* **1989**, *86*, 6153-56.
- (30) Galan, M. C.; O'Connor, S.E. Semi-synthesis of secologanin analogues. *Tetrahedron Letters* **2006**, *47*, 1563-65.
- (31) Galan, M.C., McCoy, E.; O'Connor, S.E. Chemoselective derivatization of alkaloids in periwinkle. *Chemical Communications* **2007**, 3249-51.

(32) Rosenthal, C.; Mueller, U.; Panjikar, S.; Sun, L.; Ruppert, M.; Zhao, Y.; Stockigt, J. Expression, purification, crystallization and preliminary X-ray analysis of perakine reductase, a new member of the aldo-keto reductase enzyme superfamily from higher plants. *Acta Crystallographica Section F Structural Biology and Crystallization Communications* **2006**, *F62*, 1286-89.

(33) Runguphan, W.; Maresh, J. J.; O'Connor, S. E. Silencing of tryptamine biosynthesis for production of nonnatural alkaloids in plant culture. *Proceedings of the National Academy of Sciences USA* **2009**, *106*, 13673-78.

(34) Aerts, R.J.; Gisi, D.; De Carolis, E.; De Luca, V.; Baumann, T.W. Methyl jasmonate vapor increases the developmentally controlled synthesis of alkaloids in *Catharanthus* and *Cinchona* seedlings. *The Plant Journal* **1994**, *5*, 635-43.

Chapter 5: Conclusions and Future Directions

I. *Conclusions*

Terpene indole alkaloids (TIAs) are a large class of natural products produced in plants. Many TIAs have medicinal uses; for example, vinblastine **2** and vincristine **3** have anti-cancer activity, ajmalicine **4** has anti-hypertensive activity, and ajmaline **9** has anti-arrhythmic activity¹. Many TIAs most likely did not evolve to treat human diseases, however, and thus perhaps do not have optimal pharmacological properties². There are many examples of modified natural products that have improved bioactivities when compared with the unmodified natural product; for example, camptothecin **10** is too toxic and hydrophobic to be used clinically, yet the camptothecin analogs irinotecan **16** and topotecan **15** are used clinically³. In drug design, many modifications can be made to a compound to alter its pharmacological properties. For example, halogenation can improve lipophilicity^{4,5}, hydroxylation and methylation can improve water solubility⁴, and alteration of the stereochemistry at a chiral center can change the bioactivity of a drug candidate^{6,7}.

Unfortunately, the immense structural complexity of TIAs makes cost-effective industrial-scale synthesis of the majority of TIAs and TIA analogs unfeasible. The current method of isolation of medicinal TIAs is via purification from the plant; purification is no simple task, however, because numerous compounds are present. Industrial scale production of TIAs would be improved if TIAs could be produced via heterologous reconstitution of the enzymatic pathways in a heterologous organism such as yeast². However, many of the enzymes involved in TIA biosynthesis are unknown, thereby precluding these efforts. If more TIA biosynthetic enzymes were isolated and cloned, and the substrate specificity of the enzymes were known, both natural and novel TIA analogs could be more readily produced on an industrial scale.

In this thesis I developed strategies to make novel ajmalicine **4** and isositsirikine **7** analogs *in vitro*. The NADPH-dependent reductase enzymes that produce the anti-hypertensive agent ajmalicine **4** and the anti-neoplastic agent isositsirikine **7** have not been isolated. To produce ajmalicine **4** and isositsirikine **7** analogs *in vitro*, two aims must be accomplished: first, the reductases forming ajmalicine **4** and isositsirikine **7** must be partially purified, and second, the substrate specificity of the reductase enzymes ajmalicine synthase and isositsirikine synthase must be determined.

To satisfy the first of these aims, I developed a partial purification procedure for ajmalicine synthase and isositsirikine synthase from *C. roseus* hairy root and cell suspension cultures using protein precipitation, ion exchange, and gel filtration chromatography. Ajmalicine synthase and isositsirikine synthase retain activity in all steps of the purification procedure. Analysis by 2D SDS-PAGE shows that the proteins have been significantly purified. Enzymes from the 2D SDS-PAGE of an active size 200 gel filtration column fraction were sequenced, and one enzyme was found to have high sequence identity to a cinnamyl alcohol dehydrogenase. Future efforts will involve cloning and characterizing the full length gene.

In collaboration with Dr. Aimee Usera and Dr. Elizabeth McCoy, I also performed crosslinking experiments with a substrate probe in attempts to isolate ajmalicine synthase and isositsirikine synthase. In the crosslinking studies, four enzymes – Cr-2141, Cr-12, Cr-318, and Cr-611 – were isolated and cloned. Though the functions of Cr-12, Cr-318, and Cr-611 have yet to be determined, Cr-2141 was shown to have sinapyl alcohol dehydrogenase activity, reducing sinapaldehyde **96** to sinapyl alcohol **97** with a measured k_{cat} of 0.092 min^{-1} .

I determined the substrate specificities of SGD, ajmalicine synthase, and isositsirikine synthase. SGD, which deglycosylates strictosidine **1**, the central intermediate in TIA biosynthesis, does not act as a gatekeeper in TIA biosynthesis: in fact, SGD deglycosylates all indole substituted strictosidine analogs **1-c** through **1-s** tested, as well as strictosidine **1** analogs substituted at the C-5 position **1-u** and **1-v** and the methyl ester position **1-t**. An indole moiety does not appear to be required for turnover by SGD, because deglycosylation of deacetylpecosides **45-1** was observed. Additionally, strictosidine analogs containing alternate heterocycles **1-a**, **1-b**, **1-w**, and **1-x** were also deglycosylated. SGD recognizes a different stereoisomer, deglycosylating the C-3 *R* diastereomer of strictosidine **1**, vincoside **43**. Steady state kinetic analysis of indole substituted strictosidine analogs **1-d**, **1-e**, **1-g**, **1-h**, **1-j**, **1-j**, **1-r**, and **1-s** showed that the catalytic efficiencies (V_{\max}/K_m values) did not differ by more than an order of magnitude, indicating that all indole substituted strictosidine analogs assayed were accepted at similar efficiencies. Additional steady state kinetic analysis studies showed that SGD has a sixfold catalytic preference of strictosidine **1** over vincoside **43**.

Ajmalicine synthase and isositsirikine synthase also have broad substrate specificity, which is promising for the development of novel ajmalicine **4** and isositsirikine **7** analogs with potentially improved therapeutic activities. Partially purified ajmalicine synthase and isositsirikine synthase could reduce indole substituted deglycosylated strictosidine analogs **49-c** through **49-s**, as well as deglycosylated benzo strictosidine **49-a**, deglycosylated thio strictosidine **49-b**, deglycosylated pentynyl-ester strictosidine **49-t**, and deglycosylated d_4 vincoside **84**. To determine the effects of substrate specificity, I also performed steady state kinetic analysis studies. Partially purified ajmalicine synthase was found to reduce deglycosylated vincoside **84** to C-3 *R* ajmalicine **85** with a catalytic efficiency of $1.13 \times 10^{-4} \text{ min}^{-1}$

¹. Deglycosylated methyl strictosidine analogs **49-g**, **49-h**, **49-i**, and **49-j** were also reduced by partially purified ajmalicine synthase, with catalytic efficiencies of $7.08 \times 10^{-3} \text{ min}^{-1}$, $6.52 \times 10^{-3} \text{ min}^{-1}$, $11.7 \times 10^{-3} \text{ min}^{-1}$, and $7.01 \times 10^{-3} \text{ min}^{-1}$, respectively. Partially purified isositsirikine synthase reduced deglycosylated d₄ strictosidine **49-1**, deglycosylated benzo strictosidine **49-a**, and deglycosylated thio strictosidine **49-b** with catalytic efficiencies of $1.63 \times 10^{-3} \text{ min}^{-1}$, $3.36 \times 10^{-2} \text{ min}^{-1}$, and $6.03 \times 10^{-2} \text{ min}^{-1}$, respectively.

II. *Future directions*

Additional efforts will be made to clone, express, and functionally characterize the enzymes isolated via the native purification and crosslinking studies described in Chapters 3 and 4. The gene candidate identified by native purification that had sequence identity to a cinnamyl alcohol dehydrogenase will be cloned and heterologously expressed. A large-scale sequencing project scheduled to be completed in July 2010 will provide the full length sequence of this gene, after which this candidate will be amplified from *C. roseus* cDNA, placed in an expression vector, heterologously expressed in *E. coli* or yeast, and functionally characterized for ajmalicine synthase and isositsirikine synthase activity. Additionally, the function of enzymes that have already been expressed, Cr-2141, Cr-12, Cr-318, and Cr-611, will be further probed to determine their function in the plant. The functions of Cr-2141, Cr-12, Cr-318, and Cr-611 can be disrupted in the plant by using RNAi⁸ or virus-induced gene silencing (VIGS)⁹ (Liscombe, O'Connor, unpublished). After disruption of each gene, the resulting phenotype or metabolic profile can be compared with wild-type tissue to provide more information about the role of these enzymes in the plant.

Other efforts can be made to clone similar enzymes in TIA biosynthesis; for example, there are no reports in the literature of reductase(s) forming yohimbine **6**. To isolate the

reductase(s) forming yohimbine **6**, a different type of cell culture that produces large amounts of yohimbine **6** should be utilized. The PC510 *C. roseus* cell suspension culture line from DSMZ (Deutsche Sammlung von Mikroorganismen und Zellkulturen GmbH) was used for all research performed in this thesis; this line produces negligible amounts of yohimbine **6**. If a cell suspension culture line that produced more yohimbine **6**, such as *Pausinystalia yohimbe*, was used¹⁰, perhaps the reductase(s) catalyzing yohimbine **6** formation from deglycosylated strictosidine **49** could be isolated.

Additionally, numerous enzymes in TIA biosynthesis are not soluble, and we suspect that at least one membrane-bound enzyme utilizes deglycosylated strictosidine **49** as a substrate. To initiate biochemical studies of these membrane-bound enzymes, microsomes were used to develop *in vitro* enzyme assays. To obtain the microsomes, 16 g of cell suspension culture were blended in 60 mL 0.1M borate buffer, pH 7.5, containing 20 mM β -mercaptoethanol, 1 mM EDTA, 0.1% PVP, and 10% glycerol. The mixture was then ultracentrifuged at 140,000g for 1 hour. The pellet was then resuspended in 1.5 mL borate buffer, and 200 μ L 60% glycerol was added. In assays with resuspended pellet, strictosidine **1**, SGD, and NADPH, a peak with m/z 325 was observed by LCMS (Figure 5-1). This peak was not seen in LCMS traces in assays lacking strictosidine **1**. In assays using numerous other strictosidine **1** analogs (Figure 5-1), including 9-methyl strictosidine **1-g**, 11-methyl strictosidine **1-i**, and 11-methoxy strictosidine **1-s**, the corresponding analog of the parent m/z 325 compound was observed.

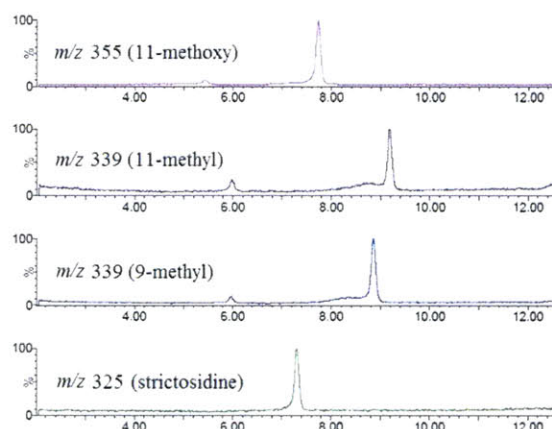


Figure 5-1: In an assay with microsomes, SGD, and NADPH, various strictosidine **1** analogs, including strictosidine **1**, 9-methyl strictosidine **1-g**, 11-methyl strictosidine **1-i**, and 11-methoxy strictosidine **1-s**, were converted to a product with m/z 325, 339 ($325 + 14$), 339 ($325 + 14$), and 355 ($325 + 30$), respectively. The x -axis is time in minutes and the y -axis is intensity.

Four potential known TIAs that the product with m/z 325 may correspond to are lochnerine **128**¹¹, rosicine **129**¹², tubotaiwin **130**¹³, and dihydroakuammicine **131**¹⁴. Unfortunately, repeated efforts to reproducibly obtain this novel activity failed. This failure may be because the cell suspension cultures lost the ability to produce the m/z 325 product; after years of subculturing, cell suspension cultures frequently lose the ability to produce natural products¹⁵. Future efforts could involve isolating microsomes from new stocks of cell suspension cultures.

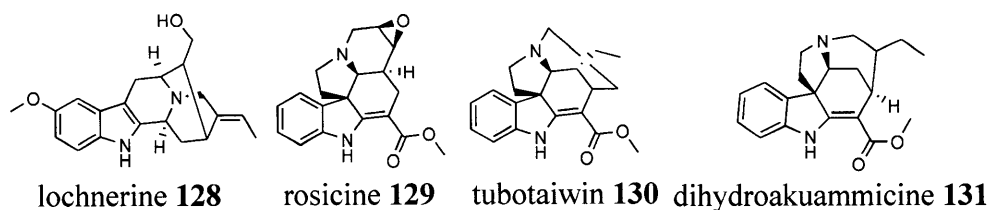


Figure 5-2: Four potential TIAs that the product with m/z 325 may correspond to are lochnerine 128¹¹, rosicine 129¹², tubotaiwin 130¹³, and dihydroakuammicine 131¹⁴.

The deglycosylated strictosidine **49** intermediate produced by SGD is reported to be extremely reactive and have low solubility in water¹⁶, and thus it can be hypothesized that ajmalicine synthase and isositsirikine synthase interact with SGD, forming a metabolon that will facilitate the shuttling of this reactive, hydrophobic intermediate. Metabolon formation has been reported in *A. thaliana*¹⁷⁻¹⁹ in phenylpropanoid and flavonoid metabolism²⁰. A co-immunoprecipitation experiment²¹ with SGD could potentially be performed to isolate ajmalicine synthase and isositsirikine synthase. SGD can be expressed as a fusion protein with glutathione-S-transferase (GST), and transformed into *C. roseus*. The transformed cells will be lysed, GST antibody will be added, and then the lysate will be passed over an IgG column. The column will be stripped, and the eluted proteins will be assayed for ajmalicine synthase and isositsirikine synthase activity. Additional methods for detecting protein-protein interactions, such as yeast two-hybrid assays, could also be performed.

Finally, the pharmaceutical activity of novel ajmalicine **4** and isositsirikine **7** analogs will be assessed. Cytotoxicity screens are already underway for various TIA analogs at Vanderbilt and the University of Illinois (Usera, Lee, O'Connor, unpublished). Additionally, crude extracts of these lysates will be sent to a natural product lysate collection at the University of Michigan.

III. Acknowledgments

I thank Professor Barbara Imperiali for allowing me to use the ultracentrifuge in her laboratory, and I thank the Imperiali laboratory members Brenda Goguen and Dr. Galen Loving for teaching me how to use it.

IV. References

- (1) O'Connor, S. E.; Maresh, J. J. Chemistry and biology of monoterpene indole alkaloid biosynthesis. *Natural Products Reports* **2006**, *23*, 532-47.
- (2) Keasling, J. From yeast to alkaloids. *Nature Chemical Biology* **2008**, *4*, 524-25.
- (3) Cragg, G.M.; Kingston, D.G.I.; Newman, D.J. *Anticancer agents from natural products*; Taylor & Francis: New York, New York, 2005.
- (4) Thomas, G. *Medicinal chemistry: an introduction*; John Wiley & Sons: New York, New York, 2000.
- (5) Wermuth, C.G. *The practice of medicinal chemistry*; Harcourt Brace and Company: New York, New York, 1996.
- (6) Silverman, R.B. *The organic chemistry of drug design and drug action*; Elsevier Academic Press: Oxford, United Kingdom, 2004.
- (7) De Camp, W.H. The FDA perspective on the development of stereoisomers. *Chirality* **1989**, *1*, 2-6.
- (8) Runguphan, W.; Maresh, J. J.; O'Connor, S. E. Silencing of tryptamine biosynthesis for production of nonnatural alkaloids in plant culture. *Proceedings of the National Academy of Sciences USA* **2009**, *106*, 13673-78.
- (9) Lu, R.; Martin-Hernandez, A.M.; Peart, J.R.; Malcuit, I.; Baulcombe, D.C. Virus-induced gene silencing in plants. *Methods* **2003**, *30*, 296-303.
- (10) Chen, Q.; Li, P.; Zhang, Z.; Li, K.; Liu, J.; Li, Q. Analysis of yohimbine alkaloid from *Pausinystalia yohimbe* by non-aqueous capillary electrophoresis and gas chromatography-mass spectrometry. *Journal of Separation Science* **2008**, *31*, 2211-18.
- (11) Banerji, A.; Chakrabarty, M. Lochvinerine: a new indole alkaloid of *vinca major*. *Phytochemistry* **1974**, *13*, 2309-12.
- (12) Cordell, G.A. *The alkaloids: chemistry and biology*; Academic Press: San Diego, California, 1998; Vol. 51.
- (13) Macabeo, A.P.G.; Krohn, K.; Gehle, D.; Read, R.W.; Brophy, J.J.; Cordell, G.A.; Franzblau, S.G.; Aguinaldo, A.M. Indole alkaloids from the leaves of Philippine *Alstonia scholaris*. *Phytochemistry* **2005**, *66*, 1158-62.
- (14) Kuehne, M.E.; Frasier, D.A.; Spitzer, T.D. Total syntheses of tubotaiwine and 19,20-dihydro-20-epi-akuammicine. *Journal of Organic Chemistry* **1990**, *56*, 2696-2700.
- (15) McCoy, E.; O'Connor, S. E. Natural products from plant cell cultures. *Progress in Drug Research* **2008**, *65*, 329, 331-70.
- (16) Barleben, L.; Panjekar, S.; Ruppert, M.; Koepke, J.; Stockigt, J. Molecular architecture of strictosidine glucosidase: the gateway to the biosynthesis of the monoterpene indole alkaloid family. *The Plant Cell* **2007**, *19*, 2886-97.

(17) Burbulis, I. E.; Winkel-Shirley, B. Interactions among enzymes of the Arabidopsis flavonoid biosynthetic pathway. *Proceedings of the National Academy of Sciences USA* **1999**, *96*, 12929-34.

(18) Jorgensen, K.; Rasmussen, A. V.; Morant, M.; Nielsen, A. H.; Bjarnholt, N.; Zagrobelny, M.; Bak, S.; Moller, B. L. Metabolon formation and metabolic channeling in the biosynthesis of plant natural products. *Current Opinion in Plant Biology* **2005**, *8*, 280-91.

(19) Nielsen, K.A.; Tattersall, D.B.; Jones, P.R.; Moller, B.L. Metabolon formation in dhurrin biosynthesis. *Phytochemistry* **2008**, *69*, 88-98.

(20) Winkel-Shirley, B. Evidence for enzyme complexes in the phenylpropanoid and flavonoid pathways. *Physiologia Plantarum* **1999**, *107*, 142-49.

(21) Alberts, B.; Johnson, A.; Lewis, J.; Raff, M.; Roberts, K.; Walter, P. *Molecular Biology of the Cell*; Garland Science: New York, New York, 2002.

Nancy Yerkes

yerkes@mit.edu / (617) 309-6458 / 56 Linnaean Street, Cambridge, MA 02138

Education:

Stanford University School of Medicine, Stanford, CA – M.D. candidate. Degree expected June 2014.

Massachusetts Institute of Technology, Cambridge, MA – Ph.D. candidate, biological chemistry. Degree expected September 2010.

Columbia University, New York, NY – B.A., Chemistry, May 2005. GPA 3.84. Graduated *magna cum laude* and with departmental honors. Dean's List all semesters. Recipient of the Jean Dreyfus Boussevain Undergraduate Scholarship for Excellence in Chemistry.

Housatonic Valley Regional High School, Falls Village, CT – Graduated *summa cum laude* and valedictorian, June 2001.

Publications:

Hyang-Yeol Lee, Nancy Yerkes, Peter Bernhardt, Sarah E. O'Connor. Aza-tryptamine substrates in natural product biosynthesis. *Chemistry and Biology* 16 (2009) 1225-1229.

Peter Bernhardt*, Nancy Yerkes*, Sarah E. O'Connor. Bypassing stereoselectivity in the early steps of alkaloid biosynthesis. *Organic and Biomolecular Chemistry* 7 (2009) 4166-4168. (*co-first authors)

Nancy Yerkes, Jia Xin Wu, Elizabeth McCoy, M. Carmen Galan, Shi Chen, Sarah E. O'Connor. Substrate specificity and diastereoselectivity of strictosidine glucosidase, a key enzyme in monoterpene indole alkaloid biosynthesis. *Bioorganic and Medicinal Chemistry Letters* 18 (2008) 3095-3098.

Wenjun Zhou, Nancy Yerkes, Jason J. Chruma, Lei Liu, Ronald Breslow. Chiral polyamines from reduction of polypeptides: asymmetric pyridoxamine-mediated transaminations. *Bioorganic and Medicinal Chemistry Letters* 15 (2005) 1351-1355.

Aimee R. Usera*, Nancy Yerkes*, Elizabeth McCoy*, David Liscombe, Nathan E. Nims, Anne C. Friedrich, Sarah E. O'Connor. Crosslinking strategies to isolate a new *C. roseus* enzyme. *Manuscript in preparation*, 2010. (* co-first authors)

Nancy Yerkes, Aimee R. Usera, Sarah E. O'Connor. Partial purification and substrate specificity of isositsirikine synthase. *Manuscript in preparation*, 2010.